THE EFFECT OF CERTAIN PARAMETERS ON THE SEPARATION OF VARIOUS LIQUID/LIQUID SYSTEMS BY A HYDROCYCLONE

by

WALTER MALCOLM SCOTT

B.Eng (Civil)

A Thesis
Submitted to the School of Graduate Studies
in Partial Fulfilment of the Requirements
for the Degree
Master of Engineering

McMaster University
September 1980.

MASTER OF ENGINEERING (1980)
(Civil)

McMaster University
Hamilton, Ontario.

TITLE: The Effect of Certain Parameters on the Separation of Various Liquid/Liquid Systems by a Hydrocyclone.

AUTHOR: Walter Malcolm Scott, B.Eng. (McMaster University)

SUPERVISOR: Professor D.R. Woods

NUMBER OF PAGES: xvi, 211

SCOPE AND CONTENTS

A 2 inch diameter, conical-shaped glass hydrocyclone, operating without an air core, was used in this study. The geometric dimensions of the cyclone followed closely with the optimum design conditions determined for solid/liquid systems by Rietema (R-1) and used by Burrill and Woods (B-3) for liquid/liquid systems. Distilled water was used as the continuous phase. Dispersed oil phases studied include: butanol, methyl isobutyl ketone (MIBK), toluene and kerosene.

For each of the liquid/liquid systems, the efficiency of separation was determined as a function of volume split, oil/water phase ratio and feed flowrate. Differentiation of the liquid/liquid systems, in terms of physical properties, was based primarily on interfacial tension. Density difference and viscosity of the dispersed phase, were comparable from one system to another. Mixing energy used to disperse the oil phase in the water phase, geometric dimensions and temperature were constant throughout the work. The range of the operating variables were as follows:

i)	oil/water phase ratio	0.160 to 1.00
ii)	feed flowrate	100 to 365 mL/s
iii)	interfacial tension	2.0 to 30.0 mN/m
iv)	volume split	0.17 to 3.90

For each system studied, photographs were taken at the inlet and outlets leading to and from the cyclone, respectively, to determine the drop size of the dispersed phase.

The second part of the present work considered the influence that the mixing energy had on the effects of oil/water ratio and feed flowrate

as studied in the first part.

The efficiency of separation (E_s) is defined as follows:

$$E_s = \frac{Q_o}{Q_f}\left[\frac{Y_o - Y_f}{1 - Y_f}\right] + \frac{Q_u}{Q_f}\left[\frac{Y_f - Y_u}{Y_f}\right]$$

where Y and Q represent volume fraction of light phase and flowrate, respectively, while the subscripts denote a specific orifice location on the hydrocyclone.

From the first part the efficiency of separation in the cyclone was a very important function of volume split. The effect of the feed flowrate on separation in the cyclone was dependent on the interfacial tension. The effect of oil/water ratio was dependent on the rate of coalescence. Based on the photographic work, coalescence occurred in the cyclone for several of the systems studied.

The majority of past work has varied the mixing energy with a change in the feed flowrate. As a result, drop size varied. Present work revealed that this reversed the effect that feed flowrate had on the separation in the cyclone with mixing energy constant.

It was not possible to obtain two pure phases from the hydrocyclone for any of the systems studied. One pure phase, however, was achieved for three of the four systems studied. A relatively pure water phase (≥ 99%) was obtained at the underflow for the MIBK/water, toluene/water and kerosene/water systems. The highest values of the optimum E_s were 67, 57 and 62%, respectively, for each of these systems. For toluene/water and kerosene/water systems, the interfacial tension was sufficiently high to prevent significant drop breakup when the feed flowrate was increased. Under similar circumstances, drop breakup predominated for MIBK/water and butanol/water

systems due to the lower values of interfacial tension. With butanol/water, a significant amount of light phase was found in the underflow. The optimum E_s for this system was only 26%.

It was noted that the efficiency of separation, E_s, increased sharply at first and then decreased gradually with increasing volume split. The optimum volume split occurred at a value greater than the feed phase ratio for all systems studied. The optimum value ranged from 100 to 500% greater than the feed phase ratio. Since complete coalescence does not occur inside the cyclone, it is not possible to have the optimum split equivalent to the feed phase ratio. Continuous phase trapped in the intersticies results in the optimum split equivalent to a value greater than the feed phase ratio. A simple mass balance model was used to describe the effects of volume split. From this model the interstitial volume could be inferred for all conditions. Combining this information with models for breakup, coalescence and hindered settling yielded a semi-quantitative explanation of all the trends observed.

The feasibility of using the hydrocyclone to separate emulsions is based on achieving at least one pure phase. If this achievement is accomplished, then it is possible to reduce the volume requirement of a gravity settler. The role of the hydrocyclone is basically one of a preliminary stage in the physical separation process. If, on the other hand, it is not possible to have one pure phase, no useful purpose is served by the cyclone. Consequently, the butanol/water system can not be considered a feasible system to be separated by a hydrocyclone.

ACKNOWLEDGEMENTS

I wish to express my deep gratitude to Dr. D.R. Woods for his endless enthusiasm and helpful suggestions during the course of this research work.

Special thanks is also extended to Dr. S. Vijayan for his assistance with the surface/interfacial tension work, to Messrs. R.Dunn and J. Newton for their help in constructing and assembling equipment and to Messrs. H. Behmann and U. Goults for their assistance and suggestions with the photographic work.

Financial assistance in the form of an N.R.C. research grant, and a teaching assistantship from the Civil Engineering Department, was gratefully appreciated.

A sincere thanks is extended to my parents for their encouragement throughout my education.

Finally, an expression of thanks is extended to Mrs. Amy Stott and Mrs. Grace Wang for their conscientous work in typing this thesis.

Walter M. Scott
September 1980
Hamilton.

TABLE OF CONTENTS

PAGE

LIST OF TABLES

LIST OF FIGURES

LIST OF FIGURES (cont'd)

LIST OF FIGURES (cont'd)

LIST OF ABBREVIATIONS

A_p	- projected area of droplet
b	- radius of droplet
C_D	- coefficient of drag
C_N	- clarification number
D	- pipe diameter
D_{MAX}	- largest droplet size counted
D_{MIN}	- smallest droplet size counted
D_p	- particle diameter
D_{50}	- geometric number average droplet size
D_{95}	- droplet size greater than or equal to 95% of droplets counted
D_{84}/D_{50}	- standard deviation of droplet size distribution
E_s	- efficiency of separation
F_c	- centrifugal force
F_d	- drag force
g	- gravitational constant
h	- film thickness
h_o	- initial film thickness
LL	- left limb of manometer
RL	- right limb of manometer
O/U	- volume split
O/W	- phase ratio
ΔP	- pressure drop
ΔP_o	- pressure drop in a dilute medium

p_f - pressure at feed location

p_o - pressure at overflow location

p_u - pressure at underflow location

Q_f - flowrate through feed location

Q_o - flowrate through overflow location

Q_u - flowrate through underflow location

r - radius in hydrocyclone

R - Reynolds number

U - linear velocity

V_r - radial velocity component

V_θ - tangential velocity component

V_∞ - terminal settling velocity

$\bar{X}$ - mean

Y_f - volume fraction of light phase in feed

Y_o - volume fraction of light phase in overflow

Y_u - volume fraction of light phase in underflow

Greek Letters

ε - interstitial volume

μ_c - dynamic viscosity of continuous phase

μ_d - dynamic viscosity of dispersed phase

γ - interfacial tension

ν - kinematic viscosity

ρ - density of continuous phase

$\Delta\rho$ - density difference between dispersed and continuous phase

σ - standard deviation

θ - time of coalescence

Coded

-1 - Q_{MIN} or $(O/W)_{MIN}$

0 - Q_{MID} or $(O/W)_{MID}$

+1 - Q_{MAX} or $(O/W)_{MAX}$

Subscripts

f - feed

o - overflow

u - underflow

c - continuous phase

d - dispersed phase

MIN - minimum point studied

MID - midpoint studied

MAX - maximum point studied

Other

ϕn_G^2 - constant used in Parallel Disc Model.

I OBJECTIVES

I OBJECTIVES

Past research has been concerned mainly with the study of certain operating parameters on the operation of solid/liquid and solid/gas separation processes. Applications for these processes are numerous. Only in the last 30 years or so has the liquid/liquid separation process been investigated. Rapid separation of the two liquid phases can be achieved inside the hydrocyclone. It is possible to obtain one pure phase from the cyclone. This reduces the volume required for further processing. Research in this field, however, has been limited. The most extensive work to date has been by Simkin and Olney (S-3) and Burrill and Woods (B-3). Both have shown that separation of a liquid/liquid system by a cyclone is a feasible operation. Simkin et al. studied the effect of a number of parameters on the optimum efficiency of separation; however this study was carried out in the presence of an air core and without the control of feed droplet size entering the cyclone. In addition little consideration was given to the physical properties of the liquid/liquid systems studied. Burrill et al., using a statistical design, also studied the effects of various parameters on optimum separation efficiency. He controlled feed droplet size, performed the work in the absence of an air core and paid close attention to the physical properties of the liquid/liquid system studied; however his work was limited to the study of one system only.

The problem with past work has been a lack of uniform design conditions from one study to another. This is perhaps due to the relatively recent development of this separation process. A more meaningful comparison could be gained if certain design conditions are uniform for

successive studies. The present work is tailored after that of Burrill et al.

Based on the results of past studies, the following objectives have been formulated for the present work:

1) the effect of a certain physical property of the liquid/liquid system, namely interfacial tension, on the separation process.

2) the effect of certain operating parameters, namely oil/water phase ratio and feed flowrate, on the separation process.

3) how the separation efficiency varies with volume split.

4) how the variation in feed drop size distribution can influence the results in objectives 2) and 3)

5) to predict, based on photographic work, whether breakup or coalescence predominates in the cyclone.

6) to evaluate the above objectives under the following conditions:

i) absence of an air core

ii) dimensions of cyclone fixed

iii) light phase always dispersed

iv) oil phase always lighter than continuous water phase such that it exits through the vortex finder.

II LITERATURE REVIEW

II LITERATURE REVIEW

II-a Introduction

This chapter is basically concerned with a review of literature pertaining to liquid/liquid separation in a hydrocyclone. It also describes the cyclone's development and mode of operation. Another section considers the factors which affect the separation process.

II-b Hydrocyclones

This section contains a discussion of the hydrocyclone in terms of a physical description and its historical development.

II-b.1 Physical Description

A hydrocyclone, or more simply, a cyclone, is a device which separates or classifies components of a system by centrifugal force. Liquid acts as the continuous medium. Fluid pressure, usually provided by a pump(s), ensures the driving force necessary for the separation process. Cyclones are widely used in industry for the following reasons: small space requirements, no moving parts, low initial cost and rapid separation of phases. Their use in the past, however, has been restricted mainly to liquid/solid and gas/solid separation processes.

Usually a cyclone has a cylindrical upper, and conical lower portion; however in this work a conical-shaped one was used. It has three orifices - one inlet and two outlets. The outlet orifices, termed overflow and underflow, are located at opposite ends of the cyclone's major axis. The internal projection of the overflow tube is commonly known as the "vortex finder". Its purpose is to prevent the feed dispersion from

going directly to the overflow without benefit of the cyclone's separating action - a problem known as "short circuiting".

II-b.2 Historical Development

The cyclone was first patented by Bretney in 1892. Its early use was limited to air particulate collection. In 1939 Driessen of the Dutch State Mines used the cyclone as a thickener in a coal cleaning process. This brought international interest for using liquid as the carrying medium. To date, the major emphasis on cyclone development has been in the liquid/solid and gas/solid systems.

II-c Study of Liquid/Liquid Separation

This section is basically concerned with justifying the study of liquid/liquid separation. It discusses present or potential applications. It also contains a review of significant observations made from past research.

II-c.1 Applications

Hydrocyclones can be used in solvent extraction where the solvent should be recovered because of its expense. Further consideration of this process should also be given to the treatment of industrial wastes such as refinery oil, rendering fats and edible oil.

II-c.2 Methods of Processing

Two methods of processing a liquid/liquid system through a cyclone are employed. One, with the underflow open to the atmosphere, allows an air core to form the full length of the cyclone along the major axis. Allowing an air core to form reduces the pressure drop and energy usage.

The second method, with the underflow flooded by a liquid, prevents

formation of an air core. The underflow line may be used to transport the effluent to further downstream processing. Without an air core, pressure losses are roughly doubled. Absence of an air core is important when dealing with volatile food processing liquids where oxygen is not a desired constituent.

Past research has predominantly been carried out in the presence of an air core. The only published results without air core formation were performed by Knowles (K-3), Hsiang and Woods (H-4), Witbeck (W-1) and Burrill and Woods (B-3).

II-c.3 Past Research

Two dramatically different views, about liquid/liquid separation, are prevailant in the literature.

On one hand, Svarovsky (S-6), Bradley (B-1) and Tepe and Woods (T-2) all expressed doubt that a liquid/liquid system could be successfully separated with a hydrocyclone. Svarovsky stated that "for the separation of immiscible liquids that the efficiency was poor and the existence of shear caused emulsification of the two phases". Bradley reiterated this statement. Tepe and Woods, studying an isobutanol/water system, found the separation to be "poor due to the problem of emulsification". From the aforementioned work, it may be concluded that a cyclone is not an effective tool in separating liquid/liquid systems.

Contrary to this, liquid/liquid systems studied by Simkin and Olney (S-3), Mahajan and Pai (M-1), Hitchon (H-3), Sheng et al. (S-1) and Burrill and Woods (B-3), have shown that efficient separation was possible; however for certain operating conditions a significant decrease in separation efficiency was observed. The most comprehensive studies were by

Simkin et al. and Burrill et al. Simkin et al. with kerosene/water and white oil/water showed that the optimum separation efficiency, E_s, was dependent on volume split, phase ratio and feed flowrate. Burrill et al. with a carbon tetrachloride/water system maintained a constant flowrate and found that efficiency of separation was affected by volume split, phase ratio, and droplet size, in that order, respectively.

According to Simkin et al., the optimum E_s decreased with increasing flowrate. This was verified by Mahajan et al. and Sheng et al. Flowrate can be expressed in terms of the Reynolds number which is defined as:

$$R = \frac{U\ D}{\upsilon} \qquad \text{(II-1)}$$

This dimensionless number represents the ratio of inertial to viscous forces. Even for solid/liquid systems the effect on optimum E_s with a change in Reynolds number is not well known. Since solid particles will not breakup with an increase in centrifugal force, separation should be enhanced with an increase in Reynolds number. Van Kooy (V-1), expressing separation efficiency in terms of a clarification number, found that as Reynolds number increased, C_N increased to an optimum. Any further increase in flowrate resulted in no significant increase in C_N. Hsiang and Woods (H-4), also studying solid/liquid separation, stated that an increase in flowrate improved the separation efficiency; however they found that this increase was influenced by cyclone shape.

The effect of phase ratio was inconclusive from the work of Simkin et al. The range studied was sufficiently wide that the oil

phase was dispersed at the lower values and was continuous at the upper ones. Sheng et al., however, studying a somewhat smaller range, found that the optimum E_s increased with an increase in phase ratio. Burrill et al., studying the effect over a small range, noted a decrease in the optimum E_s with an increase in phase ratio; however the volume split was held constant with a change in phase ratio for this work.

Simkin et al. noted that E_s initially increased rapidly to an optimum value with an increase in volume split; E_s then decreased slowly with a further increase in the split. This was verified by Sheng et al. and Mahajan et al. Burrill et al. noted the same trend; however with the heavy phase dispersed, E_s initially increased slowly with increasing volume split and then dropped off rapidly with a further increase.

Burrill et al. determined that a decrease in droplet size decreased the optimum E_s. He controlled droplet size by varying the head loss through a valve located downstream of the mixing tee.

Regrettably, only Burrill et al. measured and stated interfacial tension for each system studied. In addition, no other research has attempted to control drop size distribution entering the cyclone. Generally mixing of the pure phases occurred at a tee section located upstream of the cyclone inlet. Since no by-pass line was located between the tee section and the cyclone inlet, mixing energy varied according to inlet Reynolds number. According to McDonough et al. (M-3), interfacial area is increased with an increase in pressure drop across the mixing tee. This means that an increase in flowrate decreases the geometric number average droplet size. As a result, drop size distribution entering the cyclone was dependent on the inlet Reynolds number.

Hence inlet Reynolds number and droplet size were not independent variables.

A summary of systems studied and operating conditions is shown in Table II-1.

II-c.4 Separation Efficiency Defined

Efficiency of separation can be defined in a number of ways; yet for liquid/liquid systems the definition that is most applicable is based on the ability of the cyclone to maximize the quantity and quality of the final products with respect to the original mixture. The equation used is as follows:

$$E_s = \frac{Q_o}{Q_f} \left[\frac{Y_o - Y_f}{1 - Y_f}\right] + \frac{Q_u}{Q_f} \left[\frac{Y_f - Y_u}{Y_f}\right] \qquad \text{(II-2)}$$

The above equation can be used to predict the shape of the E_s versus volume split curve, if the interstitial volume and feed concentration are specified. For the purposes of this work, interstitial volume is defined as the volume fraction of water which leaves through the overflow because it is trapped in the gaps between the packed oil droplets. This definition is based on the oil remaining as the dispersed phase despite the change in phase ratio. Volume split is defined as the ratio of the flowrate out the overflow to that out the underflow.

Figure A5-2 is a plot of E_s versus volume split for a given feed concentration and a variable interstitial volume. It can be noted that the curve passes through an optimum E_s for each interstitial volume. With an interstitial volume of 0.30, the optimum volume split is 50% greater than the feed concentration; however if interstitial volume is

Summary of Past Research

Table II-1

Parameter	Researchers			
	Simkin and Olney	Mahajan and Pai	Sheng *et al.*	Burrill and Woods
system(s) studied	(i) kerosene/water (ii) white oil/water	kerosene/water	paraffinic mixture/water	carbon tetrachloride/water
interfacial tension (mN/m)	not measured	not measured	not measured	39
Density difference (gm/cm^3)	(i) 0.20 (ii) 0.16	not measured	0.24	0.58
viscosity of organic phase (c.p.)	(i) 1.4 (ii) 8.9	not measured	not measured	0.9
cyclone shape	cylindrical upper, conical lower.	cylindrical upper, conical lower.	conical	conical
geometric dimensions varied	yes	yes	yes	no

Table II-1 cont'd

Parameter	Researchers			
	Simkin and Olney	Mahajan and Pai	Sheng *et al.*	Burrill and Woods
air core present	yes	yes	yes	no
type of mixing energy	variable	variable	variable	constant
Reynolds number in cyclone	(i) 16000-80000 (ii) 32000-64000	15000-31000	11000-16000	35000
residence time in cyclone (s)	(i) 1.4 - 6.8 (ii) 1.7 - 3.4	cyclone volume not known	0.5 - 0.8	0.7
phase ratio (O/W)	(i) 0.33 - 9.0 (ii) 0.33 - 9.0	1.0	0.5 - 2.0	0.13 - 0.21

assumed to be zero, then the optimum split is equivalent to the feed concentration.

II-d Mechanisms Affecting the Separation Process

The following section is concerned with describing what influences the breakup and coalescence mechanisms inside the cyclone. It also considers how each of these influence droplet movement. Droplets of the dispersed phase may either coalesce to form larger droplets or breakup into smaller ones depending on the magnitude of shear forces in the cyclone. The relative amounts of each liquid phase determines which one is dispersed; the dispersed phased being defined as that phase which is completely surrounded by the other one.

II-d.1 Droplet Breakup

A certain amount of disagreement prevails as to the relative importance of certain forces in promoting breakup. Work by Taylor (T-1), stated that motion of fluid around a droplet generates a stress system which can be resolved into tangential and normal stresses; they act at the drop interface. The tangential component produces velocity gradients within the droplet while the normal component generates a pressure differential across the interface.

Models have been proposed to predict the maximum stable drop size generated in a section of pipe, under specific inertial conditions, for a liquid/liquid system. Stable drop sizes are characterized by the Weber number and they include all sizes less than the critical value necessary for breakup. The critical Weber number, $\frac{d_{MAX}\ \rho_c\ U^2}{\gamma}$ is a dimensionless group, which defines the ratio of inertial to surface forces. The maximum stable drop size is defined as being that size

which, if flowrate is incrementally increased, would breakup. Hinze (H-1) felt that dynamic pressure forces rather than viscous shear forces controlled the breakup process. Sleicher (S-4) maintained, however, that viscous forces within the droplet are important is resisting the stretching caused by the flow field. The two models are shown below:

$$\text{Hinze}: \quad d_{95} = 1.51 \left| \frac{\gamma}{D\,\rho_c\,U^2} \right|^{0.6} R^{0.1}\,D \qquad \text{(II-3)}$$

$$\text{Sleicher}: \quad D_{MAX} = \frac{38 + 26.6 \left(\frac{\mu_d\,U}{\gamma}\right)^{0.7}}{\frac{\rho_c\,U^2}{\gamma} \left(\frac{\mu_c\,U}{\gamma}\right)^{0.5}} \qquad \text{(II-4)}$$

Work by Karabelas (K-1) found better agreement with the Hinze equation for a highly viscous continuous phase (0.15 gm/cm-s), while both equations appeared to be fairly adequate for the lower viscosity continuous phase (0.02 gm/cm-s).

It is not certain how closely the drop size models are in predicting behaviour inside the cyclone. According to Rietema (R-2), turbulent motion does not occur in the cyclone. With pipe flow, turbulent motion occurs above a Reynolds number of roughly 2000. Regardless of the flow regime, the models specify the parameters considered important in predicting droplet breakup.

Mason and Rumscheidt (M-2), photographed various stages of drop breakup in a well defined laminar field with velocity gradients. The dispersed phase formed a long cylindrical chain which changed to regions

of swelling and shrinking due to pressure differentials. Breakup occurred when the thinned down regions reached a point of instability.

Raja Gopal (R-1) determined that due to the statistical nature of the turbulent flow in emulsification a log-normal drop size distribution results. Burrill and Woods (B-3) verified that the dispersion generated through a mixing valve obeyed the log-normal distribution.

II-d.2 Droplet Coalescence

Coalescence of droplets is a thermodynamically spontaneous process while production of a dispersion requires an expenditure of energy. Most dispersions are unstable; after agitation has ceased, individual droplets coalesce. In addition an equilibrium exists between breakup and coalescence even in a system which is being agitated. Shinnar and Church (S-2) noted that coalescence is prevented if the kinetic energy of relative motion between two drops is larger than the energy of adhesion.

Liem and Woods (L-1), used the Parallel Disc Model to predict the time of coalescence for drop/drop and drop/interface contact. Consider the following model:

$$\theta = \frac{\mu \Delta \rho g b^5}{\gamma^2} \left(\frac{1}{h^2} - \frac{1}{h_o^2}\right) \frac{\phi n_G^2}{16} \qquad \text{(II-5)}$$

The value ϕn_G^2 is dependent on the assumptions made. The assumptions are based on whether two approaching droplets circulate or deform during coalescence. The main parameters affecting the time of coalescence are droplet size and interfacial tension. For thick dispersion bands, Allak and Jeffreys (A-1) determined that the time of coalescence varied directly to the droplet size to roughly the third power.

This dependency was less than is noted for the Parallel Disc Model.

It has been noted by Burrill and Woods (B-3) that the hydrocyclone can not yield two pure phases since complete coalescence within the cyclone rarely occurs. They found that coalescence was not significant for the carbon tetrachloride/water system. Some of the continuous light phase was always trapped in the dispersed heavy phase, thereby exiting through the underflow.

While breakup reduces the separation efficiency, coalescence can enhance it by increasing droplet size and reducing interfacial area.

II-d.3 Droplet Movement

The extent of droplet movement in the cyclone will determine how successful the separation process is.

The tangential motion of the liquids generate a centrifugal force which promotes separation. Centrifugal force is defined as follows:

$$F_c = \frac{\pi}{6} D_p^3 \frac{V_\theta^2}{r} (\rho \ell_1 - \rho \ell_2) \qquad \text{(II-6)}$$

Due to the centrifugal force, the dispersed liquid drops acquire a radial velocity with respect to the continuous liquid. This relative motion between the two liquids exerts a drag force on the dispersed liquid. Drag force is defined as follows:

$$F_d = C_D \frac{A_p \rho U^2}{2g} \qquad \text{(II-7)}$$

If we assume that the Stoke's region is approximately correct, then $C_D = 24/\frac{UD}{\gamma}$, such that F_d reduces to:

$$F_d = 3\pi D_p \mu_c U \qquad \text{(II-8)}$$

A droplet under a centrifugal force accelerates until the drag force is equivalent to the centrifugal force, it then falls at a constant velocity known as the terminal velocity (V_∞):

$$V_\infty = \frac{V_\theta^2}{r} \frac{(\rho\ell_1 - \rho\ell_2) D_p^2}{18 \mu_c} \qquad \text{(II-9)}$$

where V_θ = local tangential velocity of the dispersed phase in the cyclone

r = radial position

The tangential velocities have been measured in cyclones by Knowles et al. (K-3), Kelsall (K-2) and Ohasi and Maeda (O-1). An increase in drop diameter, density difference, centrifugal acceleration and a decrease in continuous phase viscosity increases V_∞ and therefore E_s.

Increasing the throughput means that a droplet experiences a greater centrifugal force; however due to the decreased residence time, a droplet may not possess sufficient time to separate from the continuous phase before reaching the apex. A reduction in residence time also decreases the possibility of drop coalescence in the cyclone. An increase in centrifugal force increases all velocity components in the cyclone.

The tangential velocity is probably responsible for most of the drop breakup due to its relatively steep velocity gradient and large magnitude. The radial velocity, which is substantially smaller in magnitude, has only a slight gradient. The axial velocity, which has a significant gradient, is smaller in magnitude than the tangential com-

ponent. Axial fluid movement is in two directions. The loci of zero vertical velocity points separates the upward movement of fluid through the overflow from the downward movement out the underflow. As the volume split is changed, the loci of points shifts either inwards or outwards to accomodate the differing portions leaving each of the outlets. If a light phase droplet is able to reach the region of upward axial velocity before reaching the apex of the cyclone, then separation has been accomplished.

When the concentration of droplets increase, the terminal settling velocity can no longer be predicted by Equation II-9. Equations have been developed which account for the hindered settling velocity in terms of interstitial volume. Consider the following equation, developed by Happel and Brenner (H-1), for a concentrated system:

$$\frac{U}{U_o} = \left(\frac{3 - {}^{9}/_{2}\,\varepsilon + {}^{9}/_{2}\,\varepsilon^5 - 3\,\varepsilon^6}{3 + 2\,\varepsilon^5} \right) \frac{\Delta P}{\Delta P_o} \qquad \text{(II-10)}$$

For sedimentation problems, assume $\Delta P = \Delta P_o$

III EXPERIMENTAL APPROACH

III EXPERIMENTAL APPROACH

III-a Introduction

The apparatus used in this research can be divided into two parts; one deals with hardware and the other, with reagents. The hardware can be subdivided into three components - feed, test and sampling sections. Experimental procedure is divided into two areas of study. The first is concerned with evaluation of separating efficiency; the second deals with droplet size measurement.

III-b Hardware

A description of each of the major sections is considered. A schematic layout is shown in Figure A1-1.

III-b.1 Feed Section

The primary function of the feed section was to provide a similar droplet size distribution, yet a variable flowrate, to the test section. Mutually saturated pure phases were pumped from separate glass containers to calibrated rotameters. The oil and water phases were located in 25 and 50 Imperial gallon vessels, respectively. Rotameters for each phase were calibrated before initiating a series of runs. These calibrations are shown in Figures A1-4 to A1-8.

Pumping pure phases with separate pumps prevented excessive breakup caused by the shearing action of the impellers. It also avoided the problem of calibrating a rotameter for a variable dispersed phase concentration. Mixing of the two phases occurred at a tee section, located past the rotameters.

A Bourdon pressure gauge was situated immediately past the mixing tee. A diversion line, downstream of the gauge, enabled variable flow to the cyclone by providing a by-pass route to the separator tank.

III-b.2 Test Section

The function of the test section was to separate the feed mixture, by centrifugal force, into light and heavy phases.

The hydrocyclone, conical in shape and of glass construction, had geometric dimensions similar to those used by Burrill and Woods (B-3). It was surrounded at the inlet to and outlets from the cyclone by three manometers and optical cells. Gate valves were located at the outlet ends of the cyclone. These valves served two functions. First they provided a wide range of volume splits to study. The valve at the underflow allowed flooding of this outlet, thus preventing the formation of an air core.

III-b.3 Sampling Section

The function of the sampling section was to provide a means of monitoring the effluent from the test section.

Switch valves, located at the overflow and underflow outlet lines, diverted effluent to two 4000 mL Erhlenmeyer flasks. Otherwise, the effluent emptied into a 100 Imperial gallon glass and stainless steel separator ~~tank~~. Valves, located near the bottom of this tank, allowed recycle of the clarified effluent back into the glass vessels.

III-c Reagent Selection and Measurement.

The following discussion describes the basis for selecting reagents and the measurement of certain properties.

III-c.1 Reagent Selection

Reagents were selected primarily on interfacial tension with water. Density difference and oil phase viscosity were comparable for all systems selected. Solvents selected include: butanol, methyl isobutyl ketone (MIBK), toluene and kerosene. With the exception of kerosene, all oil phase liquids were of analytical reagent grade.

III-c.2 Measurement of Some Properties.

Surface and interfacial tension measurements were made on both the oil and water phases with a Fisher 215 Autotensiomat after completion of the experimental runs. Surface tension of distilled water used for the experimental runs ranged from 65 to 70 mN/m. Other surface/interfacial tension measurements are shown in Table A3-2. Conductivity measurements were made on the distilled water samples, collected before starting and after completing a particular system with a Radiometer Copenhagen. Temperature of both phases was measured to be 18 $\pm$ 3°C. throughout the experimental runs.

A complete description of the measurement techniques are given in Appendix A3.

III-d Experimental Procedure

The experimental procedure can be divided into two major sections. One deals with the determination of separation efficiency for the various liquid/liquid systems; the other relates to the droplet size measurement for each of these systems.

III-d.1 Efficiency of Separation Study

After the pumps were started, the globe valves on the rotameters

were opened to supply a total flowrate of 365 mL/s ± 10% at the mixing tee and a particular oil/water ratio. Flowrate to the cyclone was varied by partially closing gate valves at the outlet ends from the cyclone and, or, by opening the gate valve on the diversion line. The outlet valves were also used to control the relative flowrate existing at the overflow and underflow.

Normally a period of 45 to 60 s. was allowed between start-up and sampling. Results showed that steady state was reached well within this time allotment. During this period, pressure readings were noted at each of the four locations.

The collected samples were transferred to graduated cylinders where the relative proportions of light and heavy phase was determined. An equation, proposed by Simkin and Olney (S-3) was employed to determine separation efficiency. The equation was as follows:

$$E_s = \frac{Q_o}{Q_f}\left[\frac{Y_o - Y_f}{1 - Y_f}\right] + \frac{Q_u}{Q_f}\left[\frac{Y_f - Y_u}{Y_f}\right] \qquad \text{(III-1)}$$

A mass balance was performed to determine if flowrate and phase ratio of the collected sample were within 10% of the rotameter settings. If the discrepancy was greater than 10%, the run was disregarded. An exception was made for the minimum flowrate studied, Q_{MIN}, where a deviation of 15% was allowed. This was permitted due to the difficulty encountered in maintaining this low flowrate.

The number of runs performed per day was governed by the amount of pure phase in each vessel. Immediate recycle was not used since the

contents of the separator tank had not completely separated. Recycle of phases to each vessel occurred some hours later or the next day.

A detailed experimental procedure is given in Appendix A1.

III-d.2 Droplet Size Study

An Asahi Pentax camera, complete with extension tube and bellows, was used. An arrangement was constructed which attached the camera to the system pipe work. An electronic flash unit was used to illuminate the optical cell. Photographs were taken at the feed, overflow and underflow optical cells. An effort was made to perform the photographic work at optimum volume split. Samples were taken at the overflow and underflow, while photographs were being taken, to ensure the volume split requirement.

Droplets were counted and sized from print blow-ups with a Zeiss TRG-3 Particle Size Analyzer. The number of droplets counted ranged from 50 to 2,600, depending on photo quality. Droplet sizes, plotted on log-probability paper, are shown in Figures A2-4 to A2-17.

All photographic work was performed at a phase ratio of $(O/W)_{MIN}$ and a feed flowrate of Q_{MIN}. This ensured a reasonable photograph quality.

A complete description of the photographic method is given in Appendix A2.

IV. RESULTS AND DISCUSSION

IV RESULTS AND DISCUSSIONS

IV-a Introduction

An important control variable is the drop size distribution of the emulsion fed to the hydrocyclone. A study of the effect of feed Reynolds number on the separation efficiency was desired; however the drop size distribution is a function of Reynolds number. Two distinct sets of experiments were performed to clarify this problem. With the first method, maximum flow was always fed to the mixing tee to yield a fixed drop size distribution. The feed Reynolds number was controlled by regulating the amount of the dispersion that was allowed to by-pass the cyclone. Consequently, the drop size was controlled independent of the Reynolds number of the cyclone feed. This method was used for most of the data collection in this work because the objective was to independently study the effect of Reynolds number.

In the second method (with no by-pass of the hydrocyclone) changing the Reynolds number to the hydrocyclone also changed the feed drop size distribution. This method has been used exclusively by others, notably Simkin and Olney (S-3) - and was used in this work for the kerosene/water system.

The feed drop size distribution for all systems studied was photographed. As noted in Figures A2-4 to A2-17, distributions were log-normal. Estimates of the maximum and minimum diameters, geometric number average diameter (D_{50}) and the geometric standard deviation are summarized in Table IV-1. Results for both the toluene/water and kerosene/water systems were difficult to obtain with the photographic set-up used in this study.

Droplet Size Distribution for Various Liquid/Liquid Systems Table IV-1

System	Location of Measurement	Number of Droplets Counted	D_{50}	D_{95}	D_{MAX}	D_{MIN}	$\frac{D_{84}}{D_{50}}$
			(microns)				
MIBK/ Water	Feed	550	225	355	470	60	1.31
	Underflow	460	355	660	970	100	1.44
	Overflow	1008	330	530	1010	70	1.33
Butanol/ Water	Feed	703	95	140	175	40	1.26
	Underflow	1686	110	165	255	40	1.27
	Overflow	2638	110	175	350	40	1.32
Toluene/ Water	Feed	105	175	270	395	90	1.29
	Underflow	762	140	195	305	50	1.21
	Overflow	50	140	205	250	90	1.25
Kerosene/ Water	Feed[a]	623	285	570	1255	100	1.51
	Feed[b]	138	360	1385	1980	100	2.06
	Underflow[b]	118	650	1480	1785	210	1.62
	Overflow[b]	47	790	1550	1605	295	1.39

Note: With the exception of the Kerosene/water system mixing energy was at Q_{MAX}

a - mixing energy at Q_{MID}

b - mixing energy at Q_{MIN}

From the theory of Hinze, drop diameters can be predicted. If it is assumed that mixing energy is constant and that the theory applies for D_{50} and not just the maximum size, the diameters will relate as follows:

$$\frac{D_{50_1}}{D_{50_2}} = \left(\frac{\gamma_1}{\gamma_2}\right)^{0.6} \qquad \text{(IV-1)}$$

If the assumption is made that the results of the butanol/water system in Table IV-1 are correct, then it is possible to calculate drop diameters for the same mixing energy and pipe diameter but with a different interfacial tension. Calculated values from Eq. IV-1 are shown in Table IV-2. The agreement is good for the MIBK/water system but is quite poor for toluene/water and kerosene/water. The measured values for these two systems are suspect. D_{50} should be closer to 380 and 480 microns, respectively.

IV-b General Separation Efficiency

Perhaps the simplest way to explore how separation efficiency varies with all the parameters studied is to look initially at how efficiency varies with volume split. Some researchers (B-3), (S-3) have suggested that volume split is the most important of the various operating parameters. Efficiency of separation can be calculated as a function of volume split by using the following equation:

$$E_s = \frac{Q_o}{Q_f}\left[\frac{Y_o - Y_f}{1 - Y_f}\right] + \frac{Q_u}{Q_f}\left[\frac{Y_f - Y_u}{Y_f}\right] \qquad \text{(IV-2)}$$

Droplet Size (D_{50}) as Predicted by the Hinze Equation — Table IV-2

System	D_{50} (Microns)		
	Measured	Calculated based on MIBK/Water	Calculated based on Butanol/Water
Butanol/Water	95	86	-
MIBK/Water	225	-	250
Toluene/Water	175	341	380
Kerosene/Water	285	438	482

In order to use Eq. IV-2 two variables must be specified. The void or interstitial volume fraction in the dispersed phase leaving through either the underflow or overflow must be defined. In addition, the percentage of dispersed phase which can be separated from the continuous phase by centrifugal action must also be specified. For example if centrifugal force is insufficient, one may suggest that only 60 or 70% of the dispersed phase gets separated from the continuous phase.

The calculated E_s versus volume split curve, plotted in Figure IV-1, shows that as volume split is increased from zero, E_s increases until it passes through a maximum. This maximum, assuming complete coalescence of the dispersed phase, or $\varepsilon=0$, occurs at a volume split equivalent to the phase ratio. As the interstitial volume is increased, the intersection of the interstitial and complete separation curve moves to the right. As a result, the optimum E_s decreases with an increase in interstitial volume. A family of curves exist which relate E_s for a given volume split and interstitial volume. At volume splits greater than the optimum value, all curves are co-linear. The co-linear region represents volume splits where a pure heavy phase appears at the underflow. It is assumed that in this situation that the heavy phase is continuous. For example, in Figure IV-1 for an interstitial volume less than or equal to 0.70, a pure heavy phase will appear at the underflow for a volume split greater than or equal to 0.85.

Phase ratio also has an effect on the shape of the E_s versus volume split curve. As noted in Figure IV-2, the higher the phase ratio, the higher the volume split at which optimum E_s occurs. The slope of the curve from the origin to the optimum split varies with change in

Figure IV — 1 E_S versus Volume Split at a Phase Ratio of $(O/W)_{MIN}$ for Various Interstitial Volumes Assuming 100% Centrifugal Acceleration Utilized.

Calculated interstitial volume: (as a fraction)
$\varepsilon = 0.8$; $\varepsilon = 0.7$; $\varepsilon = 0.6$;
$\varepsilon = 0.5$; $\varepsilon = 0.4$; $\varepsilon = 0.3$;
$\varepsilon = 0.15$; $\varepsilon = 0$

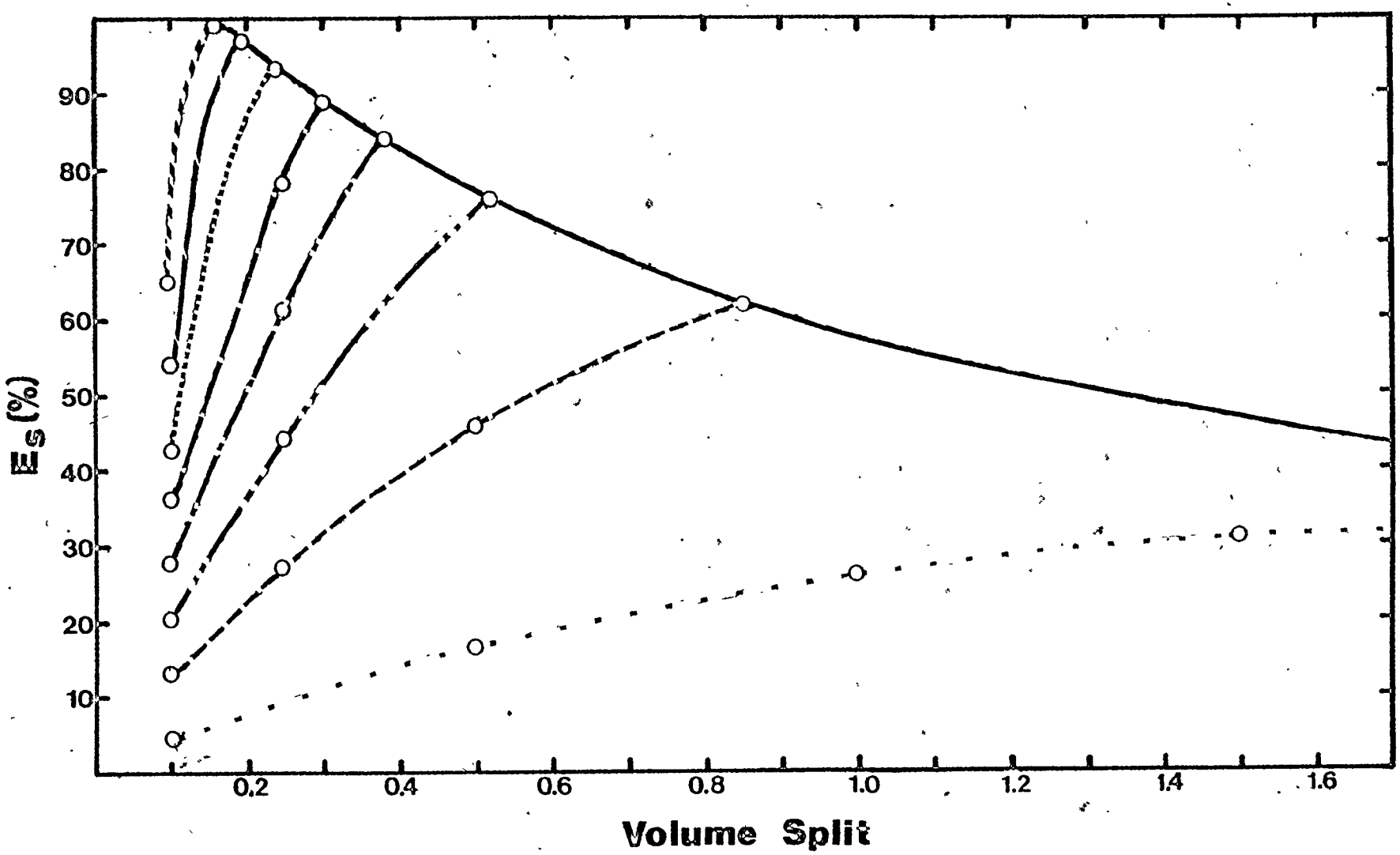

Figure IV — 2 E_s versus Volume Split at an Interstitial Volume $\varepsilon=0$ for Various Phase Ratios Assuming 100% Centrifugal Acceleration Utilized.

Oil/Water phase ratio: $(O/W)_{MIN}$ - - - - - - ; $(O/W)_{MID}$ ——— ; $(O/W)_{MAX}$ - - - - - - .

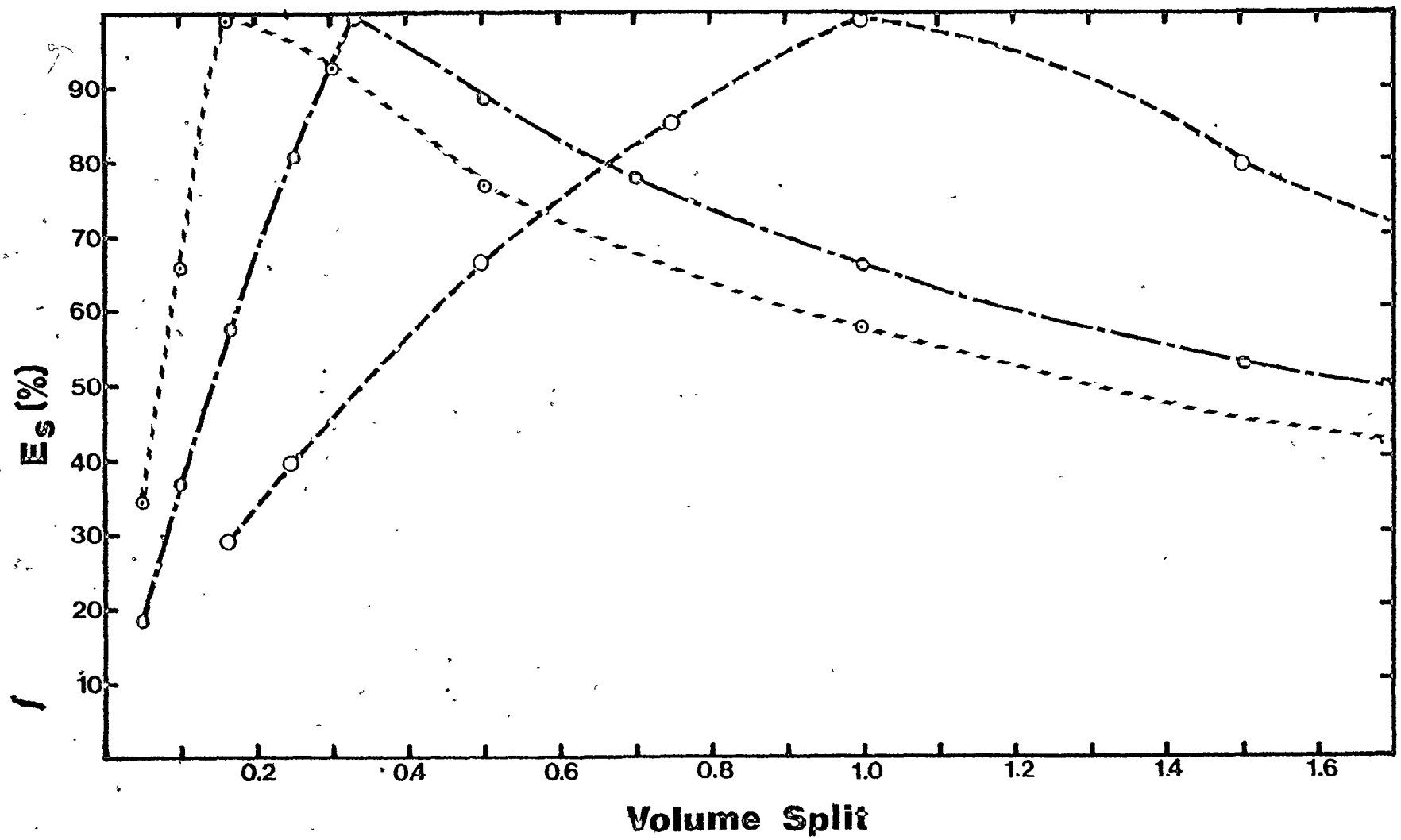

phase ratio. An increase in phase ratio decreases the slope for this portion of the curve.

Centrifugal separation is a measure of the ability, in this research, to produce a pure continuous heavy phase at the underflow. Complete separation, 100%, means that all the dispersion crossed the zero axial velocity loci of points. The interstitial volume reflects the degree of packing or concentrating of the light dispersed phase in the overflow. The lower the interstitial volume, the higher the concentration of dispersed light phase in the overflow.

The theoretical curves mentioned earlier have no significance by themselves. When used in conjunction, however, with the experimental data, an inference can be made regarding what is happening in the cyclone.

Figures IV-3 to IV-11 show the plotted data together with pertinent sections of the theoretical curves. Results from these plots are summarized in Table IV-3. The table suggests that rarely is a dense suspension achieved. For example ε is often greater than 0.6; often centrifugal separation is less than 100%. The figures also show that the curves are sensitive to oil/water phase ratio and inlet feed flowrate. Table IV-4 illustrates how the interstitial volume and centrifugal separation vary with change in operating conditions.

The following observations are noted from Table IV-4. For butanol/water increasing the feed flowrate caused a slight (< 10%) increase in the interstitial volume and a 10% decrease in centrifugal separation. If there is no drop breakup, these effects are opposite to what is noted above. For MIBK/water increasing the feed flowrate

Figure IV — 3 E_s versus Volume Split for Butanol/Water at a Phase Ratio of $(O/W)_{MIN}$ at 20°C, performed at a Feed Flowrate of: Q_{MID} (o); Q_{MAX} (O).

Parameters are: calculated interstitial volume (as a fraction) and the calculated centrifugal acceleration (as a percentage).

calculated interstitial volume: $\varepsilon = 0.8$ - - - - ; $\varepsilon = 0.7$ — — — — ;

calculated centrifugal acceleration: 100% ——— ; 70% — — — ; 60% —·—

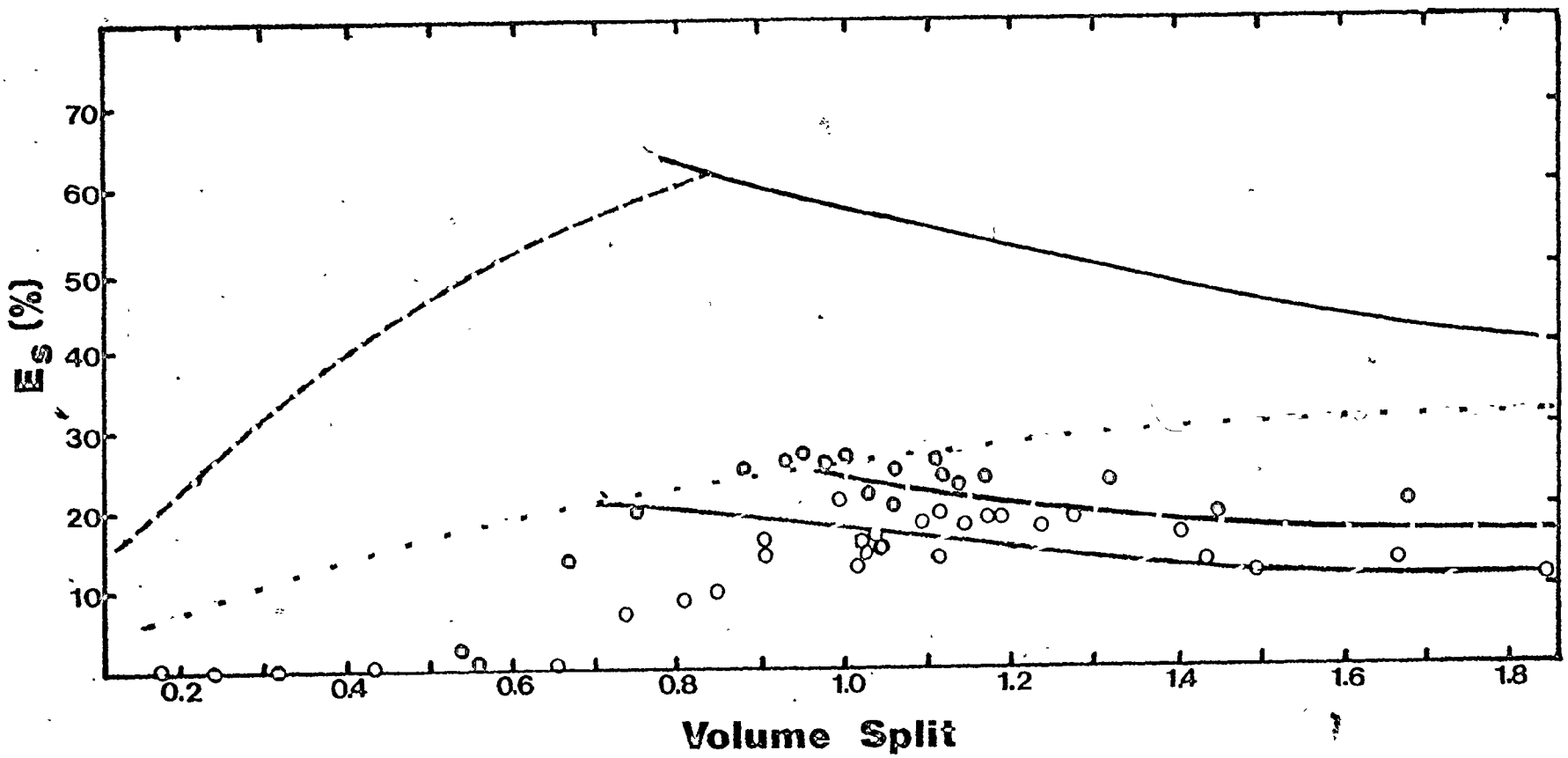

Figure IV — 4 E_s versus Volume Split for Butanol/Water at a Phase Ratio of $(O/W)_{MID}$ at 20°C, performed at a Feed Flowrate of: Q_{MID}(o); Q_{MAX}(o).

Parameters are: calculated interstitial volume (as a fraction) and the calculated centrifugal acceleration (as a percentage).

calculated interstitial volume: $\varepsilon = 0.7$; $\varepsilon = 0.6$;

calculated centrifugal acceleration: 100% ; 60% ; 50%

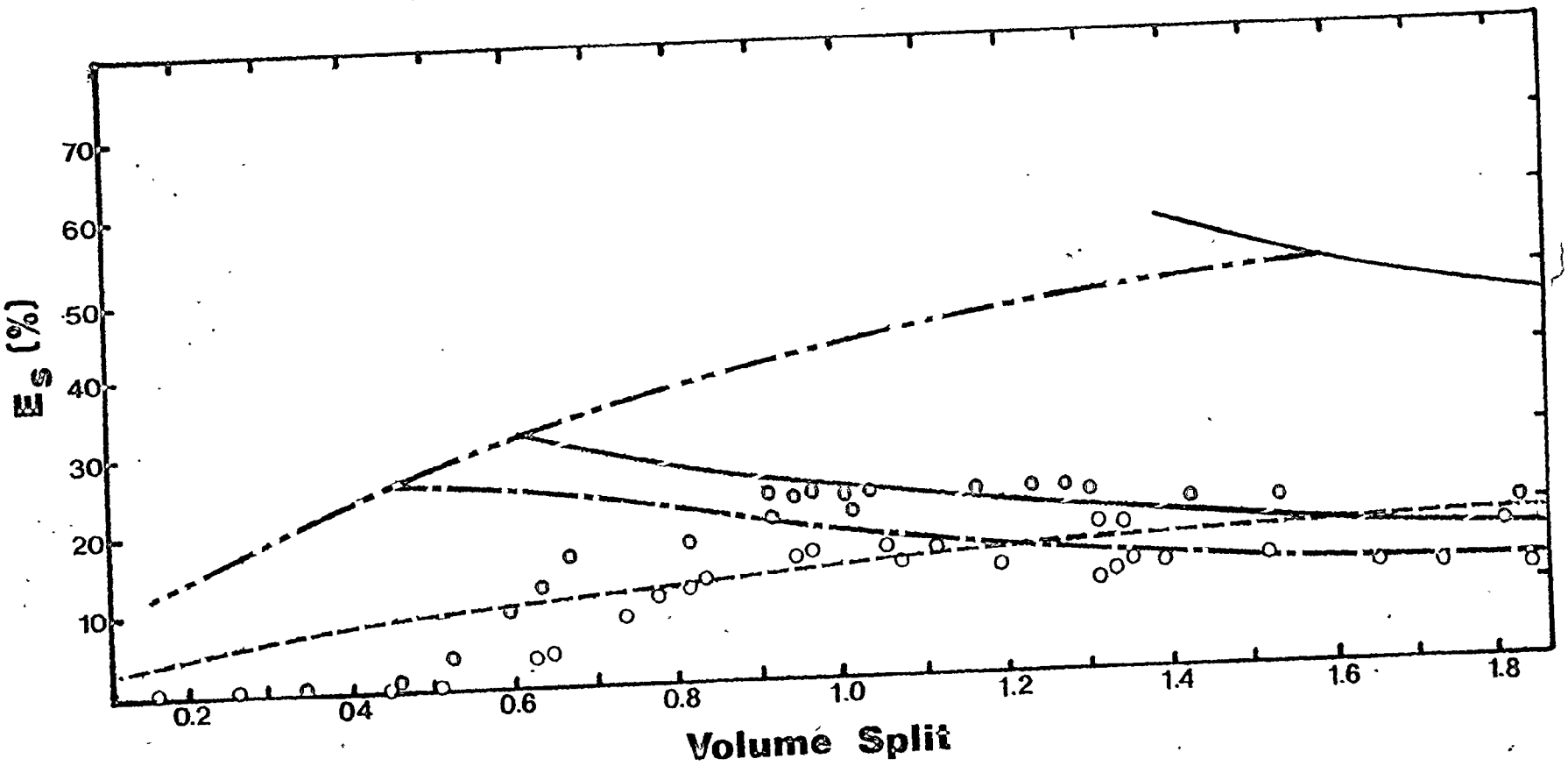

Figure IV — 5 E_s versus Volume Split for MIBK/Water at a Phase Ratio of $(O/W)_{MIN}$ at 20°C, performed at a Feed Flowrate of: Q_{MIN} (⊙); Q_{MID} (⊙); Q_{MAX} (O).

Parameters are: calculated interstitial volume (as a fraction) and the calculated centrifugal acceleration (as a percentage).

calculated interstitial volume: $\varepsilon = 0.8$ - - - ; $\varepsilon = 0.7$ ·—·—·— ; $\varepsilon = 0.6$ - - —— - -

calculated centrifugal acceleration: 100% ——

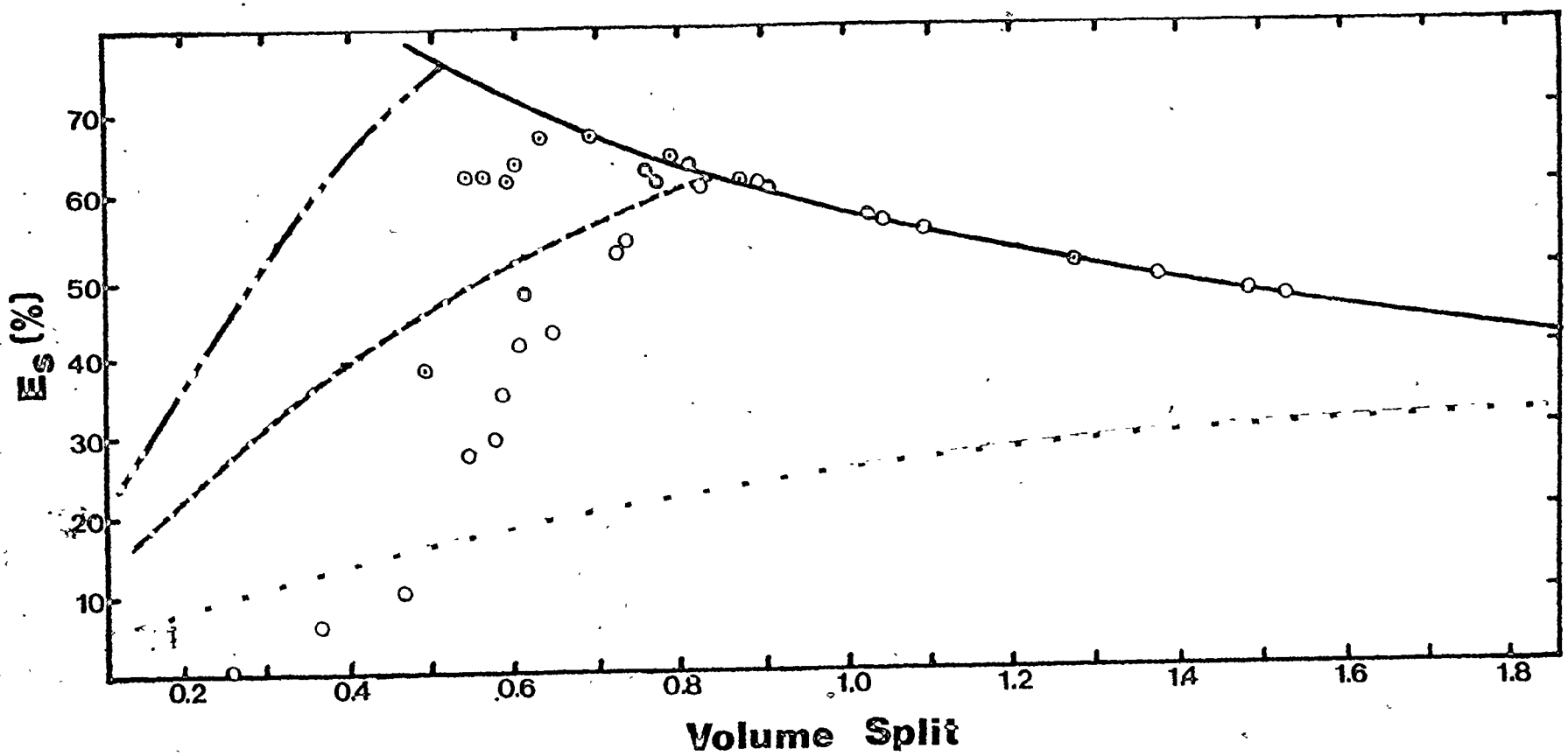

Figure IV — 6 E_s versus Volume Split for MIBK/Water at a Phase Ratio of $(O/W)_{MID}$ at $20^{o}C$, performed at a Feed Flowrate of: Q_{MIN}(⊙); Q_{MAX}(O).

Parameters are: calculated interstitial volume(as a fraction) and the calculated centrifugal acceleration (as a percentage).

calculated interstitial volume: $\varepsilon = 0.7$; $\varepsilon = 0.6$; $\varepsilon = 0.5$;
$\varepsilon = 0.4$.

calculated centrifugal acceleration: 100% .

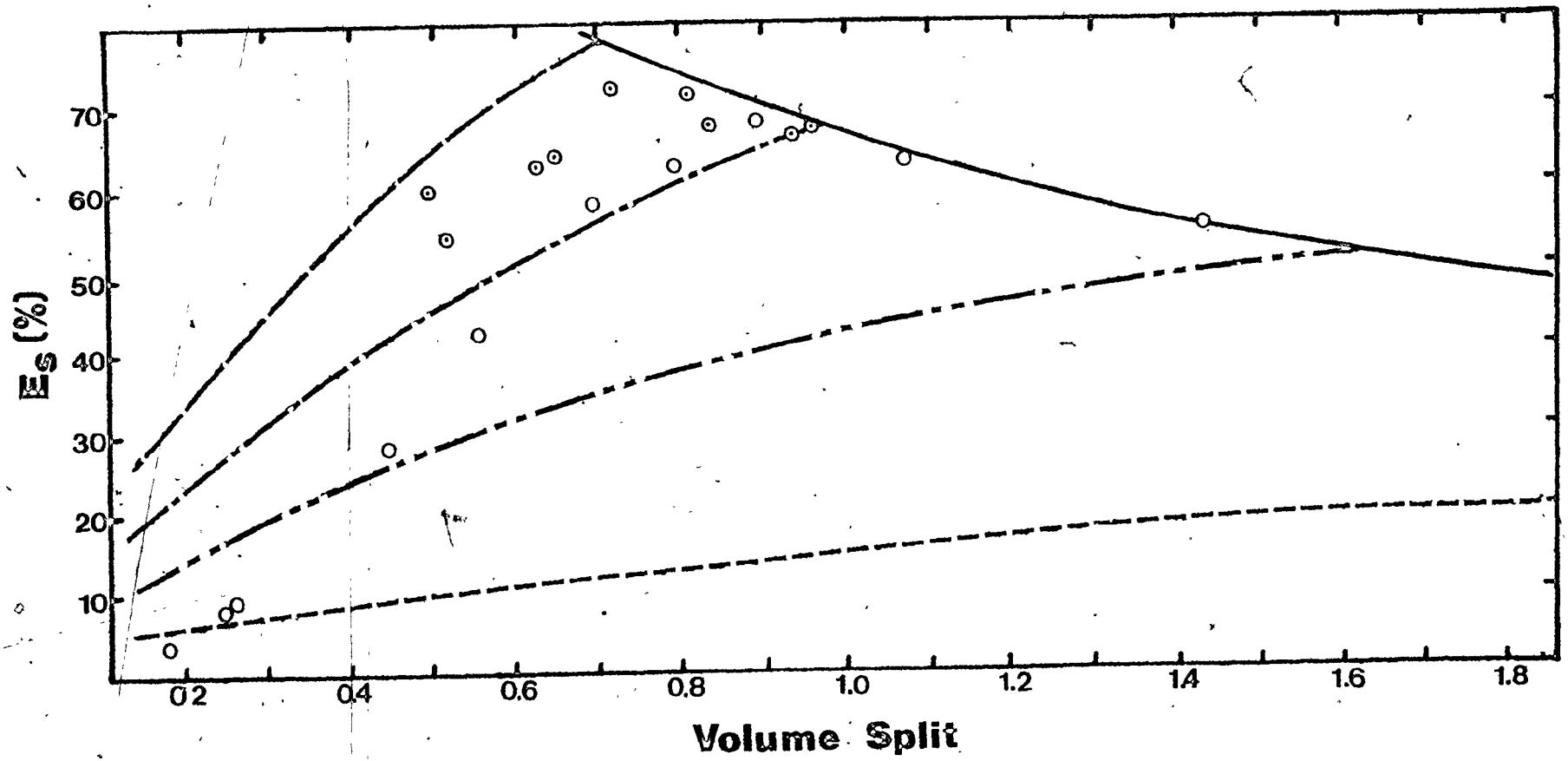

Figure IV — 7 E_s versus Volume Split for Toluene/Water at a Phase Ratio of $(O/W)_{MIN}$ at 20°C, performed at a Feed Flowrate of: Q_{MIN}(⊙); Q_{MAX}(O).

Parameters are: calculated interstitial volume (as a fraction) and the calculated centrifugal acceleration (as a percentage).

calculated interstitial volume: $\varepsilon = 0.8$ - - - - ; $\varepsilon = 0.7$ — — — —

calculated centrifugal acceleration: 100% ———— ; 90% - - - - - - ; 70% — — — —

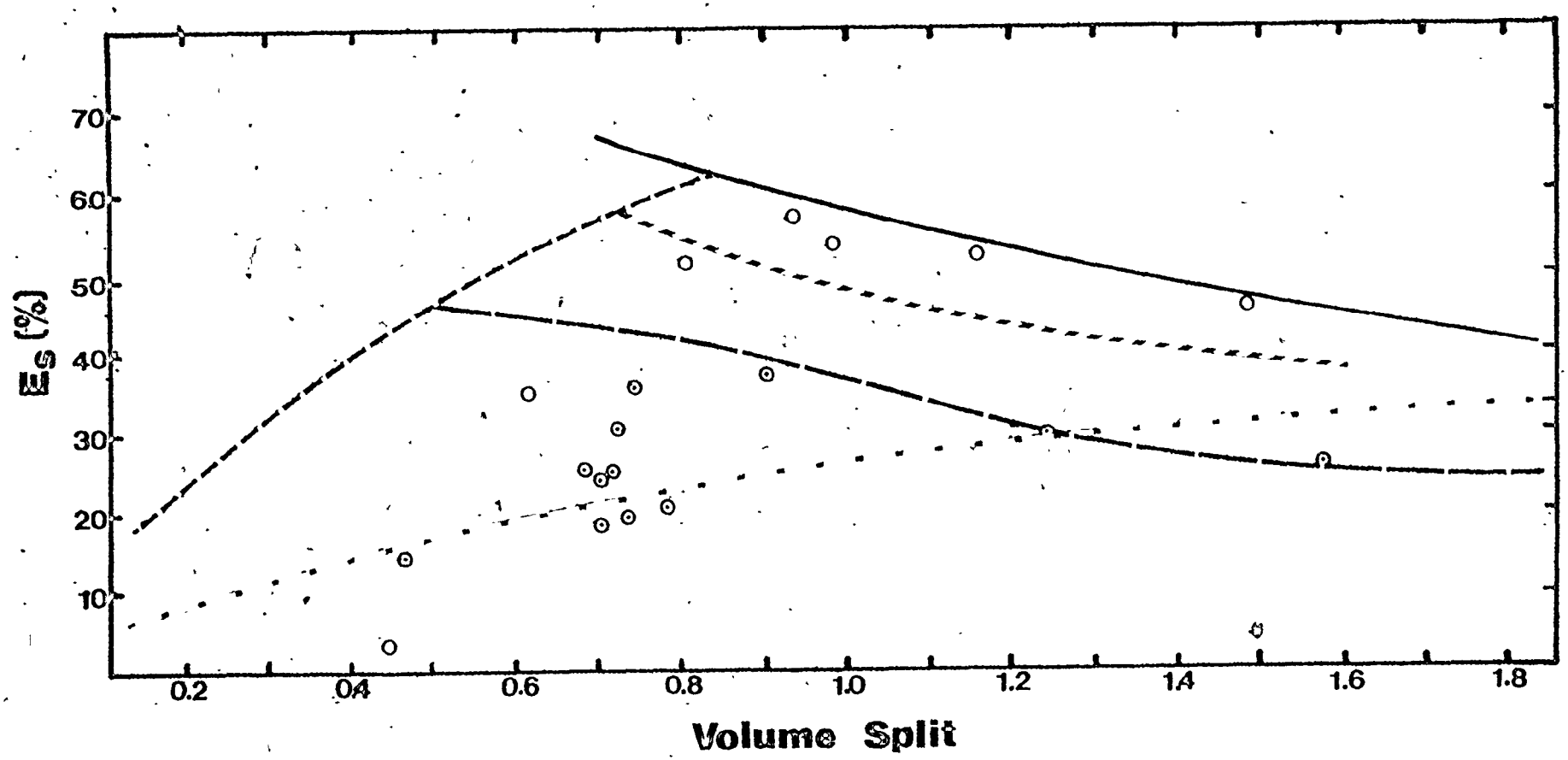

Figure IV — 8 E_s versus Volume Split for Toluene/Water at a Phase Ratio of $(O/W)_{MID}$ at 20°C, performed at a Feed Flowrate of: Q_{MIN}(⊙); Q_{MAX}(O).

Parameters are: calculated interstitial volume (as a fraction) and the calculated centrifugal acceleration (as a percentage).

calculated interstitial volume: $\varepsilon = 0.7$; $\varepsilon = 0.6$; $\varepsilon = 0.5$.

calculated centrifugal acceleration: 100% ; 90% ; 70% .

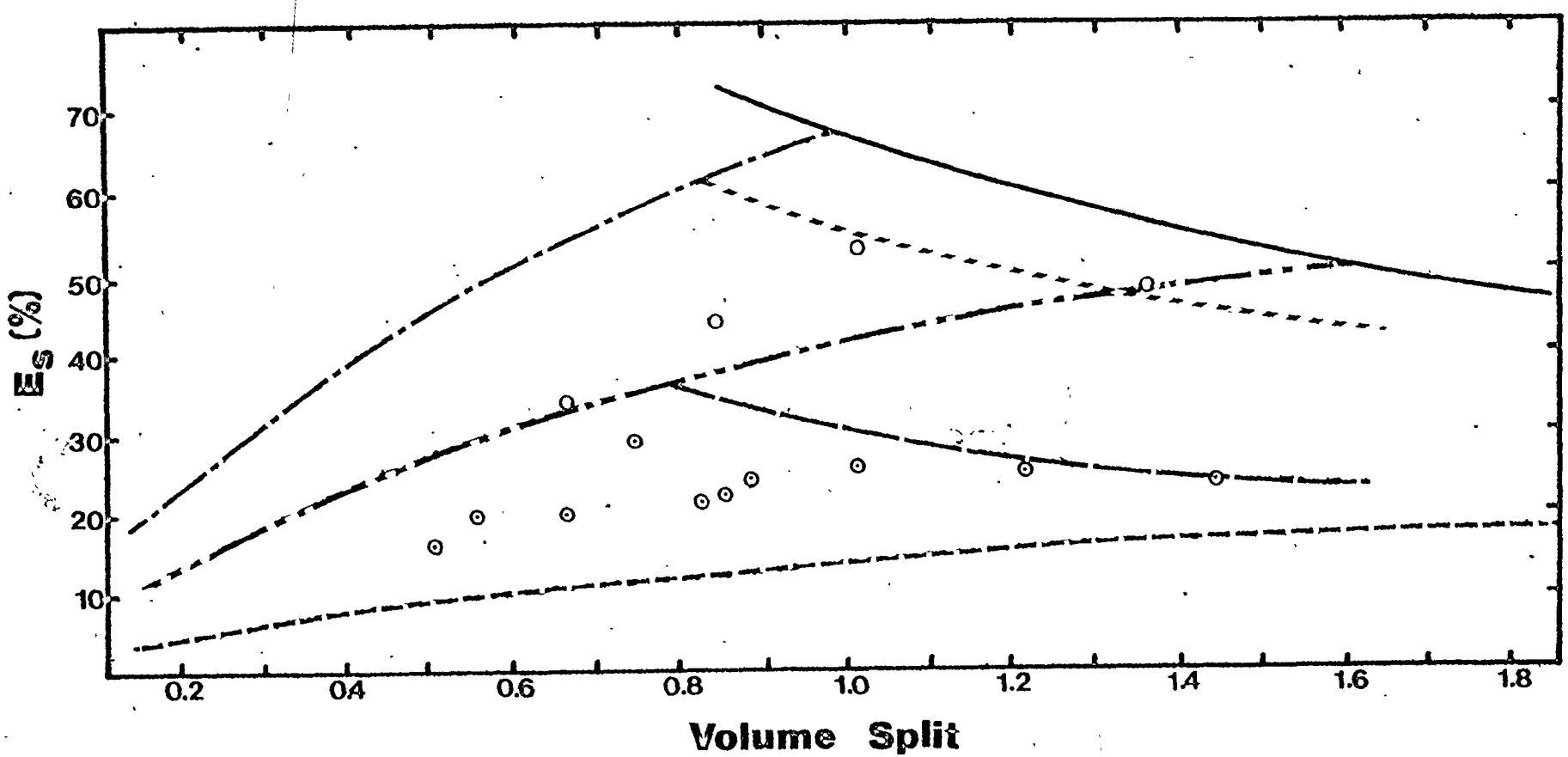

Figure IV — 9 E_s versus Volume Split for Kerosene/Water at a Phase Ratio of $(O/W)_{MIN}$ at 20°C, performed at a Feed Flowrate of: Q_{MIN}(⊙); Q_{MID}(O); Q_{MAX}(O).

Parameters are: calculated interstitial volume (as a fraction) and the calculated centrifugal acceleration (as a percentage).

calculated interstitial volume: $\varepsilon = 0.8$; $\varepsilon = 0.7$

calculated centrifugal acceleration: 100% ; 90% ; 80%

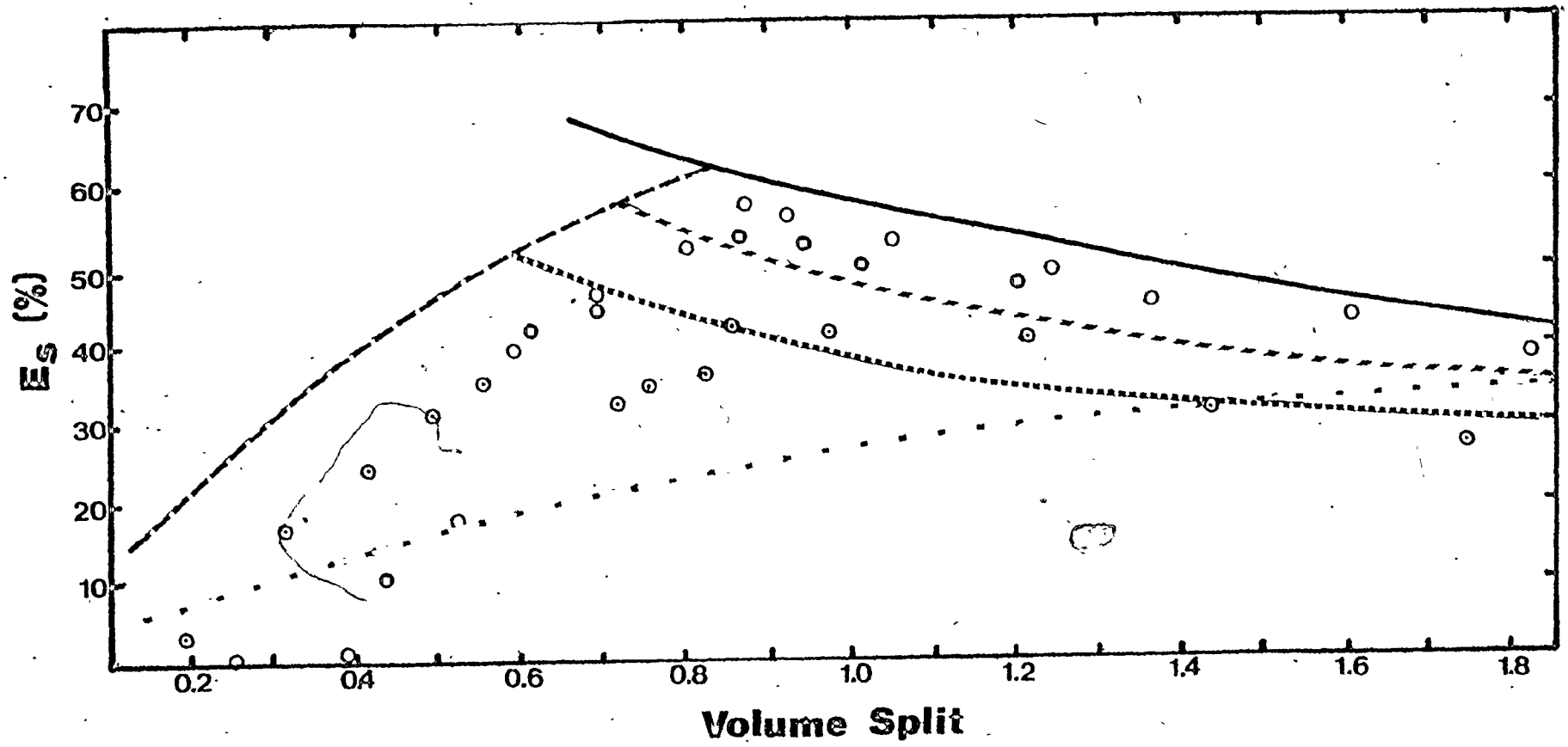

Figure IV — 10 E_s versus Volume Split for Kerosene/Water at a Phase Ratio of $(O/W)_{MID}$ at 20°C, performed at a Feed Flowrate of: Q_{MIN}(⊙); Q_{MID}(⊙); Q_{MAX}(O).

Parameters are: calculated interstitial volume (as a fraction) and the calculated centrifugal acceleration (as a percentage).

calculated interstitial volume: $\varepsilon = 0.7$; $\varepsilon = 0.6$; $\varepsilon = 0.5$

calculated centrifugal acceleration: 100% ; 90% ; 80%

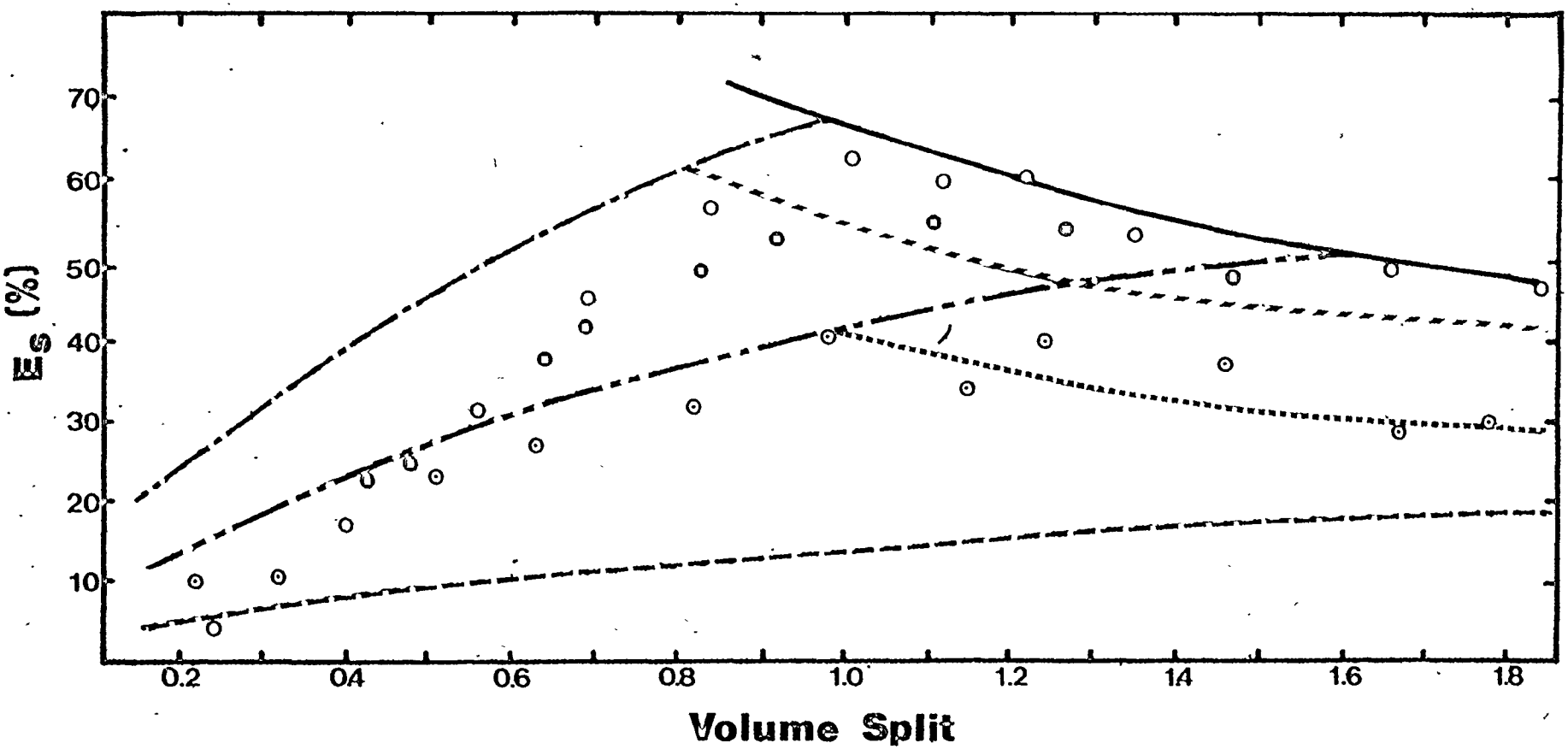

Figure IV — 11 E_s versus Volume Split for Kerosene/Water at a Phase Ratio of $(O/W)_{MAX}$ at 20°C, performed at a Feed Flowrate of: Q_{MIN}(⊙); Q_{MID}(⊙); Q_{MAX}(○).

Parameters are: calculated interstitial volume (as a fraction) and the calculated centrifugal acceleration (as a percentage).

calculated interstitial volume: ε = 0.4 ; ε = 0.3 .

calculated centrifugal acceleration: 100% ; 90% ; 60%

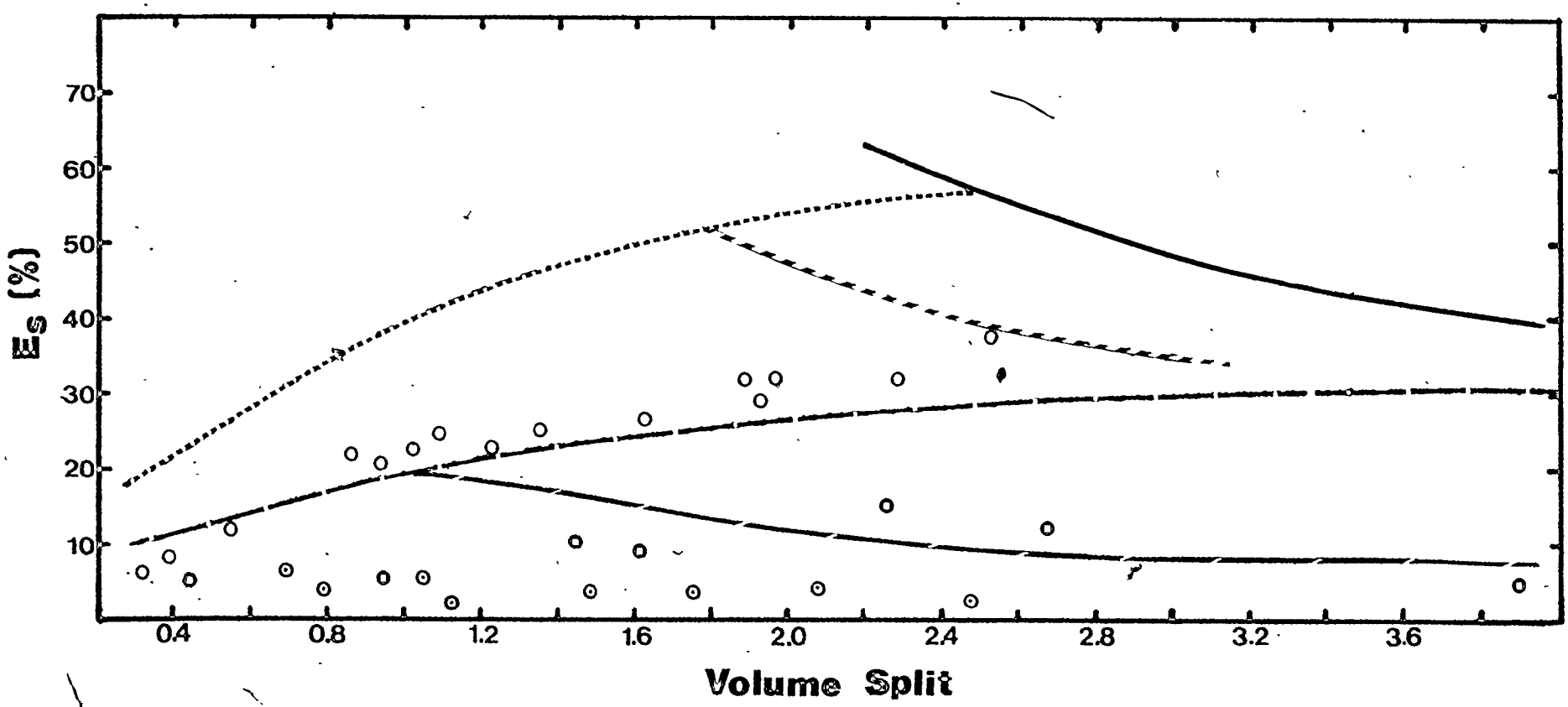

Table IV-3

Summary of Results from E_s versus Volume Split Curves

System	Interstitial Volume Range	Centrifugal Separation Range (%)	Optimum E_s (%)
Butanol/Water	0.67 - 0.81	50 - 70	26
MIBK/Water	0.43 - 0.70	100	73
Toluene/Water	0.56 - 0.77	70 - 95	57
Kerosene/Water	0.37 - 0.75	60 - 100	62

Summary of E_s versus Volume Split Graphs

Table IV-4

System	Conditions (coded)		Centrifugal Acceleration Utilized ±5%	Interstitial Volume at Optimum E_s ±0.01
	O/W	Q		
Butanol/Water	-1	+1	60	0.81
	-1	0	70	0.80
	0	+1	50	0.69
	0	0	60	0.67
MIBK/Water	-1	+1	100	0.70
	-1	0	100	0.69
	-1	-1	100	0.67
	0	-1	100	0.43
Toluene/Water	-1	+1	95	0.72
	-1	-1	70	0.77
	0	+1	90	0.56
	0	-1	70	0.63

Table IV-4 cont'd

Summary	Conditions (coded)		Centrifugal Acceleration Utilized ±5%	Interstitial Volume at Optimum E_s ±0.01
	O/W	Q		
Kerosene/ Water	-1	+1	95	0.72
	-1	0	90	0.73
	-1	-1	80	0.75
	0	+1	100	0.52
	0	0	95	0.56
	0	-1	80	0.60
	+1	+1	90	0.37
	+1	0	60	0.44
	+1	-1	20	-
*	-1	0	95	0.69
*	-1	-1	95	0.64
*	0	0	100	0.47
*	0	-1	100	0.37
*	+1	0	95	0.25
*	+1	+1	100	0.18

*variable mixing energy method.

increased the interstitial volume slightly; the centrifugal separation was not affected. Both these effects suggest that the dispersion was breaking up and yielding a looser central dispersion with an increase in feed flowrate. This is expected with lower interfacial tension systems. For both kerosene/water and toluene/water systems, increasing the feed flowrate decreased the interstitial volume by 5 to 35% and 5 to 10% respectively and increased the centrifugal separation by 5 to 40% and 20 to 30%, respectively.

By visual observation it is possible to roughly determine whether or not complete centrifugal separation in the cyclone was occurring. Complete separation was marked by a clear region in the outer portion of the cyclone interior that surrounded a milky core. With less than complete centrifugal separation, a milky appearance was noted across the entire cross-section of the cyclone interior.

Breakup in the cyclone for butanol/water was sufficiently large to prevent complete separation of the two phases. For MIBK/water, despite the tendency for greater breakup with increasing feed flowrate, complete separation was achieved. Breakup was sufficiently small that complete separation was still possible. For toluene/water and kerosene/water less than complete separation was achieved at the lower feed flowrates. Only with an increase in flowrate was sufficient centrifugal force developed to separate the two phases.

From Figure IV-1 simple calculations from Eq. IV-2 show that, for a given phase ratio and volume split, increasing the optimum E_s corresponds with a decrease in interstitial volume for the overflow sample and an increase in % centrifugal separation. From Table IV-4,

based on the above trends, it is possible to determine which set of operating conditions yield the optimum E_s for each liquid/liquid system. For each phase ratio studied, an increase in % centrifugal separation is associated with a decrease in interstitial volume. For MIBK/water, with complete separation of the phases inside the cyclone, under all conditions, interstitial volume decreased with decreasing feed flowrate. To increase the optimum E_s with decreasing flowrate, optimum volume split was decreased. This was necessary in order to take full advantage of the denser packing of the dispersed light phase.

Burrill and Woods (B-3) noted that a pure continuous light phase was achieved at the overflow for the $CC\ell_4$/water system. The interstitial volume in the underflow at optimum volume split equalled 0.28. For the present work, a value of 0.70 was noted for MIBK/water under comparable conditions, although in Burrill's et al. work the dispersed phase went out the underflow. While both systems accomplished separation of pure continuous phases within the cyclone, settling velocity of the droplets varied substantially. With the higher interfacial tension and density difference, settling velocity was significantly higher for $CC\ell_4$/water. Consequently for the same residence time, these droplets travel further. This produces a tighter packing of the dispersed phase, with the result that the interstitial volume was much lower. This was reflected in the optimum E_s for each system, 94 and 61% for $CC\ell_4$/water and MIBK/water, respectively. For the former system, the dispersed phase was the heavier of the two phases. As a result, the plot of E_s versus volume split for different interstitial volumes is a mirror image of that for the latter system. As opposed to the case where the light phase is dispersed, the

complete separation curve lies to the left of the optimum splits, for different interstitial volumes.

If complete coalescence occurs in the cyclone, the optimum E_s equivalent to 100% can be achieved at a volume split equal to the phase ratio. Optimum volume split for all liquid/liquid systems studied was located to the right of the complete coalescence value. With increasing interstitial volume in the overflow sample, an increase in optimum split was combined with a decrease in the optimum E_s. An optimum split, greater than that which corresponds to the complete coalescence value, suggests that the light phase was dispersed throughout the present work.

With an increase in the phase ratio, the tendency for dispersed phase reversal is greater. Phase reversal was noted in the work by Sheng et al. (S-1) and Simkin and Olney (S-3). For example, Simkin et al. found that at an oil/water phase ratio of 3/1 and 9/1, the optimum split occurred at roughly 2/1 and 6/1, respectively, for a kerosene/water system. This meant that the optimum E_s was located to the left of the phase ratio, whereas without phase inversion, the optimum split was to the right of it.

IV-b.1 Summary

The overflow/underflow ratio or volume split is the most important parameter affecting the efficiency of separation. Depending on the volume split, E_s varies from zero to an optimum value. The optimum value varied from 26 to 73% for the liquid/liquid systems studied in this work. If it is assumed that complete coalescence does not occur and that the light phase remains dispersed throughout the study, then the optimum volume split is greater than the oil/water phase ratio. Reduction in

interstitial volume or tighter packing of the dispersed phase decreases the optimum split and increases the optimum E_s. Whenever complete centrifugal separation is achieved inside the cyclone, it is possible to obtain a pure continuous phase at volume splits greater than the optimum value.

IV-c The Effect of Feed Flowrate on the Optimum E_s

Two opposite effects occurred, depending on the liquid/liquid system studied. For lower interfacial tensions, less than or equal to 10 mN/m, increasing the feed flowrate caused a decrease in the optimum E_s. For higher interfacial tension systems, greater than or equal to 20 mN/m, increasing the flowrate caused an increase in the optimum E_s.

IV-c.1 An Explanation of the Feed Flowrate Effect

The apparently contradictory results can be explained if three theoretical ideas are explored. Consider these ideas as follows:

a) The movement of droplets radially inwards in the centrifugal field can be approximated by Stoke's Law:

$$V_\infty \propto \left(\frac{\Delta\rho\ D_{50}^2}{\mu}\right)\frac{V_\theta^2}{r} \qquad \text{(IV-3)}$$

The geometric number average diameter is summarized in Table IV-1. The tangential velocity component inside the cyclone is shown in Figure IV-12 based on work of Knowles et al. (K-3).

b) The droplets may coalesce inside the cyclone as suggested from the data in Table IV-1 for all systems but toluene/water. The time for coalescence to occur can be approximated by a modified version of the Parallel Disc Model:

Tangential Velocity Profiles in a Hydrocyclone

Figure IV — 12

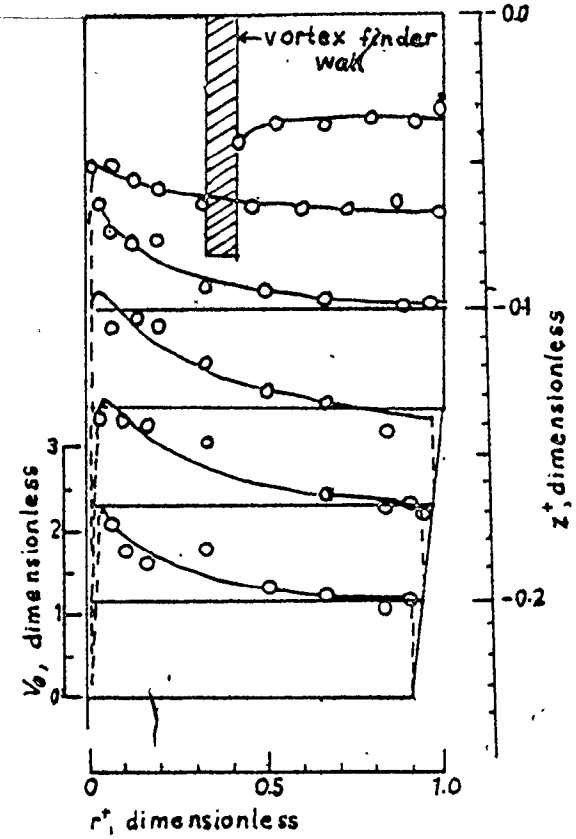

Note: o indicates data from view A

The Effect of a Velocity Gradient on an Oil Drop

Figure IV — 13

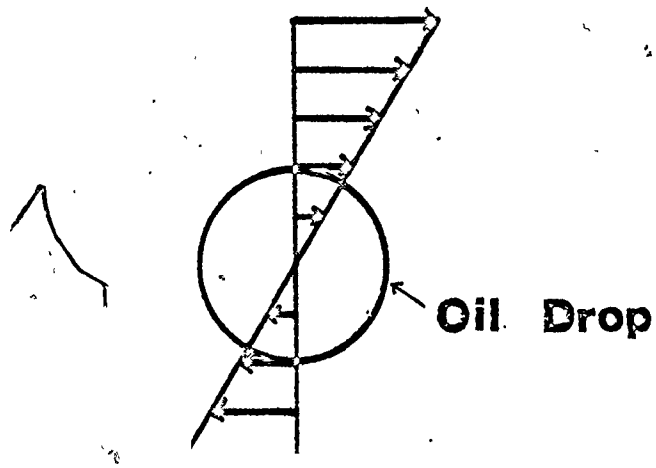

$$\theta \alpha \frac{\mu \Delta \rho g b^2}{\gamma^2} \left(\frac{1}{h^2}\right) \qquad \text{(IV-4)}$$

c) The droplets may breakup because of the velocity gradients as shown in Figure IV-13. The breakup inside the cyclone can be approximated by the Hinze equation:

$$d_{95} \alpha \left(\frac{\gamma}{D\rho_c U^2}\right)^{0.6} R^{0.1} D \qquad \text{(IV-5)}$$

These principles are now used to interpret the data.

From Table IV-5 the relative decrease in the optimum E_s for a 100% increase in feed flowrate was roughly 20% for butanol/water and 2 to 6% for MIBK/water. Hinze (H-2) and Sleicher (S-4) correlated the maximum stable droplet size that can exist in a pipe in terms of the Weber and the Reynolds numbers. Eq. IV-5 verifies that an increase in flowrate reduces the maximum stable droplet size. The relative decrease was less for MIBK/water because its higher interfacial tension afforded greater resistance to the inertial force which promotes breakup. Regardless, breakup predominates for these two systems. As a result, the optimum E_s decreases since the effect of decreased droplet size is more significant than the effect of increased centrifugal acceleration.

A relative increase in the optimum E_s, for a 100% increase in feed flowrate, ranged from 18 to 27% and 9 to 33% for toluene/water and kerosene/water, respectively. This increase is probably due to an increase in droplet size and, or, to an increase in centrifugal acceleration. An increase in droplet size suggests that the rate of coalescence

The Effect of Flowrate on Optimum E_s Table IV-5

System	Interfacial Tension (mN/m)	Phase Ratio (coded)	Flowrate From (coded)	Flowrate To (coded)	% Increase in Flowrate	% Increase in E_s
Butanol/ Water	2	-1	0	+1	89 (100)	- 19 (-21)
		0	0	+1	85 (100)	- 19 (-22)
MIBK/ Water	10	-1	-1	0	86 (100)	- 4 (-5)
		-1	0	+1	91 (100)	- 5 (-6)
		0	-1	+1	268 (100)	- 6 (-2)
Toluene/ Water	20	-1	-1	+1	286 (100)	+ 55 (+18)
		0	-1	+1	311 (100)	+ 80 (+27)
Kerosene/ Water	30	-1	-1	0	100	25
		-1	0	+1	84 (100)	+ 8 (+9)
		0	-1	0	104 (100)	+ 35 (+33)
		0	0	+1	86 (100)	+ 13 (+18)
		+1	-1	0	100	+120
		+1	0	+1	83 (100)	+138 (+166)
		* -1	-1	0	105 (100)	- 11 (-10)
		* 0	-1	0	100	- 12
		* +1	-1	0	95 (100)	- 11 (-12)

* variable mixing energy

predominates over that for breakup, if indeed, breakup does occur. Higher values of interfacial tension for these two systems help to increase the rate of coalescence as shown in Eq. IV-4. An increase in centrifugal acceleration, via a higher feed flowrate and tangential velocity, increases the centrifugal force with respect to the drag force. To benefit from an increase in the centrifugal force, the droplet must have a surface force which is strong enough to resist or minimize breakup due to an increase in the inertial force. Otherwise any increase in separation efficiency realized by an increase in centrifugal acceleration is negated by a decrease in droplet size. It is possible that breakup may occur for these systems; however the increase in centrifugal force must compensate for the breakup in order to still get an overall increase in the optimum E_s. If the droplets behave like solid particles, that is, they do not breakup with an increase in shear stress, then it is certain that an increase in the optimum E_s can be achieved. Van Kooy (V-1) noted that for a solid/liquid system, the optimum E_s increased with increasing Reynolds number over a specified range. Hsiang and Woods (H-4) verified this result. In terms of kerosene/water and toluene/water, the interfacial tension appears to be sufficiently large to resist significant breakup over the range of flowrates studied. Breakup for a particular drop size occurs only after its critical Weber number has been exceeded. Beyond the critical value, the effect of flowrate on the optimum E_s is similar to that for the butanol/water and MIBK/water systems.

These results can be conveniently summarized by plotting the relative change in separation efficiency against the interfacial tension, as is done in Figure IV-14.

Figure IV — 14 Relative Change in E_s versus Interfacial Tension for all Liquid/Liquid Systems Studied at a Phase Ratio of: $(O/W)_{MIN}$ (o); $(O/W)_{MID}$ (o).

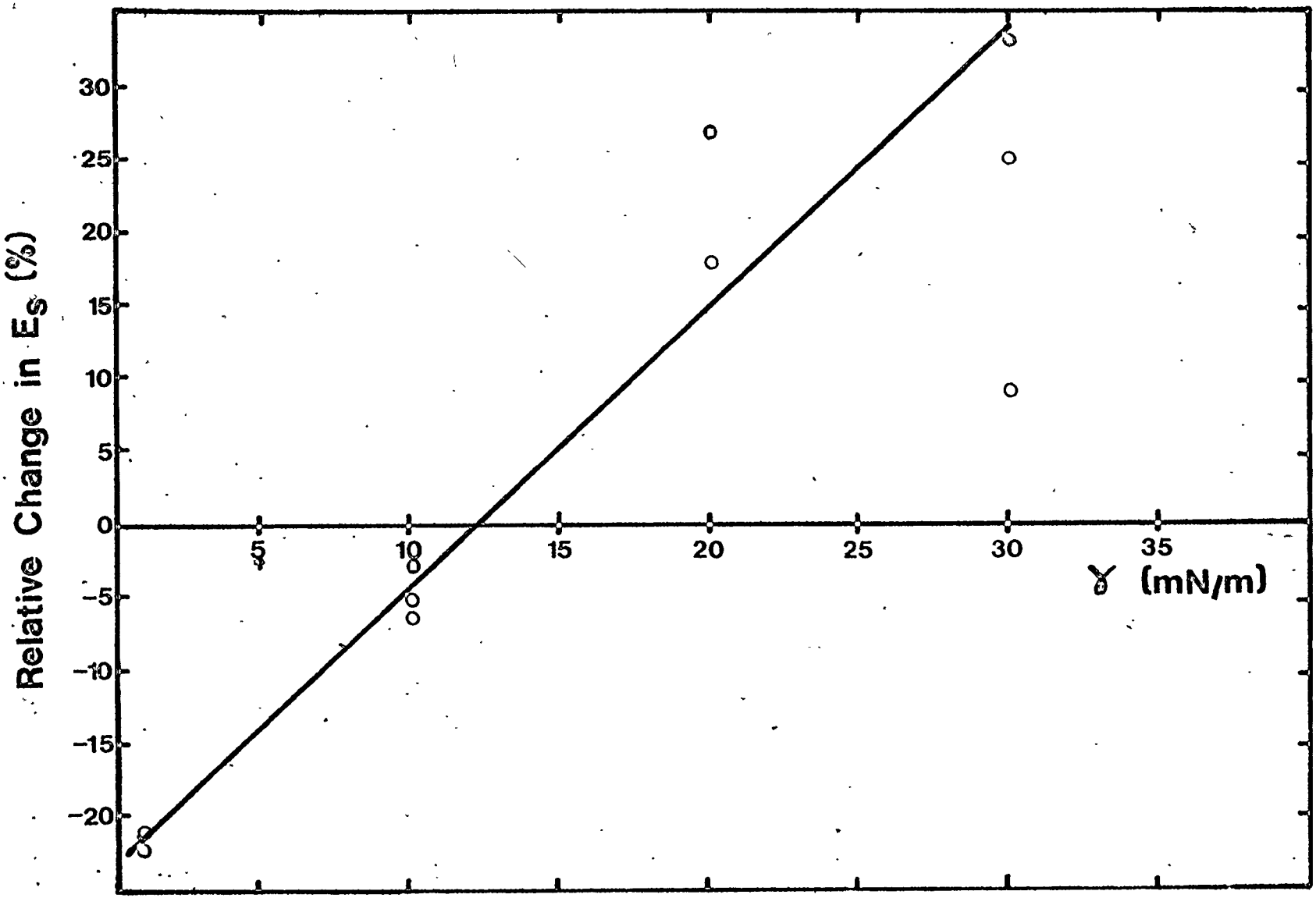

IV-c.2 The Influence of Phase Ratio on the Feed Flowrate Effect.

Figure IV-14 may be used to clarify the influence of phase ratio on the flowrate effect.

For liquid/liquid systems such as butanol/water and MIBK/water very little variation in the relative change in the optimum E_s is noted. For both these systems, the action of droplet breakup predominates over that of droplet coalescence. Consider the butanol/water system. Despite an increase in the phase ratio from $(O/W)_{MIN}$ to $(O/W)_{MID}$, relative decrease in the optimum E_s was 21 and 22%, respectively, for the same increase in flowrate.

For the kerosene/water and toluene/water systems, scatter of the data is more significant. For the same phase ratios as quoted in the previous paragraph, relative increase in the optimum E_s was 9 to 33% for the former and 18 to 27% for the latter system.

With the same increase in flowrate, the relative increase in the optimum E_s becomes larger with a higher value of phase ratio. This was noted for toluene/water and kerosene/water. This does not necessarily mean, however, that the optimum E_s increases with an associated increase in phase ratio.

IV-c.3 The Influence of Flowrate Magnitude on Flowrate Effect.

Data from the kerosene/water system provided the only information available for the study of this influence. For example a relative increase in the optimum E_s varied from 25% for a flowrate change in the range Q_{MIN} to Q_{MID} and 9% for the range Q_{MID} to Q_{MAX} at $(O/W)_{MIN}$. A similar trend was noted at $(O/W)_{MID}$. At $(O/W)_{MAX}$, however, the above trend is reversed.

A decrease in relative change of the optimum E_s with increasing feed flowrate for $(O/W)_{MIN}$ and $(O/W)_{MID}$ suggests that the maximum E_s for the system may soon be reached. An increase, as shown by $(O/W)_{MAX}$, suggests that the maximum value for the system is somewhat further away.

IV-c.4 Droplet Breakup Inside the Hydrocyclone

Droplet breakup inside the cyclone predominates for the butanol/water and MIBK/water systems with an increase in feed flowrate. It is important to understand the mechanism which promotes this breakup.

Rietema (R-2) showed that turbulent diffusion within the cyclone is non-existent. Drop size generated at the mixing tee is not likely to change significantly before it enters the cyclone because the turbulent energy remains the same (or decreases). The Reynolds number calculated immediately past the mixing tee, is roughly 40,000, well within the turbulent flow region. Turbulence, while inhibiting further droplet breakup, also prevents the possibility of droplet coalescence. Since droplet breakup does occur for the above mentioned systems, it is most likely to happen inside the cyclone itself. Any reduction in the optimum E_s must therefore be due to breakup inside the cyclone.

This breakup of droplets is due to the large magnitude and sharp gradient of the tangential velocity component. The large shear force cause stress to act on the droplet. The shear force may also be caused by other velocity components inside the cyclone; however Lilge (L-2) stated that these components were insignificant compared to the tangential velocity.

IV-c.5 Summary

The effect of feed flowrate on the optimum E_s is dependent on the interfacial tension. For toluene/water and kerosene/water, the magnitude of phase ratio influences the feed flowrate effect. Droplet breakup in the cyclone is largely due to the tangential velocity component. Liquid/liquid systems with a higher interfacial tension exhibit a greater resistance to breakup action.

IV-d The Effect of Phase Ratio on the Optimum E_s.

An increase in phase ratio can either decrease, increase or have no significant effect on the optimum E_s. For the toluene/water and butanol/water systems an increase in phase ratio decreases the optimum E_s. For the MIBK/water system an increase in phase ratio increases the optimum E_s. No clear effect is noted for the kerosene/water system.

From Table IV-6, the following results were noted. For butanol/water and toluene/water, a 100% increase in phase ratio resulted in a relative decrease in the optimum E_s from about 10%, and 8 to 22%, respectively. For MIBK/water, a relative increase of about 10% was noted; kerosene/water ranged from a decrease of 4% to an increase of 8%. A certain amount of the increase or decrease may be attributed to experimental error since it is difficult to know for certain whether the calculation of relative change is always based on the optimum values. How much the error masks the phase ratio effect is uncertain. It is certain, however, that the phase ratio has an effect on the optimum E_s. With the exception of the kerosene/water system, the effect of phase ratio is consistent within each system despite different flowrates studied.

The Effect of Phase Ratio on Optimum E_s Table IV-6

System	Flowrate (coded)	Phase Ratio From (coded)	Phase Ratio To (coded)	% Increase in Phase Ratio	% Increase in Optimum E_s
Butanol/ Water	0	-1	0	100	-10
	+1	-1	0	100	- 9
MIBK/ Water	-1	-1	0	100	+ 9
	+1	-1	0	110 (100)	+11 (+11)
Toluene/ Water	-1	-1	0	95 (100)	-21 (-22)
	+1	-1	0	95 (100)	- 8 (-8)
Kerosene/ Water	-1	-1	0	110 (100)	- 4 (-4)
	-1	0	+1	215 (100)	-80 (-40)
	0	-1	0	105 (100)	+ 2 (+2)
	0	0	+1	200 (100)	-70 (-35)
	+1	-1	0	105 (100)	+ 8 (+8)
	+1	0	+1	205 (100)	-38 (-19)
	* -1	-1	0	100	+13
	* -1	0	+1	210 (100)	- 4 (-2)
	* 0	-1	0	110 (100)	+12 (+11)
	* 0	0	+1	200 (100)	- 3 (-2)

* variable mixing energy.

For the kerosene/water system alone, a phase ratio of $(O/W)_{MAX}$ was run. As opposed to lower phase ratio runs studied for each system, the relative change in the optimum E_s is significantly higher. The difference becomes progressively less, however, as the feed flowrate increased. For example, the relative change in the optimum E_s decreased from 40 to 19% with increasing flowrate.

IV-d.1 An Explanation of the Phase Ratio Effect.

The phase ratio effect on the optimum E_s is dictated by two competing effects, that being, droplet coalescence and hindered settling. For conditions where centrifugal acceleration and volume split is constant, the only means by which the optimum E_s is increased is by increasing the droplet size. Droplet coalescence increases the droplet size and because of this, the drops can migrate more rapidly. It also reduces the interfacial area. This means that the interstitial volume is increased, thereby reducing the effect of hindered settling. Hindered settling decreases the optimum E_s since the sedimentation velocity is reduced.

The Parallel Disc Model (L-1) was used to predict the rate of coalescence for each of the liquid/liquid systems studied. Based on the coalescence study for butanol/water and MIBK/water, this model compared favourably if modified such that coalescence time varied to the droplet size to the second power. The modified model is shown in Eq. IV-4. The model predicted that the highest rate of coalescence was for kerosene/water and toluene/water, followed by MIBK/water and butanol/water in that order. If this order is correct then toluene/water should have behaved similarly to kerosene/water or MIBK/water in terms of the effect of phase ratio on the optimum E_s. Instead toluene/water shows a trend similar to

butanol/water. According to the model a decrease in separation distance brought about by an increase in phase ratio can decrease the time for coalescence. This, however, is not very significant. For example, a decrease in the separation distance of 100% can decrease the coalescence time by less than 1%. From Table IV-1, coalescence seems to have occurred for all but the toluene/water (based on the drop size data alone) for the minimum phase ratio of $(O/W)_{MIN}$. Coalescence could occur in the cyclone itself or in the overflow tube between the cyclone and the optical cell. If coalescence occurs only in the overflow tube, then the optimum E_s is not affected. For example butanol/water showed an increase in the D_{50} size from 95 to 110 microns at the feed and overflow, respectively. Since the optimum E_s decreased with an increase in phase ratio for this system, coalescence had no beneficial effect and the hindered settling effect must have dominated. The toluene/water system showed a trend similar to butanol/water. The D_{50}, however, decreased from 175 to 140 microns at the feed and overflow, respectively. This suggests that drop breakup occurs. These drop size data are suspect since results from Table IV-5 show that the optimum E_s increased with increasing flowrate. For this to occur drop breakup must not be significant. It should be remembered for this system that interfacial tension decreased from 30 to 20 mN/m throughout the course of the runs. An analysis, carried out after completion of the runs is summarized in Table A3-4. It reveals that the source of this contamination was due to the bonding agent which held the silicon sealant to the inside bottom of the tank. As a result, a dirty system can reduce the drop/drop coalescence. As opposed to toluene/water and butanol/water, coalescence is more significant for

MIBK/water and kerosene/water. Consider the MIBK/water system. Droplet size was 225 and 330 microns at the feed and overflow cells, respectively. Since the optimum E_s increased with an increase in phase ratio, it suggests that at least part of the coalescence must occur inside the cyclone.

A model proposed by Happel and Brenner (H-1), for concentrated systems, was used to predict the effect of increasing the phase ratio on settling velocity. The interstitial volume used in the model was equivalent to the value calculated at the optimum E_s and reported in Table IV-4. From this model it was predicted that a decrease in settling velocity of 50 to 80% would result from an increase in phase ratio from $(O/W)_{MIN}$ to $(O/W)_{MID}$ for the various systems studied. An apparent contradiction appears to surface. The MIBK/water system, with a decrease in settling velocity of 80% actually showed an increase in the optimum E_s with an increase in phase ratio. Perhaps it is because the coalescence effect is dominant over that of the hindered settling effect. As a result, an increase in droplet size minimizes the problems created with an increase in dispersed phase concentration. Conversely, for butanol/water and toluene/water the hindered settling effect is dominant. No dominant effect is evident for kerosene/water.

Consider the kerosene/water system as shown in Table IV-6. It is only at a phase ratio of $(O/W)_{MAX}$ that the effect of hindered settling is really noticeable. Despite the significant decrease in settling velocity predicted by the model for an increase from $(O/W)_{MIN}$ to $(O/W)_{MID}$, the relative decrease in the optimum E_s is under 20%. For an increase from $(O/W)_{MID}$ to $(O/W)_{MAX}$ relative decrease in the optimum E_s ranged from

20 to 40%. The decrease became larger with a reduction in feed flowrate. Unlike runs performed at the lower phase ratios, the magnitude of the flowrate has an influence on the phase ratio effect towards separation efficiency. Note the results in Table IV-7 for kerosene/water. At Q_{MIN} the optimum E_s was only 7%. At this flowrate residence time was at a maximum; however the centrifugal force was at a minimum. Despite the greater time for coalescence, the hindered settling effect is very dominant. By increasing the flowrate the optimum E_s is increased to 16 and 38% for Q_{MID} and Q_{MAX}, respectively. Thus by providing a greater centrifugal force, the influence of increased concentration is lessened.

IV-d.2 Summary

With the exception of kerosene/water, the trends within each system are consistent. The effect of phase ratio on the optimum E_s at $(O/W)_{MIN}$ and $(O/W)_{MID}$ is not very large. This is probably because the opposing effects of coalescence and hindered settling are fairly equal in magnitude. It is only for a phase ratio of $(O/W)_{MAX}$ that one effect is clearly dominant over the other. This dominance, however, is reduced at least for kerosene/water by an increase in the feed flowrate and hence the separating force.

IV-e The Effect of Interfacial Tension on the Optimum E_s

Depending on the magnitude of feed flowrate studied, interfacial tension may or may not be sufficiently large enough to resist droplet breakup.

IV-e.1 An Explanation of the Interfacial Tension Effect

Based on the Weber number, an increase in interfacial tension

Optimum E_s and Volume Split for Liquid/Liquid Systems Table IV-7

System		Operating Conditions (coded)		Optimum	
		Phase Ratio	Flowrate	E_s ±1%	Volume Split ±0.01
Butanol/Water		-1	0	26	0.95
		-1	+1	21	0.99
		0	0	24	0.98
		0	+1	19	1.32
MIBK/Water		-1	-1	67	0.64
		-1	0	64	0.82
		-1	+1	61	0.91
		0	-1	73	0.72
		0	+1	68	0.90
Toluene/Water		-1	-1	37	0.91
		-1	+1	57	0.94
		0	-1	19	0.75
		0	+1	52	1.03
Kerosene/Water	Constant Mixing Energy	-1	-1	42	0.86
		-1	0	54	0.87
		-1	+1	58	0.88
		0	-1	40	0.98
		0	0	55	1.11
		0	+1	62	1.01
		+1	-1	7	0.70
		+1	0	16	2.26
		+1	+1	38	2.53
	Variable Mixing Energy	-1	-1	67	0.69
		-1	0	60	0.72
		0	-1	76	0.59
		0	0	67	0.78
		+1	-1	73	1.34
		+1	0	65	1.81

increases the surface forces which resist droplet breakup. Droplets from different liquid/liquid systems, exposed to the same magnitude of flow, have varying maximum stable sizes. According to the Hinze equation, with all other factors equal, the ratio of the maximum stable droplet size varies as $(\gamma_1/\gamma_2)^{0.6}$. Predicted droplet sizes are given in Table IV-2. With the larger droplets, the terminal velocity and hence the separating ability, is enhanced. Values of the optimum E_s shown in Table IV-7 only partially bear this statement out.

If the liquid/liquid systems studied are broken into two distinct groups, the hypothesis stated in the previous paragraph holds true within each of these groups. The method of grouping the systems was based on similar trends shown in the flowrate effect discussed in section IV-c. Butanol/water and MIBK/water formed one group; kerosene/water and toluene/water formed the other. At Q_{MAX} and $(O/W)_{MID}$, the optimum E_s was 19 and 68% for butanol/water and MIBK/water, respectively. Toluene/water had an optimum E_s of 52% while for kerosene/water it was equal to 62%. Similar trends were noted at other combinations of flowrate and phase ratio. These are shown in Table IV-8.

Looking at the systems as a group under comparable operating conditions, MIBK/water has the highest optimum E_s, followed in descending order by kerosene/water, toluene/water and butanol/water. If liquid/liquid systems are compared under similar flowrate and phase ratio conditions, the main variables affecting settling velocity are interfacial tension and density difference. Based on the droplet size as predicted by the Hinze equation, kerosene/water and toluene/water should have shown a higher optimum E_s than MIBK/water. The discrepancy, at least as

The Effect of Interfacial Tension on Optimum E_s Table IV-8

System	Interfacial Tension (mN/m.)	Operating Conditions (Coded)		Optimum E_s (%)
		Phase Ratio	Flowrate	
Butanol/Water	2.0	-1	+1	21
		0	+1	19
MIBK/Water	10.0	-1	+1	61
		0	+1	68
Toluene/Water	20.0	-1	+1	57
		0	+1	52
Kerosene/Water	30.0	-1	+1	58
		0	+1	62

far as the toluene/water and MIBK/water systems are concerned, may be partially due to density difference. $\Delta\rho$ equals 0.19 for MIBK/water and 0.13 for toluene/water; $\Delta\rho$, however, is comparable for kerosene/water and MIBK/water. Based on the data summarized in Table IV-8 it is difficult to explain why kerosene/water has a lower optimum value under comparable conditions. The explanation has to consider more than just interfacial tension and density difference. As noted, density difference is comparable while interfacial tension is a factor of three times greater for kerosene/water. This alone should have resulted in a higher optimum E_s for kerosene/water.

Without the equipment constraints limiting the upper feed flowrate to Q_{MAX}, it is hypothesized that the optimum E_s, for kerosene/water and toluene/water, would have been higher than MIBK/water. At Q_{MAX} the optimum E_s was still increasing for kerosene/water and toluene/water. It is also hypothesized that for all liquid/liquid systems a range of flowrates exist where the optimum E_s increases with increasing flowrate. Beyond the upper value of this range, the optimum E_s decreases. The magnitude of flow where the trend changes depends on the interfacial tension. For the range studied, Q_{MIN} to Q_{MAX}, this critical flowrate was less than Q_{MIN} for butanol/water and MIBK/water and greater than Q_{MAX} for kerosene/water and toluene/water.

IV-e.2 Summary

For a given feed flowrate, interfacial tension controls the amount of droplet breakup in the cyclone. Interfacial tension may be sufficiently high to resist breakup over a specified feed flowrate range. The magnitude of this flowrate is dependent on the interfacial tension. As

witnessed by the comparison of the optimum E_s values between kerosene/water and MIBK/water, interfacial tension and density difference can not adequately explain the apparent discrepancy that exists. It is felt, however, that if higher feed flowrates had been studied, the optimum E_s would have more closely reflected the magnitude of interfacial tension.

IV-f The Effect of Mixing Energy on Some Operating Parameters.

The effect of volume split, phase ratio and feed flowrate on the optimum E_s can be influenced by the technique employed to mix the two phases.

For a given liquid/liquid system the droplet size generated at the mixing tee is a function of mixing energy. According to McDonough et al. (M-2) the higher the mixing energy or pressure drop, the greater the interfacial area. This suggests that the greater the combined flowrate at the tee intersection, the smaller the droplet size.

For most of the data collected in this study, the same mixing energy was maintained for all the runs performed despite the change in feed flowrate. The droplet size entering the cyclone was reproducable regardless of feed flowrate. The effect of the aforementioned operating parameters using this mixing technique have been discussed in previous sections. However, in the study of Simkin and Olney (S-3), the mixing energy varied with the feed flowrate. They found, using a kerosene/water system, that the feed flowrate effect on the optimum E_s was the opposite to these current results discussed in section IV-c. To explain this apparent contradiction, some runs were done for the kerosene/water system with the variable mixing energy technique of Simkin et al. From Table IV-5 the variable mixing energy results agreed with the trend found by

Simkin et al. Figures IV-15 to IV-17 show the plot of E_s versus volume split for the kerosene/water system, using the variable mixing energy method.

IV-f.1 Feed Flowrate

The optimum E_s, by the mixing method of Simkin et al., decreased with an increase in feed flowrate because of the smaller droplet size generated at the tee with an increase in pressure drop. Figure IV-18 contains two photos taken for kerosene/water at a mixing energy equivalent to a combined flowrate of Q_{MIN} and Q_{MID}. The change in droplet size was quite significant; D_{50} at the feed was 285 microns for Q_{MID} and 360 microns for Q_{MIN}. Because the mixing energy increased with increasing feed flowrate, the difference in the optimum E_s between this method and the constant mixing energy one, decreased. From Table IV-9, the difference decreased from 25 to 6% by increasing the feed flowrate from Q_{MIN} to Q_{MID} because the droplet size generated by both methods was approaching equivalence.

IV-f.2 Phase Ratio

As with feed flowrate, the mixing technique can influence the effect that phase ratio has on the optimum E_s. The relative increase in the optimum E_s from $(O/W)_{MIN}$ to $(O/W)_{MID}$ was about 12% as noted in Table IV-6. This increase was slightly larger than with the constant mixing energy method. As opposed to the constant mixing method, a decrease in the optimum E_s with an increase in the phase ratio from $(O/W)_{MID}$ to $(O/W)_{MAX}$ is almost insignificant for the variable method. For example, under the same conditions, the relative decrease was 40% for the former method and 2% for the latter one. The reason that the phase ratio

Figure IV — 15 E_s versus Volume Split for Kerosene/Water at a Phase Ratio of $(O/W)_{MIN}$ at 20°C, performed at a Feed Flowrate of: Q_{MIN}(⊙); Q_{MID}(o) by the Variable Mixing Energy Technique.

Parameters are: calculated interstitial volume (as a fraction) and the calculated centrifugal acceleration (as a percentage).

calculated interstitial volume: ε = 0.8 - - - - ; ε = 0.7 — — — — ; ε = 0.6 — — — — — .

calculated centrifugal acceleration: 100% ——— ; 90% - - - - - - ;

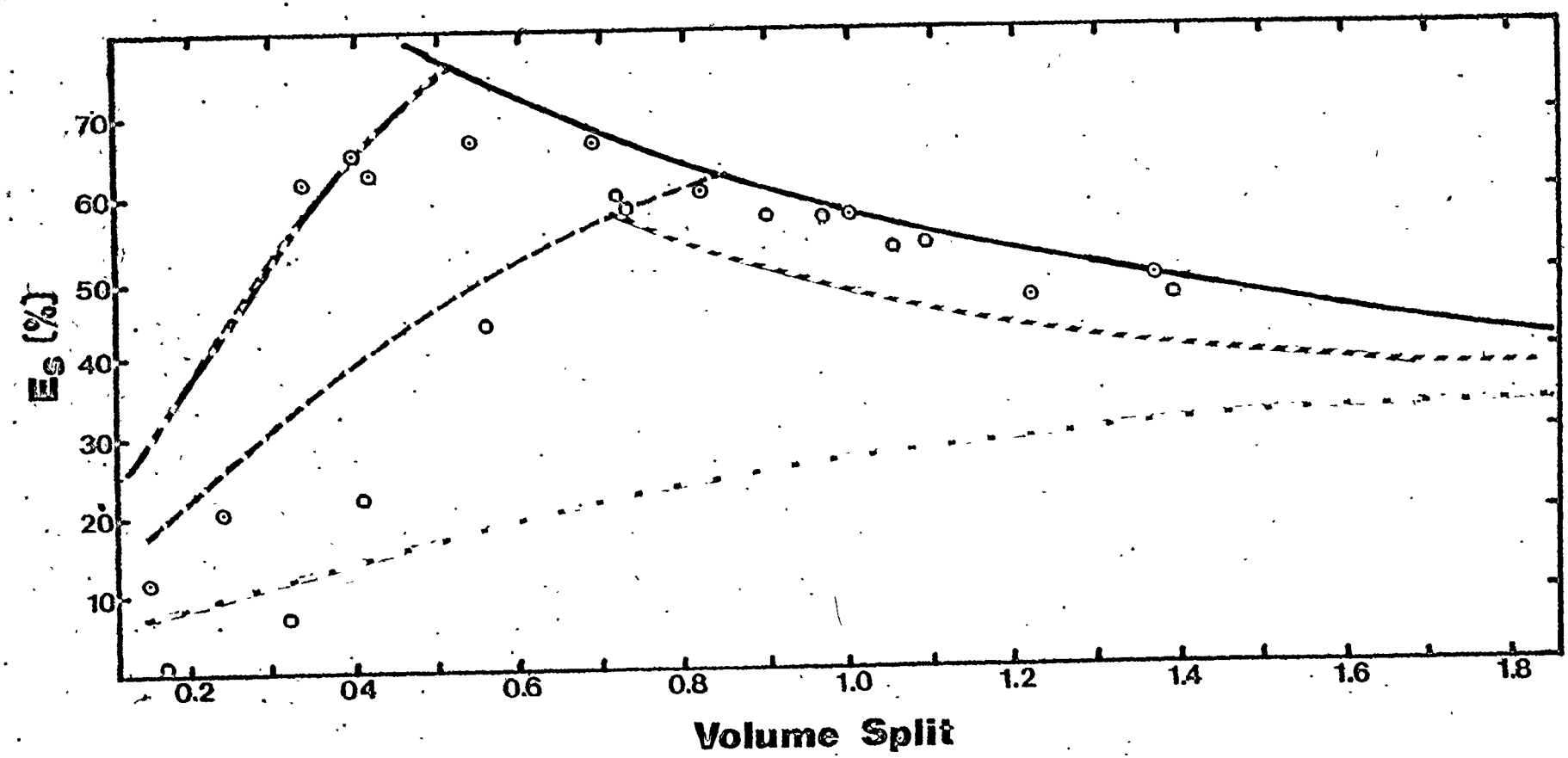

Figure IV — 16 E_s versus Volume Split for Kerosene/Water at a Phase Ratio of $(O/W)_{MID}$ at 20°C, performed at a Feed Flowrate of: Q_{MIN}(⊙); Q_{MID}(o) by the Variable Mixing Energy Techique.

Parameters are: calculated interstitial volume (as a fraction) and the calculated centrifugal acceleration (as a percentage).

calculated interstitial volume: $\varepsilon = 0.6$ - - - ——— - - ·; $\varepsilon = 0.5$ - - - ——— - - ; $\varepsilon = 0.4$ ——— ; $\varepsilon = 0.3$ ·····

calculated centrifugal acceleration: 100% ———

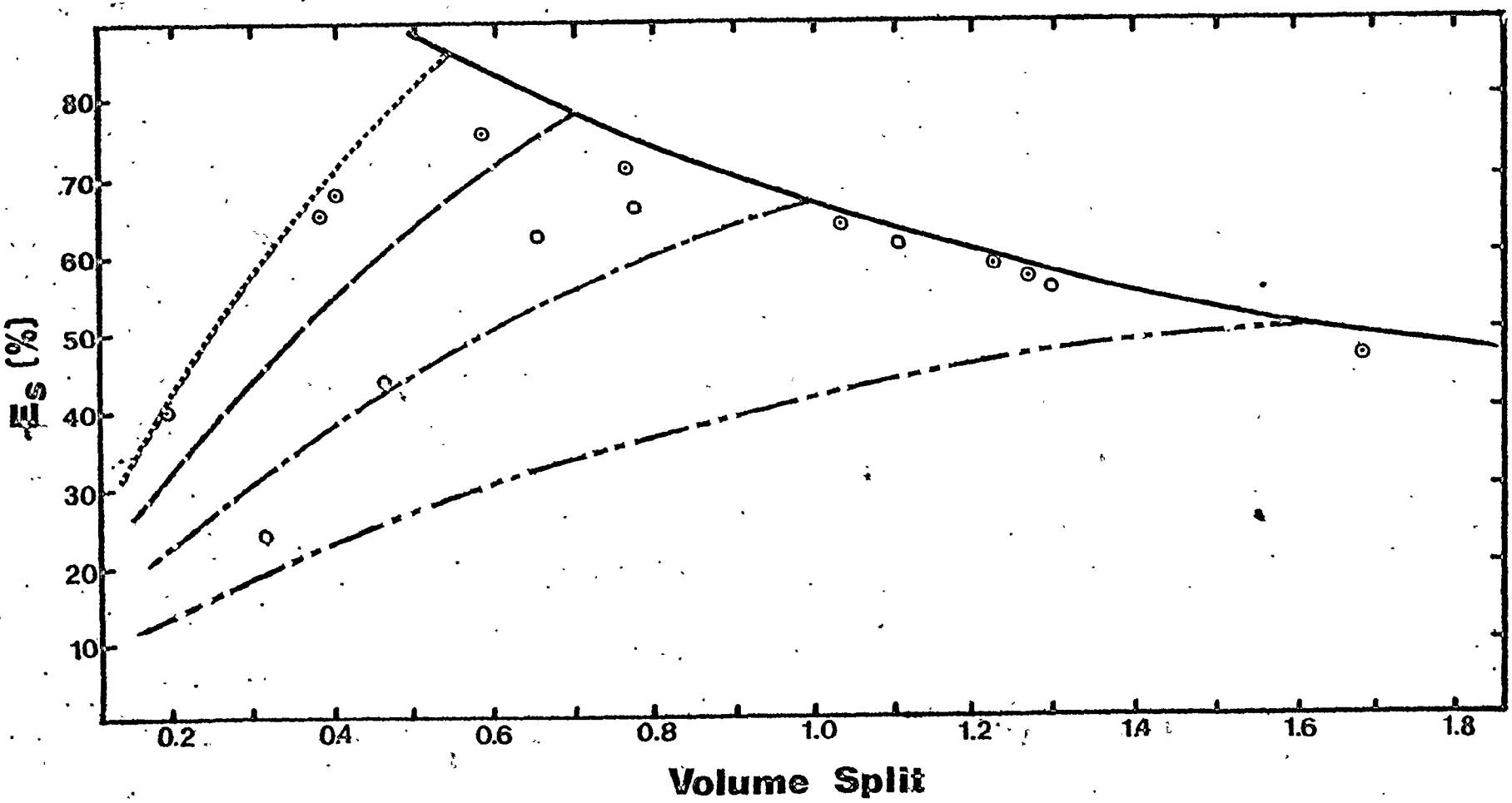

Figure IV — 17 E_s versus Volume Split for Kerosene/Water at a Phase Ratio of $(O/W)_{MAX}$ at 20°C, performed at a Feed Flowrate of: Q_{MIN}(⊙); Q_{MID}(o) by the Variable Mixing Energy Technique.

Parameters are: calculated interstitial volume (as a fraction) and the calculated centrifugal acceleration (as a percentage).

calculated interstitial volume: $\varepsilon = 0.3$ ····· ; $\varepsilon = 0.15$ —·—·—.

calculated centrifugal acceleration: 100% ——— ; 90% - - - - - - - .

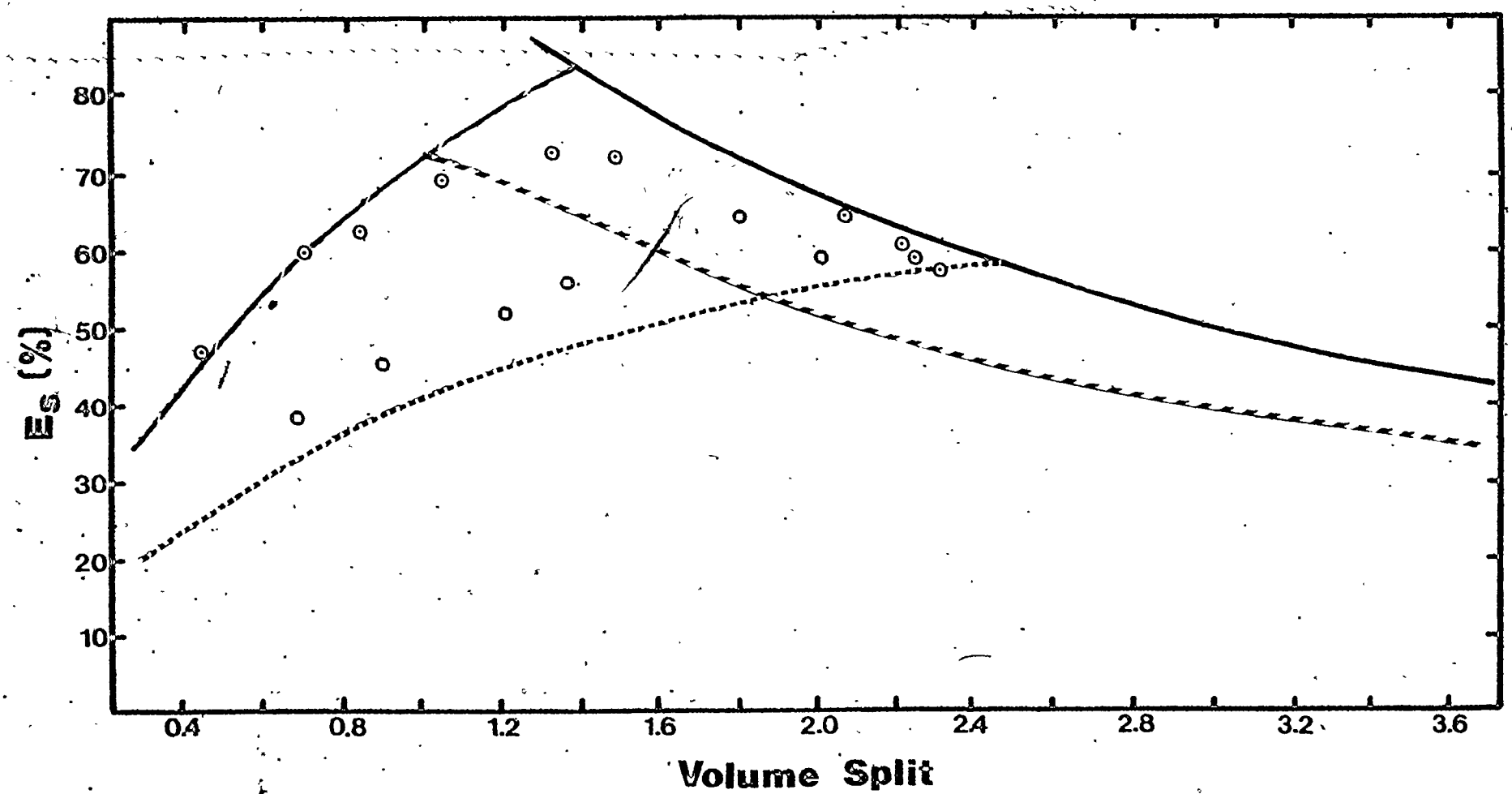

Effect of Mixing Energy on Droplet Size

Figure IV — 18

1) at Q_{MIN}

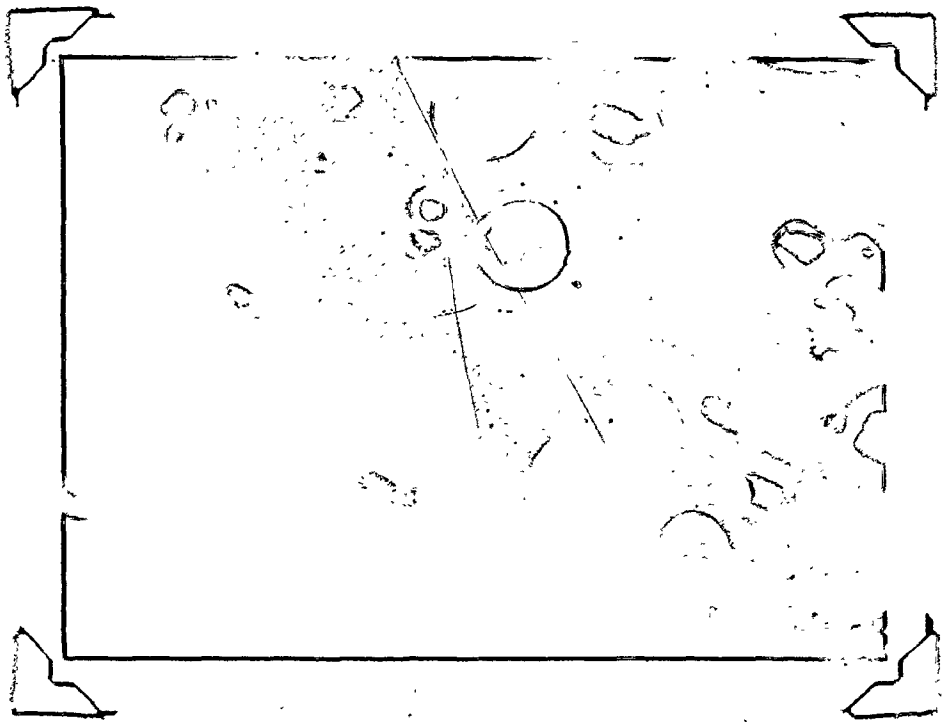

Approx. Scale (same for Q_{MIN} & Q_{MID})

microns 1000 500 0

2) at Q_{MID}

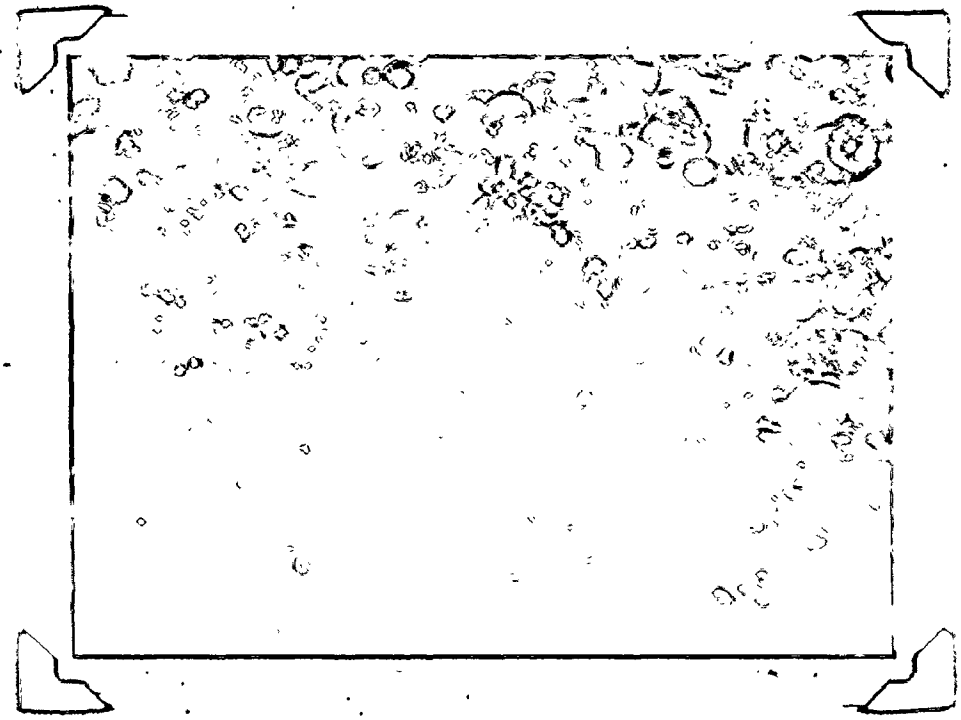

Comparison of the Optimum E_s by Different Mixing Techniques Table IV-9

Mixing Technique	Phase Ratio (coded)	Flowrate	Optimum E_s (%)	ΔE_s (%)
Variable	-1	-1	67	25
Constant	-1	-1	42	
Variable	-1	0	60	6
Constant	-1	0	54	

increase on the optimum E_s is more beneficial for the variable mixing energy system is related to droplet size. The larger the droplet size generated for a given phase ratio, the lower the interfacial area. This tends to reduce somewhat the effects of hindered settling brought about by an increase in dispersed phase concentration. In absolute terms, the optimum E_s is higher by the variable mixing method, again due to droplet size. According to Stoke's equation, an increase in droplet size, with centrifugal acceleration constant, increases the settling velocity and hence the optimum E_s. For example, in Table IV-7, under comparable conditions, the optimum E_s was 42 and 67% for the constant and variable mixing energy methods, respectively.

IV-f.3 Volume Split

The mixing method has a notable influence on how volume split affects the optimum E_s. Under comparable conditions, the optimum volume split shifted closer to a value equivalent to the phase ratio with the variable mixing method. At a mixing energy equivalent to a total flowrate of Q_{MIN}, regardless of the phase ratio, the dispersed phase concentrated in a zone extending from the major axis of the cyclone outwards. Droplet size was sufficiently large to allow a significant migration to the major axis within the residence time of the cyclone. An increase in mixing energy, with a corresponding increase in feed flowrate to Q_{MID}, initiated the formation of a region surrounding the major axis where the concentration of the dispersed light phase equals that of the feed concentration. This is a result of a decreased droplet settling velocity brought about with the increase in mixing energy. This trend was noted in varying degrees for the constant mixing energy method. Despite the formation of

this region, a pure continuous phase was achieved at the underflow under all conditions with the variable mixing method.

Unlike the constant mixing method, the minimum interstitial volume does not correspond with the optimum E_s for the variable mixing method. Instead interstitial volume is at a minimum in the vicinity of the major axis and increases to a maximum near the optimum split. This was noted at a combined mixing flowrate of Q_{MIN}; however at Q_{MID} the trend was similar to that noted for the constant mixing method.

IV-f.4 Summary

The means of mixing the two liquid phases affects the operating parameters. The reason for this variation is due largely to droplet size generated by the two mixing techniques. The optimum E_s decreases with an increase in feed flowrate because a smaller droplet size is generated in the feed mixture. The changing of the droplet size at the feed inlet also has a noticeable effect on the phase ratio and volume split.

V CONCLUSIONS AND RECOMMENDATIONS

V CONCLUSIONS AND RECOMMENDATIONS

V-a Conclusions

The conclusions from the present work can be divided into three sections - those which verify, and those which dispute past literature and those which constitute new findings in this research field.

V-a.1 Results that Verify those Reported in the Literature

The following conclusions verify those cited in past literature:

1. It is possible to separate the two phases inside the cyclone under certain operating conditions. A pure continuous phase was achieved at the underflow; however a mixture of light and heavy phases was always noted at the overflow. From the data of Simkin and Olney (S-3), a relatively pure overflow (<1% heavy phase) was noted at a oil/water phase ratio of 1/3 for kerosene/water and white oil/water.
2. The flowrate of the feed mixture into the cyclone and the volume-split of the effluent from it are important parameters affecting the optimum E_s. Burrill and Woods (B-3) noted that volume split was the most important parameter affecting the optimum E_s. Other researchers, Mahajan and Pai (M-1), Sheng et al. (S-1) and Simkin and Olney (S-3) verified this. These workers also found that feed flowrate was an important parameter.
3. For feed phase ratios less than or equal to unity, the optimum split occurs at a value greater than this phase ratio. This was noted in the E_s versus volume split plots of researchers such as Burrill and Woods (B-3), Sheng et al. (S-1) and Simkin and Olney (S-3).
4. For the range of feed flowrates studied, an increase in flowrate resulted in a decrease in the optimum E for butanol/water and

MIBK/water. These systems have an interfacial tension less than or equal to 10 mN/m. Simkin and Olney (S-3) noted this for the kerosene/water and white oil/water systems. Other researchers, Mahajan and Pai (M-1) and Sheng et al (S-1), verified this.

5. The droplet size distribution generated at the mixing tee is a function of the head loss or the flowrate through the tee section. Droplet size distribution entering or leaving the cyclone tended to obey the log-normal distribution. Burrill and Woods (B-3) noted that the drop size obeyed the log-normal distribution at the feed and overflow for the carbon tetrachloride/water system.

6. Complete coalescence does not occur inside the cyclone. It is therefore not possible to get an optimum E_s equal to 100%. Burrill and Woods (B-3) stated that no coalescence occurred inside the cyclone for the carbon tetrachloride/water system.

7. The central core region, consisting of dispersed light phase varied in width and depth with a change in volume split. As noted by Simkin and Olney (S-3), the width of the core region decreased with increasing volume split.

V-a.2 Results that Dispute those Reported in the Literature.

The following conclusions dispute those cited in past literature:

1. For toluene/water and kerosene/water, the optimum E_s, within the feed flowrate range studied, increased with increasing flowrate. The study of the kerosene/water system by Simkin and Olney (S-3) and Mahajan and Pai (M-1) found the opposite effect.

2. Results from the photographic study indicate that droplet size was larger at the overflow and underflow as compared to the feed mixture.

Whether coalescence occurs inside the cyclone or the vortex finder is dependent on the coalescence rate of the liquid/liquid system. Burrill and Woods (B-3) felt however that no coalescence occurred inside the cyclone for the carbon tetrachloride/water system.

V-a.3 New Findings

The following conclusions are new to the field of liquid/liquid separation:

1. The effect of feed flowrate on the optimum E_s is dependent on interfacial tension. For values of interfacial tension greater than or equal to 20 mN/m, the optimum E_s increased with increasing flowrate. For values of interfacial tension less than or equal to 10 mN/m, the optimum E_s decreased with an increase in flowrate.
2. For the liquid/liquid systems studied, the interstitial volume was at its minimum value at the optimum volume split. A region surrounding the major axis, where the concentration of dispersed light phase is equivalent to the feed mixture, varied in size in accordance with the feed flowrate and phase ratio used.
3. If the feasibility of separating a liquid/liquid mixture by a cyclone is based on obtaining at least one pure phase from the cyclone, then only the butanol/water system should be discounted as not being practical. All the other systems studied could be separated.
4. The spread on the droplet size, as defined by D_{84}/D_{50}, is dependent on the magnitude of the mixing energy. The higher the mixing energy, the smaller the spread or the more uniform the droplet size becomes.
5. The Parallel Disc Model proposed by Liem and Woods (L-1) was used to predict the coalescence rate for the systems studied. The following

modified version best suited the experimental data:

$$\theta \propto \frac{\mu_c \Delta \rho}{\gamma^2} \left(\frac{d_{50}}{2}\right)^2 \left(\frac{1}{h^2}\right)$$

6. Hindered settling became a significant problem at a phase ratio of $(O/W)_{MAX}$. This resulted in a decrease in the optimum E_s as compared to the lower phase ratios studied. As a result, the phase ratio becomes an important operating parameter when hindered settling is significant.

7. Controlling the droplet size distribution of the feed mixture is important in evaluating the separating ability of the cyclone alone. The droplet size is controlled by maintaining a constant mixing energy. As a result, feed flowrate to the cyclone can be varied with the certainty that a similar drop size is entering the cyclone. Without controlling the drop size of the feed, the effect of phase ratio, feed flowrate and volume split on the optimum E_s is influenced significantly.

V-b <u>Recommendations</u>

Based on the present research the following recommendations are proposed:

1. For certain liquid/liquid systems studied, the ability to achieve higher feed flowrates would be desirable. This would be particularly useful for the toluene/water and kerosene/water systems in determining how much higher the optimum E_s could increase.

2. With a study of the same feed flowrate range, liquid/liquid systems should be chosen with an interfacial tension value between 10 and 20 mN/m. This range has not been studied by past or present work. Its

study would essentially cover the full range of interfacial tension values and would give a more complete picture of its effect on phase ratio, volume split, feed flowrate and the optimum E_s.

3. The selection of liquid/liquid systems with a range of density differences but similar interfacial tensions should be considered. This would allow comparison of the relative importance of these two parameters in the separating process.

4. The simultaneous photographing of the dispersion at each of the three sampling locations should be carried out. This would ensure that comparable conditions were observed at each of the optical cells. A shorter flash duration should be considered for measuring the droplet size at higher feed flowrates. The addition of an optical cell immediately downstream of the mixing tee would allow monitoring of the droplet size generated at the tee to ensure that it is reproducable regardless of feed flowrate.

5. The exclusive use of glass vessels should be considered for storage of the liquid phases. This avoids the problems of leakage and contamination.

BIBLIOGRAPHY

BIBLIOGRAPHY

A-1 Allak, A.M. and G.V. Jeffreys, "Studies of Coalescence and Phase Separation in Thick Dispersion Bands, " A.I.Ch.E.J 20, (3), 564-581, (1974).

B-1 Bradley, D. "The Hydrocyclone," Pergamon Press (1965)

B-2 Burrill, K.A. "The Effect of Drop Size Distribution, Feed Concentration and Volume Split of Two Immiscible Liquids in a Hydrocyclone", M.Eng. Thesis (1967).

B-3 Burrill, K.A. and D.R. Woods "Separation of Two Immiscible Liquids in a Hydrocyclone", Ind. & Eng. Chem. Process Des. Develop., 9, 4, 545-552, (1970)

C-1 Coulter Electronics Literature

H-1 Happel, J. and H. Brenner "Low Reynolds Number Hydrodynamics", pg. 389, Noordhoff International Publishing (1973).

H-2 Hinze, J.O. "Fundamentals of the Hydrodynamic Mechanism of Splitting in Dispersion Processes," A.I.Ch.E.J., 1, (3), 289-295 (1955).

H-3 Hitchon, J.W. "Cyclones as Liquid-Liquid Contactor-Separators", AERE CE/R 2777, 1-17, (1959).

H-4 Hsiang, T.C.H. and D.R. Woods "The Influence of Design and Operating Variables on Energy Consumption and Separation Efficiency of a Hydrocyclonic Concentrator," C.J.Ch.E. 50, 607-610, (1972).

K-1 Karabelas, A.J. "Droplet Size Spectra Generated in Turbulent Pipe Flow of Dilute Liquid/Liquid Dispersions," A.I.Ch.E.J. 24, (2), 170-179, (1978).

K-2 Kelsall, D.F. "A Study of the Motion of Solid Particles in a Hydraulic Cyclone, Trans. Instn. Chem. Engrs. 30, 87-108, (1952).

K-3 Knowles, S.R. et al. "The Velocity Distribution Within a Hydrocyclone Operating Without an Air Core," C.J.Ch.E. 51, 263-271 (1973).

L-1 Liem, A.J.S. and D.R. Woods "Application of the Parallel Disc Model for Uneven Film Thinning," C.J.Ch.E. 52, 222-227, (1974).

L-2 Lilge, E.O. "Hydrocyclone Fundamentals," Extract from Transactions of the Institution of Mining and Metallurgy 71, (6), pg 315, (1961-1962).

M-1 Mahajan, S.P. and V.J. Pai "Liquid-Liquid Separation Efficiency and Volume Split in Hydrocyclones", Indian Chemical Engineer 19, 3-9, (1977).

M-2 McDonough, J.A. et al. "Formation of Interfacial Area in Immiscible Liquids by Orifice Mixers, A.I.Ch.E. J. 6, (4), 615-618, (1960).

O-1 Osahi, H. and S. Maeda, Chem. Eng. (Japan) 22 pg. 200, (1958).

P-1 Perry's Chem. Eng. Handbook, Fourth Edition, McGraw-Hill (1963).

R-1 Raja Gopal, E.S. Kolloidzeitschrift 162, 85-92, (1959).

R-2 Rietema, K. Chem. Eng. Science 15, 298-325, Pergamon Press (1961).

R-3 Rumscheidt, F.D. and S.G. Mason "Deformation and Burst of Fluid Drops in Shear and Hyperbolic Flow," J.Colloid Science 16, 238-261, (1961).

S-1 Sheng, H.P. et al. "Liquid/Liquid Separations in a Conventional Hydrocyclone," C.J.Ch.E. 52, 487-491, (1974).

S-2 Shinnar, R. and J.M. Church "Statistical Theories of Turbulence in Predicting Particle Size in Agitated Systems," Ind. Engng. Chem. 52, 253-256, (1960)

S-3 Simkin, D.J. and R.B. Olney "Phase Separation and Mass Transfer in a Liquid-Liquid Cyclone," A.I.Ch.E.J. 2, (4), 545-551, (1956).

S-4 Sleicher, C.A. "Maximum Stable Drop Size in Turbulent Flow, A.I.Ch.E.J. 8, (4), 471-477, (1961).

S-5 Streeter. V.L. "Fluid Mechanics", pg. 139, 5th. Edition, McGraw-Hill (1971).

S-6 Stephen, H. and T. Stephen "Solubilities of Inorganic and Organic Compounds," Pergamon Press, MacMillan Co. (1963).

S-7 Svarovsky, L. (Editor) "Solid-Liquid Separation," Chemical Engineering Series, pg. 121, (1977).

T-1 Taylor, G.I., Proc. Royal Soc. A146, 501-523, (1934).

T-2 Tepe, J.B. and W.K. Woods U.S.A.E.C. Report A.E.C.D. 2864, (1943).

V-1 Van Kooy, J.G. "The Influence of the Reynolds Number on the Operation of a Hydrocyclone," Cyclones in Industry, 64-76, (1958).

W-1 Witbeck, W.O. "Measurement of Operational Variables in a Hydrocyclone," Master's Thesis (1972).

W-2 Woods, D.R. "The Behaviour of Surfaces", McMaster University (1976).

Z-1 Zeiss Particle Size Analyzer TGZ-3 Instructional Book.

APPENDIX 1

SYSTEM DESIGN AND MEASUREMENT

A1 SYSTEM DESIGN AND MEASUREMENT

The initial objective was to establish the feasibility of the existing system in meeting the requirements of this research.

A1.1 Description of the Existing System

The existing system contained a 25 Imperial gallon glass vessel which was used to store both the light and heavy phases. The lighter liquid was pumped out the top of the vessel by a tube which extended almost to the interface of the two phases; the heavy liquid was pumped out from the bottom. The flowrate for each phase was governed by globe valves positioned directly in front of the rotameters. Downstream of the rotameters, the individual phases were mixed at a tee joint. The feed mixture flowed into the hydrocyclone. Based on volume split, the mixture was proportioned between the underflow and overflow outlets. The split was controlled by a gate valve located a short distance downstream from the overflow outlet. As the valve was closed, the proportion of liquid leaving through the overflow decreased. Further downstream of the underflow and overflow outlets, switch valves were located which allowed simultaneous sampling of each of these streams. Alternatively these valves, switched to another position, allowed the streams to empty back into the glass vessel. Pressure in the system was monitored by Bourdon gauges, which were positioned at the inlet to and outlets from the cyclone.

A1.2 Modifications and Additions to the Existing System

Based on an analysis of the requirements for this work, a number of changes were made. A schematic layout of the final experimental set-up is shown in Figure A1-1.

A1.2a Requirements for Storage

A major concern was whether the residence time in the glass vessel was sufficiently long to allow for complete coalescence of the cyclone effluent before it was pumped through the system again.

A toluene/water system was used to evaluate this requirement. Initially the two phases were clear, as the run progressed, the phases became milky in appearance as they flowed through the rotameters. This became noticeable after one to two minutes of continuous pumping. By pumping a dispersion it was no longer possible to control the feed concentration. Rotameters were calibrated based on pure phases.

It was felt that the rate of coalescence would be hastened by damping out the turbulence in the glass vessel. A cylindrical-shaped baffle was positioned around the exit from the effluent tubes; however the problem persisted.

It was decided that separate vessels would be required for each phase. The new design was based on the use of three vessels, each with a separate function. The existing vessel, located in the fume hood, contained the oil phase. A 50 Imperial gallon glass vessel, positioned outside the fume hood, contained the water phase. Draw-off of liquid from the bottom of each vessel was provided by stainless steel,

Schematic Layout of Experimental Setup

Figure A1 —

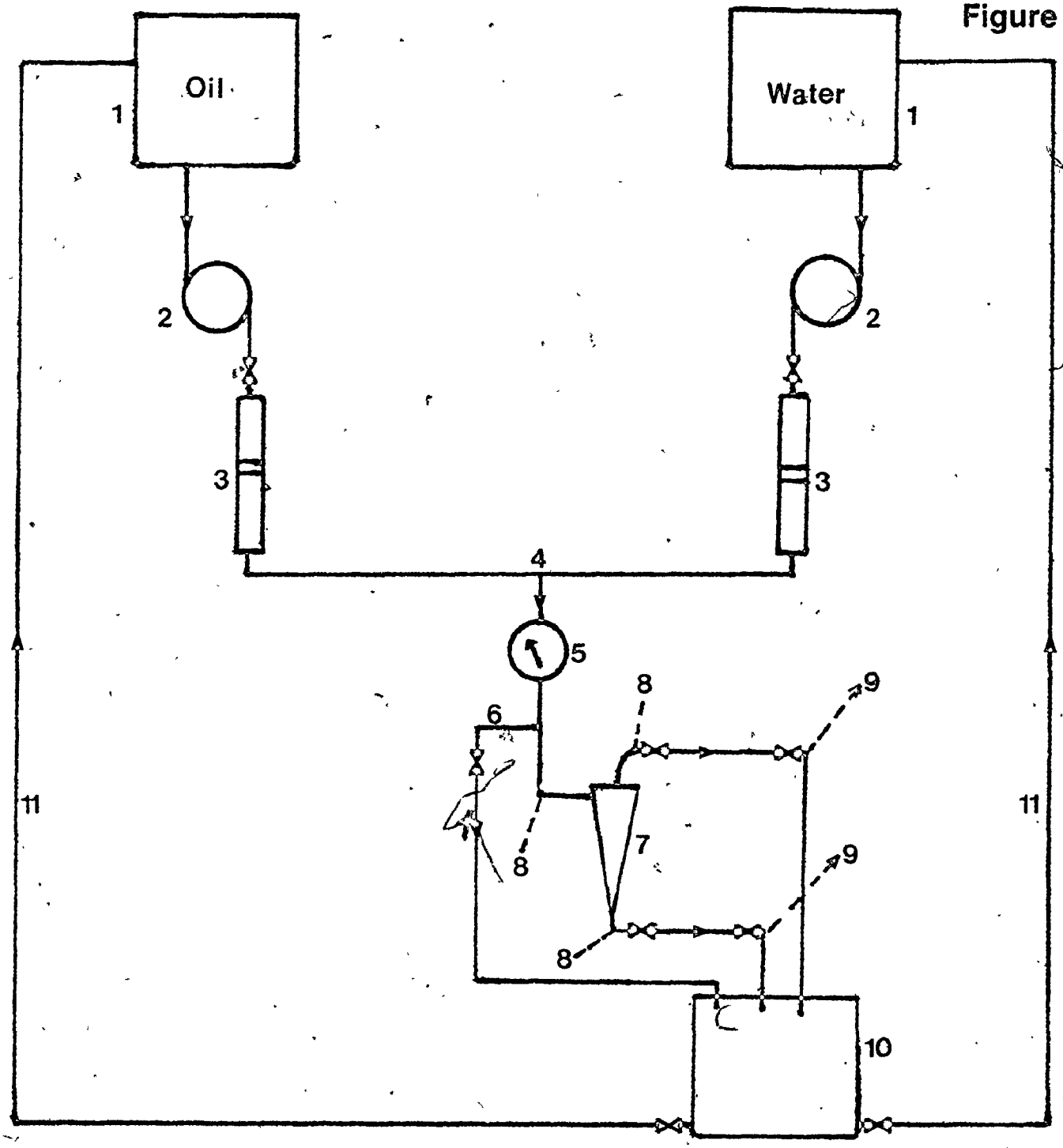

Legend

1	:Containers	7	Hydrocyclone
2 Oil and Water Phase	:Pumps	8	Connection to Manometers
3	:Rotameters	9	Connection to Sampling Points
4 Mixing Tee		10	Separator/Storage Container
5 Bourdon Pressure Gauge		11	Recyle to Oil and Water Phase Containers
6 Di			

explosion-proof pumps. A large rectangular-shaped glass and stainless steel vessel of approximately 100 Imperial gallons capacity was used to hold effluent from the cyclone. It functioned as a separator vessel. This vessel was elevated onto a four foot high metal stand. It had a plexiglass cover with a vent extending from the top of it, leading back into the fume hood. The elevated position allowed for gravity feed of the clarified effluent back into the respective glass vessels.

In addition to the effluent from the cyclone, flow from a diversion line emptied into the separator tank. This diversion line was added downstream of the mixing tee. This addition allowed the study of variable flowrate to the cyclone, independent of feed droplet size. A gate valve, located on the diversion line, controlled the flowrate through it.

A1.2b Control of Volume Split and Flowrate

To achieve a wider range of volume split, a gate valve was added at the underflow end of the cyclone. An added advantage was that it increased the range of flowrates achievable. The maximum flowrate through the cyclone was maintained at 365 mL/s ±10%. By opening the gate valve on the diversion line completely, flowrate through the cyclone was reduced to 200 mL/s ±10%. The flowrate through the cyclone was further reduced by partially closing both the underflow and overflow gate valves while leaving the diversion line valve completely open; a flowrate of 100 mL/s ±15% was achieved.

A1.2c Materials Consideration

To prevent contamination of the liquid/liquid system, inert materials such as stainless steel, #304 and #316, and glass were exclusively used in the construction of the piping. Since thin-walled tubing was being used, sections were jointed by means of Swagelok fittings. Stainless steel ferrules were predominantly used; to join glass with stainless steel sections, teflon or nylon ferrules were substituted. 1/2 and 5/8 inch outer diameter tubing was used exclusively.

A1.2d Addition of Manometers

Another concern with the existing system was the use of pressure gauges. They were not very accurate; as well, their location inside the fume hood tended to produce a cramped situation. Removal of the gauges reduced the load on the piping system considerably. One pressure gauge, positioned at the mixing tee, was retained. The remaining gauges were replaced with mercury manometers. The manometers were fastened to the outside wall of the fume hood. 3/4 inch thick plywood was used to hold the manometers in place. A 1/2 inch deep channel was routed out in the plywood so that the glass tubing could be inserted. This reduced the possibility of accidental breakage.

The three locations monitored by the manometers were as follows: one inlet to and two outlets from the cyclone. One limb of each manometer was joined to the sampling point with nylon tubing. The connection at the manometer was made with a nylon tee fitting. Extending from one end of the fitting was a piece of Tygon tubing with

a clamp on the end. This end served as a bleed line in the event that an air pocket was trapped in the nylon tubing. The other limb of the manometer was exposed to the atmosphere. At the end of this limb, a piece of Tygon tubing extended from it into a small glass jar. The purpose was to provide a trap for the mercury in case a sudden surge in pressure sent it out the top of the manometer. To dampen out sudden fluctuations in pressure, a constriction was formed at the confluence of the two limbs. Thick-walled glass was used as a preventative measure against glass breakage due to high stress development.

A1.2e Placement of the Hydrocyclone in the Piping System

The placement of the hydrocyclone was of considerable concern. With the original system this problem was averted by using a piece of flexible Tygon tubing at the underflow end of the cyclone. This facilitated the coupling operation by allowing some freedom of movement when tightening fittings; otherwise torsion between the glass and fittings would result. This caused breakage of the glass tubing which extended from the cyclone. The problem with Tygon tubing was that it reacted with organic solvents. The reaction caused the plasticizer in the tubing to be leached out, leaving it quite brittle. The tubing was replaced with a stainless steel bellows; the advantage being that it still afforded the cyclone some flexibility while not reacting with the solvents. A photograph of the cyclone and the coupling arrangement is shown in Figure A1-2.

The Hydrocyclone and Coupling Arrangement

Figure A1 — 2

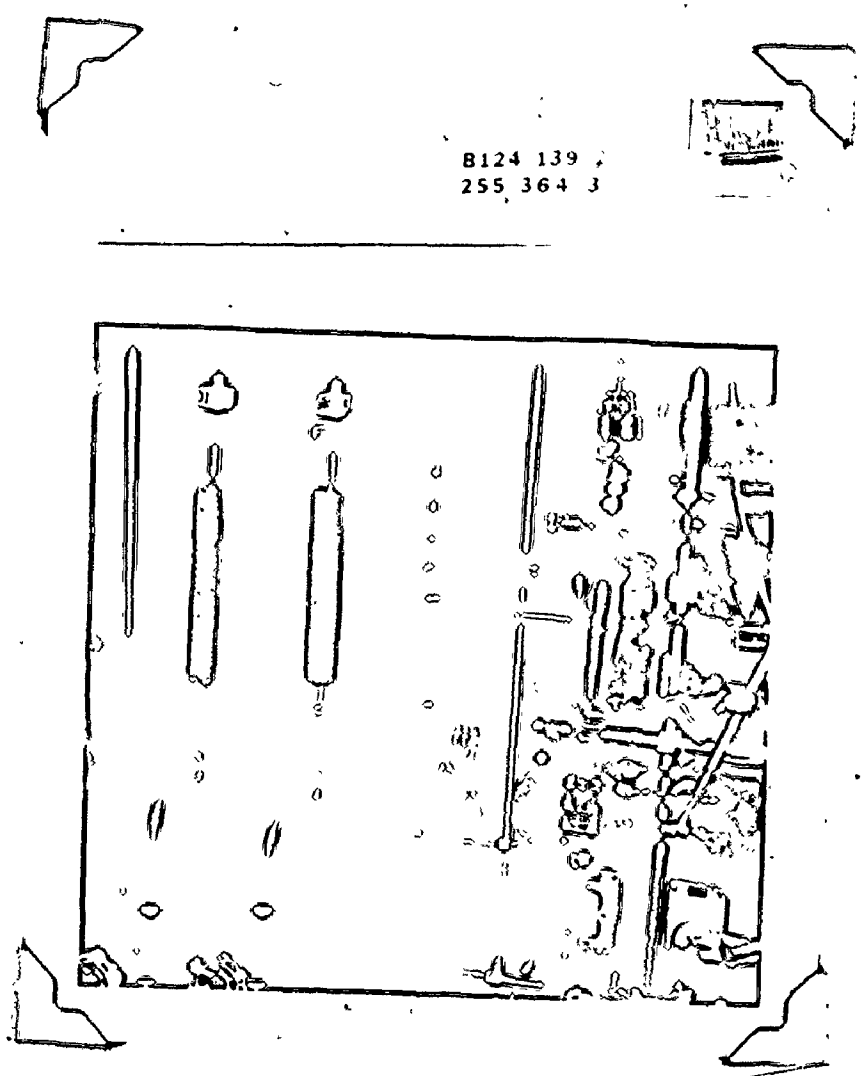

A1.2f Other Considerations

The pipe work was completely grounded to avoid build-up of static charge due to the flow of the liquids.

Due to the reactive nature of toluene and MIBK, it was necessary to replace rubber rings in the rotameter tubes with ethylene-propylene rings. They were resistant to the deteriorating action of the solvent and solvent saturated water phases.

Initial tests of adding water to the separator tank revealed a number of leaks. Application of silicon sealant on the outside edges provided a temporary solution. Halfway through the experimental work, sealant was also added to the bottom edges inside the tank. A reaction occurred between the toluene/water mixture and the sealant, causing the latter to dislodge from the contact surface.

To ensure that the rotameter levels did not change when sampling, a piece of tubing and a clamp were attached to the end of the overflow and underflow sampling points. The clamps were tightened until head loss through either the pathway to the sampling points or to the separator tank were equal. This method was used for the butanol/water and MIBK/water systems; however due to constant loosening of the clamps this method was discontinued for the other two systems. Instead, when switching to the sampling points, a quick adjustment was made with the globe valves in front of the rotameters.

A1.3 Calibration of Rotameters

Before calibrating the rotameters, the two liquids were mixed

together in the cyclone to ensure mutual saturation. The float of the rotameter was set at a specified value and then the flow was diverted from the separator vessel to the sampling points; simultaneously a timer was activated. After a short period, the flow was switched back to the separator vessel and the timer stopped. This procedure was repeated for a wide range of settings for both rotameters. A sketch of the rotameter tube and float in Figure A1-3 designates the location on the float used as the datum for all calibrations. Calibration of the water phase and each of the oil phases is shown in Figures A1-4 to A1-8. Measured flowrates were plotted as a function of the settings on the rotameters.

A1.4 Start-up Procedure

Before introducing a new liquid/liquid system, the three vessels were thoroughly washed out with tap water; no detergents whatsoever were used to cleanse the system for fear that a residual amount would be left to contaminate it. Finally a small amount of distilled water was added to rinse out the vessels and to flush out any tap water in the pipe work. While adding the oil phase from a metal container to the glass vessel, care was taken to ensure that the container had been adequately grounded. Water from the distilled water tap was added to the other vessel. Both vessels were covered with aluminum foil to prevent evaporation and contamination.

Sketch of the Rotameter Tube and Float

Figure A1 — 3

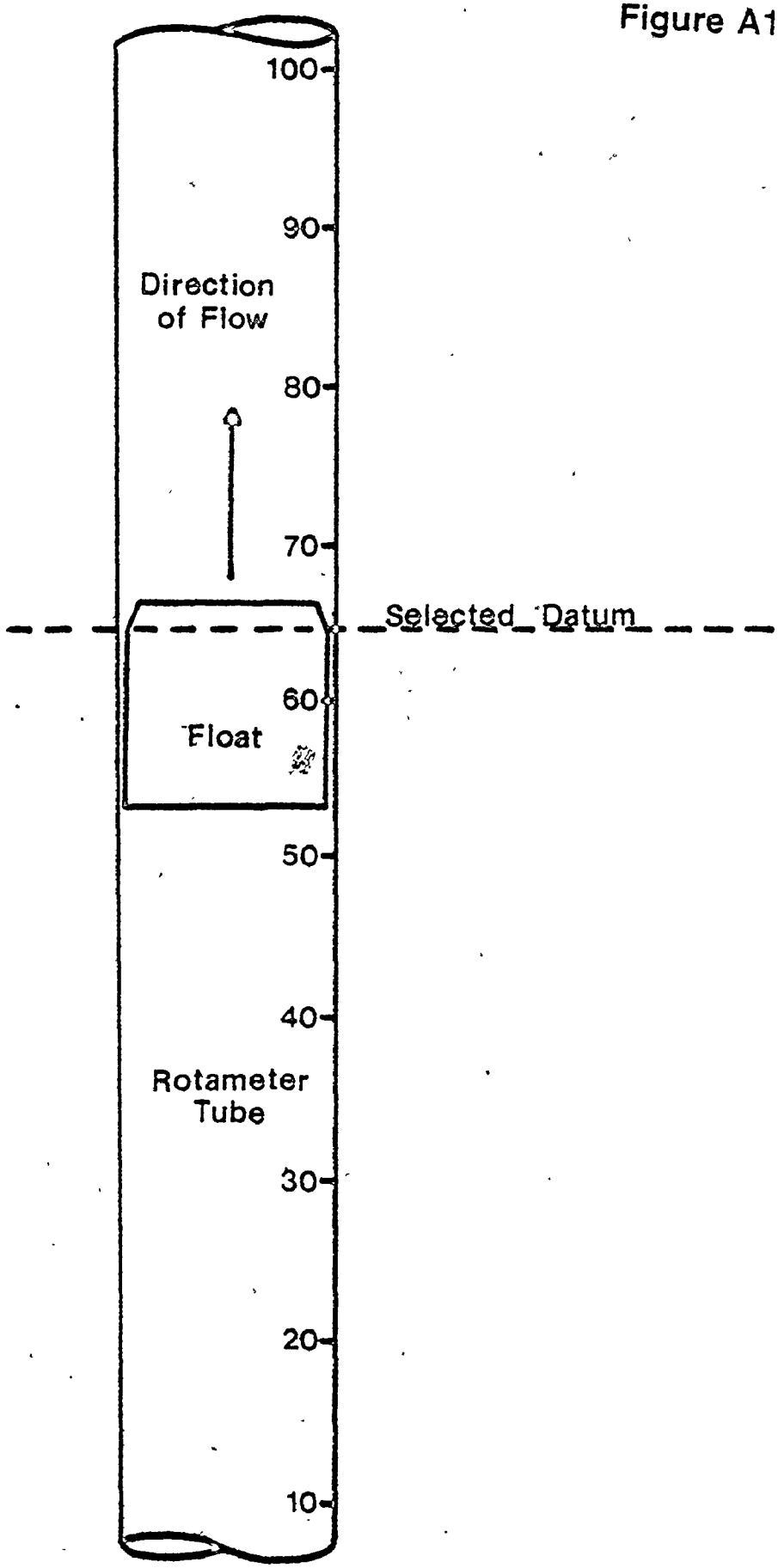

Figure A1 — 4

Rotameter Calibration Curve for Water

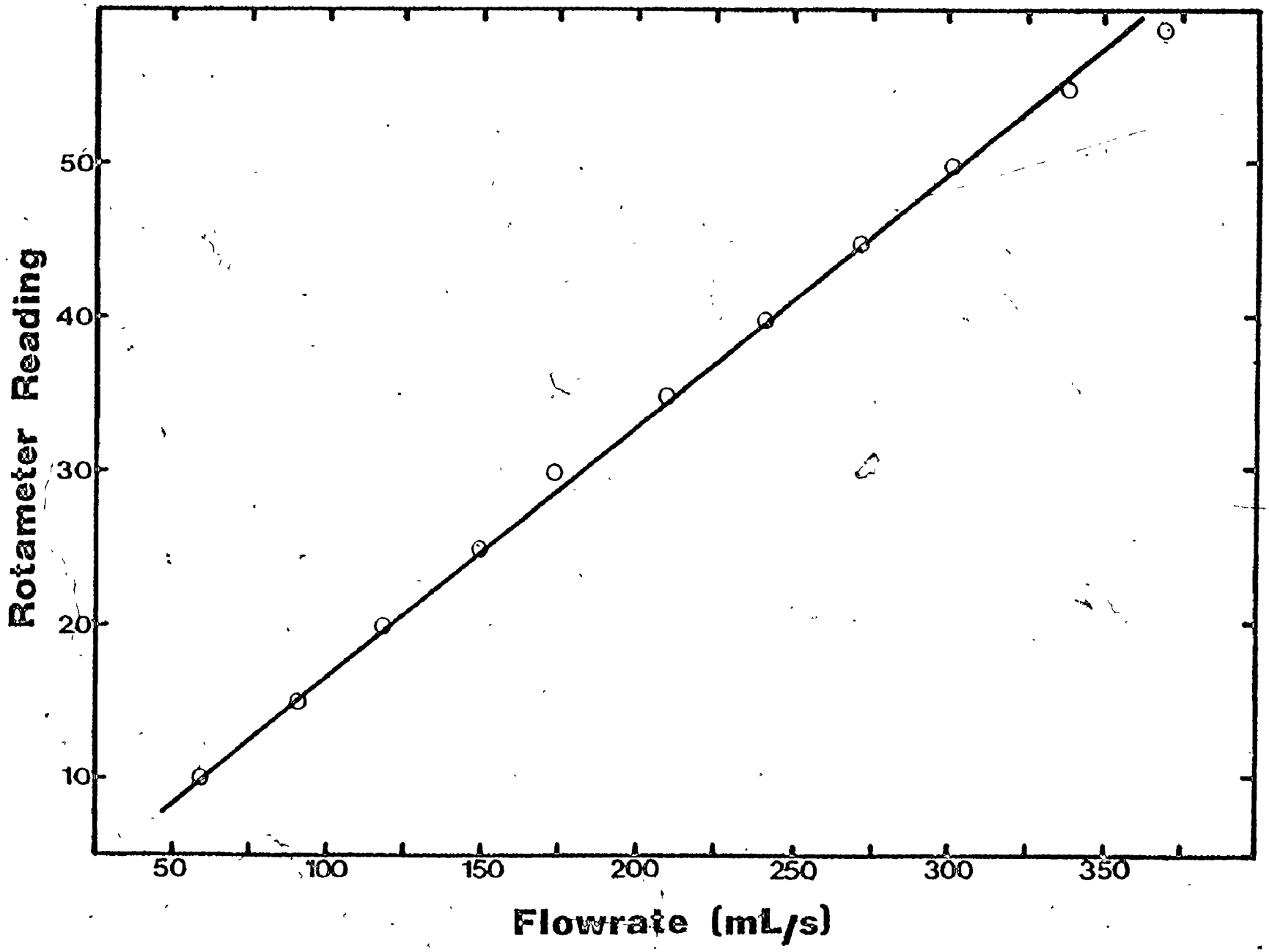

Figure A1 — 5

Rotameter Calibration Curve for Butanol

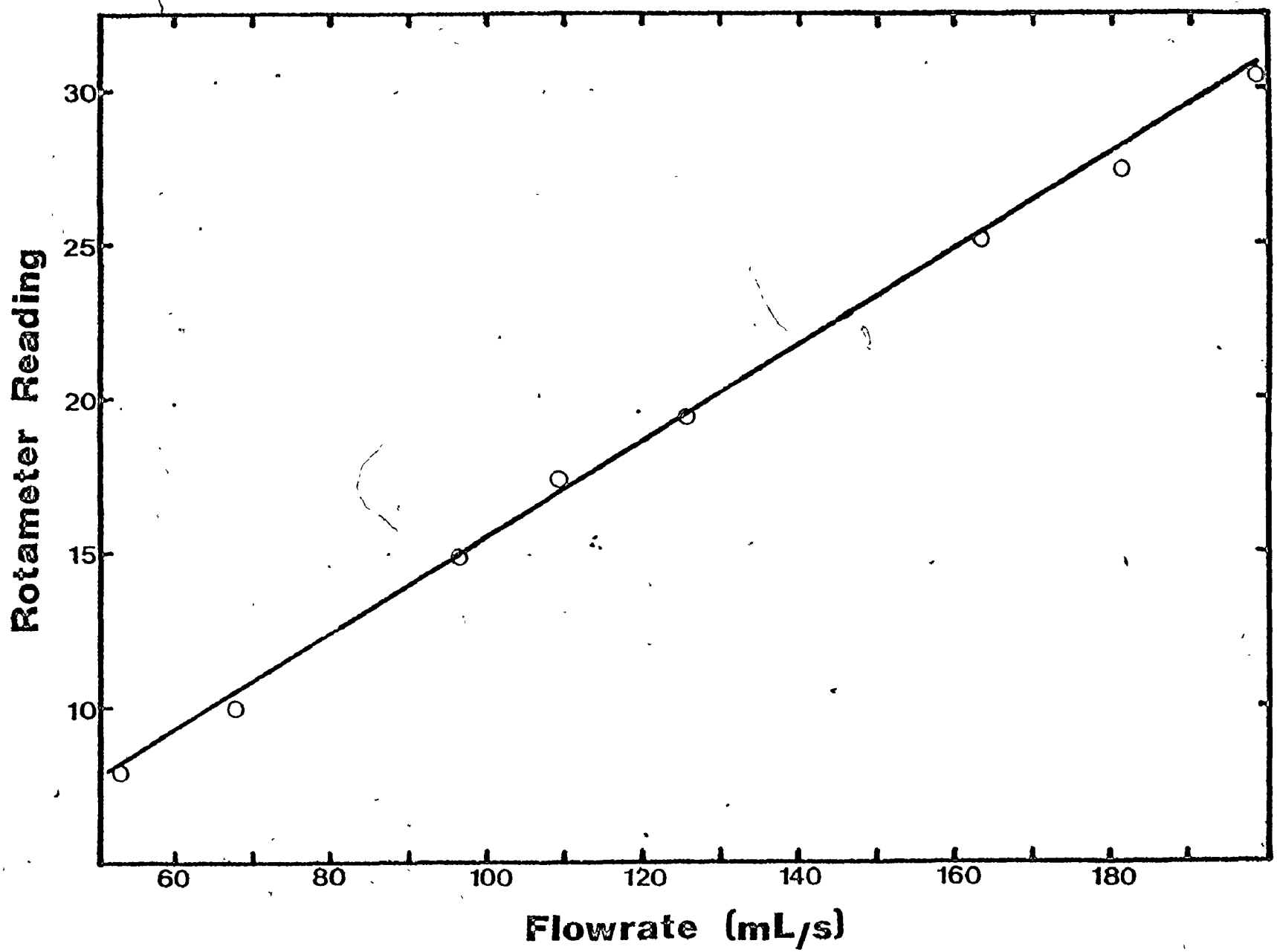

Figure A1 — 6

Rotameter Calibration Curve for MIBK

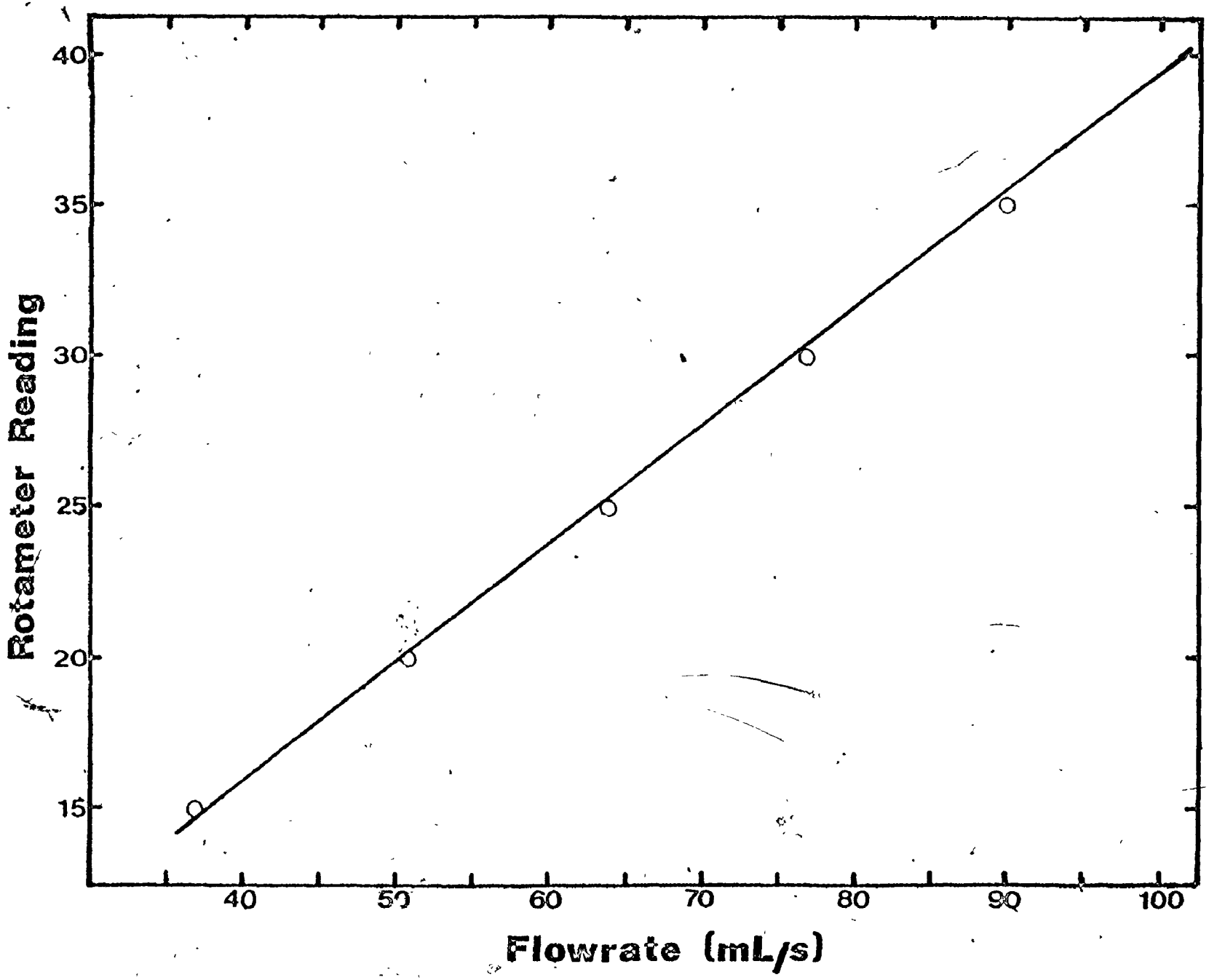

Rotameter Calibration Curve for Toluene

Figure A1 — 7

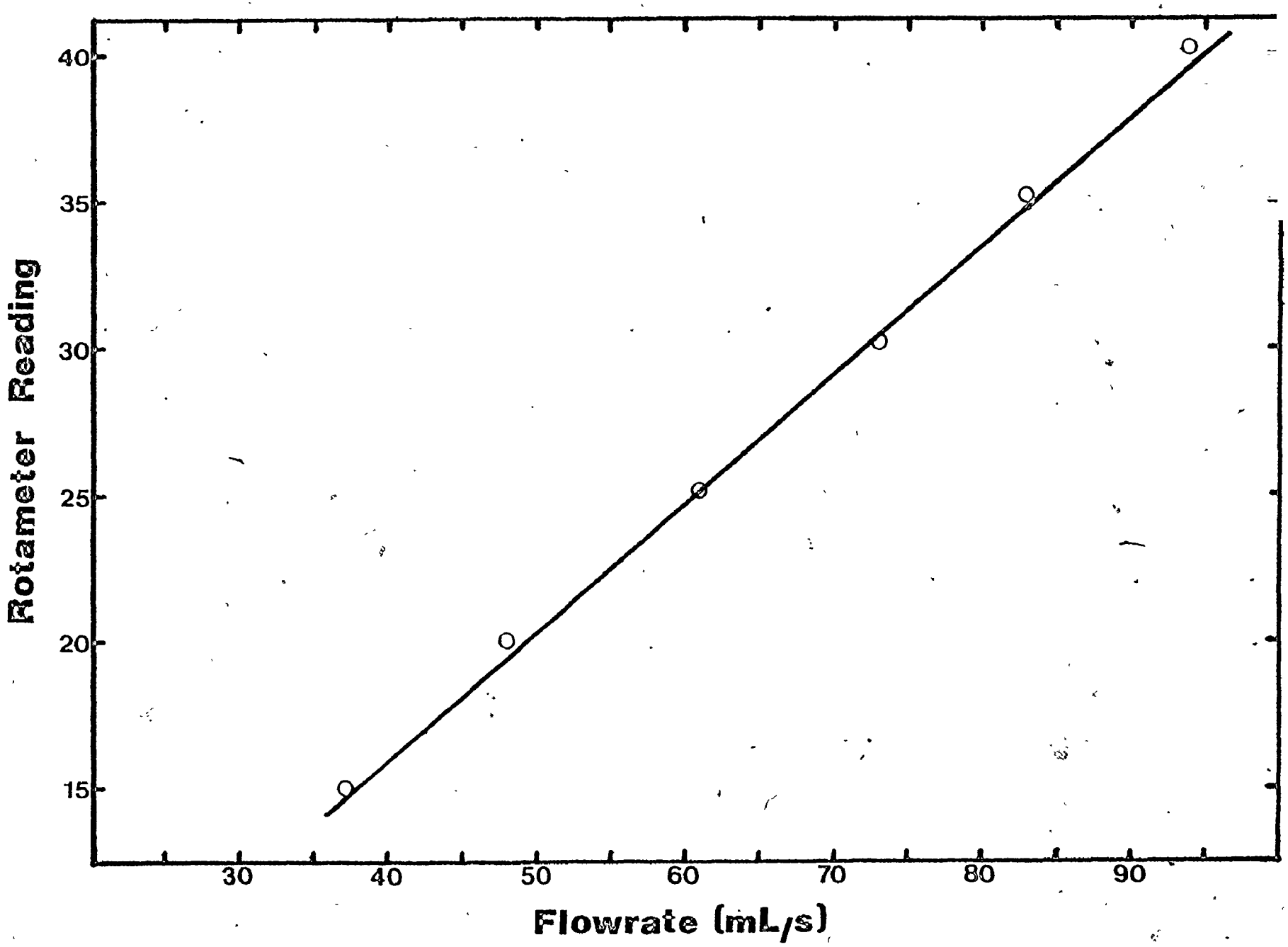

Rotameter Calibration Curve for Kerosene

Figure A1 — 8

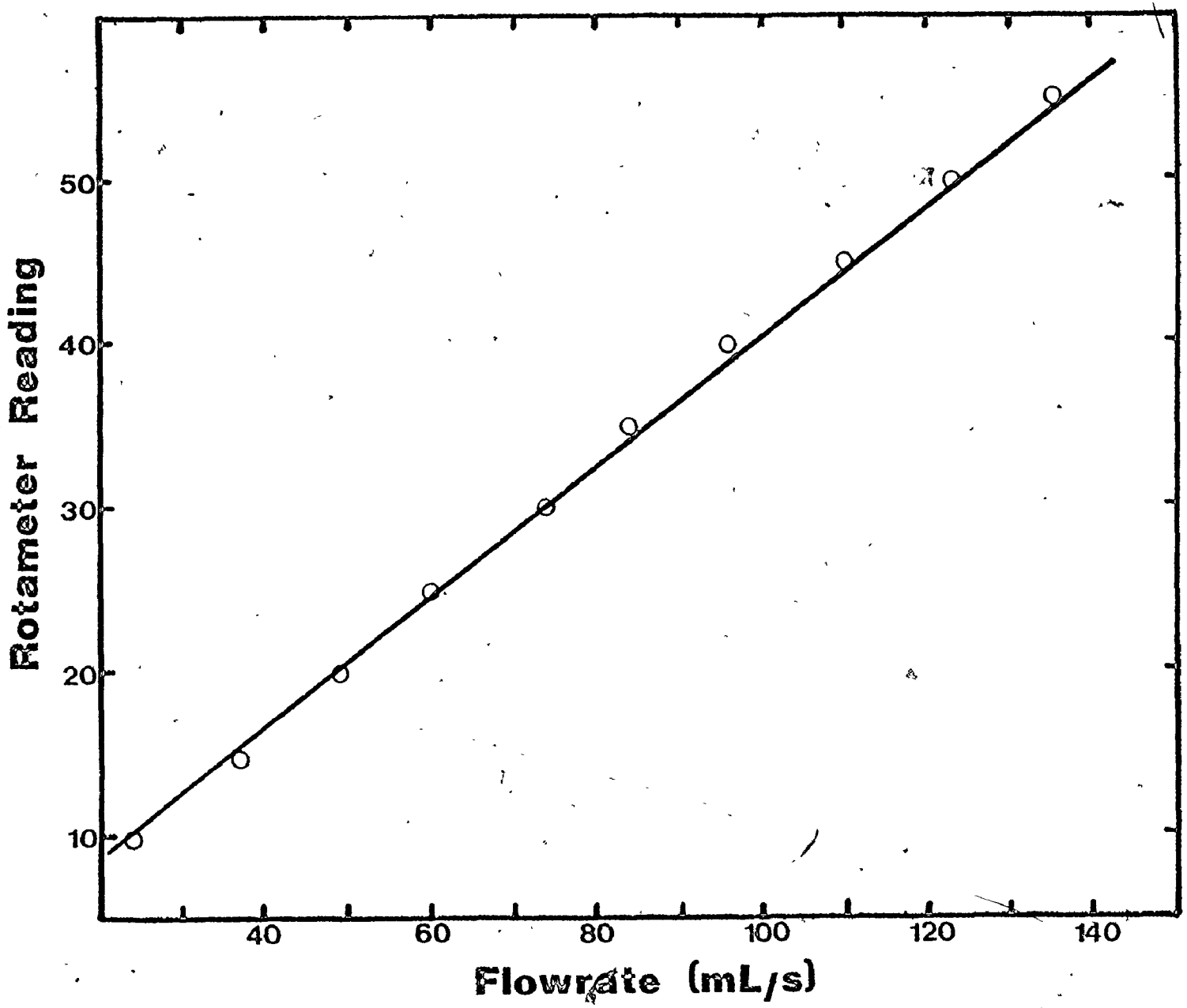

A1.5 Measurement Procedure

Based on the calibration charts, rotameters were set to reflect a particular phase ratio. After initiating flow through the system, a time allowance of 45 to 60s. was observed. A stopwatch was used to ensure observance of this time allotment. Tests verified that steady state was reached in 15s. or less. This was verified in Table A6-4, part (x), where, for time before sampling equal to 15 and 60s., E_s was 48.8 and 48.6% respectively. In addition, Burrill and Woods (B-3) using the same cyclone, noted rapid achievement of this condition. During the time allowance, readings were recorded for pressure at the four previously mentioned locations. A final check was made to ensure the rotameter readings had not deviated.

The flow was diverted to the sampling points. When the switch valves were shifted to allow sampling, the flowrate settings on the rotameters often changed. This was due to the differing resistance through the two pathways. A simple adjustment of the globe valves on the rotameters was the simplest solution.

To activated the time count while simultaneously switching flow to the sampling points, a timer was used that could be started or stopped by the press of a foot.

The collected samples were transferred from two 4000 mL. erhlenmeyer flasks to graduated cylinders to determine the proportions of the two phases in the overflow and underflow. Measured and calculated data are found in Appendices 6 and 7, respectively.

A1.6 Shut-down Procedure

After completion of runs for a particular liquid/liquid system, the water phase was disposed of via the sampling points to the drain outlet in the fume hood. The oil phase was also collected at the sampling points and placed in the solvent storage room.

A1.7 Treatment of Measured Data

Data collected, based on procedure outlined in A1.5, was formulated in Appendix 7. Calculations for E_s and pressure were performed.

First consider the derivation of the equation used to calculate E_s.

A1.7a Derivation of Efficiency of Separation Equation

For a liquid/liquid system, quality and quantity of both overflow and underflow is of interest.

Consider the overflow first. The idea was to calculate the amount of light phase leaving the overflow minus the amount of light phase leaving if no separation was occurring.

i) rate of light phase leaving overflow = $Z_oY_o = A_1$

ii) rate of light phase leaving overflow if no separation occurring: (A_2)

if X = volume of heavy phase

Y = volume of light phase

then $Y_f = Y/(Y + X)$

or $Y = X[Y_f/(1-Y_f)]$

rate of heavy phase exiting overflow = $Q_o(1-Y_o)$

$$A_2 = Q_o(1-Y_o)\,[Y_f/(1-Y_f)]$$

$$A_1 - A_2 = \frac{Q_o\,(Y_o - Y_f)}{(1-Y_f)}$$

Consider the underflow. The total rate of flow of heavy phase leaving the underflow minus the flowrate of heavy phase in the feed if no separation occurs.

i) heavy phase leaving underflow = $Q_u(1-Y_u) = B_1$

ii) heavy phase leaving underflow if no separation occurs: B_2

rate of light phase exiting underflow = $Q_u Y_u$

since $Y = X\left[\frac{Y_f}{(1-Y_f)}\right]$

$$X = Q_u Y_u \left[\frac{(1-Y_f)}{Y_f}\right] = B_2$$

$$B_1 - B_2 = \frac{Q_u(Y_f - Y_u)}{Y_f}$$

Combining the equations derived at the overflow and underflow, respectively, the equation for efficiency of separation is yielded:

$$E_s = \frac{Q_o}{Q_f}\left|\frac{(Y_o - Y_f)}{(1 - Y_f)}\right| + \frac{Q_u}{Q_f}\left|\frac{(Y_f - Y_u)}{Y_f}\right|$$

A1.7b <u>Calculation of Efficiency of Separation</u>

Based on the respective volumes of light and heavy phase at the overflow and underflow, the efficiency of separation (E_s) can be

determined.

Consider a run performed December 11 with the MIBK/water system:

Raw Data Table A1-1

	Volume (mL)	
	at underflow	at overflow
total	4120	2500
water	4060	1695
MIBK	60	805

volume split = 2500/4120 = 0.61

feed phase ratio = 865/5755 = 0.150

time of sampling = 66.8 s

feed flowrate = 6620/66.8 = 99 mL/s.

Y_f = 865/(865 + 5755) = 0.131 Y_u = 60/(60 + 4060) = 0.015

Y_o = 805/(805 + 1695) = 0.322

$$E_s = \frac{2500}{6620}\left[\frac{0.322 - 0.131}{1 - 0.131}\right] + \frac{4120}{6620}\left[\frac{0.131 - 0.015}{0.131}\right]$$

$$= 0.083 + 0.551 = 63.4\%$$

A1.7c Calculation of Pressure from Manometers

Mercury was added to the manometers. Since both limbs were exposed to the atmosphere, equivalent head was noted on both sides. For the feed and underflow a head of 82.5 cm. was noted; at the overflow the head was 82.0 cm.

Since one limb of each manometer was hooked up to the piping system, liquid filled it. This caused a head differential between the two limbs of approximately 3 cm. Consequently, the datum for the feed and underflow at the left and right limbs, respectively, was 84 and 81 cm. At the overflow, the head of the left and right limbs was 80.5 and 83.5 cm., respectively.

To determine the pressure at the feed, underflow and overflow sampling points, it was necessary to specify elevations with respect to readings on the manometers. The elevations of the feed, underflow and overflow were 150 cm. 98 cm. and 168 cm., respectively.

To demonstrate how pressure was calculated, consider the following example:

Run performed at Q_{MIN}, $(O/W)_{MIN}$ for the MIBK/water system.

feed: 101.0 cm.

underflow: 100.4 cm.

overflow: 99.5 cm.

The above values represent readings taken on the rising limb <u>or</u> the limb which is open to the atmosphere.

(i) <u>Feed</u>

$$101.0 - 84.0 = 17 \text{ cm.Hg.}$$

$$81.0 - 17.0 = 64 \text{ cm.Hg.}$$

$$\Delta h = 101.0 - 67.0 = 37 \text{ cm.Hg.}$$

Subtract from this 3 cm. due to static head

$$\Delta h_{corrected} = 37 - 3 = 34 \text{ cm.Hg.}$$

The difference in the elevation between the falling limb and the feed is (150 - 81) + (81 - 64) = 86 cm.

$$P_f = \frac{(62.4)(13.6)(34)}{(30.5)(144)} - \frac{(62.4)(86)}{(30.5)(144)} = 5.3 \text{ lb./in.}^2$$

(ii) Underflow

100.4 - 84 = 16.4 cm.Hg.

81 - 16.4 = 64.6 cm.Hg.

$\Delta h_{corrected}$ = (100.4 - 64.6) - 3 = 32.8 cm.Hg.

difference in elevation = (98 - 81) + (81 -64.6) = 33.4 cm.

$$P_u = \frac{(62.4)(13.6)(32.8)}{(30.5)(144)} - \frac{(62.4)(33.4)}{(30.5)(144)} = 5.9 \text{ lb./in.}^2$$

(iii) Overflow

99.5 - 83.5 = 16 cm.Hg.

80.5 - 16 = 64.5 cm.Hg.

$\Delta h_{corrected}$ = (99.5 - 64.5) - 3 = 32 cm.Hg.

difference in elevation = (168 - 80.5) + (80.5 - 64.5) = 103.5 cm.

$$P_o = \frac{(62.4)(13.6)(32)}{(30.5)(144)} - \frac{(62.4)(103.5)}{(30.5)(144)} = 4.7 \text{ lb/in.}^2$$

Why is the pressure greater at the underflow than at the feed? It is a result of calculating pressures at different elevations. Determine the pressure at the overflow and underflow with respect to the feed.

$\Delta h_{u/f}$ = 150 - 98 = 52 cm.

$$P_u = 5.9 - \frac{(62.4)(52)}{(30.5)(144)} = 5.2 \text{ lb/in.}^2$$

$$\Delta h_{o/f} = 168 - 150 = 18 \text{ cm.}$$

$$P_o = 4.7 + \frac{(62.4)(18)}{(30.5)(144)} = 5.0 \text{ lb/in.}^2$$

Summary

	P_f	P_u (lb./in.^{2})	P_o
unadjusted	5.3	5.9	4.7
adjusted	5.3	5.2	5.0

Calculated values for pressure in Appendix 7 are unadjusted.

APPENDIX 2

DROPLET SIZE MEASUREMENT

A2 DROPLET SIZE MEASUREMENT

For the different liquid/liquid systems studied, it was important to gain some knowledge about the droplet size entering and leaving the hydrocyclone.

A2.1 Use of the Coulter Counter

Initially it was felt that the Coulter Counter could be utilized for this purpose. Sampling points were located at the inflow to and outflow from the cyclone. Samples were withdrawn from the system by means of a syringe and needle.

The Coulter Counter under study, Model Z_B, consisted of four components. The first component, known as the sample stand, provide for the emulsion to be drawn through an orifice in a glass tube; the suction was provide by a vacuum pump. Orifice sizes ranged from 30 to 1000 microns. A size was selected which would allow all droplets to pass through. Before being drawn through the orifice, the sample was mixed with a conducting solution, known commercially as Isoton. The droplets, drawn through the orifice, were counted and sized based on the electrical resistance across the orifice. The second piece of equipment, the counter, monitored and counted the voltage pulses received from the sample stand. A pulse was registered for each droplet that passed through the orifice. The next component, known as a channelyzer, monitored the pulse received by the counter. The larger the pulse, the greater the size of the droplet. The channelyzer had the ability

to compile the size distribution passing through the orifice and transform it onto a screen, in either a linear or logarithmic mode. Finally, a teletype, which was connected to the channelyzer, converted the distribution displayed on the screen, into a print-out.

It was hoped that the emulsion, when withdrawn from the system, would behave in a stable manner. Literature forwarded by Coulter Electronics (C-1) suggested success had been met in the counting and sizing of milk solids and blood cells.

As a preliminary step, the Coulter Counter was calibrated with a known particle size; in this case it was a monodispersed polystyrene particle. A toluene/water system was run to evaluate the feasibility of this sampling method. The withdrawn sample was observed to be a very unstable dispersion. The two phases separated within seconds. Stabilization of emulsions can be achieved by either lowering the temperature or by adding another liquid to increase viscosity. Glycerol was placed in a test tube and then the liquid/liquid dispersion was added. By adding 75% volume fraction of glycerol, viscosity was increased forty fold; however a test run revealed that rapid coalescence of the dispersion still occurred.

It was decided that another method would be attempted.

A2.2 Use of a Photographic Method

Past work by Burrill and Woods (B-3) utilized a photographic method to study the oil/water dispersion in situ. This involved the construction of an optical cell. By means of O-rings, the plexiglass

cell was fitted over a transparent, thick-walled section of glass tubing. The optical cell was used to prevent distortion of the photographed droplets. This was accomplished by adding a layer of water between the inside and outside surfaces of the optical cell and glass wall, respectively.

A2.2a Method of Counting and Sizing of Droplets

Overall the photographic method was quite reliable. Its major drawback was the labourious nature involved in sizing the droplets. The Zeiss Particle Size Analyzer somewhat facilitated this task.

The principle of measuring droplet size with the Zeiss Instrument was based on approximating an equivalent diameter with a light source that has a standard size range from 1.2 to 27.7 mm. Under the reduced mode, sizes range from 0.4 to 9.2 mm. The size range was divided into 48 intervals. These intervals can either be linearly or exponentially spaced. The tally for each size interval can be set either to reflect the number of droplets within this interval or the number less than or equal to it.

Measurements were carried out in a darkened room where the effect of the illuminated light source was highlighted. After approximating the size of a particular droplet, a foot pedal was used to activate an arm with a needle attached to the end. The needle was positioned directly vertical to the light source. It punched a hole through the droplet on the blow-up, preventing it from being recounted. At the same time that the needle punctured the paper, the droplet size

was recorded on the counter.

A2.2b Selection of Other Components

A 35 mm. Pentax Asahi camera was used for this work. Black and white, Panatomic-X film of ASA 32 was used. A Braun electronic flash unit was used as the light source. The advantages of this unit were notable over that used by Burrill and Woods (B-3). First the chosen unit was light weight and compact enough to fit in the palm of one's hand. In addition, the flash unit was connected to the camera. A press of the shutter release caused the flash unit to simultaneously illuminate the optical cell. Since the unit employed by Burrill was not connected to the camera, all photographic work had to be performed in darkness. This was necessary since the camera shutter was opened in preparation for the flash of the light source. The advantage of Burrill's unit was the shorter duration of flash. This allowed the photographing of faster moving droplets.

With the conventional arrangement, it was possible to focus on objects only as close as 1.5 feet. Since it was required to focus on droplets within 1 to 2 inches from the lens, an extension tube and bellows was inserted between the camera body and lens.

Initially it was believed that a tripod would provide adequate support for the camera; however due to the confined working quarters, it was difficult not to bump against the tripod. Bumping it could result in knocking the camera out of focus after it had been properly positioned. Instead of the tripod, a three-armed arrangement was

connected directly to the pipe system by means of clamps. The camera was connected to this support by means of a C-clamp. This set-up provided a very stable arrangement without taking up a great deal of space. It was easily dismantled and reassembled from one optical cell to another in a short time. A photograph of the camera set-up is shown in Figure A2-1.

A2.2c Establishing Optimum Conditions

Initial runs were carried out to determine the proper lighting conditions. It was found that an aperture setting of f/11 with the light source at roughly 10 cm. behind the optical cell provided the best results.

All photographic work was performed at $(O/W)_{MIN}$. Under these conditions an attempt was made to obtain droplet photos at the feed optical cell for the butanol/water system. Initial attempts were unsuccessful. No droplets were distinguishable. It was performed at Q_{MAX}, which represented a velocity of roughly 10 ft./s. By opening the diversion line valve completely, the velocity past the cell was reduced to 5 ft./s. Even with the reduction, droplets were not distinguishable on the photos. To further reduce the flow, gate valves at the underflow and overflow were partially closed. This reduced the velocity past the feed cell to nearly 2.5 ft./s. At this velocity, some success was achieved. Better quality photos were obtained at the overflow and underflow cells due to the lower velocity as compared to the feed.

Setup for Photographic Work

Figure A2 — 1

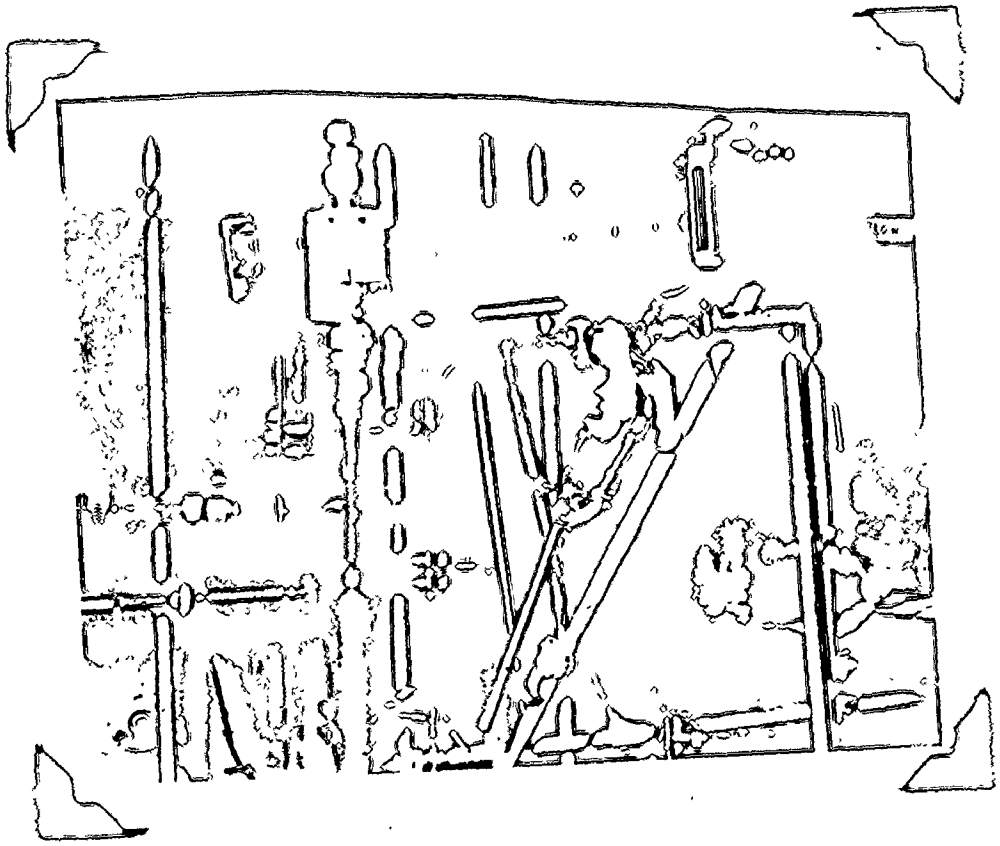

A2.3 Photographic Procedure

After the camera was attached to the support arrangement, it was focused on slow moving oil droplets inside the glass tube. After starting the system at the prescribed phase ratio, a period of 30 to 60s. was allowed before sampling to ensure a steady state condition. At this point a series of photos was taken in rapid succession, at approximately 5s. intervals. A cable release was used to reduce the chance of jarring the camera out of focus. At the same time that the photos were taken, a sample of the overflow and underflow was collected. This supplied information on volume split, phase ratio, flowrate and E_s. At each optical cell an attempt was made to photograph under comparable conditions. Ideally the best situation would be to take photos simultaneously at the three points of interest; however due to equipment requirements and lack of space, this was not practical.

It was determined that the best location to focus was just inside the inner wall of the glass tube. By focusing towards the center of the glass tube, droplets in front of the focal plane hindered the quality of the photo.

Figure A2-2 shows a photo of droplets at each cell location for the MIBK/water system.

To determine the time of coalescence for the dispersed phase, in situ, a simple technique was employed. The camera arrangement was set up at the feed optical cell. Flow through the pipes was initiated at a phase ratio of $(O/W)_{MIN}$. After allowing a short time for steady state to be reached, the flow was suddenly stopped by

MIBK Droplets at each Optical Cell

Figure A2 — 2

1) Feed

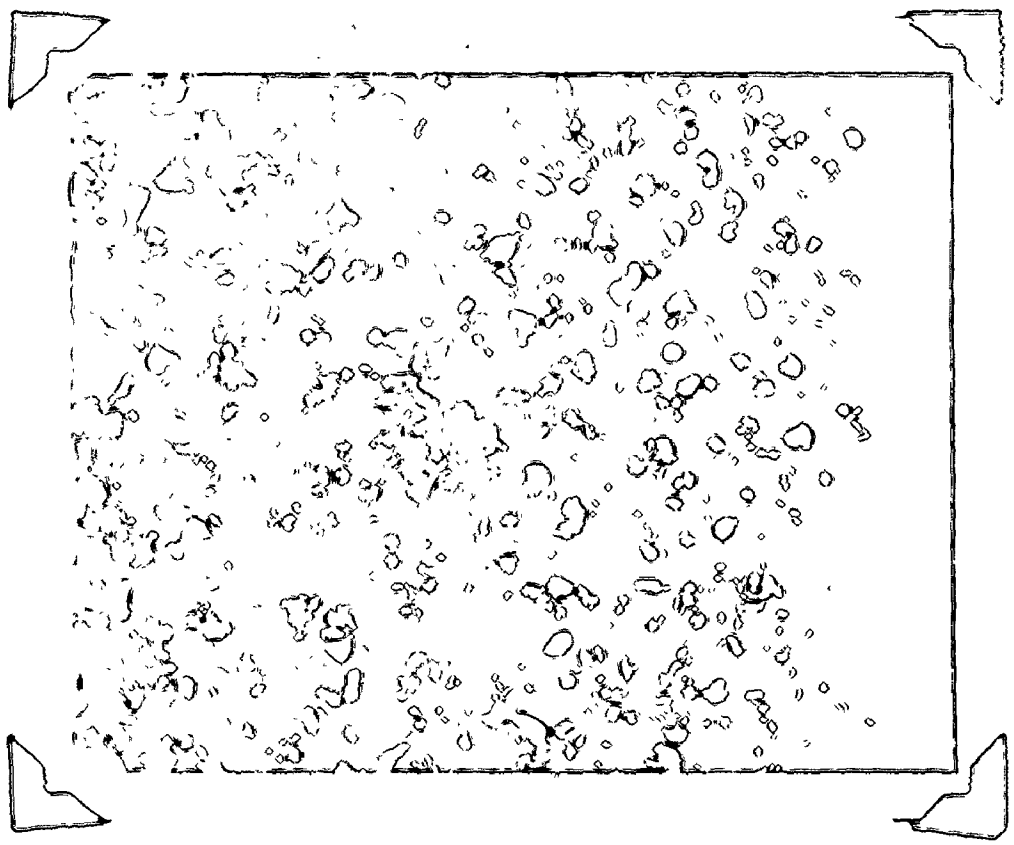

Approx
Scale
same for all
locations)

microns 1000 500 0

2) Overflow

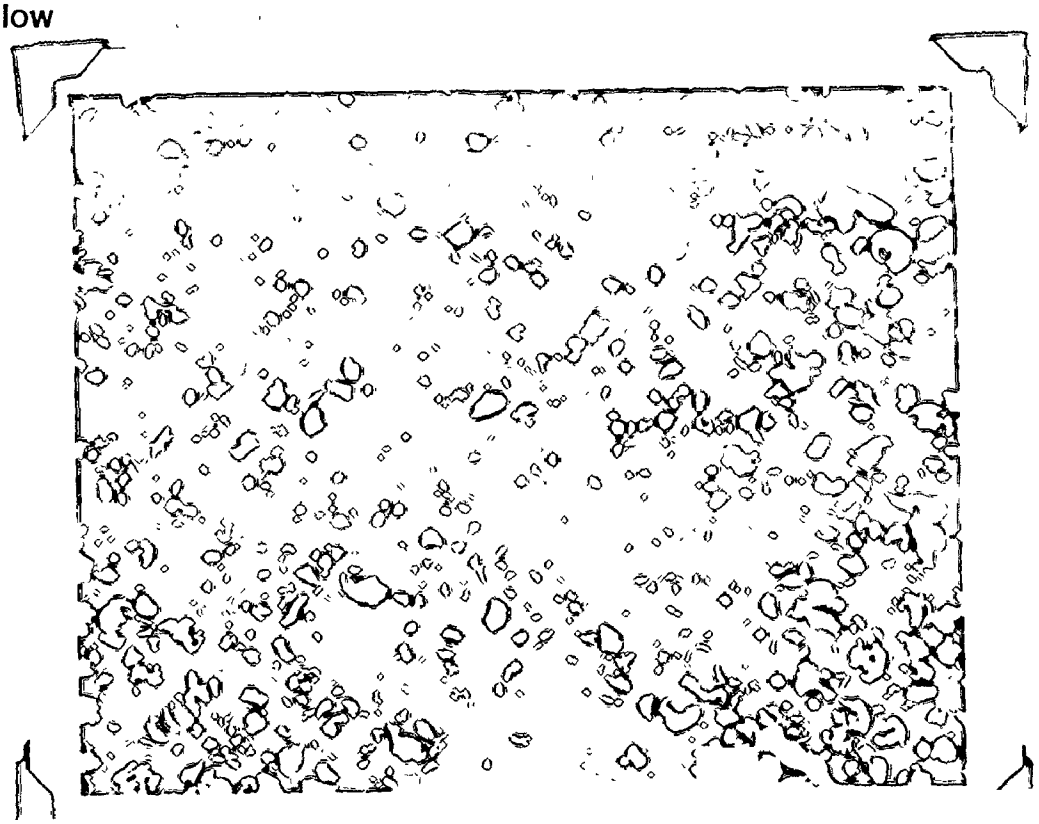

Figure A2 — 2 cont'd

3) Underflow

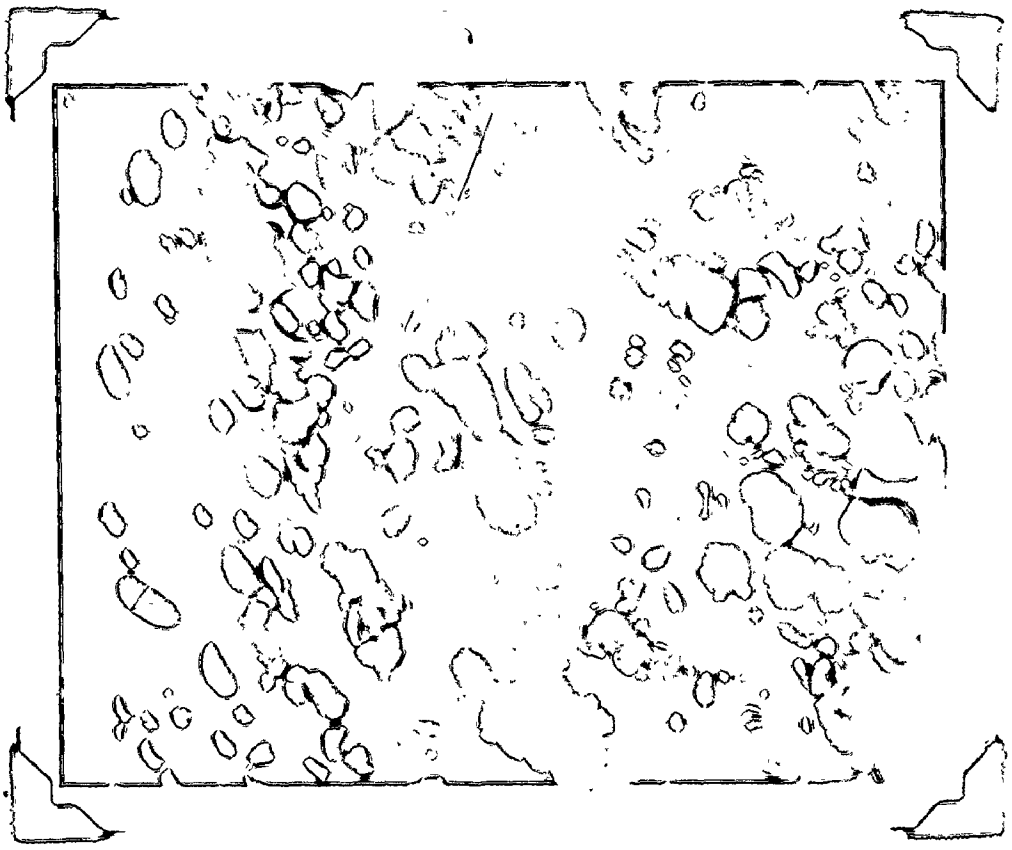

simultaneously closing both globe valves on the rotameters. At this instance, the first photo was snapped. Further photos were taken at intervals which depended on the rate of coalescence. Figure A2-3 shows the change in droplet size with increase in time of coalescence for the MIBK/water system.

A2.4 Measurement Procedure

After completing a series of shots at one location, a ruler positioned beside the optical cell was photographed. This helped to determine the magnification due to the extension tube and bellows, and print blow-up. Print blow-up was dictated by the droplet size. The smaller the droplet, the greater the magnification required. It was important that all droplet sizes were magnified to a degree which allowed them to be sized on either the standard or reduced range. Magnification due to print blow-up ranged from 3.5 to 12.0 times; due to the extension tube and bellows magnification ranged from 3.5-4.0 times, depending on the focusing at the different locations. On occasions where the photograph of the ruler did not develop, a magnification, due to extension tube and bellows, of 3.75 was assumed.

Figures A2-4 to A2-16 contains cumulative number distributions for the four liquid/liquid systems studied. Figures A2-17 and A2-18 relate specifically to the coalescence work for the butanol/water and MIBK/water systems. Based on these plots, D_{50} was determined at each time interval and plotted in Figure A2-19. Data for the coalescence work is summarized in Table A2-1.

The number of droplets counted per series of photos at a

Coalescence of MIBK Droplets

Figure A2 — 3

1) at t=0 s.

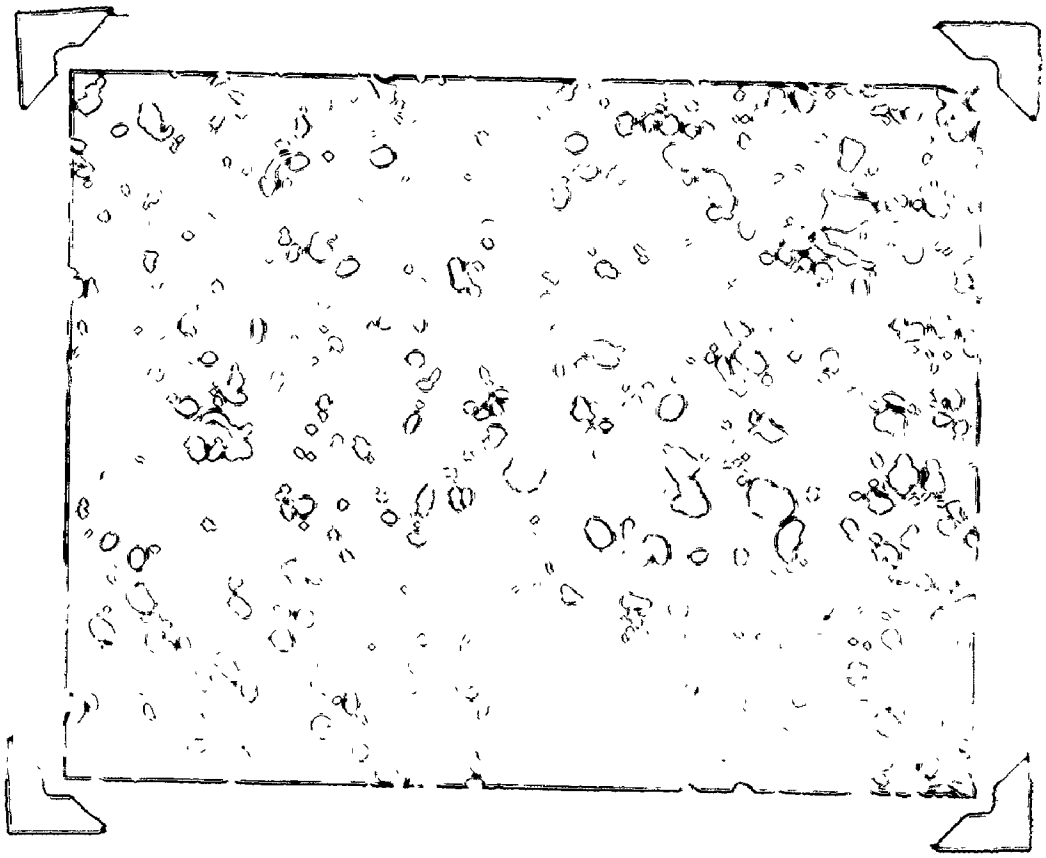

time intervals

microns 1000 500 0

2) at t=5 s.

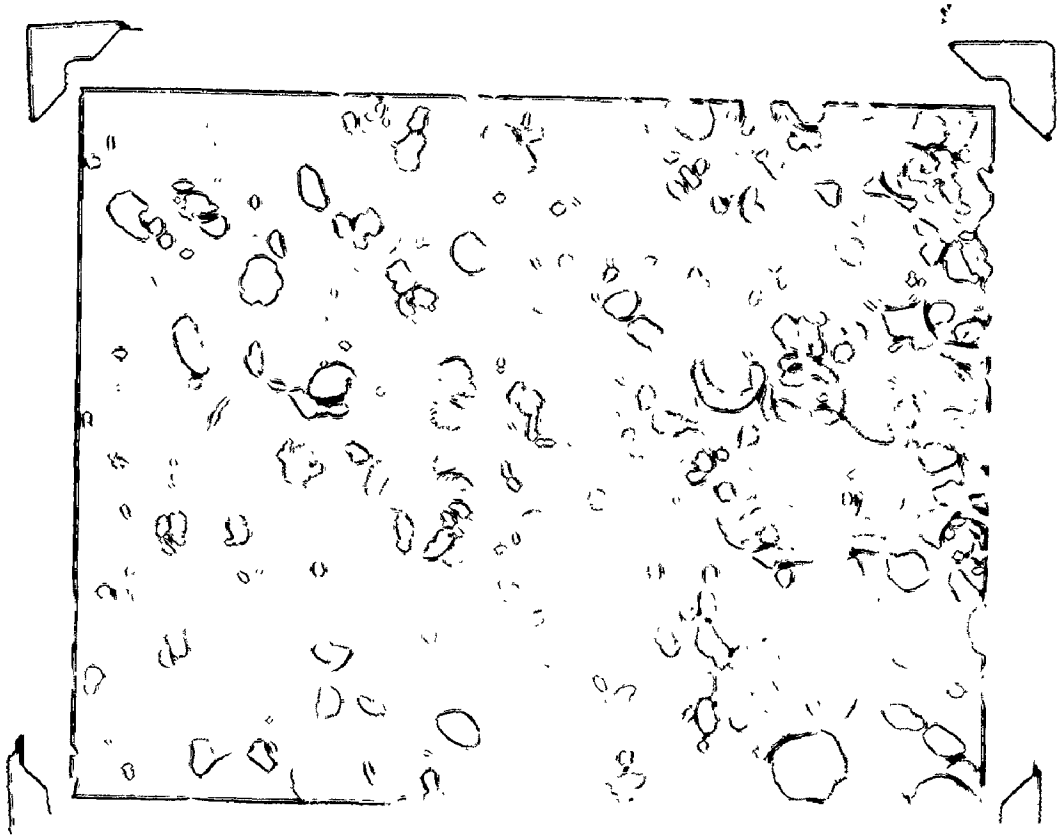

Figure A2 — 3 cont'd

3) at t = 10 s.

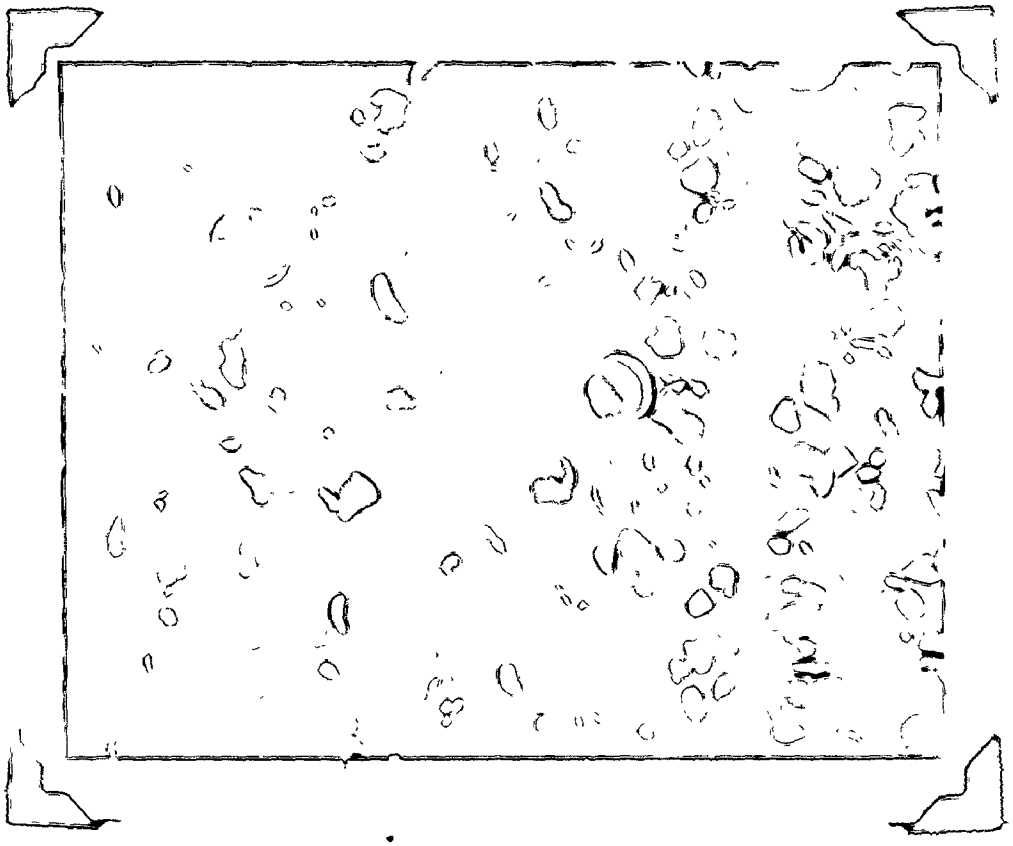

4) at t = 15 s.

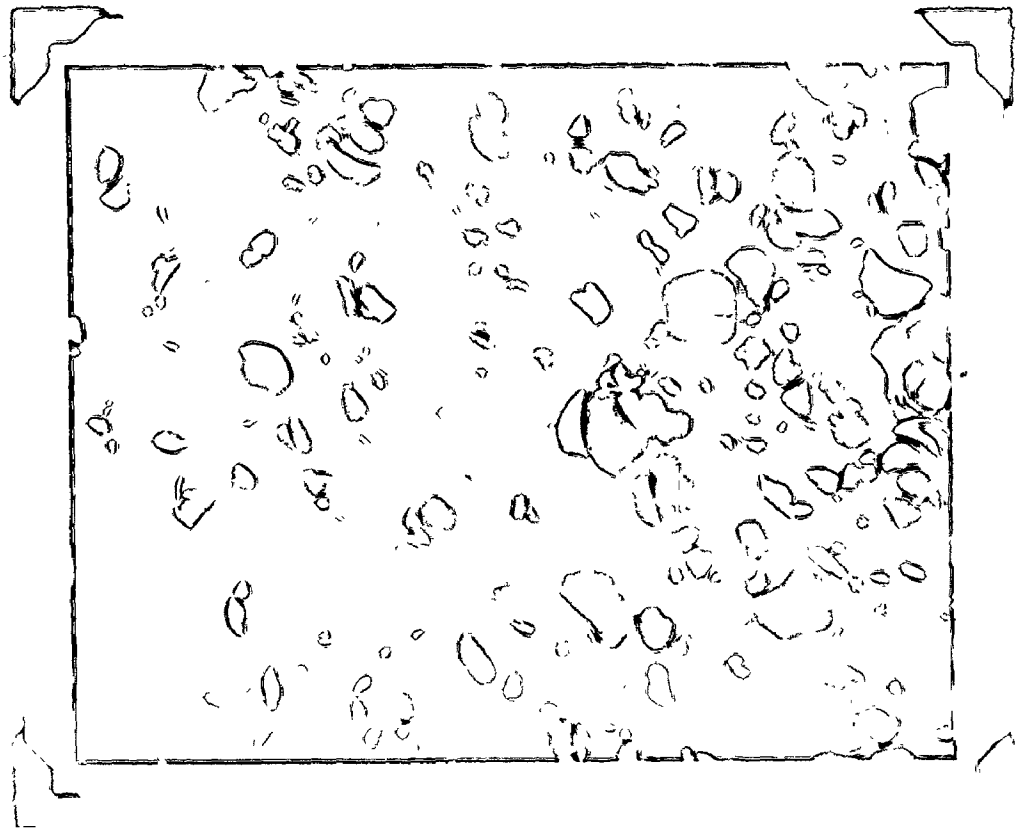

Droplet Size Distribution for Butanol/Water

Figure A2 — 4

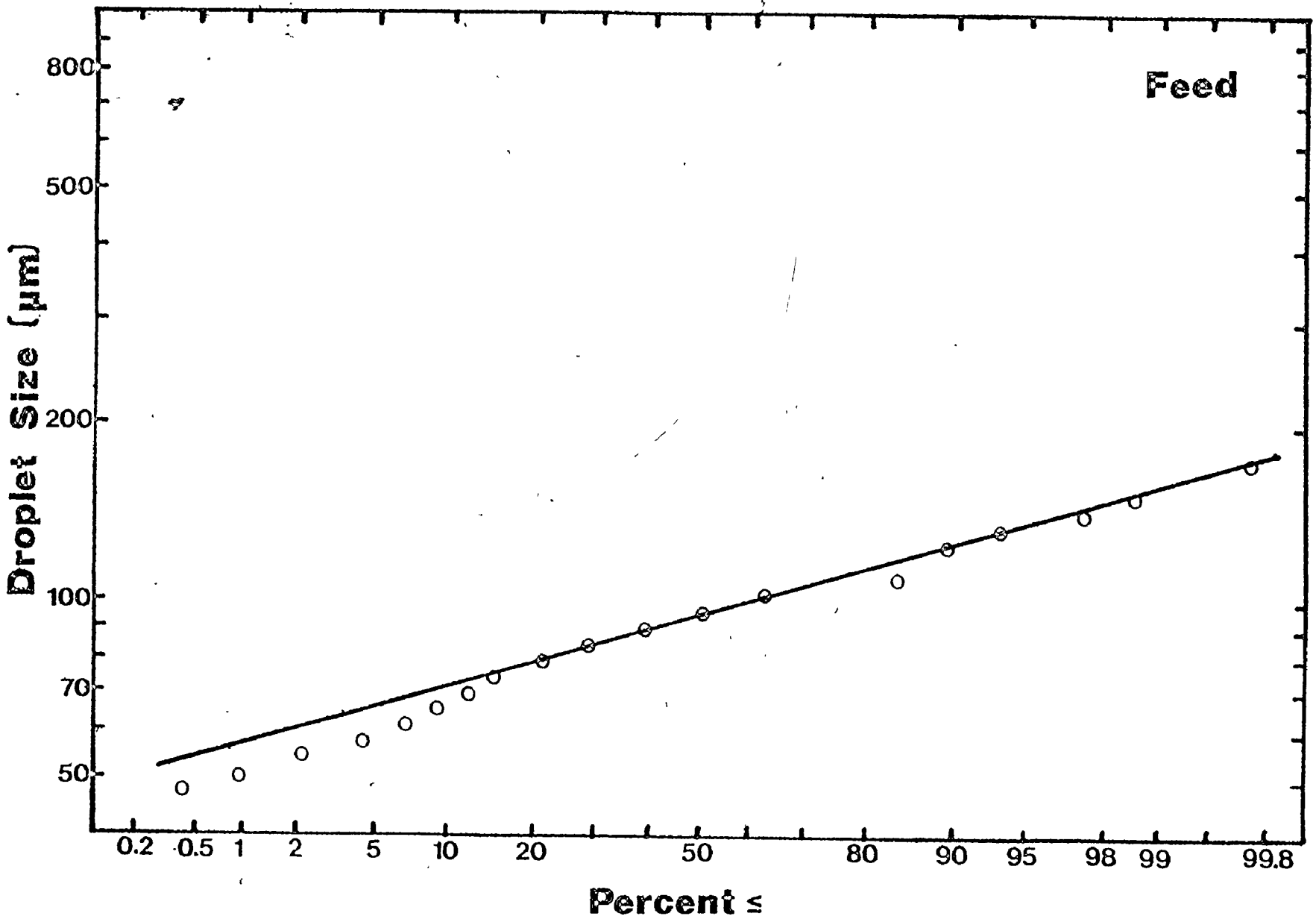

Droplet Size Distribution for Butanol/Water

Figure A2 — 5

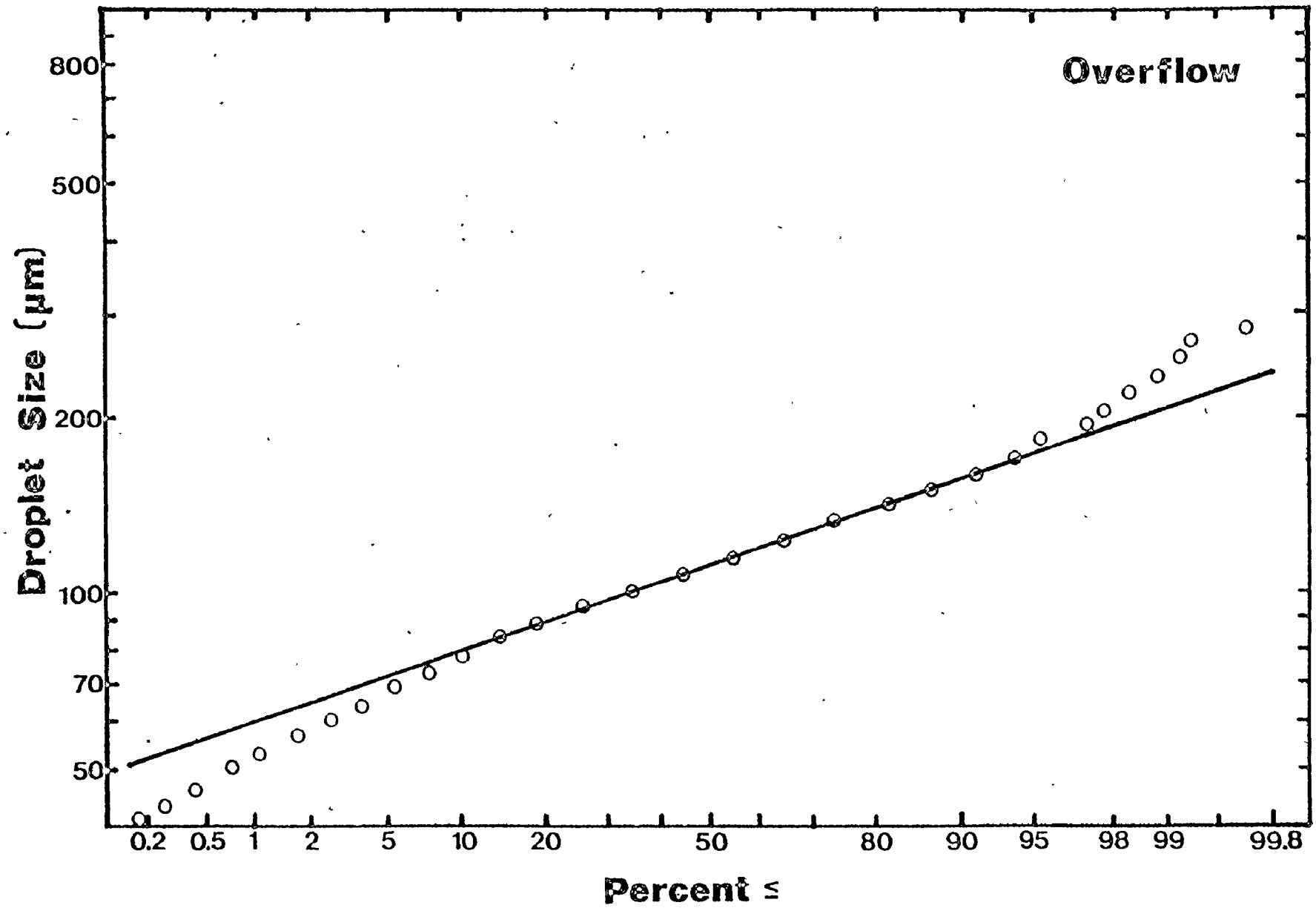

Droplet Size Distribution for Butanol/Water

Figure A2 — 6

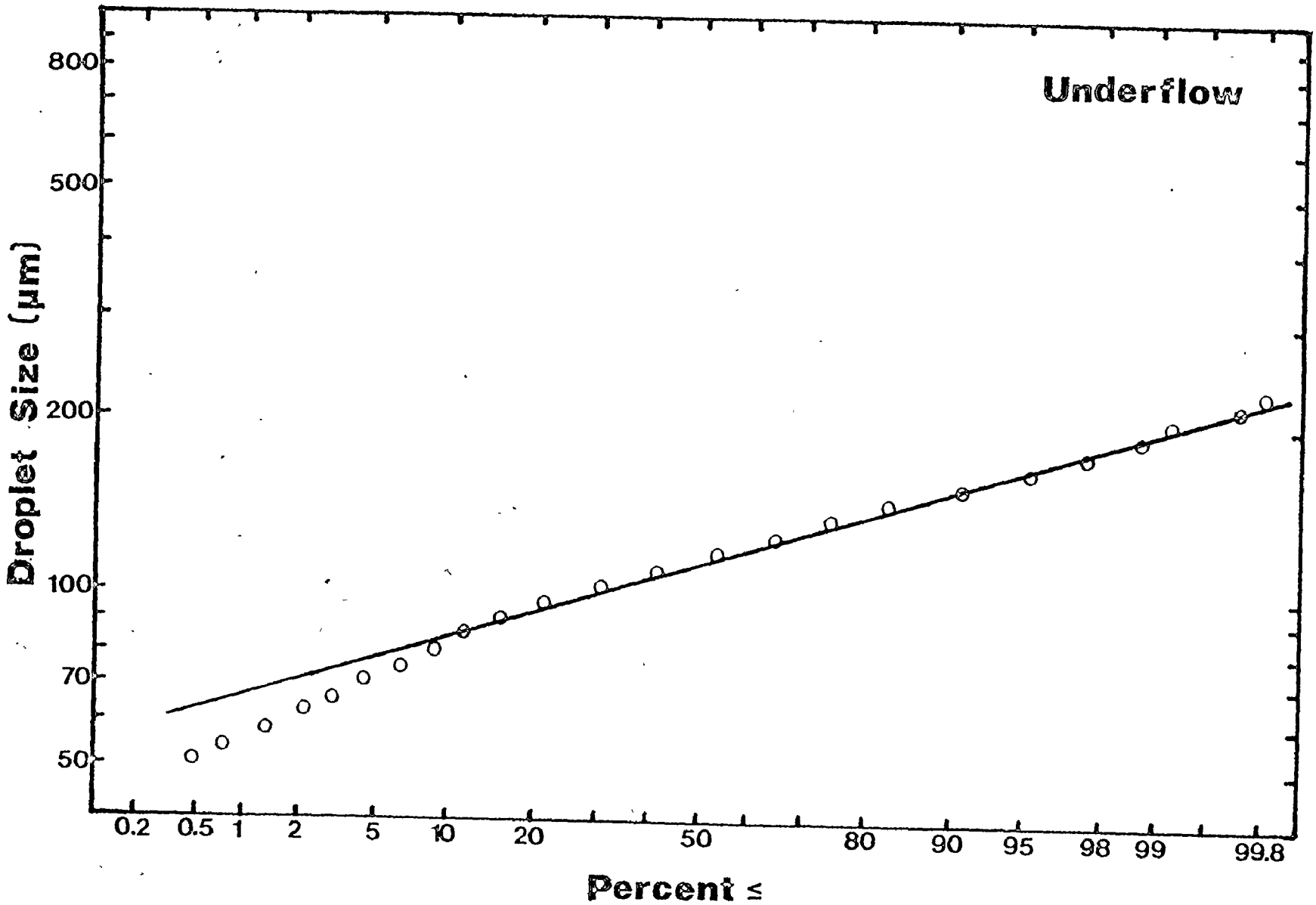

Droplet Size Distribution for MIBK/Water

Figure A2 — 7

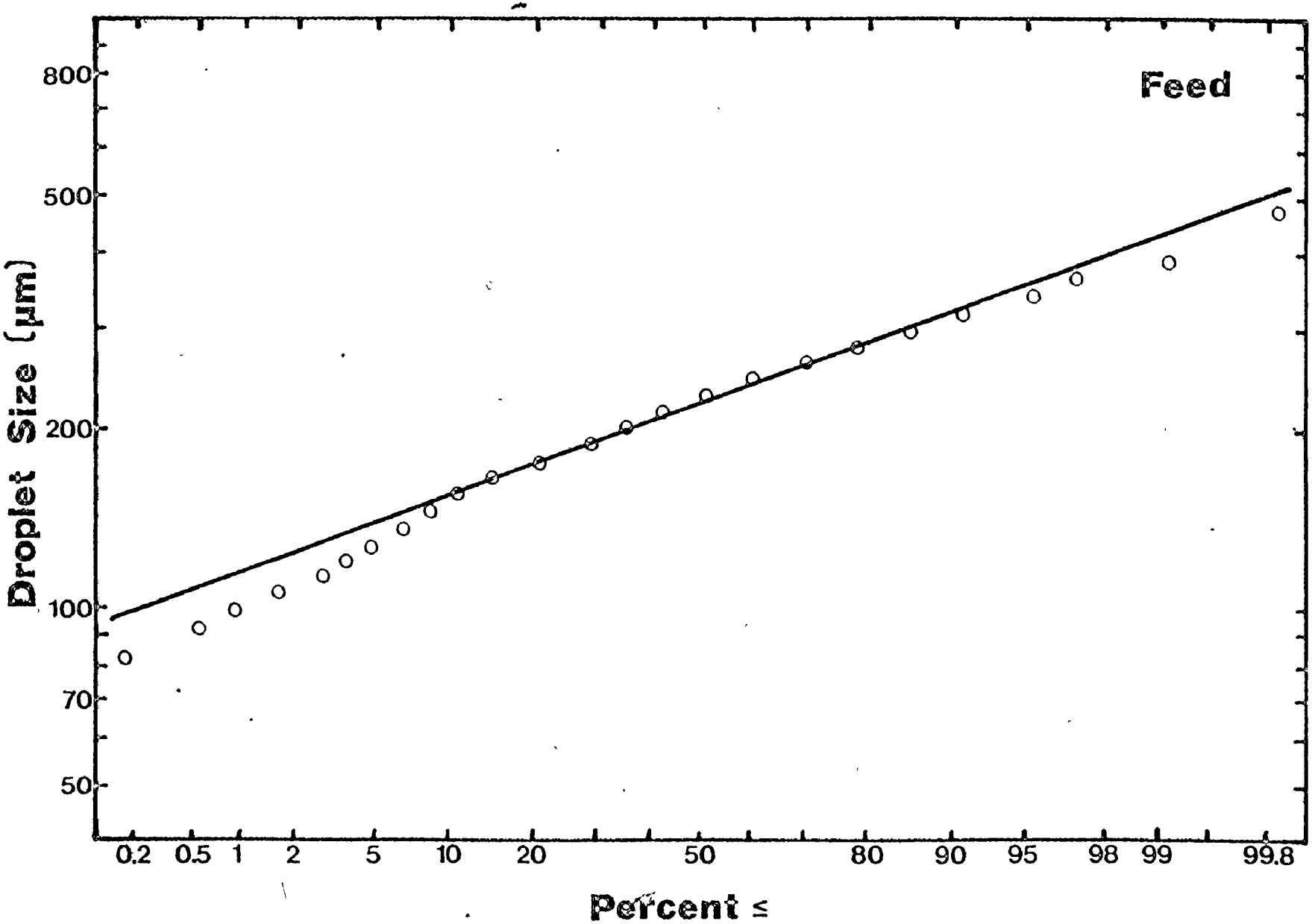

Droplet Size Distribution for MIBK/Water

Figure A2 — 8

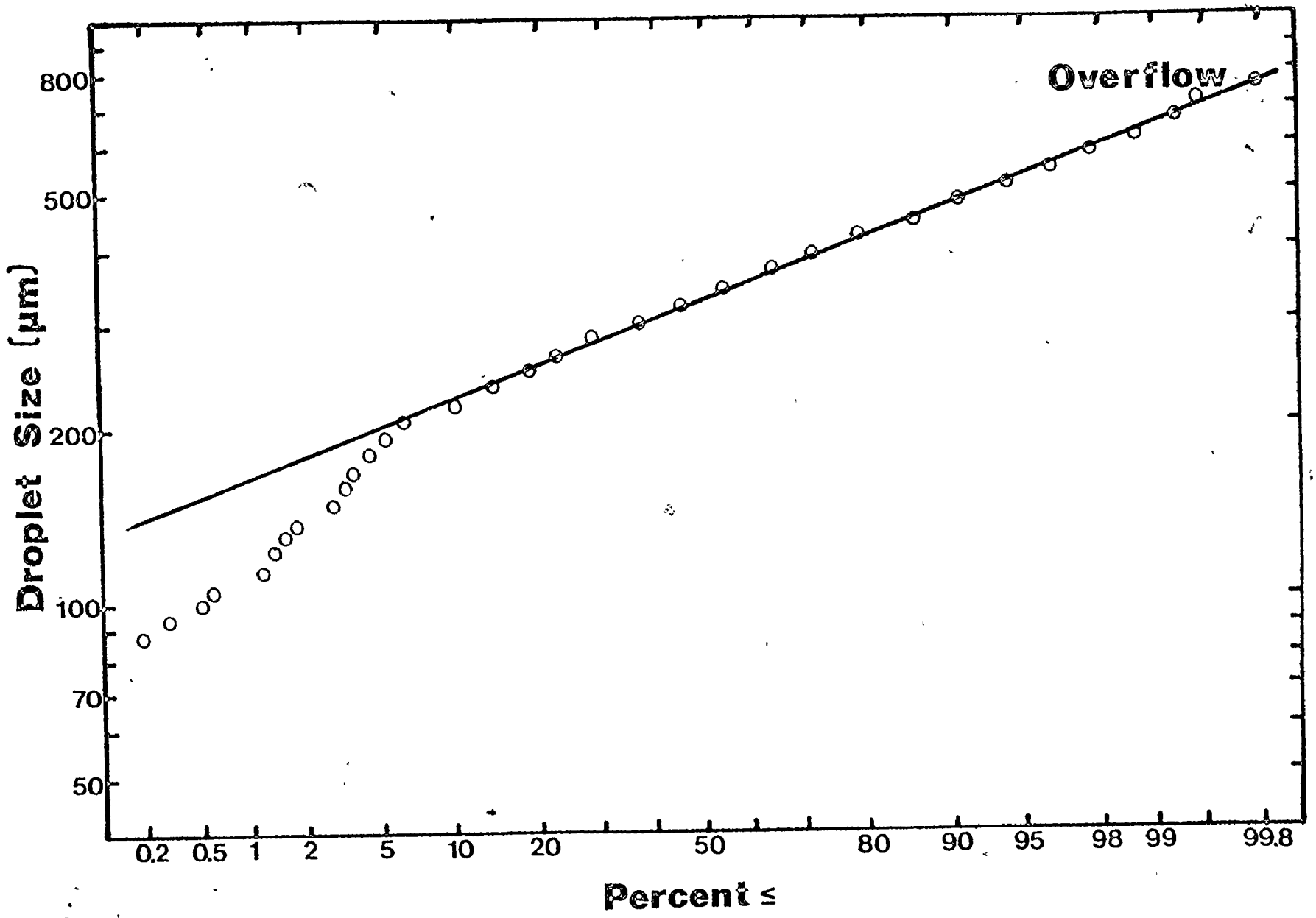

Droplet Size Distribution for MIBK/Water

Figure A2 — 9

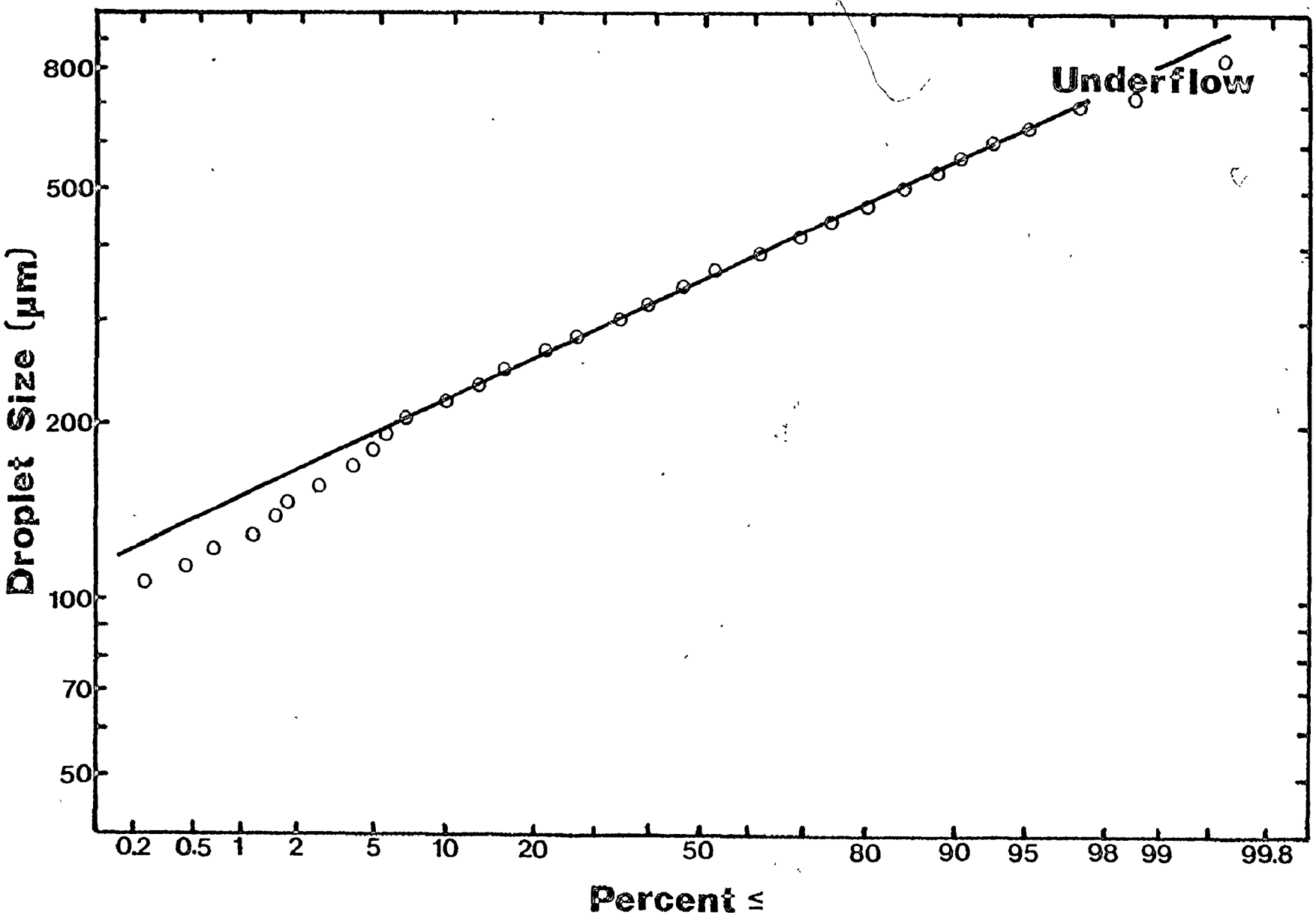

Droplet Size Distribution for Toluene/Water

Figure A2 — 10

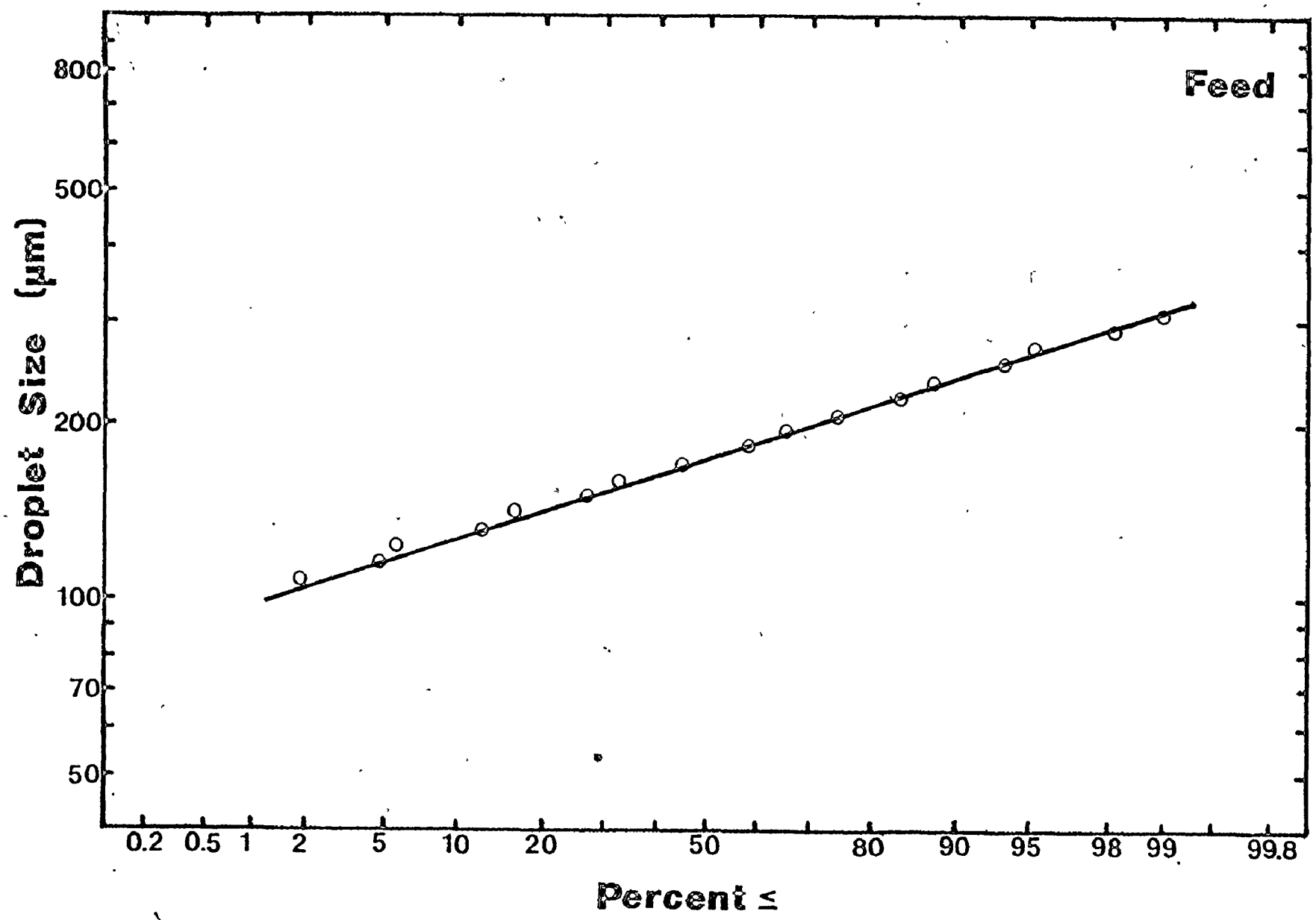

Droplet Size Distribution for Toluene/Water

Figure A2 — 11

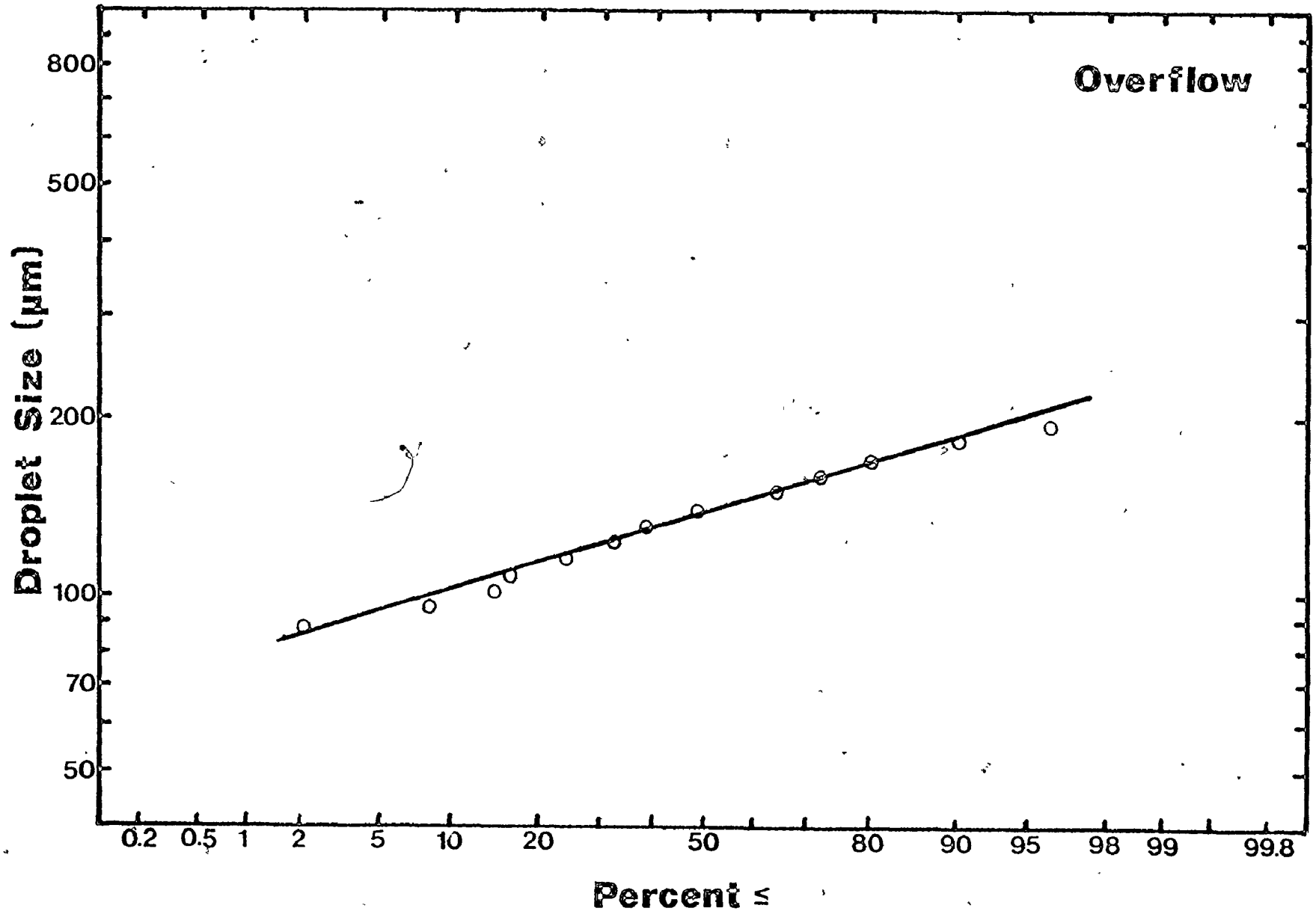

Droplet Size Distribution for Toluene/Water

Figure A2 — 12

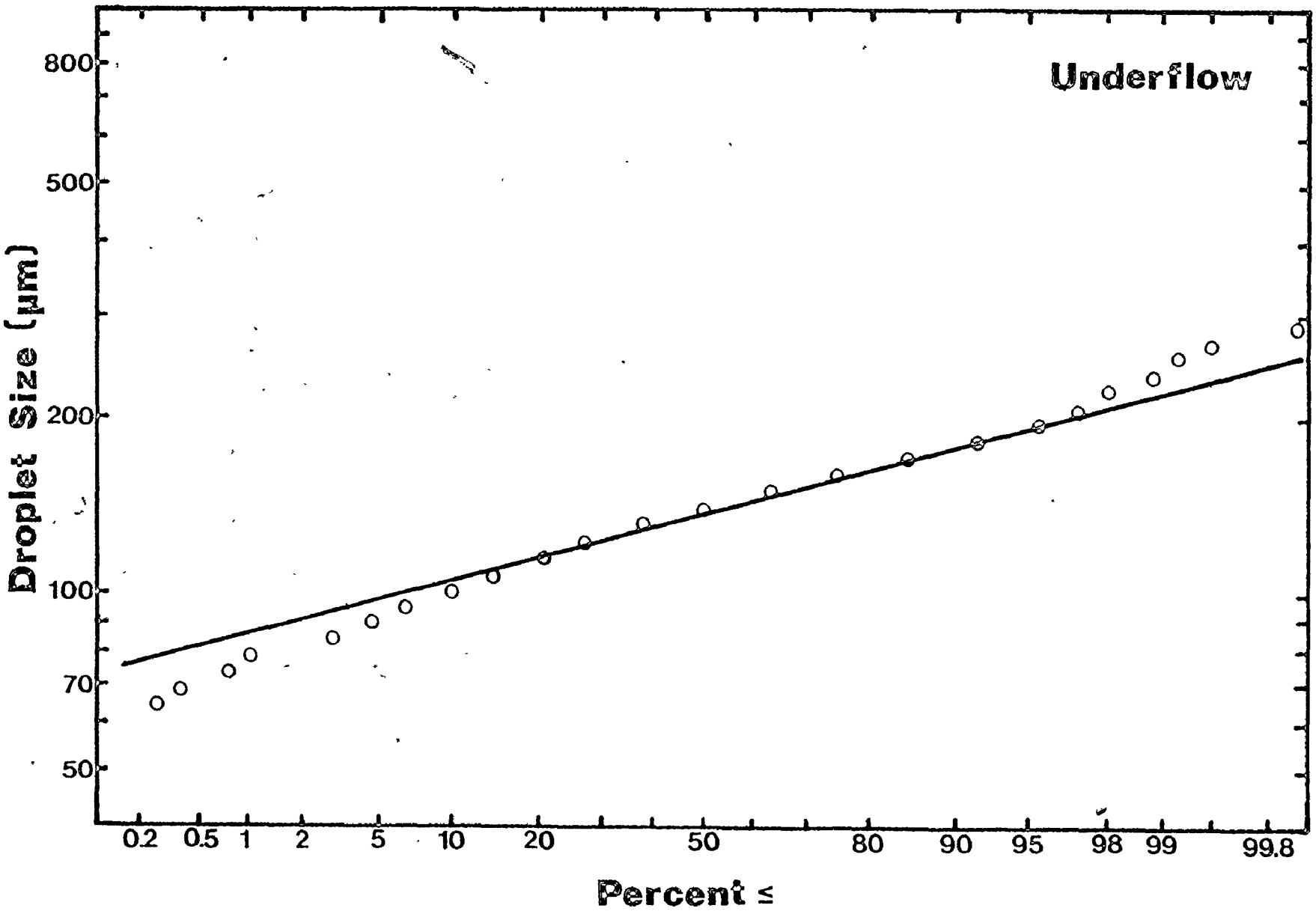

Droplet Size Distribution for Kerosene/Water

Figure A2 — 13

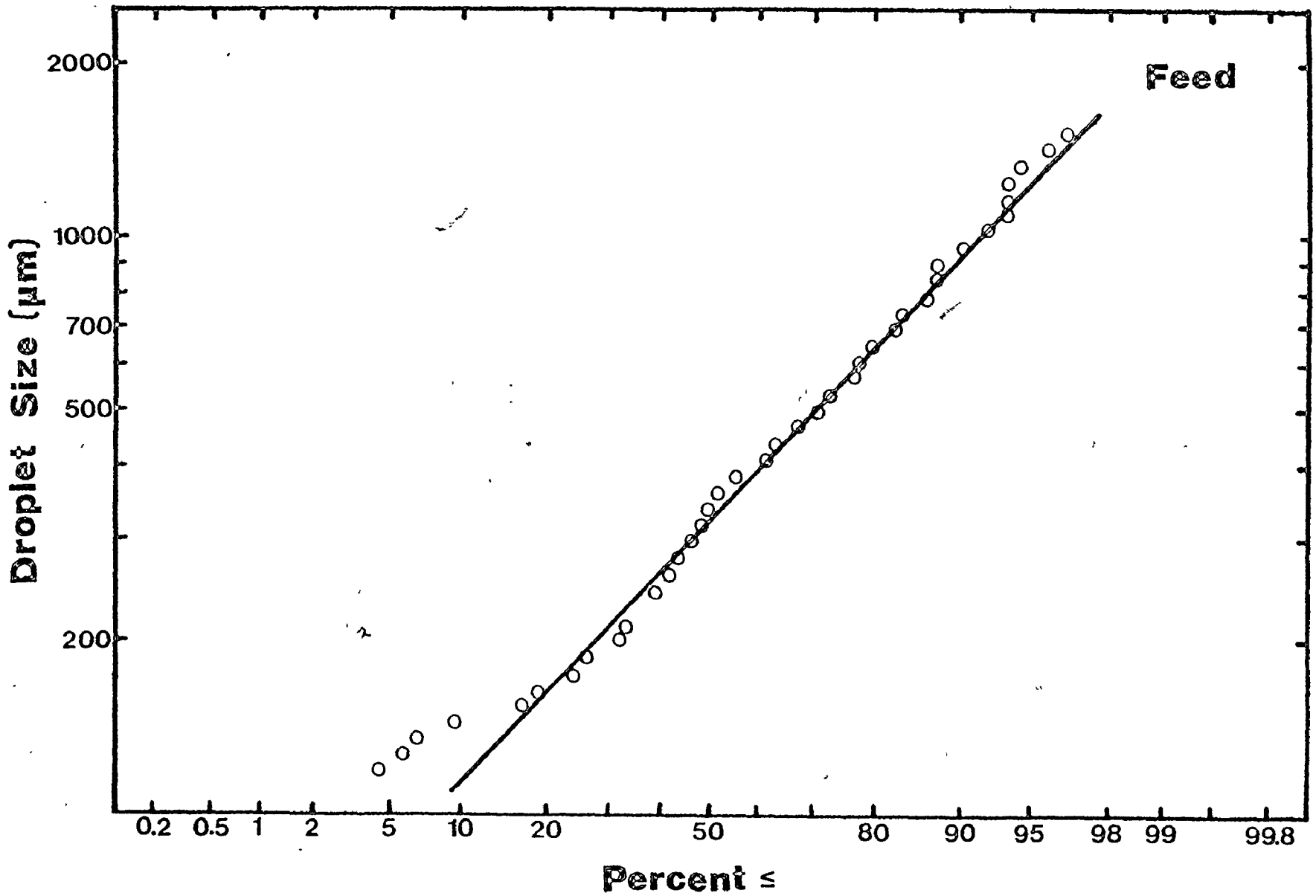

Droplet Size Distribution for Kerosene/Water

Figure A2 — 14

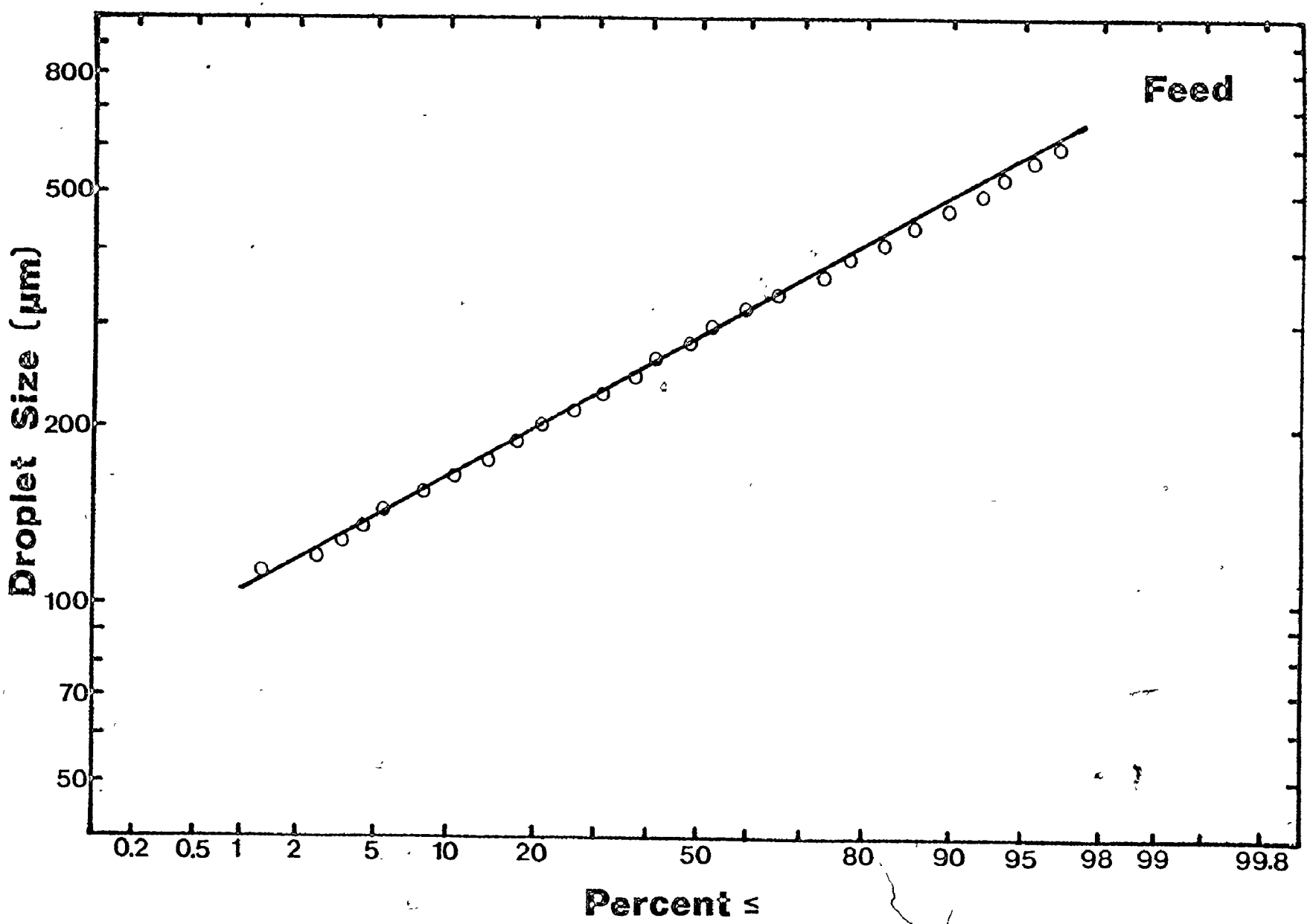

Droplet Size Distribution for Kerosene/Water

Figure A2 — 15

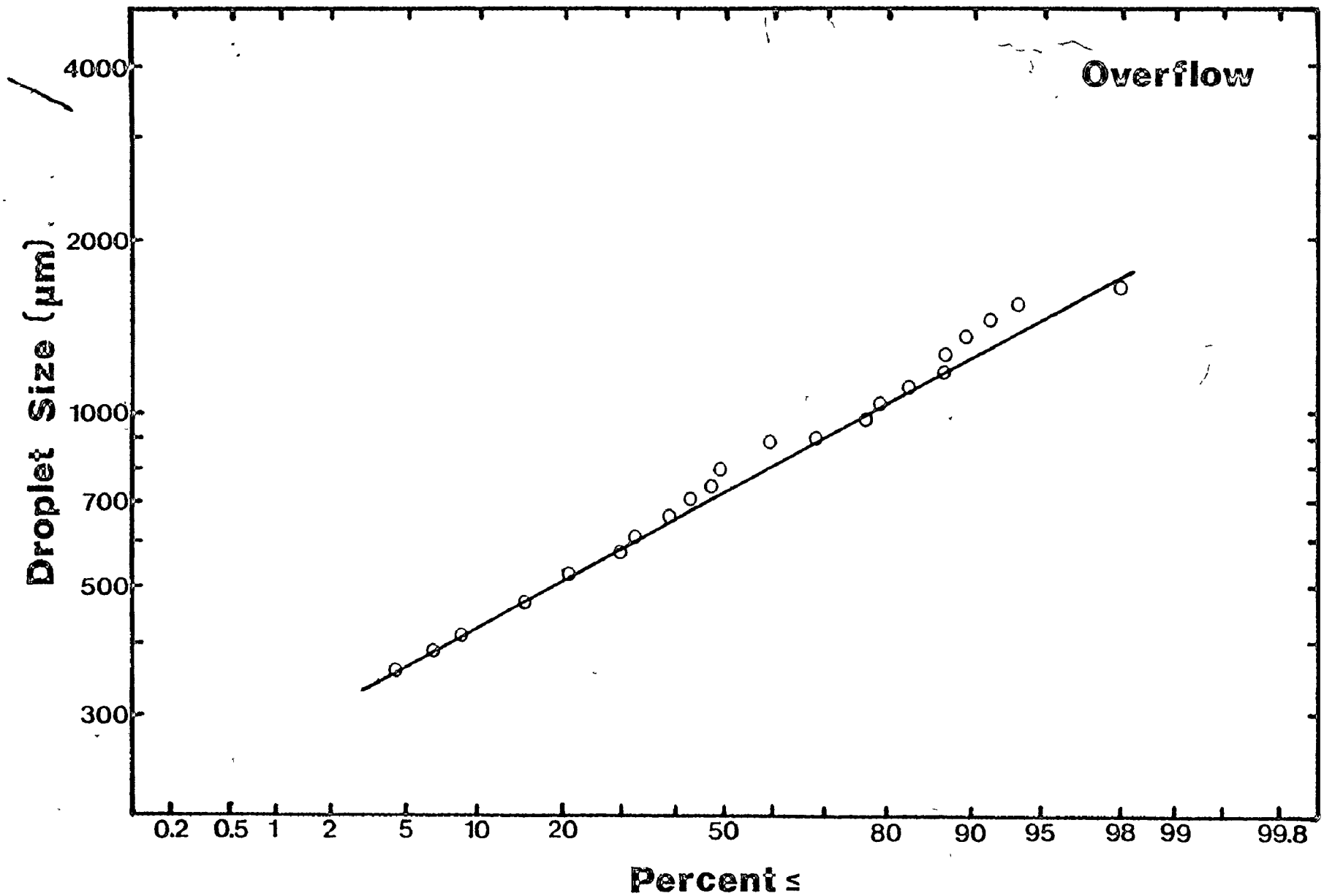

Droplet Size Distribution for Kerosene/Water

Figure A2 — 16

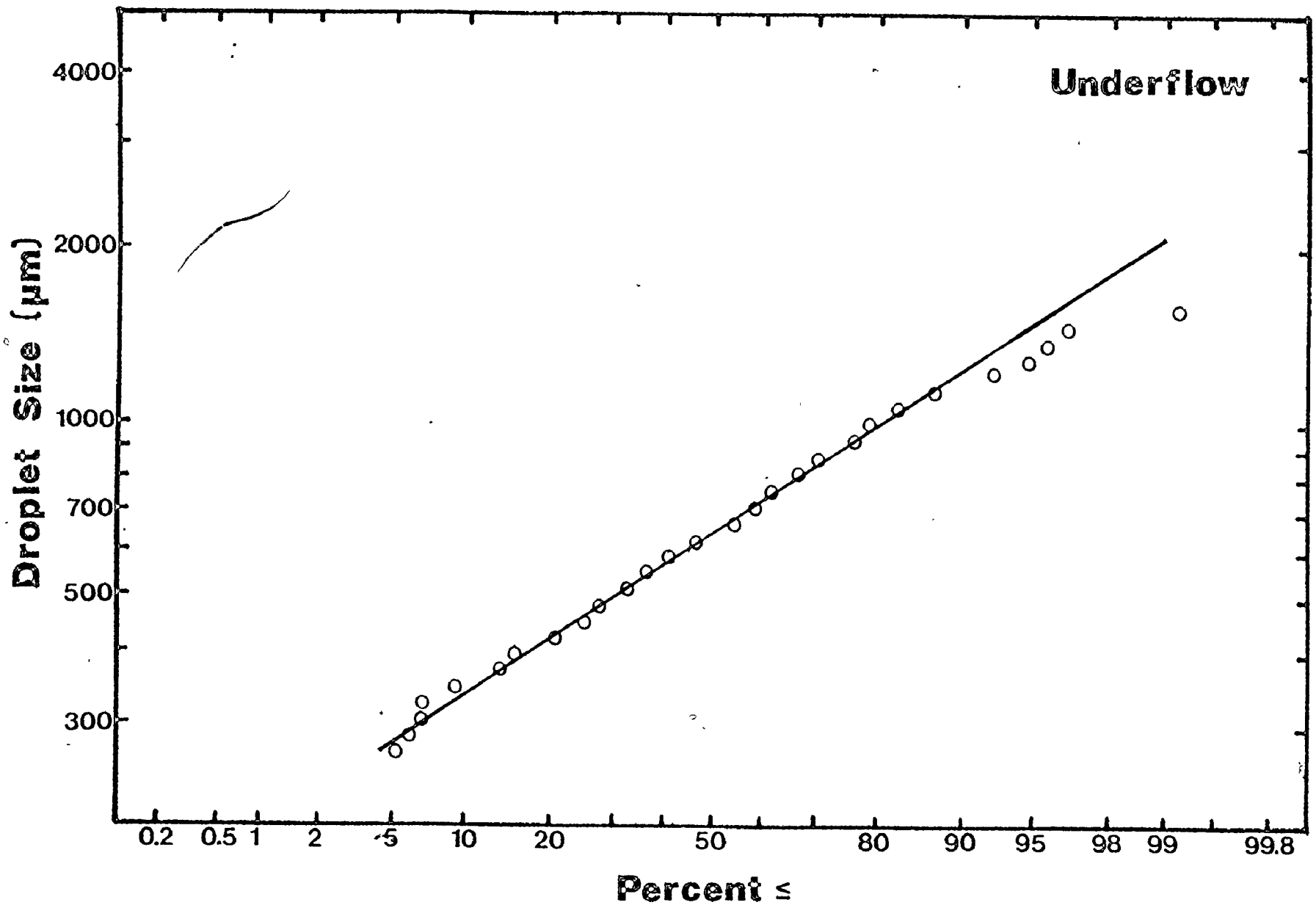

Droplet Coalescence for Butanol/Water

Figure A2 — 17

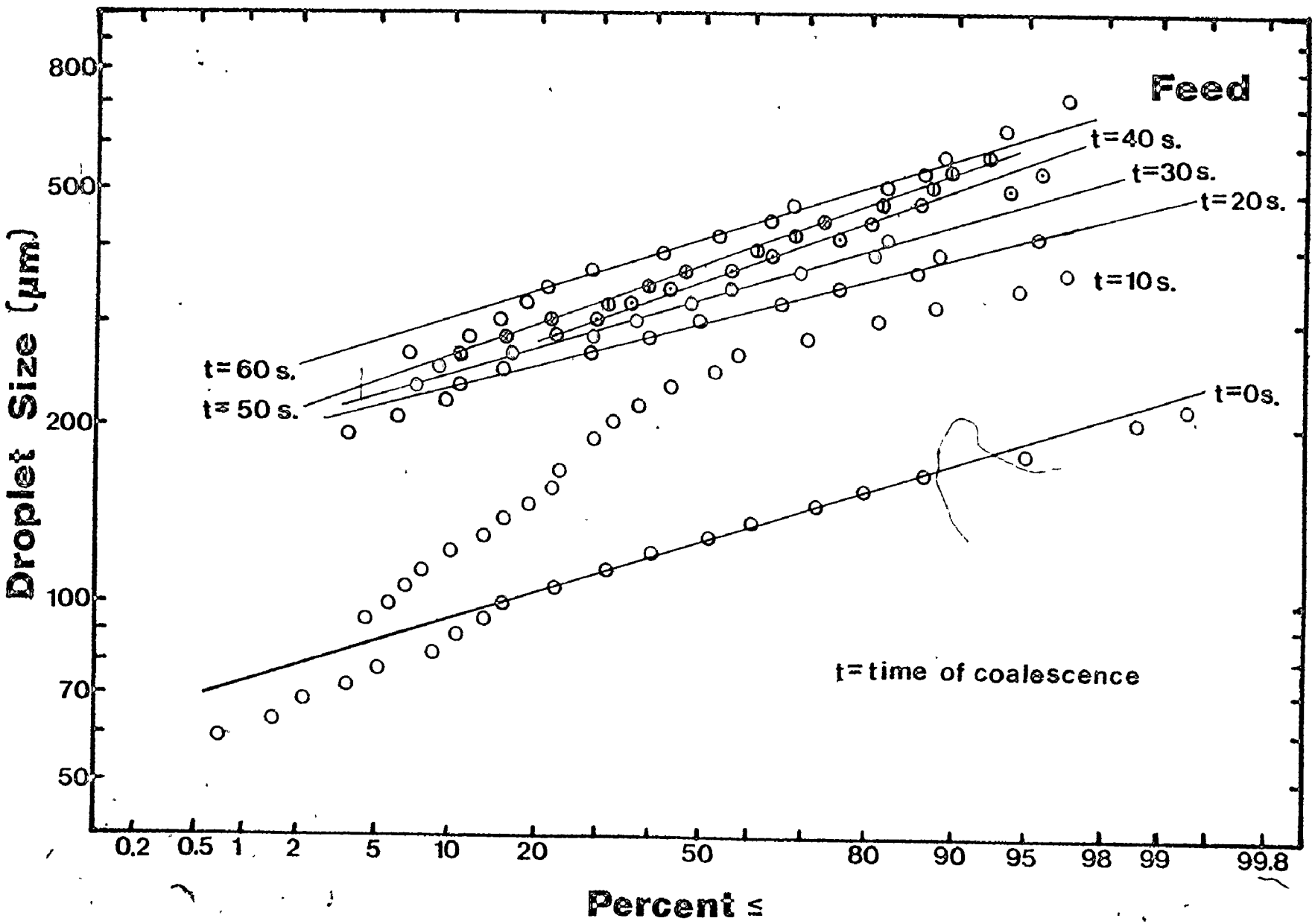

Droplet Coalescence for MIBK/Water

Figure A2 — 18

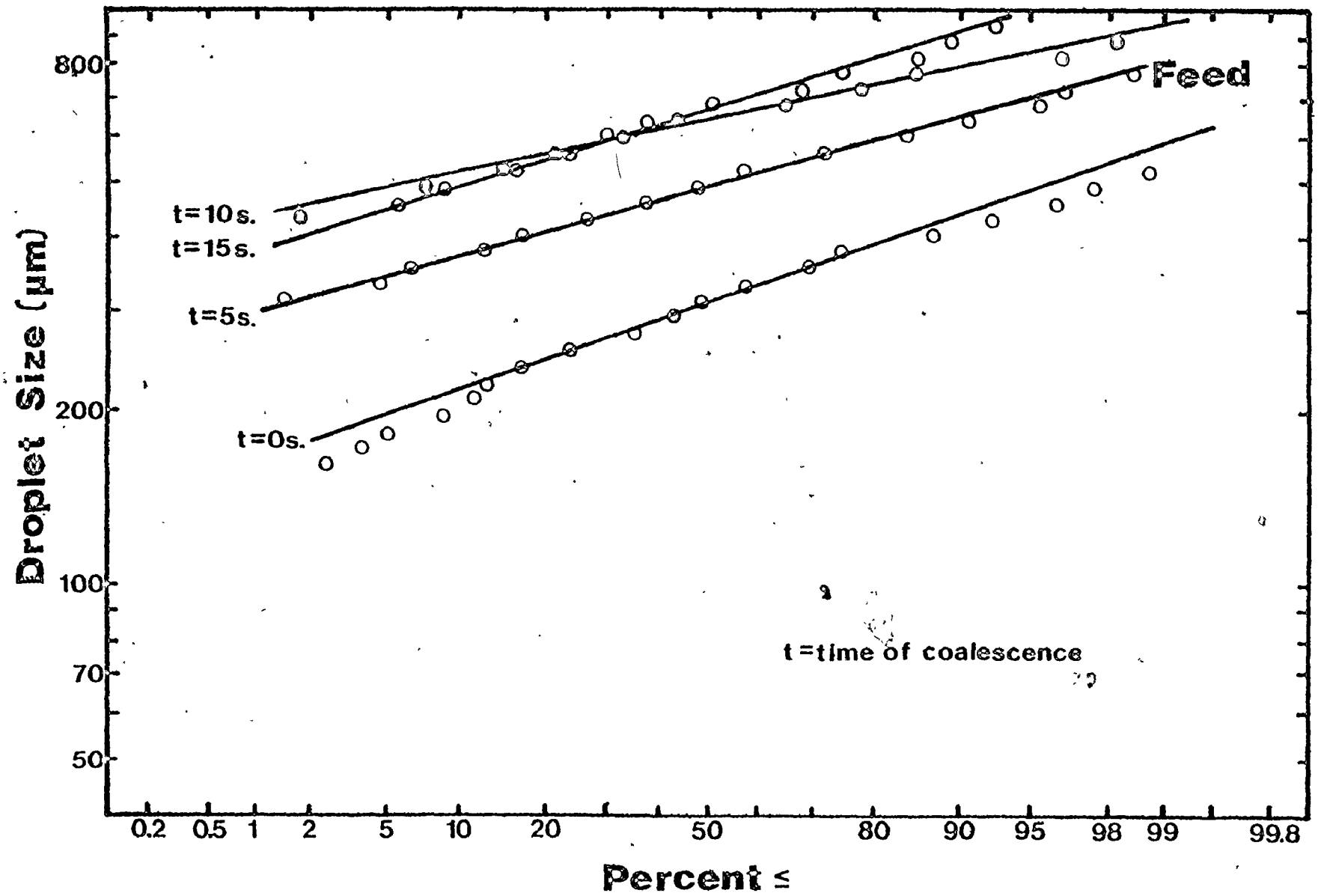

Droplet Size (D_{50}) versus Time

Figure A2 — 19

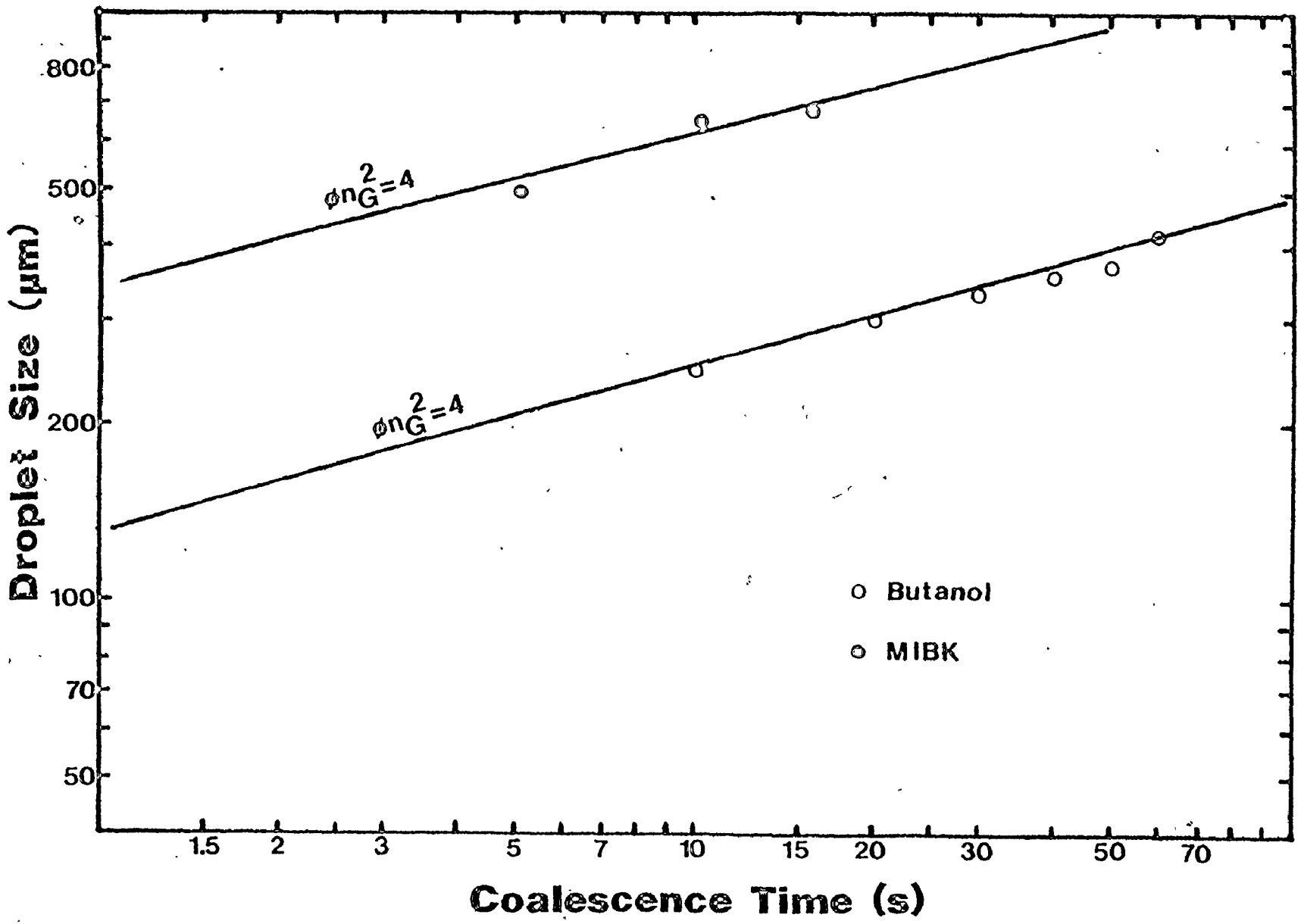

Droplet Coalescence for Two Liquid/Liquid Systems Table A2-1

System	Time after Flow Stopped (s)	Number of Droplets Counted	D_{50}	D_{95}	D_{MAX}	D_{MIN}	$\frac{D_{84}}{D_{50}}$
			(microns)				
MIBK /Water	0	80	315	495	530	165	1.32
	5	65	500	720	780	315	1.24
	10	55	650	850	890	380	1.17
	15	56	670	1000	1015	435	1.28
Butanol /Water	0	140	125	190	220	55	1.28
	10	90	245	350	370	65	1.27
	20	85	300	420	805	80	1.22
	30	56	330	480	580	150	1.26
	40	65	355	560	620	140	1.32
	50	65	370	590	805	170	1.32
	60	61	415	520	805	220	1.28

Note: All measurements made at feed optical cell.

location ranged from roughly 50 to 2600. Two reasons for this wide range were noteworthy. The larger the droplets generated, the lower the number counted per photo. Normally a dozen or so photos of droplets were taken for any one system and location. Photo quality was perhaps the most important reason for low droplet count. An attempt was made only to count those droplets which could be defined. The problem of photo quality was more acute for kerosene/water and toluene/water. Even with cleaning the inside wall of the glass tube, droplets quickly adhered to it. As a result, only the first 3 or 4 photos were satisfactory for use. Burrill and Woods (B-3) carried out his photographic work at the feed inlet with as low a phase ratio as possible. This condition was followed for the present work. By photographing at the overflow, the photo quality may be poorer due to the higher concentration of dispersed phase.

A2.5 Treatment of Data

Based on the photographs taken, droplet size was calculated for each system. Calculated values were compared to those predicted by theory. Data collected from the coalescence study was used to determine the validity of a model. This model was used to predict the rate of coalescence for the systems studied.

A2.5a Calculation of Droplet Size

The standard range which was used, projected a circle on the photographic paper varying in size from 1.2 mm - 27.7 mm. This range

was broken up into 48 exponentially spaced increments. After allocation of the droplets into the different slots by the Zeiss Particle Size Analyzer, it was possible to determine their actual size. Consider the following example:

For the butanol/water system, at the overflow optical cell, all droplets found on the photograph were located between the 5th and 39th size slots.

First it was necessary to determine the magnification of the photograph due to:

(i) extension tube and bellows

(ii) blow-up contact sheet to print size.

(i) A ruler with known divisions was held in a vertical direction beside the optical cell and photographed. Each division on the ruler was 1/32 inch. In total, 8 of these divisions are counted on the contact sheet. The vertical height of the contact photograph, from the lower to upper border, was 15/16 inch.

$$\text{Magnification} = \frac{15/16}{1/4} = 3.8$$

(ii) A ruler placed on the blow-up gave the vertical distance, from the lower to upper border, of 10-5/8 inches.

$$\text{Magnification} = \frac{10\text{-}5/8}{15/16} = 11.3$$

$$\text{total magnification} = (11.3)(3.8) = 42.6$$

Given the magnification factor, determine the smallest and largest droplet photographed.

According to Table I in the PSA TGZ-3 Instructional Book (Z-1):

(1) for the smallest droplet, in the 5th slot, it would have a diameter of 1.63 mm.

$$\text{Corrected diameter} = \frac{1.63}{42.6} = 0.038 \text{ mm}$$

$$= 38 \text{ microns}$$

(2) for the largest droplet, in the 39th slot, it would have a diameter of 14.92 mm.

$$\text{Corrected diameter} = \frac{14.92}{42.6} = 0.350 \text{ mm.}$$

$$= 350 \text{ microns}$$

A2.5b <u>Calculation of D_{50} Based on Hinze Equation</u>

Since values of D_{50} for toluene/water and kerosene/water did not follow the trend established by butanol/water and MIBK/water, D_{50} was calculated based on the latter two systems. Consider the equation as proposed by Hinze (H-2):

$$d_{95} = 1.51\nu \left(\frac{\dot{\gamma}}{D\rho_c U^2}\right)^{0.6} \left(\frac{UD}{\nu}\right)^{0.1} D$$

In comparing the two systems, it is assumed that D, ρ_c, U and ν are constant. If a log normal distribution is obeyed by these dispersions, d_{95} and d_{50} are interchangeable. For two different systems the plotted data should lie parallel. As a result the ratio of droplet sizes at d_{95} and d_{50} is equivalent:

$$\frac{D_{50_1}}{D_{50_2}} = \left(\frac{\dot{\gamma}_1}{\dot{\gamma}_2}\right)^{0.6}$$

If the MIBK/water system is used as the basis for calculation consider the following example:

$\gamma_{MIBK} = 10$ mN/m.

$\gamma_{Toluene} = 20$ mN/m.

$D_{50_{MIBK}} = 225$ microns

$$\left(\frac{10}{20}\right)^{0.6} = \left(\frac{225}{D_{50_{Toluene}}}\right)$$

$D_{50_{Toluene}} = 341$ microns

A2.5c Calculation of Rate of Coalescence

To calculate the rate of coalescence for the different liquid/liquid systems, the Parallel Disc Model studied by Liem and Woods (L-1) was applied.

The following equation was used:

$$\frac{\mu\Delta\rho g b^5}{\gamma^2}\left(\frac{1}{h^2} - \frac{1}{h_o^2}\right) = \left(\frac{16}{\emptyset n_G^2}\right)\theta$$

where (i) $\emptyset n_G^2 = 16$; if a model is assumed where the surfaces of two approaching droplets remain rigid and do not circulate.

(ii) $\emptyset n_G^2 = 1$; if neither of the above assumptions hold.

Assume $\frac{1}{h_o^2} << \frac{1}{h^2}$ such that the above equation reduces to: $\frac{\mu\Delta\rho g b^5}{\gamma^2}\left(\frac{1}{h^2}\right) = \left(\frac{16}{\emptyset n_G^2}\right)\theta$. It has been determined that h, which represents the separation distance between droplets when coalescence occurs equals 300 Å. From a plot in Figure A2-19, $\emptyset n_G^2 = 4$ best fitted the data.

Consider the following calculation for the kerosene/water system:

How long does it take two 500 micron diameter droplets to coalesce?

$$\mu = 0.01 \text{ gm/cm-s.}$$

$$\Delta\rho = 0.19 \text{ gm/cm.}^3$$

$$g = 980 \text{ cm/s.}^2$$

$$b = 250 \times 10^{-4} \text{ cm.}$$

$$\gamma = 30 \text{ mN/m} = 30 \text{ gm/s.}^2$$

$$h = 300 \times 10^{-8} \text{cm.}$$

$$\phi n_G^2 = 4$$

$$\theta = \frac{(0.01)(0.19)(980)(250 \times 10^{-4})^5}{(30)^2} \left(\frac{1}{300 \times 10^{-8}}\right) \left(\frac{4}{16}\right)$$

$$= 0.6 \text{ s.}$$

APPENDIX 3

PHYSICAL PROPERTIES OF THE LIQUID/LIQUID SYSTEMS

A3 PHYSICAL PROPERTIES OF THE LIQUID/LIQUID SYSTEMS

Physical properties cited in this section were either reported from Perry (P-1), Stephen and Stephen (S-6) and Woods (W-2) or measured during the present work. Reported properties include interfacial tension, density difference, solubility and viscosity. These values are shown in Table A3-1. Measured properties include surface and interfacial tension and specific conductivity. These values are shown in Tables A3-2 to A3-4.

The following sections describe the procedures used to measure surface and interfacial tension and specific conductivity:

A3-1 Procedure for Measurement of Surface and Interfacial Tension

This section contains a description of the equipment used and the experimental procedure followed, for the measurement of surface and interfacial tension.

A3.1a Equipment Description

The surface and interfacial tension measurements were made by a Fisher Model 215 Autotensiomat. The apparatus consisted of four components.

The first, a temperature control unit or heater, regulated the temperature at which the surface and interfacial tension measurements were made. For this work, the temperature of the circulating water was 25 ± 1°C. The sample module, in which the measurements were performed, was connected to the heater. The liquid/liquid sample was contained in a double-shelled glass vessel which was placed inside the sample module. Water from the heater circulated between the inner and outer shell of the vessel and then back to the heater. The sample module consisted of a

Reported Values of Some Important Parameters Table A3-1

System	Interfacial Tension (mN/m)	Density Difference (gm/cm^3)	Viscosity of Solvent Phase (gm/cm-s)	Solubility of Solvent Phase (gm/100mL water)
Butanol /Water	1.9	0.19	0.033	9.0
MIBK /Water	10.5	0.20	0.006	2.6
Toluene /Water	30.3	0.13	0.006	0.05
Kerosene /Water	-	0.19	0.015	0.01

Measurement of Surface/Interfacial Tension Table A3-2

System	Interfacial Tension mN/m ± 1.0	Surface Tension mN/m ± 1.0			
		Solvent phase		Water phase	
		before runs	after runs	before runs	after runs
Butanol/Water	2.0	-	23.0	68.0	28.0
MIBK/Water	10.0	-	24.0	70.0	39.0
Toluene/Water	20.0	29.0	-	70.0	57.0
Kerosene/Water	30.0	-	27.0	-	61.0

Measured Specific Conductivity of Water Phase Table A3-3

System	Specific Conductivity of Water Phase (mhos/cm)	
	*Before runs	After runs
Butanol/Water	7.6	9.1
MIBK/Water	2.8	10.5
Toluene/Water	4.9	21.5
Kerosene/Water	-	11.4
triple distilled water	1.0	
tap water	230.	

*water phase not mutually saturated.

Study of Contamination of Toluene/Water System Table A3-4

Case Considered	Measured Surface/Interfacial Tension mN/m ± 1.0
interfacial tension of pure toluene/water	31.5
surface tension of pure toluene	29.0
surface tension of pure water	69.0
interfacial tension of used toluene/water	20.0
Addition of a silicon sealant to above pure toluene/water. It was allowed to be in contact with the system for a few days. The following measurements were made:	
surface tension of toluene	26.0
surface tension of water	64.0
interfacial tension of toluene/water	21.5

balance beam arrangement. A platinum plate was attached to the beam. A control module manipulated the vertical movement and speed of the plate in and out of the liquid/liquid system. A recorder monitored the force exerted on the balance beam and plotted it on graphical paper with a marker pen.

A3.1b Measurement Procedure

For the present work, the Wilhelmy plate method was used. The force exerted on the plate represented either the surface or interfacial tension depending on the plate's position in the liquid/liquid system. To calibrate the instrument, a known weight was attached to the balance beam. The force exerted by the weight was calculated. The recorder was manipulated until it recorded a force equivalent to the calculated value.

Prior to measurement, the platinum plate was cleaned with acetone, rinsed off with distilled water and then held over a flame. This ensured the removal of contaminants which could influence measurements. The plate was then lowered into and raised from the liquid/liquid system. For each measurement two peaks were plotted; the first peak represented movement of the plate into the liquid and the second, withdrawal from it. The latter was used in the measurement of surface or interfacial tension. A print-out from the recorder, in Figure A3-1, shows the measurement of interfacial tension. The measurement was repeated a number of times for a given system until a consistent reading was obtained. Often it was found that the plate had to be cleaned after each measurement. Otherwise lower readings with successive measurements sometimes resulted. This was due to the cumulative collection of contaminants on the plate with successive measurements.

Print-out of Interfacial Tension Measurement

Figure A3 — 1

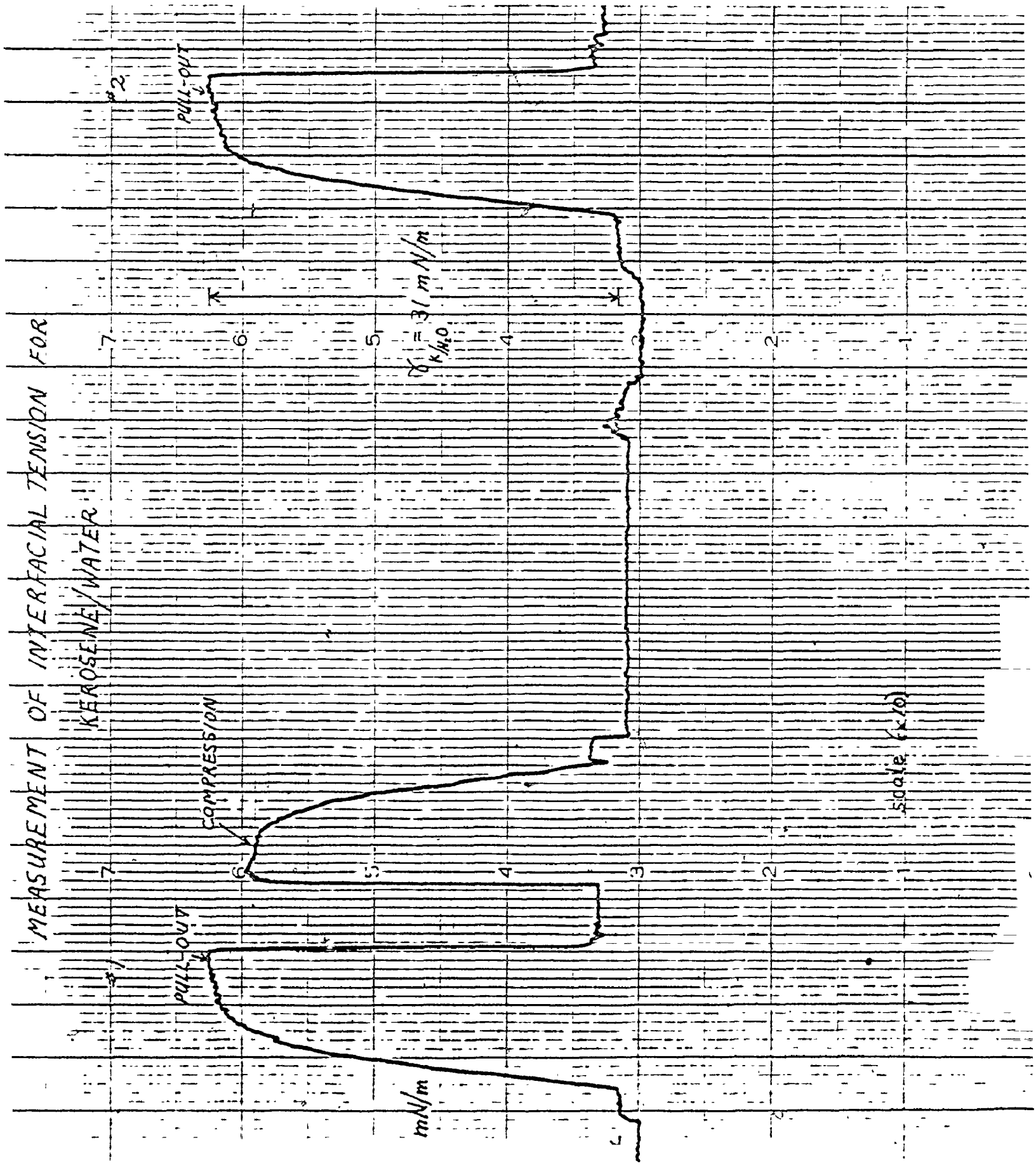

A3-2 Procedure for the Measurement of Specific Conductivity.

A Copenhagen Radiometer was used to measure the specific conductivity of the distilled water phase.

A glass probe, connected to the instrument was suspended in the water sample. Care was taken to ensure that the probe did not contact the glass sides of the sample container. Before taking a reading, a calibration check was run. If the needle did not match up with the designated value, an adjustment was made by the turn of a dial. After taking a reading the probe was thoroughly washed off with distilled water and then stored in distilled water until the next reading was taken.

Measurements were made on the distilled water samples collected before starting and after completing the runs. Samples collected after completion of the runs were mutually saturated with the oil phase; those collected before the runs started, represented a pure phase.

APPENDIX 4

EQUIPMENT SPECIFICATIONS AND SUPPLIERS

A4 EQUIPMENT SPECIFICATIONS AND SUPPLIERS

The main purpose of this brief section was to provide a complete inventory of equipment specifications and suppliers in this research. A minor section dealt with the dimensions of the test hydrocyclone. This data was used to calculate the range of residence times inside the cyclone for the liquid/liquid systems studied.

A4.1 Equipment Inventory

Table A4-1 contains a complete inventory of equipment used. It also includes equipment specifications and suppliers. This table facilitates the task of obtaining new equipment or replacing old equipment for future research.

A4.2 Hydrocyclone Dimensions

The hydrocyclone was the focus of interest in this research. Figure A4-1 contains a hydrocyclone with pertinent dimensions marked on. This cyclone is similar to the one used by Burrill and Woods (B-3). Shown below in Figure A4-2 is a calculation of the apex angle in the cyclone.

Calculation of the Apex Angle

Figure A4 — 2

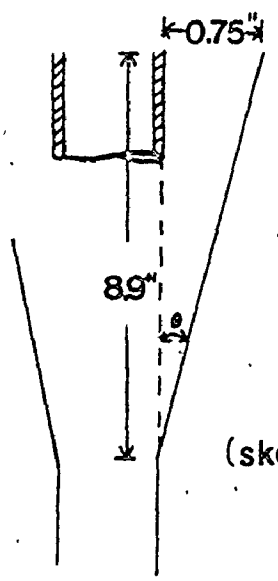

$$\tan\theta = \frac{0.75}{8.9}$$

$$\tan^{-1}\left(\frac{0.75}{8.9}\right) = 4.8^\circ$$

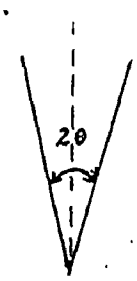

(sketch not to scale)

apex angle = 9.7°

Hydrocyclone Dimensions

Figure A4 — 1

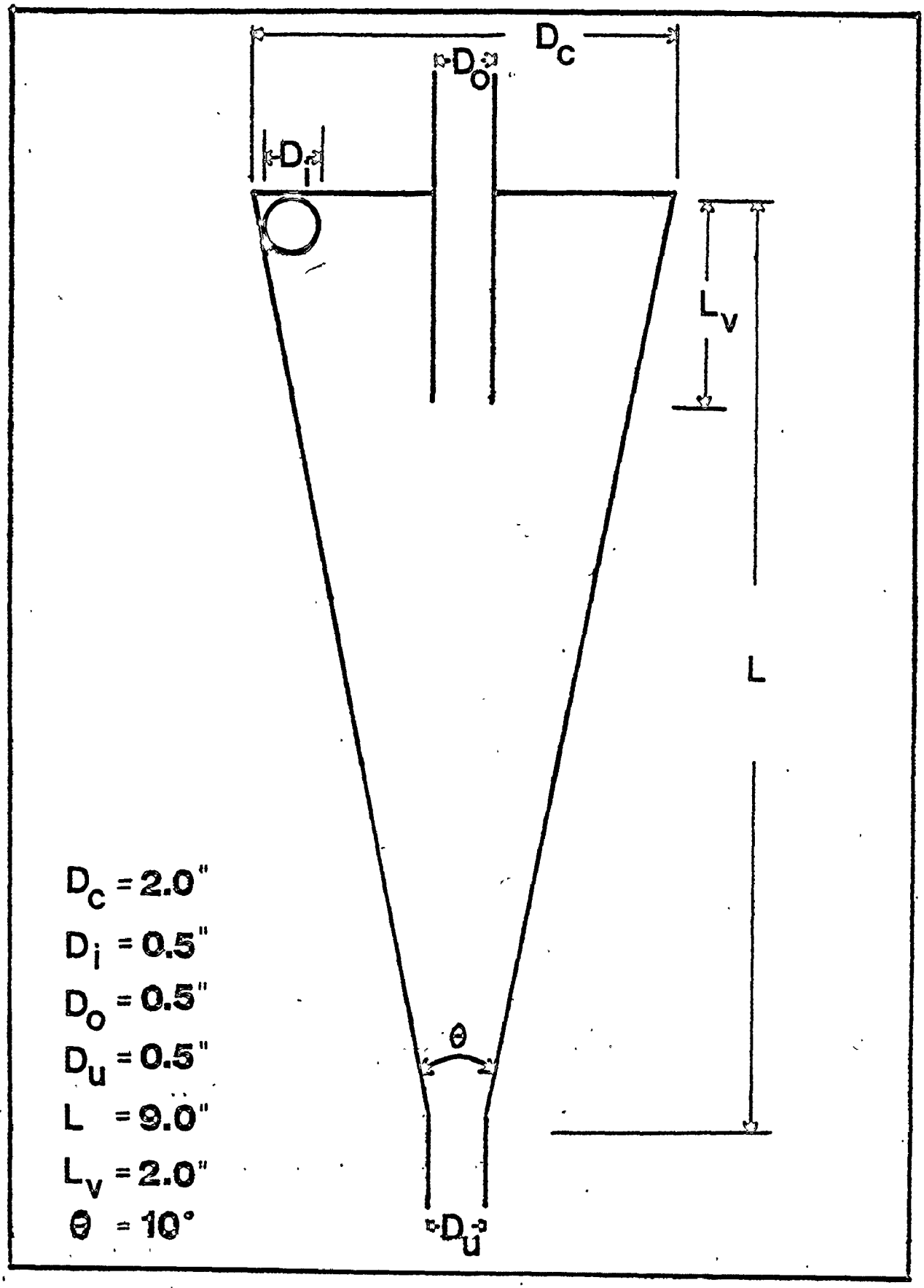

List of Equipment Used and Suppliers Table A4-1

Equipment	Comment(s)	Supplier
Braun electronic flash	- automatic unit - to illuminate optical cell	Shop Rite Store, 163 Main St. West Hamilton, Ontario
support clamp	- aid in supporting camera to piping system	Voight Photography Ltd. 592 Upper James St. Hamilton, Ontario
cable release	- to activate shutter	Connaught Camera, 127 King St. East, Hamilton, Ontario
extension cable	- to join flash unit to camera	
film	- 35mm, Panatomic - X ASA 32, black and white	Audio-Visual Dept. McMaster University, Hamilton, Ontario
1/2", 5/8" outer diameter tubing	- type #304, stainless steel - for construction of piping system	Machine Shop McMaster University, Hamilton, Ontario
Swagelok fittings	- type #316, stainless steel, tee and cross fittings	Niagara Valve and Fitting Ltd., 174 Parkdale Ave. North, Hamilton, Ontario
bellows	- type #304, flexible stainless steel - allows some freedom of movement for cyclone	
gate valve	- stainless steel - used on diversion line	Hoffman Bros. Ltd., c/o Westburne, 21 Sanford North, Hamilton, Ontario

Table A4-1 cont'd

Equipment	Comment(s)	Supplier
rotameters	- glass rotor tube and brass float - 10 USGPM capacity for water phase - 10 USGPM capacity for oil phase; due to breakage replaced by 4 USGPM capacity	Fischer and Porter, 134 NorFinch Dr., Downsview, Ontario
ethylene-propylene rings	- rings located at top and bottom of rotor tube - resistant to deterioration by solvents	Bond-Collins Ltd., 8/ - 424 Rennie Ave., Hamilton, Ontario
glass manometer	- thick-walled, U-shaped glass tube	Glass Blower, McMaster University, Hamilton, Ontario
glass hydrocyclone	- thick-walled, conical shaped glass vessel	
QVF glass vessels	- 25 and 50 Imp. Gal. spherical-shaped vessels used to store solvent and water phases, respectively	Pegasus Industrial Specialties Ltd., P.O. Box 319, Agincourt, Ontario
nylon tubing	- to join sampling locations in piping system to manometers - resistant to solvent action	Charles Jones, Industrial Ltd., 237 Arvin Ave., Stoney Creek, Ontario
electric stopwatch	- to determine sampling time of overflow and underflow	Fisher Scientific Co. Ltd., 184 Railside Dr., Don Mills, Ontario
Fisher Auto Tensiomat 15	- to determine surface/	

Table A4-1 cont'd

Equipment	Comment(s)	Supplier
support stand	- 4 foot high metal stand used to support separator tank	Chem. Eng. Machine Shop, McMaster University, Hamilton, Ontario
Radiometer Copenhagen conductivity meter	- to determine specific conductivity of water phase	Dr. D. Woods, Chem. Eng.Dept.,McMaster Univ.,Hamilton, Ont.
Wilson organic respirator	- protection against solvent fumes	Safety Supply Co., 1870 Burlington St. East, Hamilton, Ontario
kerosene	- borrowed from extraction column - used as oil phase	Dr. Baird, Chem. Eng. Dept. McMaster University, Hamilton, Ontario
butanol methyl isobutyl ketone toluene	- analytical reagent grade - used as oil phase	Scientific Stores, McMaster University, Hamilton, Ontario
rubber gloves	- protection if handling solvents	
Tygon tubing	- vent from separator tank, etc.	
mercury	- used in manometers	
erhlenmeyer flask graduated cylinder	- collection and measurement of overflow and under-flow samples	

Table A4-1 cont'd

Equipment	Comment(s)	Supplier
stopwatch	- determine time before sampling	Scientific Stores cont'd
silicon sealant	- used as sealant for separator tank	
C-clamps	- to secure plexiglass cover on separator tank	
feed pumps	- 10 USGPM at 80 feet and 3600 r.p.m. - explosive-proof - stainless steel	used from Burrill's work
Zeiss particle size analyzer	- to size and count droplets	
separator vessel	- stainless steel and glass construction	
Pentax Asahi camera	- 35 mm with 55 mm. lens	
extension tube and bellows	- to allow close-up photography	
optical cells	- plexiglass construction - O-rings used to hold optical cell in position.	
other valves	- used throughout piping system	

Table A4-1 cont'd

Equipment	Comment(s)	Supplier
Bourbon pressure gauge	- to measure pressure at mixing tee.	Burrill's cont'd.

A4.3 Residence Time in the Hydrocyclone

Over the range of flowrates studied, the minimum and maximum residence times for the liquid/liquid systems were calculated:

say $Q_{MIN} \sim 100$ mL/s.
$Q_{MAX} \sim 375$ mL/s.

$$t_r = \frac{V_c}{Q}$$

where V_c = volume of cyclone (mL)
Q = flowrate of dispersion (mL/s)

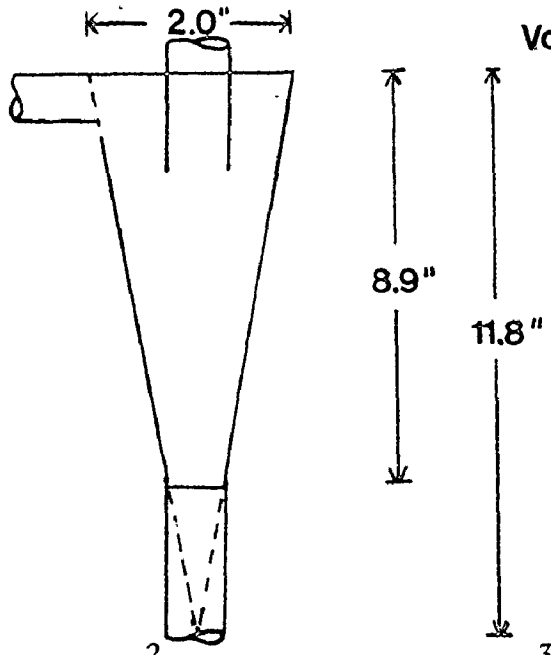

Volume of the Hydrocyclone

Figure A4 — 3

(sketch not to scale)

$$V_c = \frac{1}{3}\pi((1)^2(11.8) - (0.25)^2(11.8 - 2.9)) = 12.2 \text{ in}^3 = 200 \text{ mL}$$

at Q_{MIN} $\quad t_r = \frac{200}{100} = 2.0$s.

at Q_{MAX} $\quad t_r = \frac{200}{375} = 0.5$s.

APPENDIX 5

DERIVATION OF THEORETICAL E_s VERSUS VOLUME SPLIT CURVE

A5 DERIVATION OF THEORETICAL E_s VERSUS VOLUME SPLIT CURVE

Experimental data gathered from the efficiency of separation study for the cyclone were plotted as a function of volume split. To establish how closely the efficiency of separation (E_s) model simulated the plotted data, a theoretical curve was derived.

The E_s model assumed that complete separation of the two phases occurred within the cyclone. In addition, complete coalescence of the dispersed phase was assumed. Optimum volume split occurred at a value equivalent to that of the phase ratio. Figure A5-1 shows the derived E_s versus volume split curve for each phase ratio studied with the assumption that interstitial volume is zero.

Past research (S-3) has shown that while the data conformed to the general shape of the theoretical plot, it was frequently not co-linear.

Two significant modifications were made to the model.

It has been stated by Burrill and Woods (B-3) that no coalescence occurred in the cyclone. Assuming that the dispersed light phase droplets retained a spherical shape when concentrated in the central core, then the continuous phase would be trapped in the interstices. Depending on how tightly packed the droplets were, interstitial volume would vary. Figures A5-2 to A5-4 show the effect on interstitial volume on E_s for a given phase ratio.

In the present work, complete separation of the phases did not always occur. If the phases did not separate, it was assumed that

Figure A5 — 1 E_s versus Volume Split at an Interstitial Volume $\varepsilon=0$ for Various Phase Ratios Assuming 100% Centrifugal Acceleration Utilized.

Oil/Water phase ratio: $(O/W)_{MIN}$ - - - - - - ; $(O/W)_{MID}$ ——— ; $(O/W)_{MAX}$ - - - - - - .

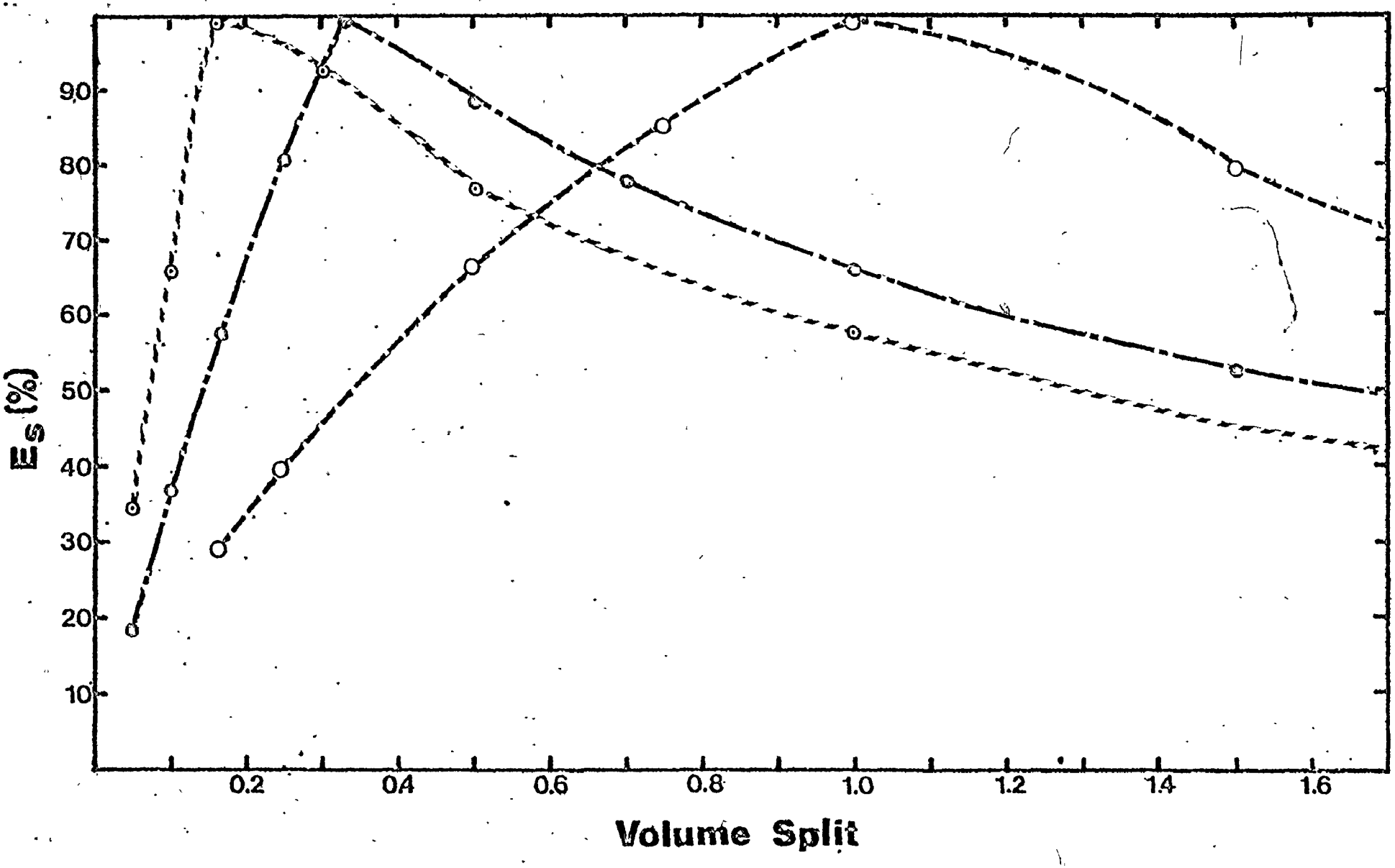

Figure A5 — 2 E_s versus Volume Split at a Phase Ratio of $(O/W)_{MIN}$ for Various Interstitial Volumes Assuming 100% Centrifugal Acceleration Utilized.

Calculated interstitial volume: (as a fraction)

$\varepsilon = 0.8$; $\varepsilon = 0.7$; $\varepsilon = 0.6$;
$\varepsilon = 0.5$; $\varepsilon = 0.4$; $\varepsilon = 0.3$;
$\varepsilon = 0.15$; $\varepsilon = 0$

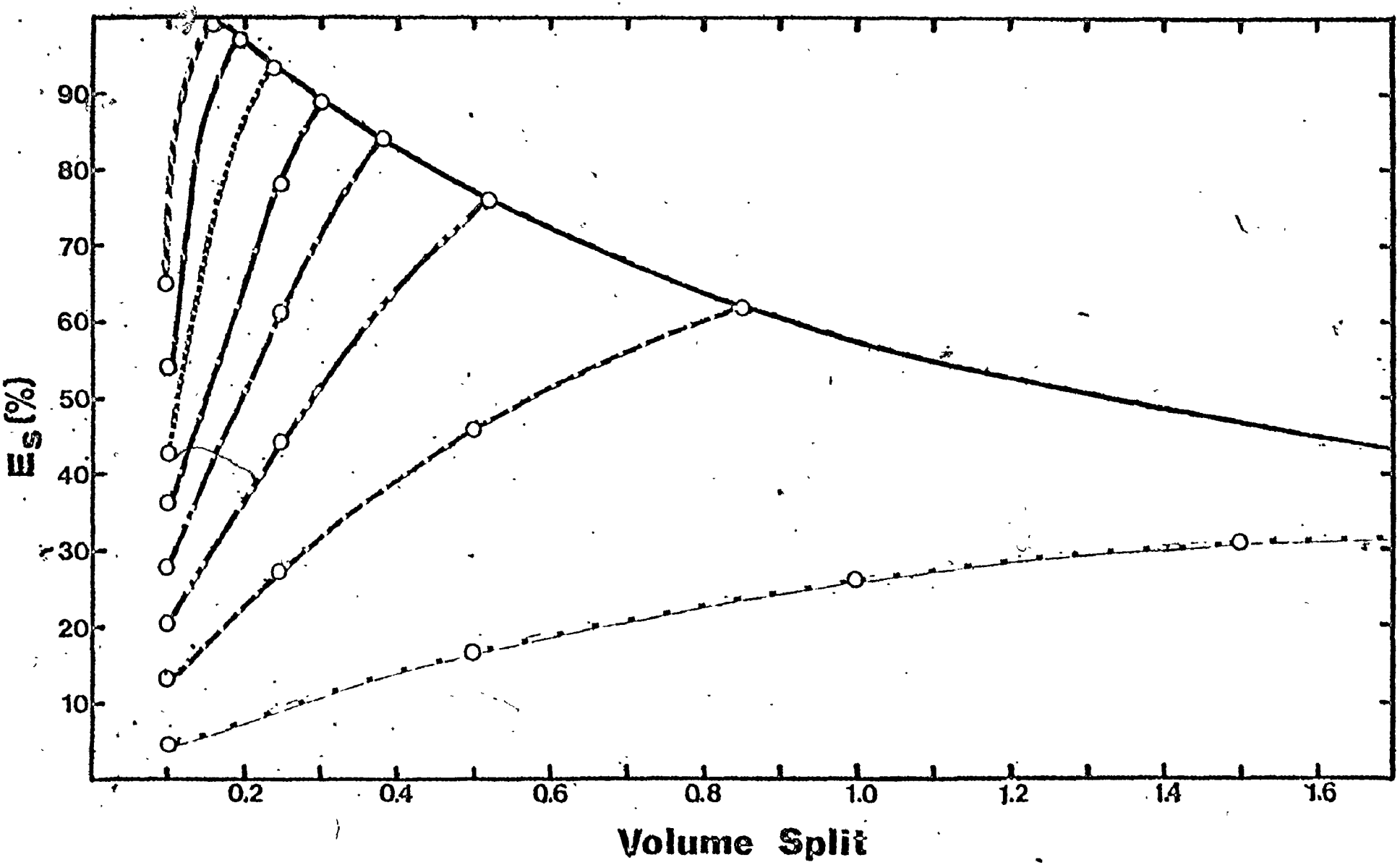

Figure A5 — 3 E_s versus Volume Split at a Phase Ratio of $(O/W)_{MID}$ for Various Interstitial Volumes Assuming 100% Centrifugal Acceleration Utilized.

Calculated interstitial volume: (as a fraction)

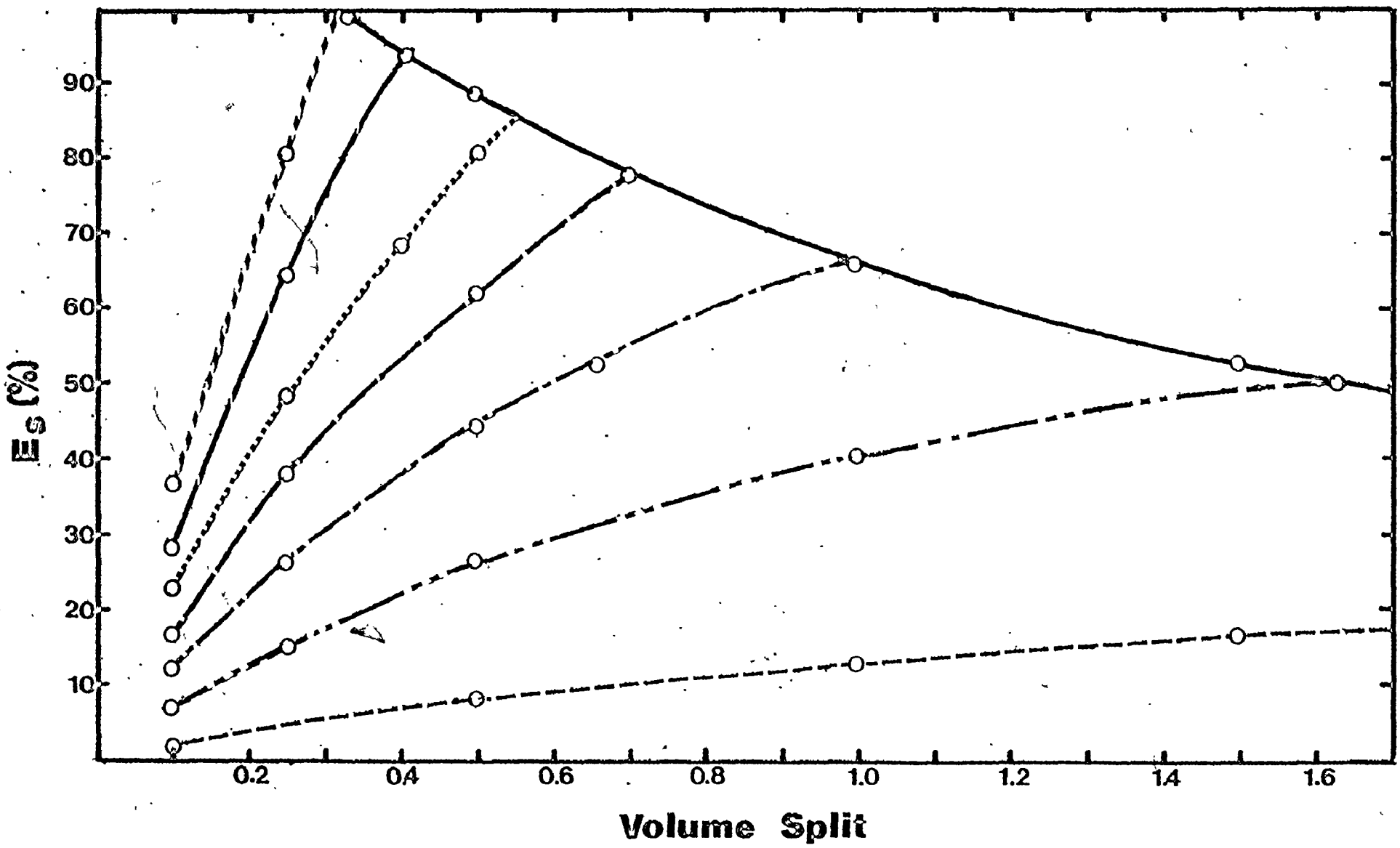

Figure A5 — 4 E_s versus Volume Split at a Phase Ratio of $(O/W)_{MAX}$ for Various Interstitial Volumes Assuming 100% Centrifugal Acceleration Utilized.

Calculated interstitial volume: (as a fraction) $\varepsilon = 0.4$; $\varepsilon = 0.3$; $\varepsilon = 0.15$; $\varepsilon = 0$.

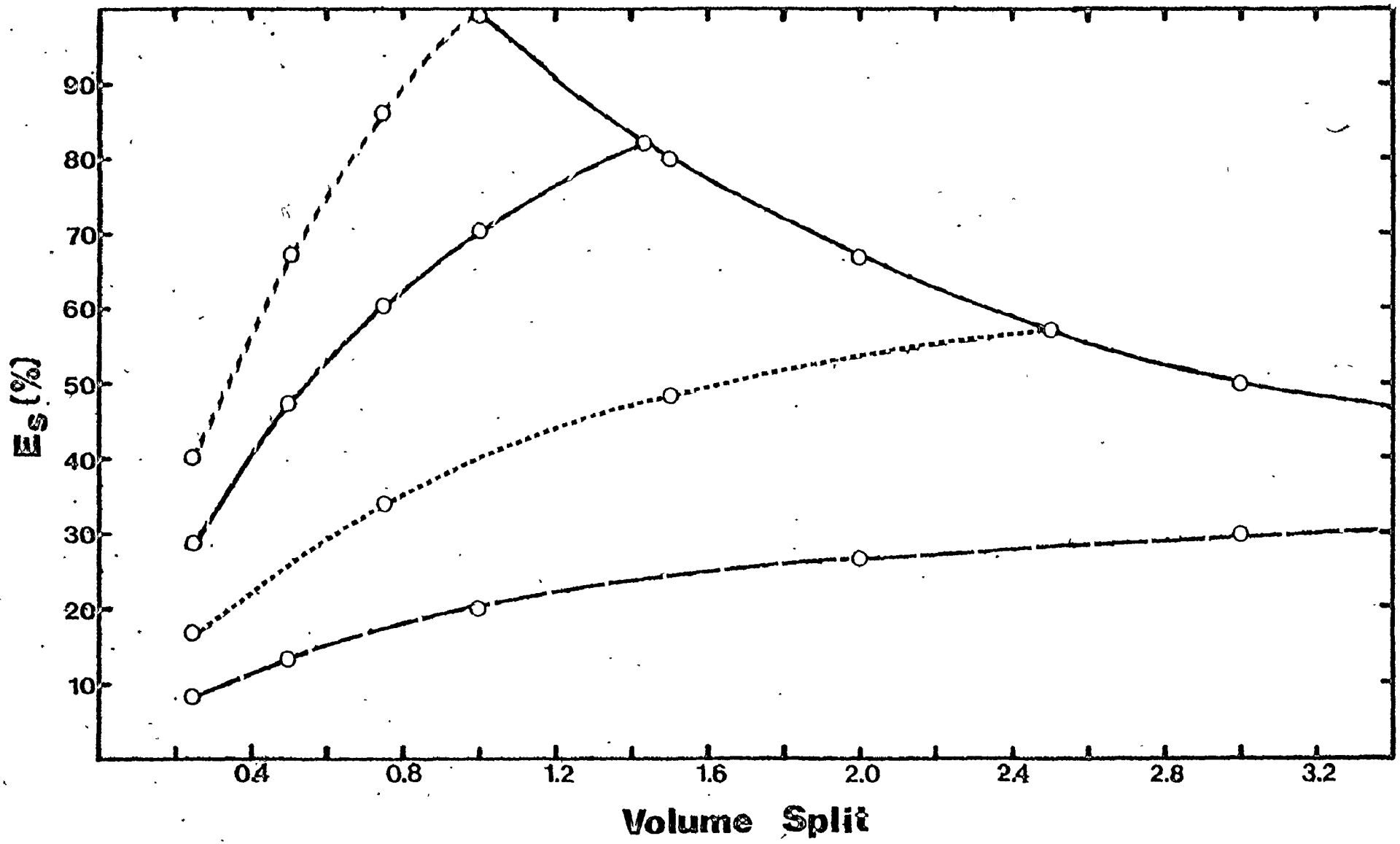

only a percentage of the centrifugal acceleration was being utilized. Figure A5-5 shows the effect of less than 100% utilization of centrifugal acceleration on E_s for a given phase ratio.

A5.1 Calculation of a Theoretical E_s versus Volume Split Curve

If the volume split and interstitial volume were specified, a theoretical E_s could be determined for a given phase ratio.

Consider the following example:

$$O/W = 1.0$$

$$O/U = 0.5$$

$$\varepsilon = 0.15$$

Since ε defined the percentage of continuous phase present in the overflow with respect to the total volume, determine the amount of continuous phase (Y) for every one part dispersed light phase.

$$\varepsilon = 0.15 = \frac{1.0}{Y + 1.0}$$

$$Y = 0.18$$

For a given phase ratio, determine the volume fraction of light phase in the feed.

$$Y_f = \frac{1.0}{1.0+1.0} = 0.50$$

For a given volume split, determine the amount actually leaving the overflow and underflow, respectively.

$$O/U = \frac{Q_o}{Q_u} = \frac{1.0 + X}{1.0 - X} = \frac{1}{2}$$

$$X = -0.33$$

$$\frac{Q_o}{Q_u} = \frac{0.67}{1.33}$$

Figure A5 — 5 E_s versus Volume Split at a Phase Ratio of $(\theta/W)_{MIN}$ Assuming less than 100% Centrifugal Acceleration Utilized.

calculated interstitial volume: $\varepsilon = 0.8$ - - - ; $\varepsilon = 0.7$; $\varepsilon = 0.5$;
(as a fraction) $\varepsilon = 0.3$.
calculated centrifugal acceleration: 100% ; 90% ; 80% ;
(as a percentage) 70% .

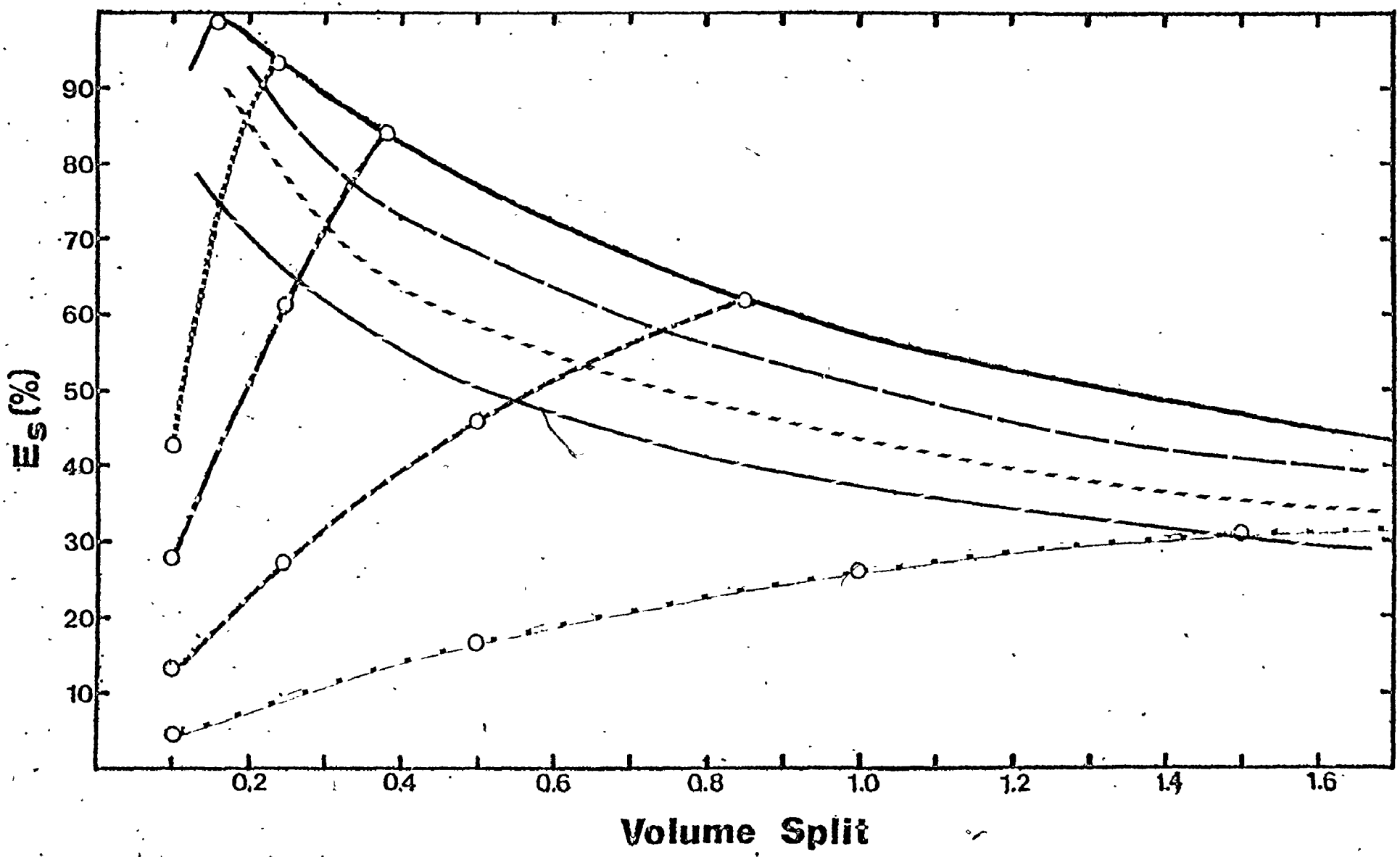

Calculate the volume fraction of light phase in the overflow and underflow, respectively.

$$Y_o = \frac{0.67 - 0.15(0.67)}{0.57 + 0.10} = 0.851$$

$$Y_u = \frac{1.0 - 0.57}{0.43 + (1.0 - 0.10)} = 0.323$$

Based on Y_f, Y_o, Y_u and volume split calculate theoretical E_s:

$$E_s = \frac{0.67}{2.00}\left[\frac{0.851 - 0.500}{1.0 - 0.500}\right] + \frac{1.33}{2.00}\left[\frac{0.500 - 0.323}{0.500}\right]$$

$$= 0.235 + 0.235$$

$$= 0.470 \quad (47.0\%)$$

A5.2 Theoretical E_s Assuming Less Than 100% Centrifugal Force

It is possible that not enough centrifugal force was available to send 100% of the dispersed light phase to the overflow. Consider the following example:

Assume a total of 100 parts oil and water.

Conditions: $(O/W)_{MID} = 25/75$

$$\varepsilon = 0.30$$

If 100% of the centrifugal force was utilized, then the optimum volume split is:

$$0.3 = \frac{X}{X + 25} \qquad \text{where } X = \text{parts of water}$$

$$X = 10.7$$

$$\therefore \text{Optimum volume split} = \frac{25 + 10.7}{75 + 10.7} = \frac{37.5}{64.3} = 0.56$$

If only 80% of the light dispersed phase was able to reach the overflow, then the optimum volume split is:

$$\frac{0.8(35.7)}{64.3 + 0.2(37.5)} = \frac{28.6}{71.4} = 0.40$$

Calculate E_s at a volume split equal to 1.0:

$$\frac{Q_o}{Q_u} = \frac{28.6 + (50 - 28.6)}{50} = \frac{50}{50}$$

At the overflow:

If 28.6 units of oil/water mixture exit through the overflow, then the amount of water in this mixture is:

$$0.3 = \frac{X}{28.6}$$

$$X = 8.6$$

Thus the mixture contained 20 parts oil, 5 parts water.

Of the remaining, (50 - 28.6) 21.4 parts total, (25 - 20) 5 parts oil would be present for every (100 - 28.6) 71.4 parts total:

$$\frac{5}{71.4} \times 21.4 = 1.5 \text{ parts oil}$$

$$21.4 - 1.5 = 19.9 \text{ parts water}$$

total oil in overflow = 20 + 1.5 = 21.5 parts

total water in overflow = 8.6 + 19.9 = 28.5 parts

$$Y_o = \frac{21.5}{21.5 + 28.5} = 0.430$$

At the underflow:

total oil in underflow = 25 - 21.5 = 3.5 parts

total water in overflow = 50 - 3.5 = 46.5 parts

$$Y_u = \frac{3.5}{3.5 + 46.5} = 0.070$$

$$E_s = \frac{50}{100}\left[\frac{0.430 - 0.250}{1.0 - 0.250}\right] + \frac{50}{100}\left[\frac{0.250 - 0.070}{0.250}\right]$$

$$= 0.12 + 0.36$$

$$= 0.48 \quad \text{or} \quad 48\%$$

APPENDIX 6

MEASURED DATA

(Tables A6-1 to A6-5)

MEASURED DATA

System I : Butanol/Water

Table A6-1

Run No.	Volume of Liquid (mL)				Time of Sampling (s)	Pressure Readings						
	Underflow		Overflow			Mixing tee (lb/in^2)	Feed		Overflow		Underflow	
	Water	Butanol	Water	Butanol			LL	RL	LL	RL	LL	RL
							cm.Hg)					
	$(i)Q_{MID}$	$(O/W)_{MIN}$										
1	2750	440	475	70	20.0	7.9	95.2	69.8	72.0	92.0	92.0	73.0
2	2800	470	670	110	22.0	7.8	94.5	70.5	72.7	91.3	91.3	73.7
3	2360	390	750	120	19.6	7.4	93.8	71.2	72.5	91.5	91.5	73.5
4	2570	410	840	130	20.4	8.0	95.0	70.0	72.8	91.2	91.3	73.7
5	2570	425	1125	175	22.6	7.1	93.4	71.6	73.7	90.3	90.6	74.4
6	2390	370	1270	225	21.7	7.0	93.0	72.0	74.3	89.7	90.3	74.7
7	2830	465	1590	270	27.3	7.0	93.0	72.0	74.4	90.6	90.2	74.8
8	2500	330	1540	355	23.8	7.0	92.7	72.3	74.9	89.1	89.9	75.1
9	2260	255	1505	380	22.3	7.0	92.6	72.4	75.0	89.0	89.7	75.3
10	2320	210	1775	455	23.5	6.6	91.8	73.2	76.2	87.8	88.8	76.2
11	2190	195	1750	470	22.5	6.7	92.1	72.9	76.0	88.0	89.0	76.0
12	2015	170	1645	425	21.2	6.6	91.7	73.3	76.5	87.5	88.6	76.4
13	2025	175	1720	440	20.6	6.8	92.2	72.8	75.8	88.2	89.3	75.7
14	2700	235	2325	615	28.5	6.7	92.2	72.8	76.0	88.0	89.2	75.8
15	2310	225	2100	500	26.1	7.0	92.3	72.7	75.7	88.3	89.4	75.6
16	1790	160	1650	425	19.6	6.7	92.3	72.7	75.7	88.3	89.3	75.7
17	1760	180	1665	400	19.6	6.9	92.1	72.9	75.8	88.2	89.2	75.8
18	2710	220	2620	640	-	7.0	92.6	72.4	75.2	88.8	89.8	75.2
19	2210	190	2150	535	26.0	7.0	92.5	72.5	75.0	89.0	89.7	75.3
20	2155	195	2160	530	25.2	6.7	92.3	72.7	75.7	88.3	89.4	75.6
21	2110	180	2150	525	25.2	6.9	92.3	72.7	75.7	88.3	89.4	75.6
22	1420	120	1640	400	17.8	7.0	92.6	72.4	75.0	89.0	90.0	75.0

Butanol/Water (i) cont'd

Run No.	Volume of Liquid (mL)				Time of Sampling (s)	Pressure Readings						
	Underflow		Overflow			Mixing tee (lb/in^2)	Feed		Overflow		Underflow	
	Water	Butanol	Water	Butanol			LL	RL	LL (cm.Hg)	RL	LL	RL
23	2180	205	2815	635	28.6	7.0	92.6	72.4	75.4	88.6	89.9	75.1
24	1610	125	2400	520	24.3	7.0	93.0	72.0	75.0	89.0	90.5	74.5
25	1555	135	2830	580	25.8	7.2	93.3	71.7	74.7	89.3	90.9	74.1
26	1510	120	2930	610	26.1	7.3	93.5	71.5	74.3	89.7	91.2	73.8
27	1250	90	2750	570	24.2	7.1	93.4	71.6	74.5	89.5	91.1	73.9
28	1030	85	2955	585	-	7.4	94.4	70.6	73.4	90.6	92.4	72.6
(ii)	Q_{MID}	$(O/W)_{MID}$										
29	2650	865	940	295	24.3	7.8	94.6	70.4	72.4	91.6	92.0	73.0
30	2200	730	990	345	21.4	7.5	94.0	71.0	73.3	90.7	91.1	73.9
31	2555	805	1275	490	25.3	7.5	93.6	71.4	73.7	90.3	90.9	74.1
32	2495	695	1340	575	25.0	7.4	93.4	71.6	74.1	89.9	90.5	74.5
33	2540	675	1425	640	25.6	7.3	93.4	71.6	74.2	89.8	90.4	74.6
34	2405	570	1465	685	24.9	7.3	93.0	72.0	74.9	89.1	90.0	75.0
35	2650	600	1800	860	28.0	7.1	92.3	72.7	75.7	88.3	89.3	75.7
36	1980	390	1440	745	22.0	7.0	92.3	72.7	76.0	88.0	89.0	76.0
37	2665	570	1990	985	28.8	7.1	92.4	72.6	75.8	88.2	89.3	75.7
38	2480	500	1870	970	27.3	7.1	92.5	72.5	75.7	88.3	89.5	75.5
39	2630	510	2015	1030	29.2	7.0	92.4	72.6	75.8	88.2	89.2	75.8
40	2440	470	1875	965	27.1	7.0	92.3	72.7	76.1	87.9	89.0	76.0
41	2470	480	1980	1000	27.2	7.2	92.8	72.2	75.4	88.6	89.7	75.3
42	2380	485	1975	945	27.2	7.1	92.4	72.6	75.8	88.2	89.2	75.8
43	2595	495	2140	1085	30.1	7.0	92.3	72.7	76.0	88.0	89.2	75.8
44	2430	455	2260	1115	29.3	7.1	92.6	72.4	75.7	88.3	89.5	75.5
45	2355	440	2295	1170	30.1	7.4	93.4	71.6	74.7	89.3	90.6	74.4
46	2170	390	2205	1075	27.6	7.2	93.0	72.0	75.1	88.9	90.0	75.0
47	2010	380	2085	1045	27.0	7.3	93.2	71.8	74.9	89.1	90.4	74.6

Butanol/Water (ii) cont'd

Run No.	Volume of Liquid (mL)				Time of Sampling (s)	Pressure Readings						
	Underflow		Overflow			Mixing tee (lb/in^2)	Feed		Overflow		Underflow	
	Water	Butanol	Water	Butanol			LL	RL	LL	RL	LL	RL
							(cm.Hg)					
48	1850	335	2125	990	25.5	7.1	92.7	72.3	75.3	88.7	90.0	75.0
49	1870	330	2320	1060	26.8	7.3	93.1	71.9	75.0	89.0	90.4	74.6
50	1650	315	2505	1060	26.2	7.4	93.3	71.7	75.0	89.0	90.5	74.5
51	1470	255	2175	975	-	7.5	93.6	71.4	74.2	89.8	91.1	73.9
(iii)	Q_{MAX}	$(O/W)_{MIN}$										
52	3200	495	550	85	11.8	20.5	122.5	42.5	53.3	110.7	110.0	55.0
53	3270	565	1440	220	14.7	18.0	118.5	46.5	57.6	106.4	107.1	57.9
54	3235	535	2040	330	16.3	16.5	114.5	50.5	62.2	101.8	103.0	62.0
55	2900	480	1870	310	15.3	16.3	110.0	55.0	68.3	995.7	97.5	67.5
56	3045	515	1985	320	16.0	16.3	110.5	54.5	68.3	95.7	97.5	67.5
57	3220	460	2240	435	17.1	15.9	113.0	52.0	63.7	100.3	101.8	63.2
58	3290	440	2500	490	18.1	16.0	110.7	54.3	68.5	95.5	97.3	67.7
59	2810	350	2210	430	15.6	16.5	111.5	53.5	67.7	96.3	98.5	66.5
60	3010	350	2480	530	17.2	16.5	111.5	53.5	67.7	96.3	98.0	67.0
61	2460	290	2020	465	14.0	15.0	108.3	56.7	69.5	94.5	96.4	68.6
62	2900	295	2545	625	16.7	14.5	109.7	55.3	68.2	95.8	98.1	66.9
63	2645	325	2480	530	16.4	17.0	112.3	52.7	67.3	96.7	99.3	65.7
64	2780	330	2610	560	17.1	17.0	113.0	52.0	67.0	97.0	99.7	65.3
65	3125	360	2925	645	18.9	14.5	109.3	55.7	68.3	95.7	98.3	66.7
66	3170	350	2980	660	19.1	14.5	109.4	55.6	68.3	95.7	98.4	66.6
67	2900	330	2760	590	17.4	16.5	111.5	53.5	68.0	96.0	98.5	66.5
68	2800	290	2750	620	17.4	15.5	112.3	52.7	66.2	97.8	100.8	64.2
69	2600	255	2580	580	16.3	15.5	112.3	52.7	66.0	98.0	101.0	64.0
70	2700	305	2780	560	16.7	17.0	112.5	52.5	67.0	97.0	99.3	65.7
71	2595	265	2670	600	16.5	15.4	112.0	53.0	66.2	97.8	100.5	64.5

Butanol/Water (iii) cont'd

Run No.	Volume of Liquid (mL)				Time of Sampling (s)	Pressure Readings						
	Underflow		Overflow			Mixing tee (lb/in^2)	Feed		Overflow		Underflow	
	Water	Butanol	Water	Butanol			LL	RL	LL	RL	LL	RL
							(cm Hg)					
72	2620	255	2750	610	16.6	15.5	112.3	52.7	66.0	98.0	100.7	64.3
73	2335	235	2465	565	15.4	15.0	110.0	55.0	67.5	96.5	99.0	66.0
74	2710	280	2995	675	17.8	15.4	112.1	52.9	66.2	97.8	100.7	64.3
75	2400	230	2740	600	16.1	15.5	112.5	52.5	65.5	98.5	101.3	63.7
76	2125	225	2680	600	14.8	15.5	112.2	52.8	66.0	98.0	100.7	64.3
77	1995	225	2650	535	14.7	18.8	117.3	47.7	63.3	100.7	104.5	60.5
78	2255	260	3130	610	16.9	18.7	117.5	47.5	62.7	101.3	104.7	60.3
79	1940	215	2960	610	14.9	16.8	118.5	46.5	62.8	101.2	105.0	60.0
80	1610	180	2840	530	13.9	19.5	119.0	46.0	62.5	101.5	105.5	59.5
81	1560	170	2750	510	13.0	19.8	120.0	45.0	61.2	102.8	106.7	58.3
(iv)	Q_{MAX}	$(O/W)_{MID}$										
82	2950	960	500	160	11.8	22.0	125.5	39.5	50.7	113.3	112.3	52.7
83	2600	860	720	220	12.2	20.5	122.0	43.0	53.7	110.3	110.0	55.0
84	2740	945	1260	395	13.7	19.0	120.5	44.5	56.0	108.0	108.5	56.5
85	2650	895	1275	400	13.7	19.0	120.8	44.2	55.1	108.9	109.3	55.7
86	2930	970	1520	485	15.4	18.4	118.8	46.2	57.5	106.5	107.3	57.7
87	2600	820	1555	585	14.4	17.5	113.0	52.0	65.0	99.0	100.3	64.7
88	2600	800	1645	580	15.1	17.8	113.3	51.7	64.7	99.3	103.3	61.7
89	2330	630	1570	615	13.7	17.0	111.3	53.7	67.3	96.7	98.3	66.7
90	2290	620	1580	680	13.2	17.3	112.0	53.0	67.0	97.0	98.7	66.3
91	2505	655	1790	790	14.8	16.8	111.0	54.0	67.7	96.3	98.3	66.7
92	2750	700	2020	890	15.9	17.0	111.0	54.0	68.0	96.0	97.7	67.3
93	2245	540	1810	830	-	17.0	113.0	52.0	67.0	97.0	99.5	65.5
94	2880	665	2370	1065	17.9	15.3	110.8	54.2	66.7	97.3	100.0	65.0
95	2720	630	2440	1120	18.7	13.2	106.3	58.7	69.5	94.5	96.8	68.2
96	2230	520	2080	890	14.8	18.4	115.0	50.0	66.5	97.5	100.3	64.7
97	2630	580	2505	1095	17.1	18.2	114.5	50.5	65.0	99.0	101.5	63.5

Butanol/Water (iv) cont'd

Run No.	Volume of Liquid (m/L)				Time of Sampling (s)	Pressure Readings						
	Underflow		Overflow			Mixing tee (lb/in²)	Feed		Overflow		Underflow	
	Water	Butanol	Water	Butanol			LL	RL	LL	RL	LL	RL
							(cm.Hg)					
98	1975	470	2060	880	13.6	18.1	114.5	50.5	64.7	99.3	102.0	63.0
99	2230	430	2440	1080	-	16.4	113.7	51.3	64.7	99.3	102.3	62.7
100	1890	445	2235	855	13.9	18.4	115.3	49.7	64.3	99.7	102.8	62.2
101	1855	440	2175	895	14.0	17.0	115.0	50.0	63.3	100.7	104.0	61.0
102	2070	410	2310	1030	18.1	16.5	114.3	50.7	64.5	99.5	104.4	60.6
103	2395	550	2830	1185	14.8	16.7	114.5	50.5	63.6	100.4	102.5	62.5
104	2065	485	2505	1055	16.0	16.9	114.8	50.2	63.5	100.5	104.3	60.7
105	1905	435	2500	1050	15.3	17.4	116.4	48.6	62.0	102.0	105.8	59.2
106	1820	420	2640	1080	15.1	18.0	117.8	47.2	60.7	103.3	107.3	57.7
107	1960	430	2995	1155	16.7	20.5	121.0	44.0	60.0	104.0	108.0	57.0
108	1540	360	2500	1000	13.6	20.5	120.7	44.3	59.7	104.3	108.3	56.7
(v)	$(O/W)_{MIN}$, Q variable											
109	2520	380	610	90	20.9	7.5	93.7	71.3	73.0	91.0	91.0	74.0
110	3135	505	1000	150	14.5	16.0	112.3	52.7	61.5	102.5	102.5	62.5
111	2220	195	1870	480	30.6	7.5	97.3	67.7	69.2	94.8	95.6	69.4
112	2545	250	2180	540	17.7	11.0	101.5	63.5	71.9	92.1	93.9	71.1
113	1975	165	1700	425	51.1	11.5	105.6	59.4	59.2	104.8	105.3	59.7
114	2595	235	2240	570	20.7	8.8	96.8	68.2	74.1	89.9	91.3	73.7
115	2590	230	2260	590	25.4	7.1	93.0	72.0	75.7	88.3	89.4	75.6
116	2750	265	2420	620	53.8	10.0	102.8	62.2	64.0	100.0	100.9	64.1
117	1665	155	1470	385	33.5	10.0	101.8	63.2	63.7	100.3	101.2	63.8
118	2740	260	2575	545	72.4	11.0	105.0	60.0	60.5	103.5	104.5	60.5
119	1810	150	1700	400	36.5	10.1	102.1	62.9	63.6	100.4	101.4	63.6
120	2430	220	2400	560	21.3	9.5	98.5	66.5	72.3	91.7	93.3	71.1
121	1480	125	1470	350	40.6	11.5	106.0	59.0	59.4	104.6	105.5	59.5
122	2320	225	2335	550	35.5	8.5	97.3	67.7	69.2	94.8	95.7	69.3
123	2395	210	2350	585	26.0	7.5	93.7	71.3	74.7	89.3	90.5	74.5

Butanol/Water (v) cont'd

Run No.	Volume of Liquid (mL)				Time of Sampling (s)	Pressure Readings						
	Underflow		Overflow			Mixing tee (lb/in^2)	Feed		Overflow		Underflow	
	Water	Butanol	Water	Butanol			LL	RL	LL	RL	LL	RL
							(cm.Hg)					
124	2635	255	2640	620	19.8	11.8	104.0	61.0	69.7	94.3	96.5	68.5
125	2110	170	2215	485	43.5	10.0	101.4	63.6	64.0	100.0	100.8	64.2
126	540	40	1770	340	43.2	12.5	109.0	56.0	56.5	107.5	108.5	56.5
(vi)	$(O/W)_{MID}$, $Q_{variable}$											
127	2155	645	1340	480	18.1	10.0	97.8	67.2	72.3	91.7	92.3	72.7
128	1810	505	1210	480	13.5	11.5	101.0	64.0	72.0	92.0	93.5	71.5
129	2725	600	2135	985	20.7	11.0	102.0	63.0	70.5	93.5	95.0	70.0
130	2750	625	2180	1020	19.4	12.1	104.0	610	69.9	94.1	95.9	69.1
131	1890	355	1445	740	27.2	9.0	98.2	66.8	68.3	95.7	96.5	68.5
132	2395	525	2010	950	21.5	9.4	97.5	67.5	73.1	90.9	92.2	72.8
133	1730	320	1405	735	36.7	10.7	103.3	61.7	62.5	101.5	102.5	62.5
134	1510	255	1220	635	40.4	12.0	106.7	58.3	58.4	105.5	106.4	58.6
135	2670	570	2445	1145	27.3	8.2	94.8	70.2	74.4	89.6	90.8	74.2
136	2540	530	2350	1090	28.5	7.5	93.5	71.5	75.1	88.9	90.0	75.0
137	2480	570	2330	1080	23.3	9.3	97.1	67.9	73.7	90.3	91.8	73.2
138	2060	405	1920	910	32.9	9.0	98.3	66.7	68.2	95.8	96.6	68.4
(vii)	Q_{MAX}, $(O/W)_{MIN}$; time allowed before sampling : (No.139) = 1.0 min, (No.140) = 1.5 min, (No.141) = 1.75 min											
	O/U constant											
139	2480	225	2540	500	16.5	15.3	111.5	53.5	66.5	97.5	100.3	64.7
140	2705	270	2640	615	16.9	-	112.0	53.0	66.0	98.0	101.0	64.0
141	2820	255	2730	605	17.4	15.5	111.8	53.2	66.0	98.0	100.7	64.3

System II : MIBK/Water

Table A6-2

Run No.	Volume of Liquid (mL)				Time of Sampling (s)	Pressure Readings						
	Underflow		Overflow				Feed		Overflow		Underflow	
	Water	MIBK	Water	MIBK		Mixing tee (lb/in^2)	LL	RL	LL (cm.Hg)	RL	LL	RL
(i)	Q_{MIN},	$(O/W)_{MIN}$										
1	2890	230	1135	440	43.9	9.5	100.8	64.2	64.8	99.2	100.0	65.0
2	2060	50	750	400	32.3	9.8	101.1	63.9	64.0	100.0	100.6	64.4
3	1465	35	560	300	-	9.5	100.0	65.0	65.0	99.0	99.4	65.6
4	3180	70	1280	680	49.4	9.7	101.0	64.0	64.3	99.7	100.3	64.7
5	3960	60	1695	805	66.8	9.5	101.0	64.0	64.5	99.5	100.4	64.6
6	3820	65	1590	830	59.4	9.5	100.9	64.1	64.8	99.2	99.9	65.1
7	1905	15	800	435	30.3	9.6	101.0	64.0	64.5	99.5	100.3	64.7
8	1635	5	765	390	27.0	9.7	101.1	63.9	64.4	99.6	100.4	64.6
9	1870	0	1020	480	32.2	9.5	100.8	64.2	64.9	99.1	100.0	65.0
10	1490	0	930	395	30.0	10.1	102.4	62.6	63.0	101.0	101.9	63.1
11	1200	0	1160	380	29.2	10.0	102.0	63.0	63.2	100.8	101.6	63.4
(ii)	Q_{MIN},	$(O/W)_{MID}$										
12	1870	160	420	595	35.4	10.1	102.9	62.1	62.3	101.7	102.3	62.7
13	1560	155	420	475	-	9.5	100.7	64.3	64.7	99.3	99.7	65.3
14	1300	80	380	485	22.0	9.8	101.6	63.4	63.7	100.3	101.0	64.0
15	1620	90	495	575	25.9	9.8	101.3	63.7	64.1	99.9	100.5	64.5
16	1760	95	530	670	28.8	9.5	100.8	64.2	64.7	99.3	100.0	65.0
17	1320	20	410	555	22.1	9.7	101.0	64.0	64.2	99.8	100.5	64.5
18	1400	5	515	625	28.3	10.1	102.5	62.5	62.8	101.2	102.1	62.9
19	1305	20	525	590	-	9.7	101.4	63.6	63.9	100.1	100.8	64.2
20	1080	5	510	505	22.3	10.0	102.0	63.0	63.4	100.6	101.4	63.6
21	995	0	475	485	21.2	10.0	102.1	62.9	63.0	101.0	101.6	63.4
(iii)	Q_{MID},	$(O/W)_{MIN}$										
22	2950	140	1360	560	26.6	6.5	91.7	73.3	76.0	88.0	88.7	76.3

MIBK/Water (iii) cont'd

Run No.	Volume of Liquid (mL)				Time of Sampling (s)	Pressure Readings						
	Underflow		Overflow			Mixing tee (lb/in^2)	Feed		Overflow		Underflow	
	Water	MIBK	Water	MIBK			LL	RL	LL	RL	LL	RL
							(cm.Hg)					
23	2560	20	1340	640	23.7	6.5	91.8	73.2	76.0	88.0	88.8	76.2
24	3090	20	1735	705	29.9	6.3	91.6	73.4	76.1	87.9	88.7	76.3
25	2960	0	1650	790	27.7	6.5	91.7	73.3	76.4	87.6	88.6	76.4
26	2260	0	1420	615	22.7	6.6	92.4	72.6	75.6	88.4	89.5	75.5
27	2050	0	1530	615	21.9	6.7	92.4	72.6	75.6	88.4	89.7	75.3
(iv)	Q_{MAX}	$(O/W)_{MIN}$										
28	3080	500	820	115	12.6	20.0	125.0	40.0	50.5	113.5	113.0	52.0
29	2800	420	1000	200	12.3	18.3	120.0	45.0	56.1	107.9	107.6	57.4
30	3270	430	1430	300	15.1	17.4	119.0	46.0	58.7	105.3	105.7	59.3
31	2910	290	1340	420	13.9	14.3	110.5	54.5	67.1	96.9	98.0	67.0
32	3260	280	1555	515	15.3	16.3	114.5	50.5	62.5	101.5	102.5	62.5
33	2925	240	1380	485	14.2	14.5	110.2	54.8	67.0	97.0	98.2	66.8
34	1555	115	755	270	7.2	15.7	113.4	51.6	63.7	100.3	101.5	63.5
35	3130	170	1585	545	14.6	15.7	113.0	52.0	65.0	99.0	100.5	64.5
36	3065	100	1600	700	15.3	15.0	111.4	53.6	67.5	96.5	99.2	65.8
37	3175	85	1720	685	15.8	14.6	110.9	54.1	67.4	96.6	99.0	66.0
38	3225	20	1900	805	16.4	14.5	110.3	54.7	67.2	96.8	98.5	66.5
39	3360	0	2120	920	17.4	14.3	109.6	55.4	68.0	96.0	97.6	67.4
40	2660	0	2070	720	15.1	13.9	109.0	56.0	69.2	94.8	96.7	68.3
41	2700	0	2205	765	16.5	17.0	116.3	48.7	62.5	101.5	105.0	60.0
42	2590	0	2680	900	16.7	15.5	112.6	52.4	66.0	98.0	101.2	63.8
43	2620	0	2710	905	17.3	15.6	112.8	52.2	65.7	98.3	101.6	63.4
44	2270	0	2570	810	15.5	16.3	114.8	50.2	64.0	100.0	103.5	61.5
45	2180	0	2500	830	15.1	15.6	113.2	51.8	65.3	98.7	102.0	63.0
46	1685	0	2840	710	14.5	17.0	116.7	48.3	62.4	101.6	105.6	59.4
(v)	Q_{MAX},	$(O/W)_{MID}$										
47	2540	795	410	175	11.2	20.5	125.7	39.3	49.0	115.0	113.5	51.5

MIBK/Water (v) cont'd

Run No.	Volume of Liquid (mL)				Time of Sampling (s)	Pressure Readings						
	Underflow		Overflow			Mixing tee (lb/in^2)	Feed		Overflow		Underflow	
	Water	MIBK	Water	MIBK			LL	RL	LL	RL	LL	RL
							(cm.Hg)					
48	2705	815	590	280	12.3	20.0	124.6	40.4	50.8	113.2	112.4	52.6
49	2550	760	580	295	11.7	19.3	123.0	42.0	52.2	111.8	111.0	54.0
50	2660	560	835	620	12.9	16.7	116.1	48.9	59.9	104.1	104.5	60.5
51	2810	405	950	845	13.8	16.0	113.9	51.1	62.7	101.3	102.3	62.7
52	2450	170	880	960	12.3	14.6	110.8	54.2	66.0	98.0	99.4	65.6
53	2620	110	1045	1140	13.5	14.5	110.3	54.7	67.1	96.9	98.6	66.4
54	2690	25	1145	1295	14.2	13.0	108.0	57.0	69.2	94.8	996.7	68.3
55	2205	10	1245	1155	12.7	15.0	112.0	53.0	65.6	98.4	101.0	64.0
56	2180	0	1795	1335	14.6	15.8	114.0	51.0	64.0	100.0	103.4	61.6
57	1820	0	2105	1315	14.4	17.1	117.4	47.6	61.1	102.9	107.0	58.0
(vi)	$(O/W)_{MIN}$, Q varied, volume split constant.											
58	1610	50	675	315	20.6	12.5	109.0	56.0	57.0	107.0	107.7	57.3
59	2270	90	1135	480	13.4	11.1	102.7	62.3	69.9	94.1	95.3	69.7
60	1705	30	820	380	17.8	17.8	122.0	43.0	44.7	119.3	120.3	44.7
61	2085	55	1070	480	14.9	9.0	97.4	67.6	72.8	91.2	92.3	72.7

System III : Toluene/Water

Table A6-3

Run No.	Volume of Liquid (mL)				Time of Sampling (s)	Pressure Readings						
	Underflow		Overflow			Mixing tee (lb/in^2)	Feed		Overflow		Underflow	
	Water	Toluene	Water	Toluene			LL	RL	LL (cm Hg)	RL	LL	RL
(i)	Q_{MAX}, $(O/W)_{MIN}$; preliminary runs											
1	2830	90	1585	625	14.0	14.6	110.5	54.5	66.2	97.8	99.3	65.7
2	3135	40	1900	830	16.1	14.2	109.0	56.0	67.7	96.3	98.0	67.0
3	2875	5	1925	785	15.3	-	-	-	-	-	-	-
(ii)	Q_{MIN}, $(O/W)_{MIN}$											
4	1080	150	460	120	17.0	9.5	100.5	64.5	65.0	99.0	99.6	65.4
5	2910	285	1720	480	56.5	10.5	103.4	61.6	62.2	101.8	102.6	62.4
6	2465	270	1560	380	48.4	10.5	103.0	62.0	62.2	101.8	102.6	62.4
7	2380	240	1450	410	44.8	10.5	103.2	61.8	62.3	101.7	102.6	62.4
8	3380	330	2105	575	61.5	10.3	102.7	62.3	62.8	101.2	102.3	62.7
9	2595	215	1570	490	48.2	10.5	103.4	61.6	62.1	101.9	102.8	62.2
10	1720	190	1140	280	37.0	10.5	103.3	61.7	61.7	102.3	102.8	62.2
11	1240	80	760	230	23.7	10.6	103.6	61.4	62.0	102.0	103.0	62.0
12	2190	230	1540	380	44.0	10.3	102.7	62.3	62.6	101.4	102.3	62.7
13	1040	60	770	230	23.2	11.1	104.9	60.1	60.6	103.4	104.4	60.6
14	840	55	880	240	24.8	-	106.0	59.0	59.2	104.8	105.4	59.6
15	735	45	995	235	26.4	11.7	106.5	58.5	58.8	105.2	106.2	58.8
(iii)	Q_{MIN}, $(O/W)_{MID}$											
16	1260	320	540	270	22.3	9.5	100.8	64.2	64.7	99.3	100.0	65.0
17	1120	260	505	265	23.2	9.7	101.1	63.9	64.2	99.8	100.5	64.5
18	915	195	500	240	19.6	10.0	101.9	63.1	63.4	100.6	101.3	63.7
19	1400	250	780	460	29.4	10.0	102.4	62.6	63.0	101.0	101.8	63.2
20	840	180	565	285	22.0	10.6	103.7	61.3	61.6	102.4	103.3	61.7
21	930	185	640	315	-	10.5	103.3	61.7	62.0	102.0	102.8	62.2
22	830	160	580	300	22.4	10.5	103.4	61.6	62.0	102.0	102.9	62.1

Toluene/Water (iii) cont'd

Run No.	Volume of Liquid (mL)				Time of Sampling (s)	Pressure Readings						
	Underflow		Overflow			Mixing tee (lb/in^2)	Feed		Overflow		Underflow	
	Water	Toluene	Water	Toluene			LL	RL	LL	RL	LL	RL
							(cm.Hg)					
23	740	130	590	300	21.2	11.0	104.4	60.6	60.8	103.2	104.0	61.0
24	585	95	560	270	19.8	11.0	104.9	60.1	60.2	103.8	104.5	60.5
25	570	90	660	300	22.3	11.1	105.3	59.7	59.8	104.2	105.0	60.0
(iv)	Q_{MAX},	$(O/W)_{MIN}$										
26	2900	440	1270	230	13.4	18.1	119.2	45.8	56.5	107.5	107.5	57.5
27	3155	245	1610	530	-	16.6	115.0	50.0	61.2	102.8	104.2	60.8
28	2815	90	1685	670	14.1	15.3	111.7	53.3	64.5	99.5	101.0	64.0
29	2885	25	1960	775	15.5	14.8	110.5	54.5	66.2	97.8	99.7	65.3
30	30.5	40	2195	835	16.6	14.7	110.3	54.7	66.8	97.2	99.3	65.7
31	2525	15	2175	765	14.9	13.8	108.0	57.0	68.8	95.2	97.4	67.6
32	2250	10	2590	785	15.5	15.3	111.8	53.2	65.5	98.5	101.3	63.7
(v)	Q_{MAX},	$(O/W)_{MID}$										
33	2720	430	1290	835	14.5	14.0	109.4	55.6	66.7	97.3	98.5	66.5
34	2650	280	1450	1050	-	14.0	109.0	56.0	67.5	96.5	98.2	66.8
35	2400	120	1480	1120	14.1	13.2	107.0	58.0	69.7	94.3	96.3	68.7
36	2145	85	1830	1220	14.6	14.3	109.8	55.2	67.2	96.8	99.4	65.6

System IV : Kerosene/Water

Table A6-4

Run No.	Volume of Liquid (mL)				Time of Sampling (s)	Pressure Readings						
	Underflow		Overflow			Mixing tee (lb/in^2)	Feed		Overflow		Underflow	
	Water	Kerosene	Water	Kerosene			LL	RL	LL	RL	LL	RL
							(cm.Hg)					
(i)	Q_{MIN},	$(O/W)_{MIN}$										
1	1800	285	350	70	25.8	9.9	101.6	63.4	63.6	100.4	101.0	64.0
2	1850	230	520	150	24.3	9.7	100.8	64.2	64.4	99.6	100.0	65.0
3	1790	195	640	200	28.2	9.8	101.4	63.6	63.7	100.3	100.8	64.2
4	1680	140	695	215	30.0	10.4	102.8	62.2	62.2	101.8	102.5	62.5
5	1620	115	740	230	25.7	9.6	100.9	64.1	63.1	100.9	100.0	65.0
6	1445	115	860	270	26.7	9.5	101.0	64.0	64.2	99.8	100.4	64.6
7	840	60	515	165	15.7	10.0	101.9	63.1	63.7	100.3	101.3	63.7
8	1340	90	890	290	27.4	10.0	102.0	63.0	62.2	101.8	101.5	63.5
9	1060	50	720	240	23.2	10.2	102.5	62.5	63.0	101.0	102.0	63.0
10	1335	55	1055	325	28.4	9.7	101.4	63.6	64.0	100.0	100.7	64.3
11	1400	40	1375	380	31.3	9.5	100.7	64.3	64.7	99.3	100.0	65.0
12	1020	50	1220	320	25.6	10.0	101.7	63.3	63.7	100.3	101.2	63.8
13	725	40	1080	260	23.5	10.3	102.8	62.2	62.5	101.5	102.4	62.6
(ii)	Q_{MIN},	$(O/W)_{MID}$										
14	1835	555	340	190	25.7	9.0	99.6	65.4	65.5	98.5	98.6	66.4
15	1450	420	395	200	23.2	9.2	100.0	65.0	65.0	99.0	99.4	65.6
16	1150	260	450	270	24.8	10.0	102.5	62.5	62.7	101.3	101.9	63.1
17	1100	220	510	325	24.8	10.0	102.3	62.7	62.7	101.3	101.8	63.2
18	1175	195	690	430	26.1	9.8	101.7	63.3	63.2	100.8	101.3	63.7
19	1115	125	720	490	25.5	9.5	101.0	64.0	64.2	99.8	100.5	64.5
20	1065	125	855	520	27.5	9.8	101.5	63.5	63.7	100.3	101.1	63.9
21	1040	95	860	545	26.6	9.5	101.3	63.7	64.0	100.0	100.8	64.2
22	970	85	970	570	26.0	9.5	100.8	64.2	64.4	99.6	100.3	64.7
23	705	90	870	460	25.6	10.2	102.7	62.3	62.4	101.6	102.4	62.6
24	810	80	1070	510	28.0	10.0	102.0	63.0	63.2	100.8	101.5	63.5

Kerosene/Water cont'd.

Run No.	Volume of Liquid (mL)				Time of Sampling (s)	Pressure Readings						
	Underflow		Overflow			Mixing tee (lb/in^2)	Feed		Overflow		Underflow	
	Water	Kerosene	Water	Kerosene			LL	RL	LL (cm.Hg)	RL	LL	RL
(iii)	Q_{MIN},	$(O/W)_{MAX}$										
25	930	900	580	700	29.8	10.5	103.5	61.5	62.0	102.0	102.8	62.2
26	610	590	440	515	21.0	11.0	104.5	60.5	61.3	102.7	104.0	61.0
27	710	660	660	790	24.7	10.0	102.3	62.7	63.2	100.8	101.5	63.5
28	630	635	670	765	25.7	10.8	104.5	60.5	61.0	103.0	103.5	61.5
29	470	450	640	730	22.2	10.4	103.3	61.7	62.2	101.8	102.8	62.2
30	380	360	610	690	21.0	11.2	105.0	60.0	60.5	103.5	104.4	70.6
31	260	240	490	550	17.1	11.0	105.0	60.0	60.5	103.5	104.5	60.5
32	320	305	740	810	22.0	11.0	109.3	60.7	61.2	102.8	103.8	61.2
(iv)	Q_{MID},	$(O/W)_{MIN}$										
33	2680	360	1090	240	23.4	6.8	92.6	72.4	74.7	89.3	89.9	75.1
34	2590	150	1260	445	23.1	6.5	91.8	73.2	75.8	88.2	89.0	76.0
35	2545	135	1360	515	23.0	6.7	92.4	72.6	75.3	88.7	89.5	75.5
36	2360	50	1490	600	22.1	6.6	92.1	72.9	75.8	88.2	89.2	75.8
37	2475	45	1730	675	24.3	6.5	91.7	73.3	76.4	87.6	88.7	76.3
38	2215	40	1700	610	22.3	6.5	91.5	73.5	76.6	87.4	88.5	76.5
39	2015	30	1845	625	22.3	6.5	91.5	73.5	76.5	87.5	88.7	76.3
(v)	Q_{MID},	$(O/W)_{MID}$										
40	2450	590	800	520	23.6	6.6	92.4	72.6	74.6	89.4	89.8	75.2
41	2530	550	895	575	24.2	6.6	92.7	72.3	74.3	89.7	90.2	74.8
42	2310	370	960	760	23.0	6.4	91.9	73.1	75.4	88.6	89.3	75.7
43	2570	345	1125	895	25.4	6.4	91.9	73.1	75.4	88.6	89.3	75.7
44	2540	235	1235	1065	25.6	6.4	91.7	73.3	75.7	88.3	89.1	75.9
45	1725	120	900	800	17.6	6.3	92.0	73.0	75.7	88.3	89.3	75.7
46	2215	85	1385	1165	24.5	6.3	91.5	73.5	76.0	88.0	89.0	76.0

Kerosene/Water (v) cont'd

Run No.	Volume of Liquid (mL)				Time of Sampling (s)	Pressure Readings						
	Underflow		Overflow			Mixing tee (lb/in^2)	Feed		Overflow		Underflow	
	Water	Kerosene	Water	Kerosene			LL	RL	LL	RL	LL	RL
							(cm.Hg)					
47	2120	50	1535	1215	25.4	6.4	91.8	73.2	75.7	88.3	89.3	75.7
48	1880	60	1680	1170	24.7	6.5	92.2	72.8	75.3	88.7	89.8	75.2
(vi)	Q_{MID},	$(O/W)_{MAX}$										
49	1375	1355	535	700	19.9	7.8	95.0	70.0	71.5	92.5	92.8	72.2
50	1335	1270	1110	1360	23.1	7.5	93.8	71.2	73.1	90.9	91.5	73.5
51	930	750	1075	1355	20.1	7.6	94.8	70.2	72.2	91.8	93.0	72.0
52	840	690	1125	1355	19.6	8.0	95.3	69.7	72.0	92.0	93.3	71.7
53	790	490	1260	1630	21.3	8.0	95.5	69.5	71.6	92.4	93.9	71.1
54	660	440	1310	1635	21.3	7.9	95.8	69.2	71.2	92.8	94.3	70.7
55	460	390	1570	1745	21.3	8.7	97.7	67.3	69.5	94.5	96.5	68.5
(vii)	Q_{MAX},	$(O/W)_{MIN}$										
56	3400	585	905	115	13.5	18.3	120.5	44.5	55.5	108.5	108.3	56.7
57	3250	510	1275	215	14.4	16.5	115.5	49.5	61.0	103.0	103.5	61.5
58	3025	370	1430	370	14.0	15.7	113.5	51.5	63.5	100.5	101.5	63.5
59	3360	220	1595	560	15.7	15.3	112.3	52.7	64.6	99.4	100.4	64.6
60	3120	150	1645	645	15.4	15.0	111.3	53.7	65.7	98.3	99.6	65.4
61	2995	85	1775	715	15.2	14.5	110.0	55.0	66.5	97.5	98.3	66.7
62	2890	30	1830	740	15.4	13.7	108.3	56.7	68.5	95.5	97.3	67.7
63	3000	30	2010	805	15.7	14.3	109.0	56.0	68.2	95.8	97.8	67.2
64	2615	25	2065	735	15.0	13.5	107.5	57.5	70.1	93.9	96.0	69.0
65	2915	25	2745	935	18.1	-	-	-	-	-	-	-
66	2545	30	2680	840	16.8	14.8	111.0	54.0	67.2	96.8	99.5	65.5
67	2430	10	3030	895	17.6	15.0	111.5	53.5	66.2	97.8	101.0	64.0
68	1940	20	2865	720	15.2	15.7	113.5	51.5	64.8	99.2	102.5	62.5

Kerosene/Water cont'd

Run No.	Volume of Liquid (mL)				Time of Sampling (s)	Pressure Readings						
	Underflow		Overflow			Mixing tee (lb/in^2)	Feed		Overflow		Underflow	
	Water	Kerosene	Water	Kerosene			LL	RL	LL	RL	LL	RL
							(cm.Hg)					
(viii)	Q_{MAX},	$(O/W)_{MID}$										
69	2610	840	600	240	11.9	17.4	118.3	46.7	56.2	107.8	107.3	57.7
70	2370	630	765	445	11.6	15.8	114.4	50.6	61.0	103.0	103.4	61.6
71	2680	530	1050	760	14.0	14.5	110.7	54.3	64.7	99.3	100.0	65.0
72	2790	350	1165	995	14.7	14.0	109.5	55.5	66.2	97.8	99.0	66.0
73	3065	190	1400	1335	16.5	13.5	108.0	57.0	68.0	96.0	97.5	67.5
74	2045	30	1110	995	11.5	12.7	106.6	58.4	68.2	95.8	96.6	68.4
75	2710	40	1640	1445	16.2	13.5	108.3	56.7	68.0	96.0	98.0	67.0
76	2620	25	1770	1465	16.3	13.8	108.9	56.1	67.5	96.5	98.7	66.3
77	2410	50	1890	1440	16.1	14.3	110.0	55.0	66.7	97.3	99.8	65.2
78	2065	25	2070	1405	15.7	14.8	111.3	53.7	65.7	98.3	101.3	63.7
79	1990	15	2255	1425	15.8	15.0	112.0	53.0	65.0	99.0	102.3	62.7
(ix)	Q_{MAX},	$(O/W)_{MAX}$										
80	1870	1810	520	690	13.0	15.5	114.0	51.0	58.0	106.0	106.0	69.0
81	1795	1685	575	805	13.2	16.8	115.7	49.3	57.5	106.5	106.5	58.5
83	2100	1815	890	1300	16.2	15.1	111.8	53.2	61.7	102.3	102.5	62.5
83	1965	1340	1070	1805	16.7	14.0	108.5	56.5	65.3	98.7	99.5	65.5
84	1990	1360	1210	1970	17.8	14.8	110.3	54.7	63.5	100.5	102.0	63.0
85	2030	1280	1305	2090	18.2	15.0	111.3	53.7	62.7	101.3	103.7	61.3
86	1835	1120	1205	2055	16.9	15.3	112.0	53.0	61.7	102.3	104.3	60.7
87	1680	1030	1290	2065	16.5	15.8	113.3	51.7	61.2	102.8	105.0	60.0
88	1720	960	1395	2260	17.2	16.3	114.3	50.7	59.7	104.3	106.5	58.5
89	1595	765	1505	2335	16.6	17.3	116.7	48.3	58.0	106.0	108.0	57.0
90	1420	560	1350	2390	15.5	17.5	118.5	46.5	57.0	107.0	110.5	54.5
91	1780	280	1340	2590	17.1	17.2	118.0	47.0	57.2	106.8	109.8	55.2
92	1400	625	1430	2485	15.9	19.5	-	-	-	-	-	-

Kerosene/Water (ix) cont'd

Run No.	Volume of Liquid (mL)				Time of Sampling (s)	Pressure Readings						
	Underflow		Overflow			Mixing tee (lb/in^2)	Feed		Overflow		Underflow	
	Water	Kerosene	Water	Kerosene			LL	RL	LL	RL	LL	RL
							(cm.Hg)					
93	1460	550	1440	2520	16.2	18.7	121.0	44.0	55.0	109.0	112.5	52.5
94	1260	415	1420	2415	14.7	20.0	123.5	41.5	52.7	111.3	115.3	49.7
95	1240	275	1350	2480	14.2	20.5	125.0	40.0	51.7	112.3	116.8	48.2
(x)	Q_{MAX}, $(O/W)_{MIN}$; check for steady state; time allowed before sampling: (No. 96) = 15s, (No. 97) = 60s.											
96	2915	25	2745	935	18.1	-	-	-	-	-	-	-
97	2775	15	2850	970	18.4	14.2	109.6	55.4	68.0	96.0	98.4	66.6
(xi)-(xvi) represent cases where flowrate at the mixing tee is equivalent to that through the hydrocyclone												
(xi)	Q_{MIN}, $(O/W)_{MIN}$											
98	2190	305	290	90	29.7	2.8	87.5	77.5	77.7	86.3	86.8	78.2
99	1880	200	335	165	26.8	2.8	87.3	77.7	77.8	86.2	86.6	78.4
100	2545	125	520	380	37.1	2.5	86.5	78.5	78.6	85.4	85.8	79.2
101	2150	70	515	380	32.0	2.5	86.5	78.5	78.7	85.3	85.8	79.2
102	1790	60	470	300	27.0	2.8	87.4	77.6	78.0	86.0	86.6	78.4
103	1835	30	640	370	29.5	2.6	86.9	78.1	78.3	85.7	86.3	78.7
104	1820	10	820	435	31.9	2.5	86.5	78.5	79.0	85.0	85.8	79.2
105	1805	15	1050	450	34.7	2.4	86.3	78.7	79.2	84.8	85.6	79.4
106	1440	0	1060	380	30.3	2.4	86.2	78.8	79.2	84.8	85.5	79.5
107	1220	20	1130	380	27.8	2.5	86.8	78.2	78.6	85.4	86.2	78.8
108	980	0	1000	340	24.0	2.6	86.9	78.1	78.5	85.5	86.3	78.7
(xii)	Q_{MIN}, $(O/W)_{MID}$											
109	2380	430	190	380	34.5	2.7	87.5	77.5	77.5	86.5	87.0	78.0
110	2265	190	315	635	34.7	2.6	87.2	77.8	78.0	86.0	86.5	78.5

Kerosene/Water (xii) cont'd

Run No.	Volume of Liquid (mL)				Time of Sampling (s)	Pressure Readings						
	Underflow		Overflow			Mixing tee (lb/in^2)	Feed		Overflow		Underflow	
	Water	Kerosene	Water	Kerosene			LL	RL	LL	RL	LL	RL
							(cm.Hg)					
111	2050	140	310	590	31.3	2.8	87.7	77.3	77.3	86.7	87.1	77.9
112	2090	45	480	770	34.6	2.5	86.9	78.1	78.2	85.8	86.3	78.7
113	1750	20	615	755	32.5	2.4	86.7	78.3	78.5	85.5	86.0	79.0
114	1560	10	840	795	33.1	2.5	86.7	78.3	78.5	85.5	86.1	78.9
115	1340	10	880	780	31.2	2.5	86.8	78.2	78.3	85.7	86.3	78.7
116	1365	5	980	765	31.7	2.5	86.8	78.2	78.4	85.6	86.3	78.7
117	1250	20	1280	870	35.1	2.6	87.2	77.8	78.2	85.8	86.5	78.5
(xiii)	Q_{MIN},	$(O/W)_{MAX}$										
118	1200	560	110	680	25.2	2.8	87.5	77.5	77.5	86.5	87.0	78.0
119	1270	410	180	1020	28.2	2.6	87.5	77.5	77.5	86.5	87.0	78.0
120	1420	395	250	1290	32.7	2.6	87.3	77.7	77.7	86.3	86.5	78.5
121	1355	235	270	1370	31.3	2.8	87.8	77.2	77.3	86.7	87.2	77.8
122	1275	125	320	1550	31.9	3.0	88.3	76.7	76.7	87.3	87.7	77.3
123	1320	80	400	1680	33.9	2.7	87.7	77.3	77.4	86.6	87.3	77.7
124	930	20	480	1490	28.4	3.2	88.9	76.1	76.4	87.6	88.4	76.6
125	910	20	560	1500	29.1	3.3	89.0	76.0	76.2	87.8	88.5	76.5
126	920	35	575	1570	30.2	3.1	88.8	76.2	76.5	87.5	88.3	76.7
127	800	25	545	1370	26.5	3.6	89.8	75.2	75.6	88.4	89.3	75.7
(xiv)	Q_{MID},	$(O/W)_{MIN}$										
128	3210	525	570	75	22.2	7.0	96.5	68.5	70.7	93.3	93.3	71.7
129	2470	365	760	160	19.0	6.3	94.8	70.2	72.9	91.1	91.6	73.4
130	3135	350	1115	325	25.0	5.8	93.5	71.5	74.0	90.0	90.5	74.5
131	2690	165	1140	460	22.5	5.6	92.9	72.1	74.8	89.2	89.9	75.1
132	3370	50	1715	740	30.0	5.1	91.6	73.4	76.0	88.0	88.8	76.2
133	2335	50	1190	550	20.9	5.3	92.3	72.7	75.7	88.3	89.3	75.7
134	2915	25	1890	745	28.2	5.1	91.5	73.5	76.2	87.8	88.7	76.3

Kerosene/Water (xiv) cont'd

Run No.	Volume of Liquid (mL)				Time of Sampling (s)	Pressure Readings						
	Underflow		Overflow			Mixing tee (lb/in²)	Feed		Overflow		Underflow	
	Water	Kerosene	Water	Kerosene			LL	RL	LL	RL	LL	RL
							(cm.Hg)					
135	2840	10	2010	770	28.6	4.9	90.8	74.2	76.9	87.1	88.0	77.0
136	2640	10	2110	690	29.0	4.8	90.8	74.2	76.7	87.3	88.3	76.7
137	2860	5	2330	810	30.4	5.1	91.8	73.2	76.1	87.9	88.9	76.1
138	2505	5	2695	815	30.6	5.1	91.7	73.3	76.2	87.8	88.9	76.1
(xv)	Q_{MID},	$(O/W)_{MID}$										
139	2740	620	610	460	23.2	5.7	93.5	71.5	73.6	90.4	90.6	74.4
140	2750	410	735	765	23.6	6.0	94.0	71.0	73.3	90.7	91.2	73.8
141	2640	165	825	1015	23.8	5.4	92.4	72.6	75.0	89.0	89.6	75.4
142	2720	80	1000	1180	25.4	5.3	92.4	72.6	75.1	88.9	89.6	75.4
143	2220	15	1315	1175	24.0	5.3	92.3	72.7	75.4	88.6	89.5	75.5
144	2140	20	1560	1240	25.0	5.5	92.6	72.4	75.0	89.0	90.0	75.0
(xvi)	Q_{MID},	$(O/W)_{MAX}$										
145	2105	1095	580	1630	26.4	6.0	94.4	70.6	73.0	91.0	91.4	73.6
146	1980	815	655	1885	26.3	6.5	95.7	69.3	71.7	92.3	93.0	72.0
147	1700	470	690	1950	23.6	7.5	98.0	67.0	69.6	94.4	95.4	69.6
148	1645	335	700	2040	23.3	7.0	97.1	67.9	70.5	93.5	94.7	70.3
149	1810	50	900	2460	27.6	7.5	98.5	66.5	69.1	94.9	96.3	68.7
150	1780	120	1045	2790	28.3	8.4	100.5	64.5	67.5	96.5	98.0	67.0

Mean and Standard Deviation of Measured Data Table A6-5

System	Conditions		Mean ($\bar{X}$)	Standard Deviation (σ)
Butanol/Water	(i)	Q_{MID}	198	7
		$(O/W)_{MIN}$	0.165	0.004
	(ii)	Q_{MAX}	374	7
		$(O/W)_{MIN}$	0.164	0.004
	(iii)	Q_{MID}	209	5
		$(O/W)_{MID}$	0.334	0.006
	(iv)	Q_{MAX}	387	9
		$(O/W)_{MID}$	0.330	0.007
	(v)	$Q_{variable}$	-	-
		$(O/W)_{MIN}$	0.163	0.007
	(vi)	$Q_{variable}$	-	-
		$(O/W)_{MID}$	0.331	0.006
	(vii)	$(O/U)_{constant}$	1.10	0.021
		$(O/W)_{MIN}$	0.155	0.011
MIBK/Water	(i)	Q_{MIN}	102	5
		$(O/W)_{MIN}$	0.163	0.004
	(ii)	Q_{MID}	190	3
		$(O/W)_{MIN}$	0.165	0.008
	(iii)	Q_{MAX}	362	7
		$(O/W)_{MID}$	0.163	0.007
	(iv)	Q_{MIN}	98	8
		$(O/W)_{MID}$	0.328	0.007

Table A6-5 cont'd

System	Conditions		Mean ($\bar{X}$)	Standard Deviation (σ)
MIBK/Water cont'd	(v)	Q_{MAX}	361	4
		$(O/W)_{MID}$	0.336	0.004
	(vi)	$(O/U)_{constant}$	0.67	0.05
		$(O/W)_{MIN}$	0.165	0.005
Toluene/Water	(i)	Q_{MID}	95	9
		$(O/W)_{MIN}$	0.165	0.006
	(ii)	Q_{MAX}	367	4
		$(O/W)_{MIN}$	0.165	0.003
	(iii)	Q_{MIN}	88	10
		$(O/W)_{MID}$	0.322	0.007
	(iv)	Q_{MAX}	362	2
		$(O/W)_{MID}$	0.322	0.006
Kerosene/Water	(i)	Q_{MIN}	99	7
		$(O/W)_{MIN}$	0.161	0.008
	(ii)	Q_{MID}	199	7
		$(O/W)_{MIN}$	0.165	0.006
	(iii)	Q_{MAX}	366	4
		$(O/W)_{MIN}$	0.164	0.005
	(iv)	Q_{MIN}	95	9
		$(O/W)_{MID}$	0.335	0.008
	(v)	Q_{MID}	194	6
		$(O/W)_{MID}$	0.343	0.007

Table A6-5 cont'd

System	Conditions		Mean ($\bar{X}$)	Standard Deviation (σ)
Kerosene/Water cont'd	(vi)	Q_{MAX} $(O/W)_{MID}$	361 0.340	3 0.006
	(vii)	Q_{MIN} $(O/W)_{MAX}$	102 1.06	7 0.010
	(viii)	Q_{MID} $(O/W)_{MAX}$	202 1.04	10 0.03
	(ix)	Q_{MAX} $(O/W)_{MAX}$	370 1.04	6 0.04
	(x)	Q_{MIN} $(O/W)_{MIN}$	96 0.164	2 0.006
	(xi)	Q_{MID} $(O/W)_{MIN}$	197 0.159	3 0.005
	(xii)	Q_{MIN} $(O/W)_{MID}$	98 0.329	1 0.016
	(xiii)	Q_{MID} $(O/W)_{MID}$	196 0.336	3 0.007
	(xiv)	Q_{MIN} $(O/W)_{MAX}$	103 1.02	1 0.04
	(xv)	Q_{MID} $(O/W)_{MAX}$	201 1.00	6 0.04

The units for mean flowrate are mL/s.

APPENDIX 7

CALCULATED DATA

(Tables A7-1 to A7-4)

CALCULATED DATA

System I : Butanol/Water

Table A7-1

Run No.	O/U (v./v.)	Q_f (mL/s)	O/W (v./v.)	Pressure (lb/in^2)			Concentration of Light Phase (v./v.) (%)			E_s (%)
				P_f	P_o	P_u	Y_f	Y_o	Y_u	
(i)										
1	0.17	187	0.158	3.2	1.9	2.7	13.7	12.8	13.8	0
2	0.24	184	0.167	2.9	1.7	2.5	14.3	14.1	14.4	0
3	0.32	185	0.164	2.7	1.8	2.6	14.1	13.8	14.2	0
4	0.33	194	0.158	3.1	1.6	2.5	13.7	13.4	13.8	0
5	0.43	190	0.162	2.5	1.3	2.2	13.9	13.5	14.2	0
6	0.54	196	0.163	2.4	1.1	2.1	14.0	15.1	13.4	3.2
7	0.56	189	0.166	2.4	1.0	2.1	14.3	14.5	14.1	1.0
8	0.67	199	0.170	2.3	0.9	2.0	14.5	18.7	11.7	13.5
9	0.75	197	0.169	2.2	0.8	1.9	14.4	20.2	10.1	20.0
10	0.88	203	0.162	1.9	0.4	1.6	14.0	24.0	8.3	25.1
11	0.93	205	0.169	2.1	0.5	1.6	14.4	21.2	8.2	26.1
12	0.95	201	0.163	1.9	0.3	1.5	14.0	20.5	7.8	26.4
13	0.98	212	0.164	2.1	0.5	1.7	14.1	20.4	8.0	25.5
14	1.00	206	0.169	2.1	0.5	1.7	14.5	20.9	8.0	26.1
15	1.03	197	0.164	2.1	0.6	1.8	14.1	19.2	8.9	21.2
16	1.06	206	0.170	2.1	0.6	1.7	14.5	20.5	8.2	24.7
17	1.06	204	0.169	2.1	0.5	1.7	14.5	19.4	9.3	20.3
18	1.11	-	0.161	2.2	0.8	1.9	13.9	19.6	7.5	25.3
19	1.12	196	0.166	2.2	0.8	1.9	14.3	199	7.9	24.6
20	1.14	200	0.168	2.1	0.6	1.8	14.4	19.7	8.3	23.1
21	1.17	197	0.165	2.1	0.6	1.8	14.2	19.6	7.9	23.9
22	1.32	201	0.170	2.2	0.8	2.0	14.5	19.6	7.8	23.3
23	1.45	204	0.168	2.2	0.7	2.0	14.4	18.4	8.6	19.2

Butanol/Water (i) cont'd

Run No.	O/U (v./v.)	Q_f (mL/s)	O/W (v./v.)	Pressure (lb/in²)			Concentration of Light Phase (v./v.) (%)			E_s (%)
				P_f	P_o	P_u	Y_f	Y_o	Y_u	
24	1.68	192	0.161	2.4	0.8	2.2	13.9	17.8	7.2	20.8
25	2.02	198	0.163	2.5	0.9	2.3	14.0	17.0	8.0	16.5
26	2.17	198	0.164	2.6	1.1	2.4	14.1	17.2	7.4	17.5
27	2.48	193	0.165	2.5	1.0	2.4	14.2	17.2	6.7	17.7
28	3.7	-	0.168	2.9	1.4	2.9	14.4	16.5	7.6	13.2
(ii)										
29	0.35	196	0.323	3.0	1.8	2.7	24.4	23.9	24.6	0
30	0.46	199	0.337	2.8	1.5	2.4	25.2	25.8	24.9	1.1
31	0.53	203	0.338	2.6	1.3	2.3	25.3	27.8	24.0	4.5
32	0.60	205	0.331	2.5	1.2	2.2	24.9	30.0	21.8	10.3
33	0.64	206	0.332	2.5	1.1	2.1	24.9	31.0	21.0	12.7
34	0.72	206	0.324	2.4	0.9	2.0	24.5	31.9	19.2	16.7
35	0.82	211	0.328	2.1	0.6	1.7	24.7	32.3	18.5	18.3
36	0.92	208	0.332	2.1	0.5	1.6	24.9	34.1	16.5	23.4
37	0.92	216	0.334	2.2	0.5	1.7	25.0	33.1	17.6	20.6
38	0.95	213	0.338	2.2	0.6	1.8	25.3	34.2	16.8	22.9
39	0.97	212	0.332	2.2	0.5	1.7	24.9	33.8	16.2	23.6
40	0.98	212	0.333	2.1	0.4	1.6	25.0	34.0	16.2	23.7
41	1.01	218	0.333	2.3	0.7	1.9	25.0	33.6	16.3	23.1
42	1.02	213	0.328	2.2	0.5	1.7	24.7	32.4	16.9	20.8
43	1.04	210	0.334	2.1	0.5	1.7	25.0	33.6	16.0	23.5
44	1.17	214	0.334	2.2	0.6	1.8	25.1	33.0	15.8	22.8
45	1.24	208	0.346	2.5	0.9	2.2	25.7	33.8	15.7	23.4
46	1.28	212	0.335	2.4	0.8	2.0	25.1	32.8	15.2	23.1
47	1.31	205	0.348	2.5	0.9	2.1	25.8	33.4	15.9	22.4
48	1.43	208	0.333	2.3	0.7	2.0	25.0	31.8	15.3	21.3
49	1.54	208	0.332	2.4	0.8	2.1	24.9	31.4	15.0	20.9
50	1.81	211	0.331	2.5	0.8	2.2	24.9	29.7	16.0	16.8
51	1.83	-	0.337	2.6	1.1	2.4	25.2	31.0	14.8	19.6

Butanol/Water cont'd

Run No.	$O/_U$ (v./v.)	Q_f (mL/s)	$O/_W$ (v./v.)	Pressure (lb/in^2)			Concentration of Light Phase (v./v.) (%)			E_s (%)
				P_f	P_o	P_u	Y_f	Y_o	Y_u	
(iii)										
52	0.17	369	0.155	13.4	8.9	9.4	13.4	13.4	13.4	0
53	0.43	374	0.167	11.9	7.3	8.4	14.3	13.3	14.7	0
54	0.63	377	0.164	10.4	5.6	6.8	14.1	13.9	14.2	0
55	0.65	363	0.166	8.7	3.3	4.8	14.2	14.2	14.2	0
56	0.65	367	0.166	8.9	3.3	4.8	14.2	13.9	14.5	0
57	0.73	373	0.164	9.8	5.0	6.4	14.1	16.3	12.5	7.7
58	0.80	371	0.161	9.0	3.2	4.7	13.8	16.4	11.8	9.4
59	0.84	372	0.155	9.3	3.5	5.2	13.4	16.3	11.1	10.9
60	0.90	371	0.160	9.3	3.5	5.0	13.8	17.6	10.4	15.1
61	0.90	375	0.169	8.1	2.9	4.4	14.4	18.7	10.5	16.6
62	0.99	381	0.169	8.6	3.4	5.0	14.5	19.7	9.2	21.4
63	1.01	365	0.169	9.6	3.7	5.5	14.3	17.6	10.9	13.7
64	1.02	367	0.165	9.8	3.8	5.6	14.2	17.7	10.6	14.6
65	1.02	373	0.166	8.5	3.3	5.1	14.2	18.1	10.3	15.9
66	1.03	375	0.164	8.5	3.3	5.1	14.1	18.1	9.9	17.0
67	1.04	378	0.163	9.3	3.4	5.2	14.0	17.6	10.2	15.5
68	1.09	371	0.164	9.6	4.1	6.0	14.1	18.4	9.4	18.6
69	1.11	369	0.161	9.6	4.2	6.1	13.9	18.4	8.9	19.8
70	1.11	381	0.158	9.6	3.8	5.5	13.6	16.8	10.1	14.1
71	1.14	372	0.164	9.5	4.1	5.9	14.1	18.3	9.3	18.3
72	1.17	377	0.161	9.6	4.2	6.0	13.9	18.2	8.9	19.3
73	1.18	364	0.167	8.7	3.6	5.3	14.3	18.6	9.1	19.4
74	1.23	374	0.167	9.5	4.1	6.0	14.3	18.4	9.4	18.0
75	1.27	372	0.161	9.6	4.4	6.2	13.9	18.0	8.7	19.0
76	1.40	382	0.172	9.5	4.2	6.0	14.6	18.3	9.6	16.8
77	1.43	397	0.164	11.4	5.2	7.4	14.1	16.8	10.1	13.5
78	1.49	371	0.162	11.5	5.4	7.5	13.9	16.3	10.3	12.1

Butanol/Water (iii) cont'd

Run No.	$O/_U$ (v./v.)	Q_f (mL/s)	$O/_W$ (v./v.)	Pressure (lb/in²) P_f	P_o	P_u	Concentration of Light Phase (v./v.) (%) Y_f	Y_o	Y_u	E_s (%)
79	1.66	384	0.168	11.9	5.4	7.6	14.4	17.1	10.0	13.5
80	1.88	371	0.160	12.1	5.5	7.8	13.8	15.7	10.1	10.7
81	1.88	384	0.158	12.4	6.0	8.2	13.6	15.6	9.8	11.1
(iv)										
82	0.17	387	0.325	14.5	9.9	10.3	24.5	24.2	24.6	0
83	0.27	361	0.325	13.2	8.7	9.4	24.5	23.4	24.9	0
84	0.45	390	0.335	12.6	7.9	8.9	25.1	23.9	25.6	0
85	0.47	382	0.330	12.7	8.2	9.2	24.8	23.9	25.2	0
86	0.51	385	0.327	12.0	7.3	8.4	24.6	24.2	24.9	0
87	0.63	387	0.338	9.8	4.5	5.8	25.3	27.3	24.0	4.2
88	0.65	373	0.325	9.9	4.7	6.9	24.5	26.1	23.5	4.6
89	0.74	376	0.319	9.2	3.7	5.1	24.2	28.1	21.3	9.1
90	0.78	392	0.336	9.5	3.8	5.2	25.1	30.1	21.3	11.4
91	0.82	388	0.336	9.1	3.5	5.1	25.2	30.6	20.7	12.6
92	0.84	400	0.333	9.1	3.4	4.9	25.0	30.6	20.3	13.6
93	0.95	-	0.338	9.8	3.8	5.5	25.2	31.4	19.4	15.8
94	0.97	390	0.330	9.0	3.9	5.7	24.8	31.0	18.8	16.4
95	1.06	370	0.339	7.3	2.9	4.5	25.3	31.5	18.8	16.7
96	1.08	388	0.327	10.6	4.0	5.8	24.7	30.0	18.9	14.9
97	1.12	399	0.326	10.4	4.5	6.3	24.6	30.4	18.1	16.5
98	1.20	396	0.335	10.4	4.7	6.5	25.1	29.9	19.2	14.2
99	1.32	-	0.323	10.1	4.7	6.6	24.4	30.7	16.2	19.2
100	1.32	392	0.315	10.7	4.8	6.8	24.0	27.7	19.1	11.6
101	1.34	385	0.331	10.6	5.2	7.2	24.9	29.2	19.2	13.1
102	1.35	393	0.329	10.3	4.7	7.4	24.7	30.8	16.5	18.8
103	1.36	385	0.332	10.4	5.1	6.6	24.9	29.5	18.7	14.1
104	1.40	383	0.337	10.5	5.1	7.3	25.2	29.6	19.0	13.7

Butanol/Water (iv) cont'd

Run No.	$O/_U$ (v./v.)	Q_f (mL/s)	$O/_W$ (v./v.)	Pressure (lb/in^2)			Concentration of Light Phase (v./v.) (%)			E_s (%)
				P_f	P_o	P_u	Y_f	Y_o	Y_u	
105	1.52	385	0.337	11.1	5.7	7.9	25.2	29.6	18.6	14.0
106	1.66	395	0.336	11.6	6.1	8.4	25.2	29.0	18.8	12.7
107	1.74	392	0.320	12.8	6.4	8.7	24.2	27.8	18.0	12.4
108	1.84	397	0.337	12.7	6.5	8.8	25.2	28.6	18.9	11.7
(v)										
109	0.24	172	0.150	2.6	1.6	2.4	13.1	12.9	13.1	0
110	0.32	330	0.158	9.6	5.8	6.6	13.7	13.0	13.9	0
111	0.97	156	0.165	4.0	3.0	4.1	14.2	20.4	8.1	25.3
112	0.97	312	0.167	5.5	2.0	3.4	14.3	19.9	8.9	22.4
113	0.99	83	0.161	7.1	6.7	7.7	13.8	20.0	7.7	25.8
114	0.99	272	0.166	3.8	1.2	2.5	14.3	20.3	8.3	24.5
115	1.01	223	0.169	2.4	0.6	1.8	14.5	20.7	8.2	25.2
116	1.01	113	0.171	6.0	4.9	6.1	14.6	20.4	8.8	23.2
117	1.02	110	0.172	5.7	5.0	6.2	14.7	20.8	8.5	24.5
118	1.04	85	0.151	6.9	6.2	7.4	13.2	17.5	8.7	19.2
119	1.07	111	0.157	5.8	5.1	6.2	13.5	19.0	7.7	24.0
120	1.12	264	0.161	4.4	1.8	3.2	13.9	18.9	8.3	22.1
121	1.13	84	0.161	7.2	6.6	7.8	13.9	19.2	7.8	23.8
122	1.13	153	0.166	4.0	3.0	4.1	14.3	19.1	8.8	21.0
123	1.13	2.3	0.168	2.6	0.9	2.2	14.4	19.9	8.1	24.0
124	1.13	311	0.166	6.5	2.8	4.4	14.2	19.0	8.8	20.8
125	1.18	114	0.151	5.5	4.9	6.0	13.2	18.0	7.5	22.8
126	3.64	62	0.165	8.3	7.7	8.9	14.1	16.1	6.9	12.8
(vi)										
127	0.65	255	0.322	4.2	1.8	2.9	24.4	26.4	23.0	4.5
128	0.73	297	0.326	5.4	1.9	3.3	24.6	28.4	21.8	8.7

Butanol/Water (vi) cont'd

Run No.	$O/_U$ (v./v.)	Q_f (mL/s)	$O/_W$ (v./v.)	Pressure (lb/in^2)			Concentration of Light Phase (v./v.) (%)			E_s (%)
				P_f	P_o	P_u	Y_f	Y_o	Y_u	
129	0.94	312	0.326	5.7	2.5	3.9	24.6	31.6	18.0	18.3
130	0.95	339	0.334	6.5	2.7	4.2	25.0	31.9	18.5	17.8
131	0.97	163	0.328	4.3	3.3	4.4	24.7	33.9	15.8	24.3
132	1.01	273	0.335	4.1	1.5	2.8	25.1	32.1	18.0	18.7
133	1.04	114	0.336	6.2	5.5	6.6	25.2	34.3	15.6	24.8
134	1.05	90	0.326	7.5	7.0	8.1	24.6	34.2	14.4	26.7
135	1.11	250	0.335	3.1	1.1	2.3	25.1	31.9	17.6	18.9
136	1.12	229	0.331	2.6	0.8	2.0	24.9	31.7	17.3	19.2
137	1.12	277	0.343	3.9	1.3	2.7	25.5	31.7	18.7	17.0
138	1.15	161	0.330	4.4	3.4	4.5	24.8	32.2	16.4	21.0
(vii)										
139	1.12	348	0.144	9.3	4.0	5.8	12.6	16.4	8.3	18.4
140	1.09	369	0.166	9.5	4.2	6.1	14.2	18.9	9.1	20.0
141	1.08	368	0.155	9.4	4.2	6.0	13.4	18.1	8.3	21.1

System II : MIBK/Water

Table A7-2

Run No.	$O/_U$ (v./v.)	Q_f (mL/s)	$O/_W$ (v./v.)	Pressure (lb/in^2) P_f	P_o	P_u	Concentration of Light Phase (v./v.) (%) Y_f	Y_o	Y_u	E_s (%)
(i)										
1	0.50	107	0.166	5.3	4.6	5.7	14.3	27.9	7.4	37.4
2	0.55	101	0.160	5.4	4.9	5.9	13.8	34.8	2.4	62.1
3	0.57	-	0.165	5.0	4.5	5.5	14.2	34.9	2.3	62.1
4	0.60	105	0.168	5.4	4.8	5.8	14.4	34.7	2.2	61.7
5	0.61	99	0.153	5.4	4.7	5.9	13.3	32.2	1.5	63.4
6	0.62	106	0.165	5.3	4.6	5.7	14.2	34.3	1.7	63.2
7	0.64	104	0.166	5.4	4.7	5.8	14.3	34.2	0.8	67.0
8	0.70	104	0.165	5.4	4.8	5.9	14.1	33.8	0.3	66.9
9	0.80	105	0.166	5.3	4.6	5.7	14.2	32.0	0	64.7
10	0.89	94	0.163	5.9	5.3	6.4	14.0	29.8	0	61.5
11	1.28	94	0.161	5.7	5.2	6.3	13.9	24.7	0	50.8
(ii)										
12	0.50	86	0.330	6.1	5.6	6.6	24.8	58.6	7.9	60.4
13	0.52	-	0.318	5.3	4.9	5.6	24.1	53.1	9.0	54.3
14	0.63	102	0.336	5.6	5.0	6.1	25.2	56.1	5.8	63.2
15	0.63	107	0.314	5.5	4.9	5.9	23.9	53.7	5.3	63.0
16	0.65	106	0.334	5.3	4.7	5.7	25.0	55.8	5.1	64.4
17	0.72	104	0.332	5.4	4.8	5.9	24.9	57.5	1.5	72.8
18	0.81	90	0.329	5.9	5.4	6.5	24.8	54.8	0.4	72.2
19	0.84	102	0.333	5.5	5.0	6.0	25.0	52.9	1.5	68.0
20	0.94	94	0.321	5.7	5.1	6.2	24.3	49.8	0.5	66.9
21	0.96	92	0.330	5.8	5.3	6.3	24.8	50.5	0	67.7
(iii)										
22	0.62	188	0.162	1.9	0.5	1.5	14.0	29.2	4.5	47.3
23	0.77	192	0.169	1.9	0.5	1.6	14.5	33.0	0.8	62.9

MIBK/Water (iii) cont'd

Run No.	$O/_U$ (v./v.)	Q_f (mL/s)	$O/_W$ (v./v.)	Pressure (lb/in^2)			Concentration of Light Phase (v./v.) (%)			E_s (%)
				P_f	P_o	P_u	Y_f	Y_o	Y_u	
24	0.78	186	0.150	1.9	0.4	1.5	13.1	28.9	0.6	61.5
25	0.82	195	0.171	1.9	0.3	1.5	14.6	32.4	0	64.2
26	0.90	189	0.167	2.2	0.6	1.8	14.3	30.2	0	57.3
27	1.05	192	0.172	2.2	0.6	1.9	14.7	28.7	0	57.3
(iv)										
28	0.26	358	0.158	14.3	10.6	9.9	13.6	12.3	14.0	0
29	0.37	361	0.163	12.5	8.5	7.9	14.0	16.7	13.0	6.1
30	0.47	360	0.155	12.1	7.8	6.9	13.4	17.3	11.6	10.6
31	0.55	358	0.167	8.9	3.8	5.0	14.3	23.9	9.1	27.4
32	0.58	367	0.165	10.4	5.5	6.6	14.2	24.9	7.9	29.5
33	0.59	355	0.168	8.8	3.8	5.0	14.4	26.0	7.6	34.7
34	0.61	374	0.167	10.0	5.0	6.3	14.3	33.8	6.9	40.8
35	0.65	372	0.152	9.8	4.5	5.9	13.2	25.6	5.2	42.4
36	0.73	357	0.171	9.2	3.6	5.4	14.6	30.4	3.2	53.0
31	0.74	358	0.157	9.0	3.6	5.3	13.6	28.5	2.6	53.8
38	0.83	363	0.161	8.8	3.7	5.2	13.9	29.8	0.6	60.6
39	0.90	368	0.168	8.6	3.4	4.8	14.4	30.3	0	61.3
40	1.05	361	0.152	8.3	3.0	4.4	13.2	25.8	0	56.2
41	1.10	344	0.156	11.1	5.5	7.6	13.5	25.8	0	55.1
42	1.38	369	0.171	9.7	4.2	6.2	14.6	25.1	0	49.1
43	1.38	360	0.170	9.8	4.3	6.3	14.5	25.0	0	49.1
44	1.49	365	0.167	10.5	4.9	7.0	14.3	24.0	0	47.0
45	1.53	365	0.177	9.9	4.4	6.5	15.1	24.9	0	46.6
46	2.11	361	0.157	11.2	4.5	7.8	13.6	20.0	0	37.2
(v)										
47	0.18	352	0.329	14.6	10.5	10.7	24.7	29.9	23.8	4.1
48	0.25	357	0.332	14.1	9.8	10.3	24.9	32.1	23.2	8.7
49	0.26	359	0.337	13.5	9.3	9.8	25.2	33.7	23.0	9.3

MIBK/Water (v) cont'd

Run No.	$O/_U$ (v./v.)	Q_f (mL/s)	$O/_W$ (v./v.)	Pressure (lb/in^2)			Concentration of Light Phase (v./v.) (%)			E_s (%)
				P_f	P_o	P_u	Y_f	Y_o	Y_u	
50	0.45	362	0.338	11.0	6.4	7.4	25.2	42.6	17.4	28.5
51	0.56	363	0.332	10.2	5.4	6.6	25.0	47.1	12.6	42.4
52	0.70	364	0.339	9.0	4.2	5.5	25.3	52.2	6.5	58.6
53	0.80	364	0.341	8.8	3.8	5.2	25.4	52.2	4.0	62.8
54	0.90	363	0.344	8.0	3.0	4.5	25.6	53.1	0.9	68.3
55	1.08	363	0.337	9.5	4.3	6.1	25.2	48.5	0.5	63.4
56	1.44	364	0.336	10.2	4.9	7.0	25.1	42.7	0	55.0
57	1.88	364	0.335	11.5	6.0	8.3	25.1	38.5	0	46.4
(vi)										
58	0.60	129	0.160	8.3	7.5	8.6	13.8	31.8	3.0	56.4
59	0.68	298	0.167	6.0	2.7	4.0	14.3	29.7	3.8	50.9
60	0.69	165	0.162	13.2	12.1	13.3	14.0	31.7	1.7	60.3
61	0.72	248	0.170	4.0	1.6	2.9	14.5	31.0	2.6	55.7

System III : Toluene/Water

Table A7-3

Run No.	$O/_U$ (v./v.)	Q_f (mL/s)	$O/_W$ (v./v.)	Pressure (lb/in²)			Concentration of Light Phase (v./v.)			E_s (%)
				P_f	P_o	P_u	Y_f	Y_o	Y_u	
(i)										
1	0.76	368	0.162	8.9	4.1	5.5	13.9	28.3	3.1	51.4
2	0.86	367	0.173	8.3	3.5	5.0	14.7	30.4	1.3	57.5
3	0.94	365	0.165	-	-	-	14.1	29.0	0.2	59.2
(ii)										
4	0.47	106	0.175	5.2	4.5	5.6	14.9	20.7	12.2	14.5
5	0.69	95	0.165	6.3	5.6	6.7	14.2	21.8	8.9	25.7
6	0.71	97	0.161	6.1	5.6	6.7	13.9	19.6	9.9	19.5
7	0.71	100	0.170	6.2	5.6	6.7	14.5	22.0	9.2	25.0
8	0.72	104	0.165	6.0	5.4	6.6	14.2	21.4	8.9	25.2
9	0.73	101	0.169	6.3	5.6	6.8	14.5	23.8	7.7	21.7
10	0.74	90	0.164	6.2	5.8	6.8	14.1	19.7	9.9	19.9
11	0.75	97	0.155	6.3	5.7	6.8	13.4	23.2	6.1	35.9
12	0.79	99	0.164	6.0	5.4	6.6	14.1	19.8	9.5	21.1
13	0.91	91	0.160	6.8	6.2	7.4	13.8	23.0	5.5	36.6
14	1.25	81	0.172	7.2	6.7	7.7	14.6	21.4	6.1	30.3
15	1.58	76	0.162	7.4	6.9	8.0	13.9	19.1	5.8	26.3
(iii)										
16	0.51	98	0.326	5.3	4.7	5.7	24.7	33.3	20.2	15.9
17	0.56	93	0.323	5.4	4.8	5.9	24.4	34.4	18.8	19.4
18	0.67	94	0.307	5.7	5.1	6.2	23.5	32.4	17.6	19.8
19	0.75	98	0.326	5.9	5.3	6.4	24.6	37.1	15.2	28.9
20	0.83	85	0.331	6.4	5.8	6.9	24.9	33.5	17.6	21.2
21	0.86	85	0.318	6.2	5.7	6.8	24.2	33.0	16.6	22.3
22	0.89	83	0.326	6.3	5.7	6.8	24.6	34.1	16.2	24.0
23	1.02	83	0.323	6.6	6.1	7.2	24.4	33.7	14.9	25.4
24	1.22	76	0.319	6.8	6.3	7.4	24.2	32.5	14.0	25.0

Toluene/Water (iii) cont'd

Run No.	$O/_U$ (v./v.)	Q_f (mL/s)	$O/_W$ (v./v.)	Pressure (lb/in^2)			Concentration of Light Phase (v./v.)			E_s (%)
				P_f	P_o	P_u	Y_f	Y_o	Y_u	
25	1.45	73	0.317	7.0	6.5	7.6	24.1	31.3	13.6	23.4
(iv)										
26	0.45	361	0.161	12.1	7.7	8.5	13.8	15.3	13.2	3.5
27	0.62	-	0.163	10.6	6.0	7.3	14.0	24.8	7.2	34.7
28	0.81	374	0.169	9.3	4.7	6.1	14.4	28.5	3.1	50.7
29	0.94	365	0.165	8.9	4.1	5.6	14.2	28.3	0.9	56.6
30	0.99	367	0.168	8.8	3.9	5.5	14.4	27.6	1.3	53.4
31	1.16	368	0.166	8.0	3.1	4.8	14.2	26.0	0.6	51.8
32	1.49	365	0.164	9.4	4.4	6.2	14.1	23.3	0.4	45.4
(v)										
33	0.67	364	0.315	8.5	3.9	5.2	24.0	39.3	13.7	33.7
34	0.85	360	0.324	8.3	3.6	5.0	24.5	42.0	9.6	43.5
35	1.03	363	0.320	7.6	2.8	4.3	24.2	43.1	4.8	52.2
36	1.37	362	0.328	8.6	3.7	5.5	24.7	40.0	3.8	47.4

System IV : Kerosene/Water

Table A7-4

Run No.	$O/_U$ (v./v.)	Q_f (mL/s)	$O/_W$ (v./v.)	Pressure (lb/in²)			Concentration of Light Phase (v./v.) (%)			E_s (%)
				P_f	P_o	P_u	Y_f	Y_o	Y_u	
(i)										
1	0.20	97	0.165	5.6	5.1	6.1	14.2	16.7	13.7	3.4
2	0.32	113	0.160	5.3	4.8	5.7	13.8	22.4	11.1	17.2
3	0.42	100	0.163	5.5	5.0	6.0	14.0	23.8	9.8	24.5
4	0.50	91	0.149	6.0	5.6	6.6	13.0	23.6	7.7	31.3
5	0.56	105	0.146	5.3	5.3	5.7	12.8	23.7	6.6	35.6
6	0.72	101	0.167	5.4	4.8	5.9	14.3	23.9	7.4	32.7
7	0.76	101	0.166	5.7	5.0	6.2	14.2	24.3	6.7	35.2
8	0.83	95	0.170	5.7	5.6	6.3	14.6	24.6	6.3	36.4
9	0.86	89	0.163	5.9	5.3	6.5	14.0	25.0	4.5	42.3
10	0.98	98	0.158	5.5	4.9	6.0	13.6	23.6	4.0	41.7
11	1.22	102	0.151	5.3	4.7	5.7	13.1	21.7	2.8	40.8
12	1.44	102	0.165	5.6	5.0	6.2	14.2	20.8	4.7	31.9
13	1.75	90	0.166	6.0	5.5	6.6	14.3	19.4	5.2	26.9
(ii)										
14	0.22	114	0.343	4.8	4.4	5.2	25.5	35.8	23.2	9.9
15	0.32	106	0.336	5.0	4.5	5.5	25.2	33.6	22.5	10.8
16	0.51	86	0.331	5.9	5.4	6.4	24.9	37.5	18.4	23.0
17	0.63	87	0.339	5.8	5.4	6.4	25.3	38.9	16.7	27.9
18	0.82	95	0.335	5.6	5.2	6.2	25.1	38.4	14.2	31.9
19	0.98	96	0.335	5.4	4.8	6.0	25.1	40.5	10.1	40.4
20	1.15	93	0.336	5.5	5.0	6.1	25.1	37.8	10.5	33.8
21	1.24	96	0.337	5.5	4.9	6.0	25.2	38.8	8.4	39.9
22	1.46	100	0.338	5.3	4.8	5.8	25.2	37.0	8.1	37.0
23	1.67	83	0.343	6.0	5.5	6.6	25.5	34.6	11.3	28.4
24	1.78	88	0.314	5.7	5.2	6.3	23.9	32.3	9.0	29.6

Kerosene/Water cont'd

Run No.	$O/_U$ (v./v.)	Q_f (mL/s)	$O/_W$ (v./v.)	Pressure (lb/in^2)			Concentration of Light Phase (v./v.) (%)			E_s (%)
				P_f	P_o	P_u	Y_f	Y_o	Y_u	
(iii)										
25	0.70	104	1.06	6.3	5.7	6.8	51.4	54.7	49.2	7.1
26	0.80	103	1.05	6.7	5.9	7.2	51.3	53.9	49.2	4.7
27	1.06	114	1.06	5.8	5.2	6.3	51.4	54.5	48.2	6.3
28	1.13	105	1.08	6.7	6.0	7.0	52.0	53.0	50.2	2.8
29	1.49	103	1.06	6.2	5.6	6.8	51.5	53.3	48.9	4.2
30	1.76	97	1.06	6.9	6.2	7.4	51.5	53.1	48.6	4.1
31	2.08	90	1.05	6.9	6.2	7.4	51.3	52.9	48.0	4.3
32	2.48	99	1.05	6.6	6.0	7.1	51.3	52.3	48.8	2.9
(iv)										
33	0.44	187	0.159	2.2	0.9	2.2	13.7	18.1	11.8	11.3
34	0.62	193	0.155	1.9	0.5	1.9	13.4	26.1	5.5	41.9
35	0.70	198	0.166	2.2	0.7	2.1	14.3	27.5	5.0	44.6
36	0.87	204	0.169	2.1	0.5	1.7	14.4	28.7	2.1	53.5
37	0.95	203	0.171	1.9	0.3	1.5	14.6	28.1	1.8	52.6
38	1.02	205	0.166	1.8	0.2	1.7	14.2	26.4	1.8	50.3
39	1.21	202	0.170	1.8	0.3	1.5	14.5	25.3	1.5	47.5
(v)										
40	0.43	185	0.342	2.2	1.0	1.9	25.5	39.4	19.4	22.3
41	0.48	188	0.328	2.3	1.1	2.1	24.7	39.1	17.9	24.8
42	0.64	191	0.346	2.0	0.7	1.7	25.7	44.2	13.8	37.9
43	0.69	194	0.336	2.0	0.7	1.7	25.1	44.3	11.8	41.8
44	0.83	198	0.344	1.9	0.6	1.7	25.6	46.3	8.5	49.1
45	0.92	205	0.351	2.0	0.6	1.7	26.0	47.1	6.5	52.7
46	1.11	198	0.347	1.8	0.5	1.9	25.8	45.7	3.7	54.7
47	1.27	194	0.346	1.9	0.6	1.7	25.7	44.2	2.3	54.1
48	1.47	194	0.346	2.1	0.7	1.9	25.7	41.1	3.1	47.9

Kerosene/Water cont'd

Run No.	$O/_U$ (v./v.)	Q_f (mL/s)	$O/_W$ (v./v.)	Pressure (lb/in^2)			Concentration of Light Phase (v./v.) (%)			E_s (%)
				P_f	P_o	P_u	Y_f	Y_o	Y_u	
(vi)										
49	0.45	200	1.08	3.1	2.1	3.0	51.8	56.7	49.6	6.1
50	0.95	220	0.98	2.7	1.5	2.6	49.4	55.1	48.8	6.1
51	1.45	204	1.05	3.1	1.9	3.1	51.2	55.8	44.6	10.9
52	1.62	205	1.04	3.2	1.9	3.2	51.0	54.6	45.1	8.9
53	2.26	196	1.03	3.3	2.1	3.4	50.8	56.4	38.3	15.5
54	2.68	190	1.05	3.4	2.2	3.6	51.3	55.5	40.0	12.3
55	3.90	196	1.05	4.1	2.9	4.4	51.3	52.6	45.9	4.3
(vii)										
56	0.26	371	0.163	12.6	8.1	8.8	14.0	11.3	14.7	0
57	0.40	365	0.160	10.8	6.0	7.0	13.8	14.4	13.6	1.2
58	0.53	371	0.166	10.0	5.1	6.3	14.2	20.6	10.9	17.8
59	0.60	365	0.157	9.6	4.7	5.9	13.6	26.0	6.1	39.4
60	0.70	361	0.167	9.2	4.3	5.6	14.3	28.2	4.6	46.6
61	0.81	368	0.168	8.7	4.0	5.1	14.4	28.7	2.8	52.0
62	0.88	358	0.163	8.1	3.2	4.7	14.0	28.8	1.0	57.5
63	0.93	372	0.167	8.3	3.4	4.9	14.3	28.6	1.0	56.2
64	1.06	363	0.162	7.8	2.6	4.2	14.0	26.3	0.9	52.8
65	1.25	361	0.170	-	-	-	14.5	25.4	0.9	48.8
66	1.37	364	0.167	9.1	3.7	5.5	14.3	23.9	1.2	45.2
67	1.61	362	0.166	9.3	4.1	6.1	14.2	22.8	0.4	43.2
68	1.83	365	0.154	10.0	4.6	6.6	13.3	20.1	1.0	37.8
(viii)										
69	0.24	361	0.336	11.8	7.8	8.4	25.2	28.6	24.3	3.8
70	0.40	363	0.343	10.3	6.0	7.0	25.5	36.8	21.0	17.0
71	0.56	359	0.346	9.0	4.7	5.7	25.7	42.0	16.5	30.8
72	0.69	362	0.340	8.5	4.1	5.3	25.4	46.1	11.1	44.7
73	0.84	364	0.342	8.0	3.4	4.8	25.5	48.8	5.8	56.3

Kerosene/Water (viii) cont'd

Run No.	$O/_U$ (v./v.)	Q_f (mL/s)	$O/_W$ (v./v.)	Pressure (lb/in^2)			Concentration of Light Phase (v./v.) (%)			E_s (%)
				P_f	P_o	P_u	Y_f	Y_o	Y_u	
74	1.01	363	0.325	7.4	3.4	4.5	24.5	47.3	1.4	62.0
75	1.12	360	0.341	8.1	3.4	5.0	25.4	46.8	1.5	59.5
76	1.22	361	0.339	8.3	3.6	5.2	25.3	45.3	0.9	59.8
77	1.35	361	0.347	8.7	3.9	5.6	25.7	43.2	2.0	52.7
78	1.66	354	0.346	9.2	4.3	6.2	25.7	40.4	1.2	48.2
79	1.84	361	0.339	9.5	4.5	6.6	25.3	38.7	0.7	45.9
(ix)										
80	0.33	376	1.05	10.2	7.2	8.0	51.1	57.0	49.2	5.8
81	0.40	368	1.05	10.8	7.3	8.1	51.2	58.3	48.4	8.0
82	0.56	377	1.04	9.4	5.8	6.6	61.0	59.4	46.4	11.9
83	0.87	370	1.04	8.2	4.4	5.5	50.9	62.8	40.5	22.2
84	0.95	368	1.04	8.8	5.1	6.5	51.0	61.9	40.6	20.9
85	1.03	368	1.01	9.2	5.4	7.1	50.3	61.6	38.7	22.9
86	1.10	369	1.04	9.5	5.8	7.3	51.1	63.0	37.9	25.1
87	1.24	368	1.04	9.9	6.0	7.6	51.0	61.5	38.0	23.3
88	1.36	368	1.03	10.3	6.5	8.1	50.8	61.8	35.8	25.4
89	1.63	373	1.00	11.2	7.2	8.7	50.0	60.8	32.4	26.8
90	1.89	370	1.06	11.9	7.5	9.6	51.6	63.9	28.3	32.2
91	1.91	351	0.92	11.7	7.4	9.4	47.9	65.9	13.6	47.3
92	1.93	374	1.10	-	-	-	52.4	63.5	30.9	29.4
93	1.97	370	1.06	12.8	8.3	10.4	51.4	63.6	27.4	32.4
94	2.29	376	1.06	13.7	9.1	11.4	51.4	63.0	24.8	32.3
95	2.53	378	1.06	14.3	9.5	12.0	51.5	64.8	18.2	37.9
(x)										
96	1.25	367	0.170	-	-	-	14.5	25.4	0.9	48.8
97	1.32	365	0.175	8.6	3.4	5.1	14.9	25.4	0.5	48.6
(xi)										
98	0.15	97	0.159	0.3	negligible	0.8	13.7	23.7	12.2	11.0
99	0.24	96	0.165	0.3	negligible	0.7	14.1	33.0	9.6	30.0

Kerosene/Water (xi) cont'd

Run No.	O/U (v./v.)	Q_f (mL/s)	O/W (v./v.)	Pressure (lb/in^2) P_f	P_o	P_u	Concentration of Light Phase (v./v.) (%) Y_f	Y_o	Y_u	E_s (%)
100	0.34	91	0.165	negligible	NEGLIGIBLE	0.4	14.1	42.2	4.7	61.5
101	0.40	97	0.168	"		0.4	14.4	42.5	3.2	64.8
102	0.42	97	0.159	0.3		0.7	13.7	39.0	3.2	62.7
103	0.54	98	0.162	0.1		0.6	13.9	36.6	1.6	66.7
104	0.69	97	0.169	negligible		0.4	14.4	34.7	0.5	66.9
105	0.82	96	0.163	"		0.4	14.0	30.0	0.8	60.0
106	1.00	95	0.152	"		0.3	13.2	26.4	0	57.6
107	1.22	99	0.170	0.1		0.6	14.5	25.2	1.6	47.0
108	1.37	97	0.172	0.1		0.6	14.7	25.4	0	49.4
(xii)										
109	0.20	98	0.315	0.3	NEGLIGIBLE	0.9	24.0	66.7	15.3	39.6
110	0.39	98	0.320	0.2		0.7	24.2	66.8	7.7	64.9
111	0.41	99	0.309	0.4		0.9	23.6	65.6	6.4	67.7
112	0.59	98	0.317	0.1		0.6	24.1	61.6	2.1	75.8
113	0.77	97	0.328	negligible		0.5	24.7	55.1	1.1	71.5
114	1.04	97	0.335	"		0.5	25.1	48.6	0.6	63.8
115	1.23	97	0.356	0.1		0.6	26.2	47.0	0.7	59.2
116	1.27	98	0.329	0.1		0.6	24.8	43.8	0.4	57.3
117	1.69	97	0.352	0.2		0.7	26.0	40.5	1.6	47.1
(xiii)										
118	0.45	101	0.95	0.3	negligible	0.9	48.6	86.1	31.8	46.5
119	0.71	102	0.99	0.3	"	0.9	49.7	85.0	24.4	58.9
120	0.85	103	1.01	0.3	"	0.7	50.2	83.8	21.8	61.6
121	1.03	103	0.99	0.5	"	1.0	49.7	83.5	14.8	68.7
122	1.34	103	1.05	0.6	0.2	1.1	51.2	82.9	8.9	72.5
123	1.49	103	1.02	0.4	negligible	1.0	50.6	80.8	5.7	72.2

Kerosene/Water (xiii) cont'd

Run No.	$O/_U$ (v./v.)	Q_f (mL/s)	$O/_W$ (v./v.)	Pressure (lb/in^2)			Concentration of Light Phase (v./v.) (%)			E_s (%)
				P_f	P_o	P_u	Y_f	Y_o	Y_u	
124	2.07	103	1.07	0.9	0.3	1.4	51.7	75.6	2.1	64.6
125	2.22	103	1.03	0.9	0.4	1.4	50.8	72.8	2.2	60.6
126	2.25	103	1.07	0.8	0.3	1.4	51.8	73.2	3.7	59.3
127	2.32	103	1.04	1.2	0.6	1.7	50.9	71.5	3.0	57.6
(xiv)										
128	0.17	198	0.159	3.7	2.4	3.2	13.7	11.6	14.1	0
129	0.32	198	0.163	3.1	1.6	2.6	14.0	17.4	12.9	6.9
130	0.41	197	0.159	2.6	1.2	2.2	13.7	22.6	10.0	22.1
131	0.56	198	0.163	2.3	0.9	2.0	14.0	28.8	5.8	43.7
132	0.72	196	0.155	1.9	0.5	1.6	13.4	30.1	1.5	59.8
133	0.73	197	0.170	2.1	0.6	1.7	14.5	31.6	2.1	57.8
134	0.90	198	0.160	1.8	0.4	1.5	13.8	28.3	0.9	57.3
135	0.98	197	0.161	1.6	0.1	1.3	13.9	27.7	0.4	57.1
136	1.06	188	0.148	1.6	0.2	1.4	12.9	24.6	0.4	53.6
137	1.10	198	0.157	1.9	0.4	1.6	13.6	25.8	0.2	54.4
138	1.40	197	0.158	1.9	0.4	1.6	13.6	23.2	0.2	47.6
(xv)										
139	0.32	191	0.322	2.6	1.3	2.2	24.4	43.0	18.5	24.2
140	0.47	197	0.337	2.8	1.5	2.4	25.2	51.0	13.0	43.9
141	0.66	195	0.341	2.2	0.8	1.7	25.4	55.2	5.9	62.2
142	0.78	196	0.339	2.2	0.8	1.7	25.3	54.1	2.9	66.7
143	1.11	197	0.337	2.1	0.7	1.8	25.2	47.2	0.7	61.5
144	1.30	199	0.341	2.2	0.8	2.0	25.4	44.3	0.9	56.3
(xvi)										
145	0.69	205	1.01	2.9	1.6	2.5	50.4	73.8	34.2	38.3
146	0.91	203	1.02	3.4	2.1	3.1	50.6	74.2	29.2	44.9
147	1.22	204	1.01	4.2	2.8	4.0	50.3	73.9	21.7	51.8

Kerosene/Water (xvi) cont'd

Run No.	$O/_U$ (v./v.)	Q_f (mL/s)	$O/_W$ (v./v.)	Pressure (lb/in^2)			Concentration of Light Phase (v./v.) (%)			E_s (%)
				P_f	P_o	P_u	Y_f	Y_o	Y_u	
148	1.38	203	1.01	3.9	2.5	3.7	50.3	74.5	16.9	56.2
149	1.81	189	0.93	4.4	3.0	4.3	48.1	73.2	2.7	64.7
150	2.02	203	1.03	5.2	3.6	5.0	50.7	72.8	6.3	59.0